Targeting V-ATPase in human monocytes and macrophages to manipulate inflammation-related mediators

Dissertation

To Fulfill the
Requirements for the Degree of
„doctor rerum naturalium“ (Dr. rer. nat.)

Submitted to the Council of the Faculty
of Biological Sciences
of the Friedrich Schiller University Jena

by Zhigang Rao

born on May 4th, 1992 in Fuzhou, China

1st Reviewer: Prof. Dr.Oliver Werz, Friedrich-Schiller-Universität Jena

2nd Reviewer: Prof. Dr. Gerhard K.E. Scriba, Friedrich-Schiller-Universität Jena

3rd Reviewer: Prof. Dr. Andrea Huwiler, Universität Bern

Date of submission: November 21, 2019

Date of defense: July 3, 2020

Dissertation,Friedrich-Schiller-Universität Jena, [2020]

TABLE OF CONTENTS

ABBREVIATIONS III
SUMMARY V
ZUSAMMENFASSUNG VIII
1. INTRODUCTION 1
1.1 Inflammation 1
1.1.1 Eicosanoids and inflammation 2
1.1.1.1 Leukotrienes 3
1.1.1.2 Prostanoids 4
1.1.2 Cytokines and inflammation 5
1.2 Resolution of inflammation 6
1.2.1 Biosynthesis and biological function of SPM 6
1.2.1.1 Lipoxins and aspirin-triggered lipoxins 6
1.2.1.2 Resolvin E-series 8
1.2.1.3 Resolvin D-series, protectins and maresins 9
1.3 Monocytes and macrophages 9
1.3.1 Monocytes 9
1.3.2 Macrophages 11
1.3.2.1 M1 macrophages 12
1.3.2.2 M2 macrophages 12
1.3.2.3 Tumor associated macrophages 15
1.4 V-ATPase 15
1.4.1 Structure of V-ATPase 16
1.4.2 Biological function of V-ATPase 16
1.4.3 Pharmacological targeting V-ATPase 18
2. AIM OF THESIS 20
3. MANUSCRIPTS 21
3.1 Manuscript I 22
3.2 Manuscript II 43
3.3 Manuscript III 56
4. DISCUSSION 74
4.1 Inhibition of V-ATPase in human monocytes 74
4.2 Inhibition of V-ATPase in human M1 macrophages 77
4.3 Inhibition of V-ATPase in human M2 macrophages 81

5. REFERENCES 86
APPENDIX 1: ACKNOWLEDGEMENTS I
APPENDIX 2*:* CURRICULUM VITAE III
APPENDIX 3: LIST OF PUBLICATIONS IV
APPENDIX 4: AUTHOR CONTRIBUTION STATEMENT V
APPENDIX 5: EIGENSTÄNDIGKEITSERKLÄRUNG VIII

ABBREVIATIONS

AA	arachidonic acid
ArchA	archazolid A
AT-LX	aspirin-triggered lipoxin
ATP	adenosine triphosphate
AT-PD	aspirin-triggered protectin
A23187	calcium-ionophore
BSA	bovine serum albumin
Ca^{2+}	calcium ion
CD	cluster of differentiation
COX	cyclooxygenase
$cPLA_2$-α	cytosolic phospholipase A_2-alpha
CYP 450	cytochrome p450
Cys-LT	cysteinyl-leukotriene
DHA	docosahexaenoic acid
ERK	extracellular signal-regulated kinase
EPA	eicosapentaenoic acid
FITC	fluorescein isothiocyanate
FLAP	5-lipoxygenase-activating protein
fMLP	N-formyl-methionyl-leucyl-phenylalanine
GPCR	G-protein coupled receptor
HDHA	hydroxydocosahexaenoic acid
HEK	human embryonic kidney
HETE	hydroxyeicosatetraenoic acid
HODE	hydroxyoctadecadienoic acid
HPDHA	hydroperoxyldocosahexaenoic acid
HPETE	hydroperoxyleicosatetraenoic acid
HSC	haematopoietic stem cell
IGF-1	insulin like growth factor 1
IFNγ	Interferon γ
IκB	inhibitor of nuclear factor kappa B
IL	interleukin
iNOS	inducible nitric oxide synthase
JAK-STAT6	janus kinases-signal transducer and activator of transcription 6
Lamtor 1	late endosomal and lysosomal adaptor and MAPK and mTOR activator 1
LM	lipid mediator
LOX	lipoxygenase
LPS	lipopolysaccharide
LT	leukotriene
LTA_4H	LTA_4 hydrolase
LTC_4S	LTC_4 Synthase
LX	lipoxin
LXR	liver X receptor
MaR	maresin
MDM	monocyte-derived macrophage
MEK	mitogen-activated protein kinase kinase

MHC	major histocompatibility complex
mTORC	mechanistic target of rapamycin complex
MTT	3-(4,5-dimethylthiazol-2-yl)-2,5-diphenyltetrazolium bromide
NADPH	nicotinamide adenine dinucleotide phosphate
NF-κB	nuclear factor kappa-light-chain-enhancer of activated B cells
NSAIDs	non-steroidal anti-inflammatory drugs
p38 MAPK	p38 mitogen-activated protein kinase
PBMC	peripheral blood mononuclear cells
PBS	phosphate-buffered saline
PD	protectin
PG	prostaglandin
PI3-K	phosphoinositide 3-kinase
PMNL	polymorphonuclear neutrophil
ROI	reactive oxygen intermediate
Rv	resolvin
SAPK/JNK	stress-activated protein kinase/Jun amino-terminal kinases
SDS-PAGE	sodium dodecyl sulfate-polyacrylamide gel electrophoresis
SPM	specialized proresolving mediator
SRA	class A scavenger receptor
SRS-A	slow-reacting substance of anaphylaxis
TAMs	tumor associated macrophages
TGF-β	transforming growth factor beta
Th-1	T-helper type 1
TLR	toll-like receptor
TNF-α	tumor necrosis factor α
TX	thromboxane
UPLC-MS-MS	ultra-performance liquid chromatography–tandem mass spectrometry
V-ATPase	vacuolar (H^+)-ATPase

SUMMARY

Inflammation is a self-defensive process by the immune system that helps the body to return to homeostasis [1]. Professional innate immune cells with pivotal functions in the immune defense like human monocytes, M1 and M2 macrophages produce abundant levels of mediators including cytokines, pro-inflammatory eicosanoids, as well as specialized proresolving mediators (SPMs). These inflammation-related mediators play indispensable roles in the inflammation process. Acute inflammation is governed by the production of pro-inflammatory eicosanoids like leukotrienes (LTs) and prostaglandins (PGs). Excessive production of pro-inflammatory mediators sustains the inflammation process to a chronic inflammation state that is closely related to the pathogenesis of various diseases including Alzheimer´s diseases, cardiovascular diseases, rheumatoid arthritis, atherosclerosis and cancer [2]. The resolution of inflammation is an active process governed by the anti-inflammatory and proresolving SPMs [3].

The vacuolar (H^+)-ATPase (V-ATPase) is a universal proton pump that is involved in pH homeostasis, pathogen entry and protein degradation [4]. Although V-ATPase is fundamental in cytokine trafficking and secretion in human monocytes and was implicated in the M2 polarization of murine macrophages [5, 6], its functional roles in the biosynthesis of inflammation-related lipid mediators in human immune cells like monocytes, M1 and M2 macrophages remained elusive.

First, we discovered a differential role of V-ATPase in the expression and in the activity of cyclooxygenase (COX)-2 in human monocytes. Pharmacological targeting of V-ATPase with archazolid A (ArchA) or bafilomycin increased the expression of the COX-2 protein in lipopolysaccharide (LPS)-stimulated monocytes, which was paralleled by enhanced phosphorylation of p38 mitogen-activated protein kinase (MAPK) and extracellular signal-regulated kinase (ERK)-1/2, without impacting the nuclear factor kappa-light-chain-enhancer of activated B cells (NF-κB) and stress-activated protein kinase/Jun amino-terminal kinases (SAPK/JNK) pathways. Targeting of both p38 MAPK and ERK-1/2 pathways suggest that these kinase pathways are crucial for COX-2 expression in human monocytes. Despite increased COX-2 protein levels, however, suppression of V-ATPase activity impaired the biosynthesis of COX-related LM in monocytes without affecting 12-/15-lipoxygenase (LOX) products and only minor

suppression of 5-LOX activity. Our results indicate that changes in the intracellular pH may contribute to suppression of COX-2 activity and that V-ATPase on one hand restricts COX-2 protein levels by limiting p38 MAPK and ERK-1/2 activation, while on the other hand it governs the cellular COX-2 activity through an appropriate intracellular pH.

Next, we focused on the role of V-ATPase in the polarization of M1 macrophages. We show that targeting V-ATPase by ArchA elevated TNF-α mRNA levels and TNF-α secretion in M1 macrophages. By contrast, ArchA failed to increase TNF-α levels in uncommitted M0 or M2. Production of other relevant cytokines like IL-1β, IL-6, IL-10 or chemokines as IL-8 and monocyte chemotactic protein-1 from M1 macrophages was not affected by ArchA. Of interest, targeting V-ATPase prevented the degradation of COX-2 protein and elevated the production of related PG, which contrasts the role in monocytes. Notably, we show that the phosphorylation and nuclear translocation of the p65 subunit of NF-κB as well as phosphorylation of SAPK/JNK is enhanced by ArchA. V-ATPase is overexpressed in various types of tumor cells and targeting V-ATPase induces tumor cell apoptosis [7]. To evaluate possible benefits of V-ATPase inhibition to the anti-tumoral effects of M1 macrophages, a microfluidically-supported three-dimensional human tumor biochip model was introduced. ArchA-treated M1 macrophages significantly reduced MCF-7 tumor cell viability due to elevated TNFα secretion, whereas in models containing M2 macrophages or in models devoid of macrophages, ArchA failed in this respect. Conclusively, pharmacologically targeting V-ATPase induces COX-2 protein expression and production of PG and TNF-α levels, thus supporting the anti-tumoral effects of M1 macrophages.

Finally, IL-4-stimulated M2 macrophages possess a different LM profile compared to classical activated M1 macrophages upon challenge with pathogenic bacteria [8]. Classical M1 macrophages produce predominately pro-inflammatory LTs and PGs, while M2 macrophages biosynthesize abundant levels of SPM. V-ATPase was shown to be involved in the polarization of murine macrophages [5]. Therefore, we focused on the role of V-ATPase in LM biosynthetic pathways in human M2 macrophages. Blockade of V-ATPase during polarization of human M2 macrophages abrogated 15-lipoxygenase-1 (15-LOX-1) expression, the key enzyme in SPM biosynthesis and thus prevented the formation of 15-LOX-1-derived SPM precursors and related SPM. Targeting V-ATPase neither influenced the IL-4-triggered JAK-STAT6 pathway nor the

mTORC1 signaling cascade, but strongly suppressed phosphorylation of MEK and ERK-1/2 in M2 macrophages. The MEK inhibitor U0126 and c-Myc inhibitor JQ-1 abrogated 15-LOX-1 expression as well as SPM biosynthesis, indicating an essential role of V-ATPase in 15-LOX-1 expression and SPM formation through the MEK/ERK-1/2-c-Myc cascade in human M2 macrophages. Inhibition of V-ATPase *in vivo* delayed inflammatory resolution of zymosan-induced murine peritonitis accompanied by an increased neutrophil infiltration and decreased SPM levels without affecting the pro-inflammatory LTs or PGs. Collectively, our data propose a critical role of V-ATPase in the regulation of SPM biosynthetic pathways in M2 macrophages and has a crucial role in resolution of inflammation.

Together, this thesis provides evidence that V-ATPase differentially regulates the biosynthetic pathways of inflammation-related lipid mediators in human immune cells like monocytes, M1 and M2 macrophages. In a cell-specific manner, V-ATPase i) limits the expression of COX-2 enzyme but governs COX-2 activity via the regulation of the intracellular pH in monocytes, but ii) limits the expression of COX-2 enzyme and production of PG in M1 macrophages, and iii) is crucial for IL-4 induced expression of 15-LOX-1 as well as related SPM precursor and SPM in M2 macrophages with an essential role in resolution of inflammation.

ZUSAMMENFASSUNG

Entzündung ist ein selbstverteidigender Prozess des Immunsystems, der dem Körper hilft, zur Homöostase zurückzukehren [1]. Professionelle Zellen des angeborenen Immunsystems mit zentralen Funktionen in der Immunabwehr wie menschliche Monozyten, M1- und M2-Makrophagen produzieren reichlich Mediatoren, einschließlich Zytokine, entzündungsfördernde Eicosanoide sowie spezialisierte Pro-resolving-Mediatoren (SPMs). Diese entzündungsrelevanten Mediatoren spielen eine unverzichtbare Rolle in der Regulation des Entzündungsprozesses. Akute Entzündungen werden durch die Produktion entzündungsfördernder Eicosanoide wie Leukotriene (LTs) und Prostaglandine (PGs) gesteuert. Die übermäßige Produktion entzündungsfördernder Mediatoren führt zu einem chronischen Entzündungszustand, der eng mit der Pathogenese verschiedener Krankheiten wie Alzheimer, Herz-Kreislauf-Erkrankungen, rheumatoider Arthritis, Atherosklerose und Krebs zusammenhängt [2]. Die Auflösung der Entzündung ist ein aktiver Prozess, der von entzündungshemmenden SPMs geregelt wird [3].

Die vakuoläre (H^+) - ATPase (V-ATPase) ist eine universelle Protonenpumpe, die an der pH-Homöostase, dem Eindringen von Krankheitserregern und dem Proteinabbau beteiligt ist [4]. Die V-ATPase ist für den Zytokintransport und die Sekretion in menschlichen Monozyten von grundlegender Bedeutung und ist auch in die M2-Polarisation von Maus-Makrophagen involviert [5, 6]. Die Rolle des Enzyms bei der Biosynthese entzündungsbedingter Lipidmediatoren in menschlichen Immunzellen wie Monozyten, M1 und M2-Makrophagen ist bislang nicht geklärt.

Zunächst entdeckten wir eine unterschiedliche Rolle der V-ATPase bei der Expression und Aktivität von Cyclooxygenase (COX)-2 in menschlichen Monozyten. Das pharmakologische Targeting von V-ATPase mit Archazolid A (ArchA) oder Bafilomycin erhöhte die Expression des COX-2-Proteins in Lipopolysaccharid (LPS) -stimulierten Monozyten, was mit einer verstärkten Phosphorylierung von p38-Mitogen-aktivierter Proteinkinase (MAPK) und extrazellulär signalregulierte Kinase (ERK)-1/2 einherging, ohne den Kernfaktor kappa-light chain enhancer von aktivierten B-Zellen (NF-κB) und stressaktivierten Proteinkinase/Jun-Amino-terminalen Kinasen (SAPK/JNK) zu beeinflussen. Das Targeting von sowohl p38 MAPK- als auch ERK-1/2-Pfaden legt nahe, dass diese Kinase-Pfade für die COX-2-Expression in menschlichen Monozyten

entscheidend sind. Trotz erhöhter COX-2-Proteinspiegel beeinträchtigte die Unterdrückung der V-ATPase-Aktivität jedoch die Biosynthese von COX- abgeleiteten LM in Monozyten, ohne 12-/15-Lipoxygenase (LOX)-Produkte und, nur geringfügig, die 5-LOX-Aktivität zu beeinträchtigen. Unsere Ergebnisse deuten darauf hin, dass Änderungen des intrazellulären pH-Werts zur Unterdrückung der COX-2-Aktivität beitragen können und dass V-ATPase einerseits die COX-2-Proteinspiegel einschränkt, indem sie die Aktivierung von p38 MAPK und ERK-1/2 eingrenzt, andererseits regelt sie die zelluläre COX-2-Aktivität durch einen geeigneten intrazellulären pH-Wert.

Als nächstes konzentrierten wir uns auf die Rolle der V-ATPase bei der Polarisation von M1-Makrophagen. Wir zeigen, dass das Targeting von V-ATPase durch ArchA die TNF-α-mRNA-Spiegel und die TNF-α-Sekretion in M1-Makrophagen erhöht. Im Gegensatz dazu konnte ArchA die TNF-α-Spiegel in M0 oder M2 nicht erhöhen. Die Produktion anderer relevanter Zytokine wie IL-1β, IL-6, IL-10 oder Chemokine wie IL-8 und chemotaktisches Monozytenprotein-1 aus M1-Makrophagen wurde von ArchA nicht beeinflusst. Interessanterweise verhinderte das Targeting von V-ATPase den Abbau von COX-2-Protein und erhöhte die Produktion von verwandtem PG, was der Rolle der V-ATPase in Monozyten entgegensteht. Insbesondere zeigen wir, dass die Phosphorylierung und Kerntranslokation der p65-Untereinheit von NF-κB sowie die Phosphorylierung von SAPK/JNK durch ArchA verstärkt werden. V-ATPase wird in verschiedenen Tumorzelltypen überexprimiert und durch gezielte V-ATPase wird eine Tumorzellapoptose induziert [7]. Um die möglichen Vorteile der V-ATPase-Hemmung für die Antitumorwirkung von M1-Makrophagen zu bewerten, wurde ein mikrofluidisch unterstütztes dreidimensionales Biochip-Modell für menschliche Tumoren etabliert. ArchA-behandelte M1-Makrophagen reduzierten die Lebensfähigkeit von MCF-7-Tumorzellen aufgrund einer erhöhten TNFα-Sekretion signifikant, wohingegen ArchA in Modellen, die M2-Makrophagen enthielten, oder in Modellen, die keine Makrophagen enthielten, diesbezüglich versagte. Zusammenfassend induziert die pharmakologisch Hemmung der V-ATPase die COX-2-Proteinexpression und die Produktion von PG- und TNF-α-Spiegeln, wodurch die Antitumorwirkung von M1-Makrophagen unterstützt wird.

IL-4-stimulierte M2-Makrophagen produzieren bei Exposition mit pathogenen Bakterien ein anderes LM-Profil als klassisch aktivierte M1-Makrophagen [8]. Klassische M1-Makrophagen produzieren hauptsächlich entzündungsfördernde LTs

und PGs, während M2-Makrophagen reichlich SPM biosynthetisieren. Es wurde gezeigt, dass V-ATPase an der Polarisation von Maus-Makrophagen beteiligt ist [5]. Daher konzentrierten wir uns auf die Rolle der V-ATPase in LM-Biosynthesewegen in humanen M2-Makrophagen. Die Blockade der V-ATPase während der Polarisation von humanen M2-Makrophagen hob die 15-Lipoxygenase-1 (15-LOX-1)-Expression auf, welches das Schlüsselenzym in der SPM-Biosynthese ist, und verhinderte somit die Bildung von 15-LOX-1-abgeleiteten SPM-Vorläufern und verwandten SPM. Die Hemmung der V-ATPase beeinflusste weder den IL-4-induzierten JAK-STAT6-Signalweg noch die mTORC1-Signalkaskade, verringerte jedoch die Phosphorylierung von MEK und ERK-1/2 in M2-Makrophagen stark. Der MEK-Inhibitor U0126 und der c-Myc-Inhibitor JQ-1 verhinderten die 15-LOX-1-Expression sowie die SPM-Biosynthese, was auf eine wesentliche Rolle der V-ATPase bei der 15-LOX-1-Expression und der SPM-Bildung durch die MEK/ERK-1/2-c-Myc-Kaskade in humanen M2-Makrophagen hindeutet. Die Hemmung der V-ATPase in vivo verzögerte die Auflösung der Zymosan-induzierten murinen Peritonitis, was einherging mit einer erhöhten Neutrophilen-Infiltration und verringerten SPM-Spiegeln, ohne die proinflammatorischen LT oder PG zu beeinflussen. In der Gesamtheit zeigen unsere Daten, dass die V-ATPase eine entscheidende Rolle in der Regulation von SPM-Biosynthesewegen in M2-Makrophagen und bei der Auflösung von Entzündungen spielt.

Zusammenfassend liefert diese Arbeit Hinweise darauf, dass die V-ATPase die Biosynthesewege entzündungsbedingter Lipidmediatoren in menschlichen Immunzellen wie Monozyten, M1- und M2-Makrophagen unterschiedlich reguliert. In einer zellspezifischer Weise i) begrenzt die V-ATPase die Expression des COX-2-Enzyms in Monozyten, reguliert jedoch die COX-2-Aktivität mittels des intrazellulären pH-Wertes, ii) begrenzt die V-ATPase die Expression des COX-2-Enzyms und die Produktion von PG in M1-Makrophagen und iii) ist die V-ATPase entscheidend für die IL-4-induzierte Expression von 15-LOX-1, sowie verwandten SPM-Vorläufern und SPM in M2-Makrophagen mit einer wesentlichen Rolle bei der Auflösung von Entzündungen.

1. INTRODUCTION

1.1 Inflammation

Inflammation is a self-protective process during which the immune system defenses against exterior stimulus including tissue injury, microbial infection and many others. On challenge of harmful stimuli, various cellular processes are evoked like increase of blood flow, enhancement of capillaries permeability as well as elevated production of pro-inflammatory cytokines and eicosanoids (prostaglandins (PGs) and leukotrienes (LTs)) [1]. Cardinal signs like rubor (redness), tumor (swelling or edema), and dolor (pain) are formed during acute inflammation. One major event that governs the acute inflammatory process is the migration of neutrophils out of the capillary venules to the inflamed sites [9].

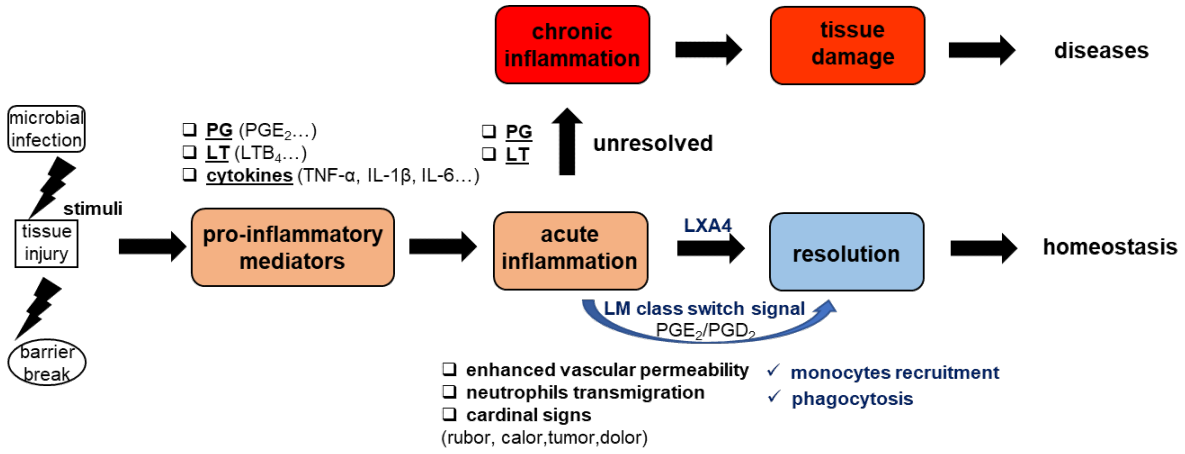

Fig.1.1 The inflammation process. Exterior stimuli (microbial infection, tissue injury and barrier break) which trigger various biological processes including increase of blood flow and vascular permeability, neutrophil transmigration, production of pro-inflammatory prostaglandins (PGs), leukotrienes (LTs) and cytokines as well as formation of cardinal signs. Excessive pro-inflammatory mediators sustain the inflammation to chronic inflammatory ones, which leads to tissue damage and is related to the pathogenesis of various diseases. Lipid mediator (LM) class switch alters the biosynthesis of PG/LT towards LXA4, which inhibits the pro-inflammatory process and programs the resolution for homeostasis.

Ideally, the inflammation process is self-limiting and acute inflammation always

accompanies with the resolution phase that helps the body return to a healthy state [10]. In the resolution phase, lipid mediators (LM) class switch signal triggered by PGE_2 and PGD_2 switches the production of pro-inflammatory LTB_4 to proresolving LXA_4 that inhibits neutrophil transmigration, recruits monocytes and programs the resolution phase for homeostasis [11]. However, unresolved inflammation would turn into a chronic inflammation state, which subsequently leads to chronic diseases such as Alzheimer´s diseases, cardiovascular diseases, rheumatoid arthritis, atherosclerosis and cancer [2].

1.1.1 Eicosanoids and inflammation

During acute inflammation, endogenously released mediators (like eicosanoids including LTs and PGs) and cytokines play pivotal roles in regulating the initiation and maintenance of the inflammatory process.

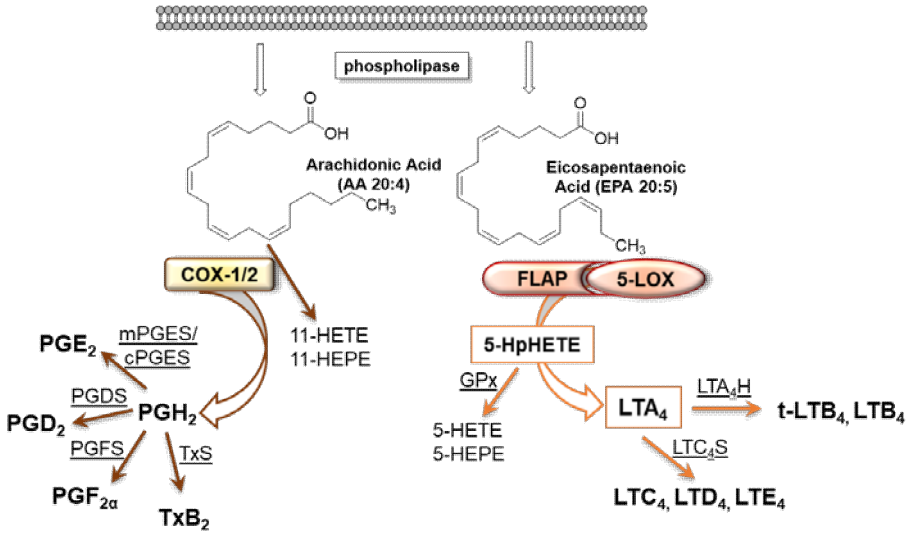

Fig.1.2 The eicosanoid biosynthesis pathway. Utilizing phospholipid-derived arachidonic acid (AA) as substrate, production of leukotrienes (LTs), prostaglandins (PGs) and thromboxane (TX) are catalyzed by various eicosanoid biosynthetic enzymes. 5-lipoxygenase (5-LOX) and 5-lipoxygenase-activating protein (FLAP) catalyze the formation of intermediate 5-HPETE, which is further converted to 5-HETE by glutathione peroxidases (GPx), to LTB_4 by LTA_4 hydrolase (LTA_4H) and Cys-LT by LTC_4 Synthase (LTC_4S). Cyclooxygenases (COX-1 and COX-2) catalyze the formation of intermediate PGH_2, which is further converted to PG and TXB_2 by PGE synthase (mPGES, cPGES), PGD synthase (PGDS),

PGF synthase (PGFS) and thromboxane synthase (TxS).

1.1.1.1 Leukotrienes

Leukotrienes (LTs) are biosynthetic eicosanoids synthesized from phospholipid-derived arachidonic acid (AA) via the 5-lipoxygenase (5-LOX) pathway [12, 13]. The catalytic activity of 5-LOX is dependent on multiple processes including the presence of 5-lipoxygenase-activating protein (FLAP), cellular AA supply, the presence of calcium ions (Ca^{2+}) and ERK-1/2 activity [14]. In the resting state, 5-LOX resides in the cytosol or the nucleoplasm. Once activated by stimuli, 5-LOX will be phosphorylated and translocated to the nuclear membrane with the help with its helper protein FLAP. Activated 5-LOX together with FLAP catalyze the formation of intermediates 5(S)-hydroperoxyeicosatetraenoic acid (HPETE) and LTA_4 from AA. Then LTA_4 is further converted to LTB_4 and cysteinyl LT (Cys-LT, including LTC_4, LTD_4 and LTE_4) with the help of LTA_4 hydrolase (LTA_4H) and LTC_4 synthases (LTC_4S) [15, 16]. Alternatively, 5(S)-HPETE can also be metabolized to 5(S)-hydroxyeicosatetraenoic acid (HETE) by glutathione peroxidase (GPx) [17]. LT are generated from a large variety of inflammatory cells including polymorphonuclear neutrophils (PMNL), eosinophils, monocytes, macrophages and mast cells. Neutrophils produce mainly LTB_4 and eosinophils produce higher amounts of LTC_4, while monocytes and macrophages produce balanced amounts of LTB_4 and cys-LTs [18, 19]. LTB_4 is among one of the most potent chemoattractant mediators that were shown to stimulate and amplify neutrophil chemotaxis in various *in vitro* and *in vivo* studies [20]. LTB_4 was shown to increase interleukin-6 (IL-6) production through activation of nuclear factor kappa-light-chain-enhancer of activated B cells (NF-κB) and NF-IL-6 in human monocytes [21]. Cys-LT are described as “slow-reacting substance of anaphylaxis” since they were shown to contract airway smooth muscles in both animal and human *in vitro* studies [22, 23]. Excessive production of leukotrienes maintains the inflammatory process and stimulates the progression of chronic inflammation, which contributes the pathogenesis of various diseases including cancer [24]. LT are critically involved in the pathogenesis of asthma, they are recognized as common therapeutic targets in the treatment of

asthma [25, 26]. The marketed drug zileuton is a common therapy for treating asthma by blockade of LT formation via inhibition of 5-LOX activity [27].

1.1.1.2 Prostanoids

Prostanoids (PG and thromboxane) are derived from AA. Cyclooxygenases (COX or named as prostaglandin H synthase) catalyze the rate-limiting step from AA to form the intermediate PGH_2. Afterwards PGH_2 is converted to PG (PGE_2, PGD_2 and PGF_2) and thromboxane (TXB_2) by specific enzymes like PGE synthase (mPGES, cPGES), PGD synthase (PGDS), PGF synthase (PGFS) and thromboxane synthase (TxS) [28]. In humans, two isoforms of COX exits, namely COX-1 and COX-2, respectively.

The COX-1 enzyme is considered to be constitutively expressed in most cells and tissues. COX-1 is responsible for the formation of gastric PG that show protective functions in stomach and intestine homeostasis. Recent evidences showed that COX-1 is also inducible upon IL-4 stimulation in alternative activated M2 macrophages [29]. However, COX-2, an inducible enzyme that can be activated by various pro-inflammatory stimuli including TNF-α, LPS and IL-1β, is critically involved in the formation of the excessive PG in inflammation.

PG play pivotal role in the initiation of inflammation, they are involved in the formation of the cardinal signs like rubor (redness), tumor (swelling or edema), and dolor (pain) in inflammation [30]. PG increase the blood flow and the permeability of venules, which cause redness and edema, and they trigger the infiltration of neutrophils to inflamed sites [31]. Their actions on peripheral sensory neurons and brain central sites are related to pain in inflammation [30]. In clinic, steroidal glucocorticoids, non-steroidal anti-inflammatory drugs (NSAIDs, like aspirin, indomethacin, ibuprofen) and selective COX-2 inhibitors coxibs (celecoxib and rofecoxib) are used to inhibit the activity of COX enzymes, especially COX-2 activity as anti-inflammatory therapy [32-35]. As doubled-edged sword, PG display dual pro-inflammatory and anti-inflammatory roles. PG as modulators rather than only mediators of inflammation down-regulate host responses and reverse the enhancement of acute allergic inflammation *in vivo*. PGE_2 triggers the

LM class switch signal and switches the production of pro-inflammatory LTB_4 to proresolving LXA_4 that inhibits neutrophil infiltration, recruits monocytes and programs the resolution phase [11]. In the gastrointestinal mucosa, abundant levels of PG are detected and play crucial cytoprotective roles to avoid gastric mucosal damage [36, 37].

1.1.2 Cytokines and inflammation

During acute inflammation, immune cells like monocytes and macrophages produce abundant levels of pro-inflammatory cytokines including interleukin-1β (IL-1β), interleukin-6 (IL-6), tumor necrosis factor (TNF-α), to name a few. Vice versa, these pro-inflammatory cytokines also stimulate and amplify the acute inflammation. Studies revealed that these pro-inflammatory cytokines are related to initiation and maintenance of the neuropathic pain [38]. IL-1β stimulates the production of other pro-inflammatory molecules like substance P and PGE_2 in neuronal cells [39, 40]. Overproduction of IL-1β and IL-6 are related to the pathogenesis of various chronic diseases like rheumatoid arthritis, inflammatory bowel disease, Alzheimer's disease and cancer [41]. TNF-α as key regulator of the inflammatory response binds TNF-α receptors and triggers cellular responses by activation of subsequent signaling. For example, TNF-α enhances leukocyte adhesion and transmigration in vascular endothelial cells [42]. TNF-α is involved in the activation of NF-κB signaling and thus induces COX-2 expression and production of PG [43].

Depending on the microenvironment, various cytokines display also anti-inflammatory effects. IL-4 is a highly pleiotropic cytokine that is produced mainly by T-helper cell type-2 (Th2) lymphocytes and in turn regulates the Th2 differentiation [44]. IL-4 displays significant anti-inflammatory roles by inhibition of production of pro-inflammatory cytokines such as IL-1β, IL-6 and TNF-α [45]. Various studies indicated that IL-6, IL-10 and IL-13 are potent deactivators of pro-inflammatory cytokine synthesis. For example, evidences proved that IL-6 stimulates anti-inflammatory responses including the synthesis of glucocorticoids and IL-1ra while it inhibited the

LPS-induced production of IL-1β and TNF-α [46]. IL-10 inhibited the activation of NF-κB and the production of TNF-α in RAW 264.7 macrophages [47]. IL-13 suppressed the production of pro-inflammatory cytokines like IL-1β, IL-6, IL-8 and TNF-α in human monocytes [48].

1.2 Resolution of inflammation

For a long period, the resolution phase was thought to be a passive process by the innate immune system. However, recent studies showed that the resolution of inflammation is an active process, which is governed by the anti-inflammatory and proresolving effects of endogenously produced specialized proresolving mediators (SPMs) [3, 49]. As functional mediators, SPMs trigger anti-inflammatory responses in acute inflammation and proresolving actions during resolution of inflammation. They are actively involved in mediating various inflammation-related processes like neutrophils transepithelial migration, phagocytosis and tissue regeneration.

1.2.1 Biosynthesis and biological function of SPM

Depending on the substrate, the SPM include lipoxins (LXs) that are derived from AA, maresins (MaRs), protectins (PDs) and resolvin D/E-series (RvDs and RvEs) that are bioactive metabolites from omega-3 essential fatty acids DHA and EPA.

1.2.1.1 Lipoxins and aspirin-triggered lipoxins

LXs are the first class of lipid mediators which are characterized to be actively involved in resolution of inflammation. Triggered by a lipid mediator class switch signal, these SPM offer “stop” signals to block the infiltration of neutrophils, end the acute inflammation and program the resolution of inflammation [11]. Other than the formation of LTs, 5-LOX derived-arachidonic acid (AA) intermediate LTA_4 can be converted to LXs (LXA4 and LXB4) with the help of 15-LOX-1 in human macrophages or 12-lipoxygenase (12-LOX) in platelets [50, 51]. Besides the classical biosynthetic pathway

for SPM, specific aspirin-triggered lipoxins (AT-LXs) are produced via the aspirin-triggered pathways when COX-2 is acetylated by aspirin [52]. The acetylated COX-2 generates 15R-H(p)ETE, which is the precursor for AT-LXs (AT-LXA4 and LT-LXB4).

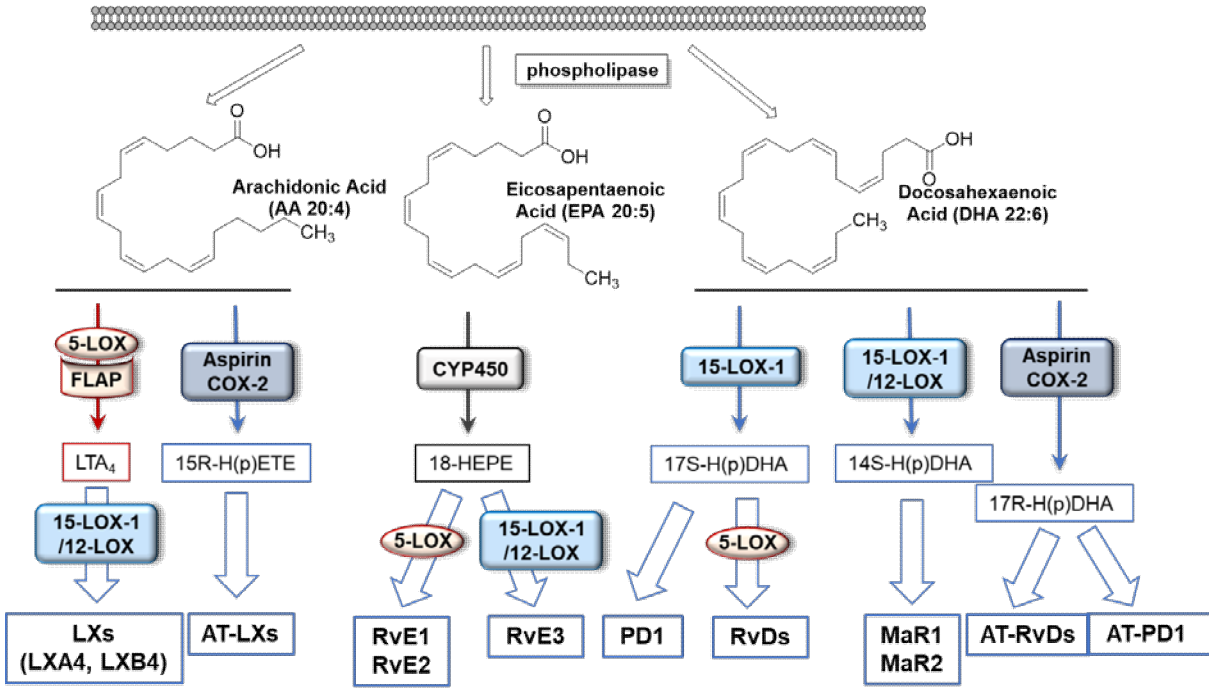

Fig.1.3 The biosynthetic pathway of specialized proresolving mediators. Various bio-functional enzymes (5-LOX, FLAP, COX-2, CYP450, 15-LOX-1 and 12-LOX) catalyze the formation of different series of specialized proresolving mediators (SPMs) including lipoxins (LXs), resolvin E-series (RvEs), protectins (PDs), resolvin D-series (RvDs), maresins (MaRs) and aspirin-triggered lipoxins/resolvins/protectins (AT-LXs, AT-RvDs and AT-PD1) from fatty acid substrates (AA, EPA and DHA).

LXs and AT-LXs achieve their biological functions via binding a specific G-protein coupled receptor (GPCR) named ALX (or called FPR) [53]. In both, *in vitro* cellular systems and *in vivo* animal disease models, LXA4 and AT-LXs are actively involved in various multicellular processes in resolution of inflammation. Various *in vitro* studies indicated that LXA4 and LXA4-derivatives inhibit human neutrophils chemotaxis and transmigration and stimulates phagocytosis of apoptotic neutrophils [54-56]. *In vivo*, LXA4-derivatives treatment showed protective roles in reducing the weight loss, intestinal bleeding and overall mice mortality in a DSS-induced murine colitis [57].

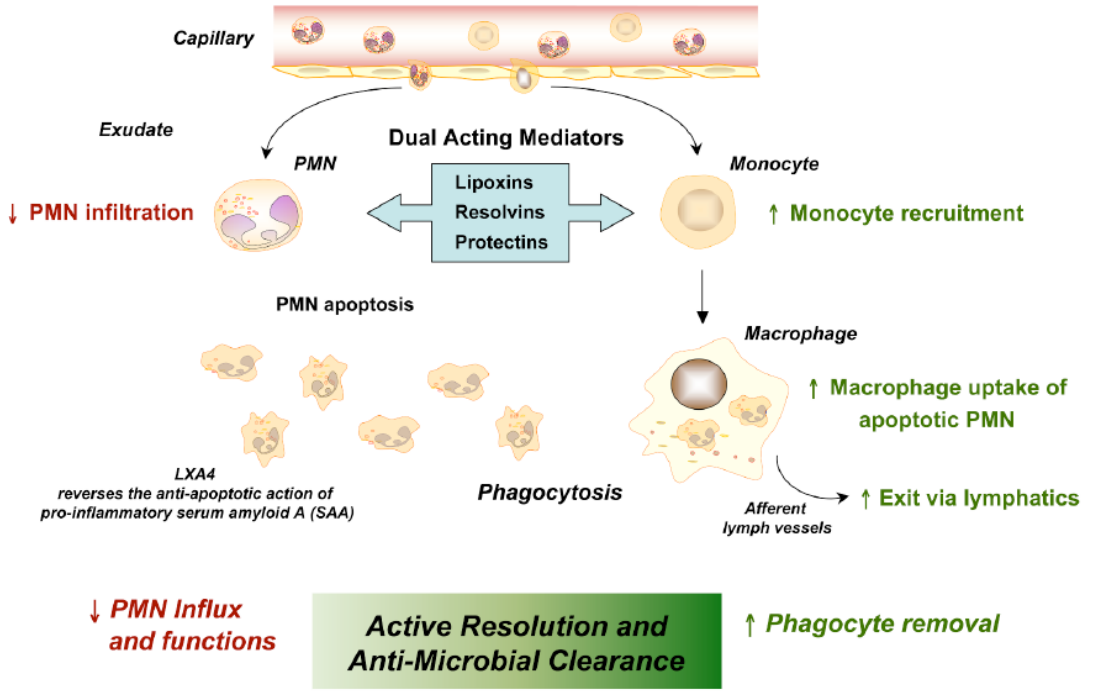

Fig.1.4 Dual anti-inflammatory and proresolving actions of specialized proresolving mediators. Specialized proresolving mediators (SPM) show dual anti-inflammatory actions including inhibition of polymorphonuclear neutrophils (PMNL) infiltration and proresolving effects including stimulation of monocyte recruitment, facilitate of macrophage phagocytosis and phagocyte removal, which help the body return to homeostasis. Figure adjusted from Serhan.CN et.al [10].

1.2.1.2 Resolvin E-series

It is well known that diets rich in essential omega-3 fatty acids including EPA and DHA are beneficial to human health, with therapeutic effects in controlling inflammation-related diseases that might even trigger cancer [58]. Several new classes of SPM derived from EPA were characterized and their connection to resolution of inflammation were investigated. Serhan et al. identified the first endogenously produced RvE1 that was proved to impede inflammation and stimulate resolution both *in vitro* and *in vivo* [59]. For the biosynthesis of EPA-derived RvEs, cytochrome P450 monooxygenase (CYP450) or aspirin-triggered acetylated COX-2 converts EPA first to 18-HEPE. Then 5-LOX catalyzes the formation of RvE1 [59] or RvE2 [60], respectively, from the mono-hydroxy precursor 18-HEPE. Alternatively, 18-HEPE can be converted by 15-LOX-1/12-LOX to RvE3 [61]. RvE2 and RvE3 exhibit potent anti-inflammatory activities by

inhibition of neutrophil chemotaxis *in vitro* and neutrophils transmigration *in vivo* in murine peritonitis [60, 61].

1.2.1.3 Resolvin D-series, protectins and maresins

In resolving exudates, other classes of SPM denoted resolvin D-series (RvDs), protectins (PDs) and maresins (MaRs) that are metabolites from DHA were discovered. For the formation of DHA derived RvDs and PDs, DHA is first metabolized to 17S-H(p)DHA by 15-LOX-1 or 17R-H(p)DHA by acetylated COX-2 [62, 63]. These intermediates are further converted to RvDs and AT-RvDs with the help of 5-LOX or to PD1 and AT-PD1 [62, 63]. RvD1 binds to ALX and GPR32 and show proresolving functions like inhibition of eosinophilia and pro-inflammatory mediators, enhancement of phagocytosis, which promotes the resolution of acute inflammation [64]. Recent reports also indicated that RvD1 is able to manipulate the polarization of macrophages by reprogramming pro-inflammatory M1 macrophages towards a proresolving phenotype [65]. Studies revealed that RvD3 and AT-RvD3 inhibit neutrophil transmigration, stimulate phagocytosis and efferocytosis and accelerate epithelial injury recovery [66, 67]. PD1 and its analogues exhibited potent anti-inflammatory and proresolving activities by blocking neutrophil transmigration and enhancing the recruitment of monocytes and lymphocytes *in vivo* in murine peritonitis [68]. Alternatively, DHA can also be converted to intermediate 14-H(p)DHA by 15-LOX-1/12-LOX. Then 14-H(p)DHA is further metabolized to its epoxy derivative and finally to MaR1 and MaR2. MaR1 and MaR2 display anti-inflammatory and proresolving actions like enhancement of human macrophage phagocytosis *in vitro* and inhibition of murine PMNL infiltration *in vivo* [69, 70].

1.3 Monocytes and macrophages

1.3.1 Monocytes

Monocytes are myeloid cells that develop in the bone marrow, circulate in the peripheral blood and migrate to specific tissues during inflammation [71, 72]. They further differentiate into various types of immune cells including macrophages and dendritic cells, mediated by specific cytokines or growth factors depending on the microenvironment [73]. For example, dendritic cells can be achieved from monocytes upon stimulation of granulocyte/macrophage colony-stimulating factor (GM-CSF) and interleukin-4 (IL-4) [74]. Monocytes can also differentiate to M1 macrophages in presence of interferon gamma (IFN-γ) and lipopolysaccharide (LPS) or to M2 macrophages after IL-4/IL-13 stimulation [75].

Human primary monocytes can be subdivided into several subsets based on their antigenic surface markers CD14 and CD16 expression. $CD14^{++}CD16^{-}$ monocytes are usually referred to as classical monocytes because they resemble more the original description of monocytes, which contribute around 90% of total circulating monocytes, express CCR2 and possess high phagocytic activity [76]. $CD14^{+}CD16^{+}$ monocytes are usually considered as non-classical monocytes while $CD14^{++}CD16^{+}$ monocytes are characterized as an intermediate phenotype [77]. $CD16^{+}$ monocytes represent around 10% of circulating monocytes and express higher CD32 and MHC class II [78]. These cells have been referred to as “resident” monocytes since they maintain the replenishment of tissue-resident macrophages and dendritic cells.

Murine monocytes subsets are distinguished based on their differential expression of Ly6C, CX3CR1 and CCR2. $Ly6C^{+}CX3CR1^{low}CCR2^{+}$ monocytes express high amounts of CD11c and MHC class II and resemble classical human $CD14^{high}CD16^{-}$ cells, which are larger in size and highly phagocytic [79]. They have a short circulation time in the bloodstream and are recruited to inflamed tissues upon inflammatory stimulation. During infection, recruited monocytes activate phagolysosome actions to display bacterial killing and clearance functions and stimulates the production of cytokines to initiate acute inflammation [80]. $Ly6C^{-}CX3CR1^{high}CCR2^{-}$ monocytes have longer circulation periods in bloodstream and resemble $CD14^{+}CD16^{+}$ human monocytes, which are smaller in size. They circulate in the peripheral blood, return to the bone

marrow, differentiate and constitutively replenish the tissue-resident macrophages and dendritic cells under homeostasis [79].

1.3.2 Macrophages

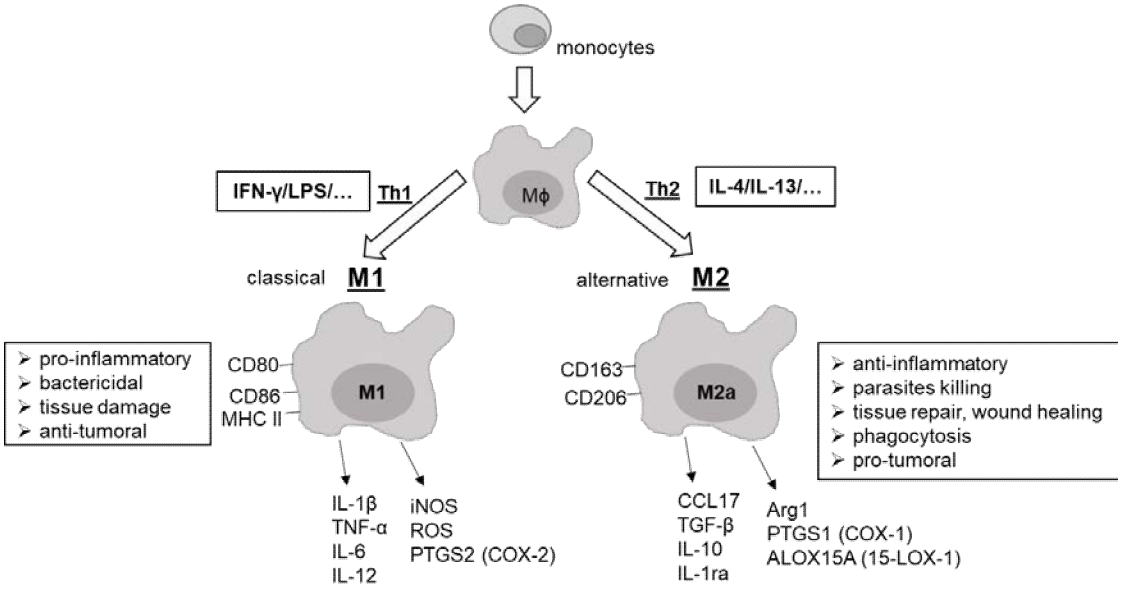

Fig.1.5 M1 and M2 macrophage polarization. Classical activated (M1) macrophages (stimulated by LPS and IFN-γ) and alternative activated (M2) macrophages (M2a stimulated in presence of IL-4 or IL-13) display distinct roles with different surface marker expression, cytokines release and gene expression.

Macrophages as prominent immune cells are widely distributed in tissues. These adult tissue macrophages were thought to be derived from circulating monocytes but recent evidence indicated that they originate mostly during embryonic development [81]. Under inflammatory conditions, circulating monocytes infiltrate from peripheral blood to inflamed tissues and polarize to macrophages [71]. Both the tissue resident macrophages and recruited monocyte-derived macrophages display indispensable roles in maintaining immune functions and homeostasis. Macrophages are professional antigen-presenting cells that collaborate with T and B cells [82]. They are also prominent phagocytic cells that phagocytose invaded microbe debris and apoptotic cells like apoptotic neutrophils [83].

Due to their plasticity and heterogeneity, macrophages can be polarized differently for

specific physiological functions depending on the microenvironment [84]. They are divided into two major functional phenotypes, classically activated M1 macrophages and alternative activated M2 macrophages. Basically, M1 macrophages are more pro-inflammatory and anti-tumoral in tumor milieu, while M2 macrophages are more anti-inflammatory but pro-tumoral in tumor microenvironment.

1.3.2.1 M1 macrophages

Classically activated M1 macrophages are developed from T-helper type 1 (Th1) cytokines interferon gamma (IFN-γ) and lipopolysaccharide (LPS) stimulation [85]. They are professional antigen-presenting cells with elevated expression of major histocompatibility complex II (MHC-II) [86, 87]. In addition, M1 macrophages express high levels of cluster of differentiation 86 (CD86) and CD80 [86]. Notably, they are responsible for the production of abundant pro-inflammatory cytokines like IL-12, IL-1β, IL-6 and TNF-α, and chemokines such as CCL15, CCL20, CXCL9, CXCL 10, CXCL11 and CXCL13 [75, 88].

Functionally, M1 macrophages are phagocytic cells that phagocytose apoptotic neutrophils and clear invaded bacterial or pathogen debris [89]. They coordinate with DC cells, natural killer cells and T cells to regulate immune cell recruitment in Th1 inflammatory responses [90]. M1 macrophages are characterized by increased microbicidal ability since they release nitric oxide and synthesize reactive oxygen intermediates (ROI) due to higher inducible nitric oxide synthase (iNOS) activity [91]. Classical M1 polarization with LPS and IFN-γ also upregulates the expression of COX-2 [92], the key enzyme in the biosynthesis of pro-inflammatory PGs. Upon challenge of pathogenic bacteria, classical M1 stimulation produces predominately pro-inflammatory LTs and PGs [8].

1.3.2.2 M2 macrophages

Different from the classical activated M1 macrophages, M2 macrophages are originally described as alternative activated macrophages that are stimulated by Th2 cytokines

IL-4 or IL-13 [93, 94]. Afterwards more stimuli including IL-10, transforming growth factor beta (TGF-β) and glucocorticoids were found to stimulate the alternative activation. M2 macrophages can be further divided into M2a (after IL-4 or IL-13 stimulation), M2b (by immune complexes and IL-1 or LPS stimulation) and M2c (by IL-10, TGF-β or glucocorticoids treatment) subtypes [95]. M2 macrophages are considered anti-inflammatory since they inhibit the production of pro-inflammatory mediators including TNF-α, IL-1β, IL-6, IL-12 and MCP-1 [96]. IL-4/IL-13 activated M2a macrophages express high levels of the mannose receptor CD206, several scavenger receptors including CD163 and class A scavenger receptor (SRA) [97]. They produce higher amounts of IL-1 receptor antagonist (IL-1ra) and the decoy IL-1β type II receptor (IL-1RII), which suppresses the release and activity of IL-1β [96, 98]. M2a macrophages express low levels of iNOS but high levels of arginase 1, which compromise the microbicidal function but stimulate tissue repair [99, 100]. Studies revealed that the expression of coagulation factor XIII-A (FXIIIA) and insulin like growth factor 1 (IGF-1) that are crucial for tissue regeneration, are mediated by IL-4 stimulated alternative macrophage activation instead of the classical activation [101]. M2a macrophages are also referred to as “wound healing macrophages” according to a functional classification proposed by Mooser et al. [90].

The Th2 cytokines IL-4/IL-13 stimulation stimulates the expression of M2-specific genes in various mammalian cells including human orbital fibroblasts, human endothelial cells, A549 cells, murine bone marrow derived macrophages and human peripheral blood monocytes [102-105]. In a gene analysis study, ALOX15 was characterized as the most strongly upregulated gene among all the genes regulated after IL-4/IL-13 mediated alternative stimulation of human monocytes [106]. ALOX15 displays dual pro-inflammatory and anti-inflammatory roles in inflammation. On the one hand, ALOX15 converts arachidonic acid (AA) to mono-hydroxylated metabolites 15-HETE, 12-HETE or 13-HODE, which were shown to be pro-inflammatory in various animal inflammation models [107]. Aberrant function of ALOX15 is also related to the pathogenesis of atherosclerosis [108]. On the other hand, 15-LOX-1 is involved in the biosynthesis of specialized proresolving mediators (SPM) that are actively involved in

the inflammation process [49]. Recent study revealed that IL-4-stimulated M2 macrophages possess different lipid mediator profile compared to classical activated M1 macrophages upon pathogenic bacterial stimulation [8]. Alternative stimulated M2 macrophages stimulate the production of bioactive SPM that are dual anti-inflammatory and proresolving.

There are several signaling pathways that might be involved in the regulation of 15-LOX-1 expression in IL-4/IL-13 stimulated macrophages. The classical IL-4/IL-13 stimulated 15-LOX-1 regulating pathway is the Janus kinases-signal transducer and activator of transcription 6 (JAK-STAT6) pathway. IL-4 or IL-13 stimulation binds the IL-4 receptor and activates JAK1 and JAK3, which phosphorylates STAT6 [109]. Phospho-STAT6 is then translocated to the nucleus and triggers the expression of IL-4 responsible genes including ALOX15 [110].

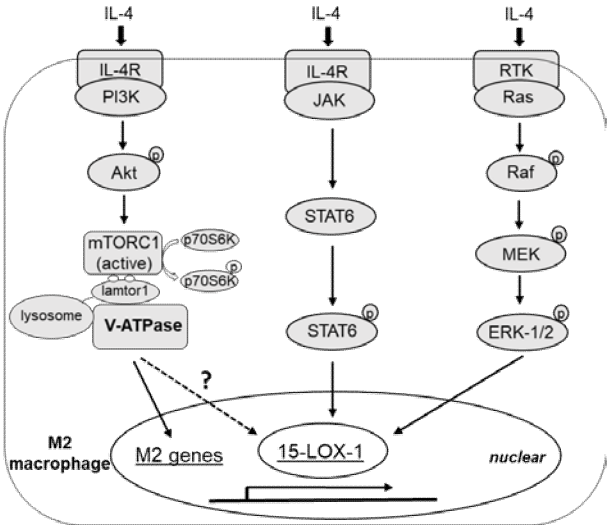

Fig.1.6 IL-4 stimulated 15-LOX-1 regulating pathway. Three signaling pathways (the JAK-STAT6 pathway, PI3K-Akt-mTORC1 pathway and the MEK/ERK-1/2 cascade) that might be involved in regulating the expression of 15-LOX-1 in IL-4 stimulated macrophages.

The PI3K-Akt-mTORC1 pathway, another pathway recognized recently, was shown to be involved in the regulation of M2-related genes expression in IL-4 stimulated bone-marrow-derived macrophages [5]. The assembly and activation of mechanistic target of rapamycin complex 1 (mTORC1) is essential for lysosomal nutrient sensing. With abundant amino acids, vacuolar H^+-ATPase (V-ATPase) interacts with the regulators and triggers the recruitment and activation of mTORC1 from the cytoplasm to the surface of lysosomes [111]. Recent study revealed that mTORC1 is involved in the regulation of IL-4 stimulated bone marrow derived macrophages polarization.

Dysfunction of mTORC1 by pharmacological interference of V-ATPase with bafilomycin blocked the expression of IL-4 triggered M2-specific genes [5]. However, the role of the PI3K-Akt-mTORC1 pathway remains to be explored in the regulation of 15-LOX-1 expression. Apart from these two pathways, Ashish Bhattacharjee et al. revealed the involvement of ERK-1/2 MAPK activity in IL-13 stimulated ALOX15 gene expression in human monocytes [112].

1.3.2.3 Tumor associated macrophages

It is well known that chronic inflammation is closely related to tumor progression. In the tumor milieu, tumor associated macrophages (TAMs) as major infiltrated inflammatory cells are present [113]. TAMs origin from both *in situ* proliferation and polarization of recruited circulating monocytes from peripheral blood [114, 115]. They contribute to the tumor milieu and were found to promote tumor growth, progression and angiogenesis in various tumor models [116-118]. TAMs resemble M2 macrophages with higher expression of anti-inflammatory IL-10 but low pro-inflammatory cytokine IL-12, which are immunosuppressive and pro-tumoral with low tumoricidal activity [119, 120]. TAMs release various cytokines and chemokines into the tumor environment, with higher levels of anti-inflammatory IL-10, CD163, VEGF and TGF-β. High levels of IL-10 and TGF-β were found to suppress dendritic cells (DCs) differentiation and maturation [121]. As anti-cancer therapy, novel strategies have been focused on reprogramming the TAMs to pro-inflammatory but anti-tumoral M1 macrophages in tumor milieu [122-124].

1.4 V-ATPase

The Vacuolar H^+-ATPase (V-ATPase) is an ATP-dependent proton pump, which has been recognized to play fundamental roles in maintaining pH homeostasis in various cell organelles in almost all eukaryotic organisms [125].

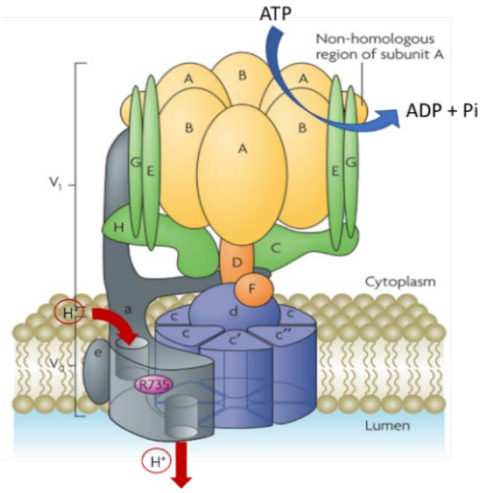

Fig.1.7 The structure of V-ATPase. V-ATPase is composed of two major domains, V0 (six subunits: a, c, c′, c″, d, and e) and V1 (eight subunits: A, B, C, D, E, F, G and H). V1 domain participates in ATP hydrolysis, which drives the rotation of central stalk D-F-d and proteolipid ring (c, c′ and c″). Rotation of the proteolipid ring in V0 triggers the proton transportation. Figure modified from Forgac et.al [4].

1.4.1 Structure of V-ATPase

The structure of V-ATPase is highly conserved in plants, animals and fungi [126]. Structurally, V-ATPase is a complex composed of two different domains with multiple subunits [127]. In detail, V-ATPase is composed of two domains V0 and V1. Anchored into the cytoplasm membrane, the transmembrane V0 domain is composed of six subunits (a, c, c′, c″, d, and e in yeast) [128]. Subunits c, c′ and c″ form a rotatory ring structure connected to subunits a, d and e [129]. The V1 domain includes eight subunits (A, B, C, D, E, F, G and H) and is located at the peripheral areas of the cytoplasm membrane [4]. The core structure of the V1 domain is a symmetric hexametric structure composed of subunits A and B [130]. The connection of the V1 domain and the V0 domain are accomplished by multiple stalks that are arranged around the hexametric A-B structure. These stalks include a central stalk D-F-d, peripheral stalks G-E-H, peripheral stalks G-E-C and the N-terminal of V0a. V-ATPase operates its proton-translocating function by a rotary mechanism driven by ATP binding and hydrolysis in the V1 domain, which cause the rotation of central stalk D-F-d as well as the connected proteolipid ring in the V0 domain. Rotation of the proteolipid ring then further activates proton transportation from the cytoplasm into the lumen or organelles in V0a [127, 129].

1.4.2 Biological function of V-ATPase

V-ATPase is functional within the membranes of various organelles (like lysosomes, endosomes and Golgi apparatus) and regulates multiple cellular processes [4]. The ATP-driven proton pump is fundamental for pH homeostasis of intracellular compartments that is crucial for various biological functions. The complete function of endosomes, lysosomes and phagolysosomes that are responsible for degradation of internalized extracellular materials as well as protein depend largely on the acidic pH environment maintained by the membrane V-ATPases [131, 132]. Autophagosomes and lysosomes mediate autophagy during which cellular dysfunctional components are degraded and recycled in order to maintain energy homeostasis [133]. V-ATPases also mediate the entry of pathogens, toxins or viruses into the cells. This process is mediated by the endosomal compartments, where the acidic pH facilitates membrane pores formation that allows entry of viral mRNA or toxins into the cytosol [134]. In our previous work, the role of V-ATPase in cytokines trafficking and secretion in human monocytes was investigated [6]. Inhibition of V-ATPase lowered the cytosolic pH but elevated the lysosomal pH and triggered endoplasmic reticulum (ER) stress, which is responsible for the accumulation of cytokines like IL-8 in ER [6]. Additionally, V-ATPase is also located at the plasma membrane in some specialized cells like renal cells, neutrophils, macrophages and osteoclasts. Plasma membrane V-ATPase is critical in maintaining cellular functions like bone resorption [135], renal acidification [136], sperm maturation [137] and neurotransmission [138]. Moreover, V-ATPases are key components and regulators of various signaling pathways including the Notch signaling, Wnt signaling and mTORC pathway [139]. In a pH-dependent manner, V-ATPase acidifies the endosomes and lysosomes and maintains low pH environment that is favorable for Notch signaling and Wnt signaling [140]. Both pathways are critically involved in cellular processes like organ development, cell proliferation and differentiation. In a pH-independent manner, V-ATPase is required in the assembly and activation of mechanistic target of rapamycin complex 1 (mTORC1) that is responsible for lysosomal nutrient sensing, protein synthesis and cell growth [141, 142].

Due to the indispensable biological roles of V-ATPase in cellular homeostasis, dysfunction or abnormal function of V-ATPase contributes to pathogenesis of diseases.

For example, the development of neurodegenerative diseases is closely related to defective lysosome function, which depends on the lysosome membrane V-ATPase machinery [143]. Intensive studies have focused on the role of V-ATPase in cancer development. Overexpression of membrane V-ATPase and particular V-ATPase subunits are detected in various cancers [144]. In tumor cells, plasma membrane V-ATPase maintains high intracellular pH that supports tumor growth and acidic extracellular environment that contributes to angiogenesis [7].

1.4.3 Pharmacological targeting V-ATPase

V-ATPase is overexpressed in tumor cells and supports tumor cells survival and angiogenesis. Additionally, tumor cells exhibit higher sensitivity to V-ATPase inhibition. Therefore, V-ATPase is characterized as interesting target for anti-cancer therapy [145]. Although not applied in clinic yet, various V-ATPase inhibitors have been developed and intensively studied for potential therapeutic purposes. In 1984, researchers characterized several new types of macrolide antibiotics including the bafilomycin derivatives and concanamycin derivatives from streptomyces [146-148]. These two new sets of antibiotics bear similar structures with a 16- or 18-membered lactone ring. Four years later, bafilomycin A1 was characterized as the first specific inhibitor of membrane V-ATPase from microorganisms, plant cells and animals [149]. Later in 1993, structure-activity relationship (SAR) studies revealed that the concanamycin derivatives were also specific inhibitors of V-ATPase [150, 151]. Both bafilomycin and concanamycin derivatives inhibits the V-ATPase activity at concentrations in the nanomolar (nM) range. Intensive studies uncovered the potential binding sites of bafilomycin and concanamycin. They bind the V0c subunit of V-ATPase and inhibit the V-ATPase function via blocking the rotatory machinery for proton transportation [152-155].

Between 1997 and 1999, researchers characterized another series of V-ATPase inhibitors from various species like murine sponge, murine tunicate, microorganisms and myxobacterium. These natural compounds are referred to as salicylihalamides,

lobatamides, oximidines and apicularens, bearing a common benzolactone enamide structure [156-159]. They show potent inhibitory effects against V-ATPase from various sources except the fungal V-ATPase at a concentration of nanomolar (nM) range [160-162]. Recently, apicularen was confirmed to bind the vicinity areas between subunit a and c of V0 domain of V-ATPase, which is a little different from the binding sites of bafilomycin and concanamycin [163].

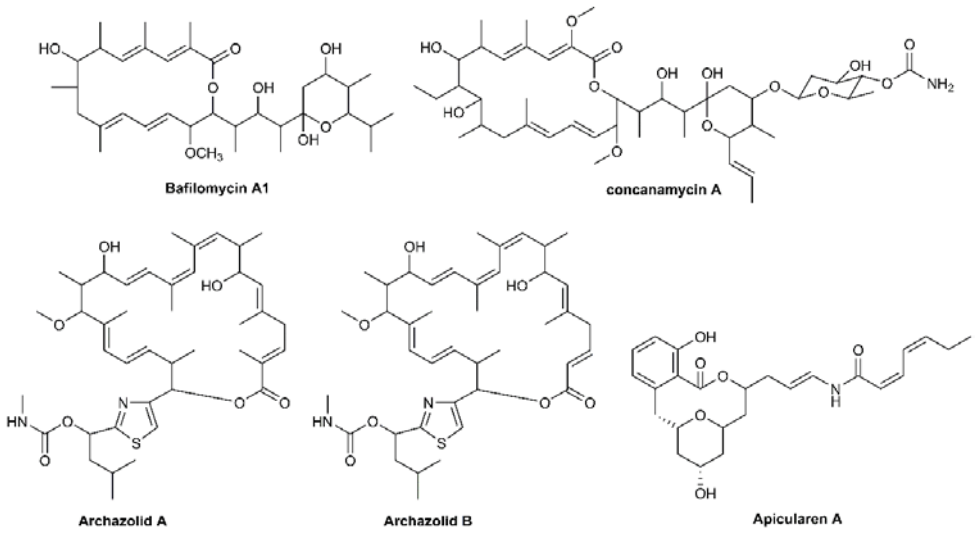

Fig.1.8 Structure of V-ATPase inhibitors Bafilomycin A1, concanamycin A, Archazolid A/B and Apicularen A.

Recently discovered from myxobacteria *Archangium gephyra* and *Cystobacter violaceus*, the archazolid derivatives represent a new class of antibiotics that target V-ATPase [164, 165]. Structurally, archazolid derivatives carry a macrocyclic lactone ring with a thiazole side chain. They are potent V-ATPase inhibitors that inhibit the activity of isolated V-ATPase enzyme and lysosomal acidification in *in vitro* cellular assays at nM range [162]. SAR studies reveal that among all archazolid derivatives that target V-ATPase, archazolid A (ArchA) and archazolid B (ArchB) are the most potent ones. These two compounds inhibit isolated V-ATPase enzyme activity with IC_{50} < 10 nM [166]. Recently, the binding site of archazolid was characterized, it binds proteolipid c ring in the V0 domain of V-ATPase, which overlaps the sites for bafilomycin and concanamycin [167].

2. AIM OF THESIS

Monocytes and macrophages as main innate immune cells play important roles in host defense during infectious inflammation. Depending on their phenotype, monocytes and M1 macrophages produce mainly pro-inflammatory PGs and LTs, while M2 macrophages produce predominantly 15-LOX-1-related LM and SPM. Acute inflammation is governed by the production of pro-inflammatory PGs and LTs. Excessive production of PGs and LTs maintains acute inflammation to a chronic state, which is related to the pathogenesis of various diseases. The resolution of inflammation is an active process governed by anti-inflammatory and proresolving SPM. Previously the role of V-ATPase in modulating cytokines release was elucidated in human primary cells. Recently V-ATPase was shown to be involved in the regulation of IL-4 stimulated polarization of murine bone-marrow-derived macrophage. However, how V-ATPase regulates human monocytes function, M1 and M2 macrophages polarization with particular respect to LM remained elusive. Therefore, we here aimed to reveal the role of V-ATPase in the regulation of LM biosynthesis in human monocytes and during human M1 and M2 macrophage polarization.

Specific objectives:

1. Explore the role of V-ATPase on LM biosynthetic pathways especially eicosanoids biosynthesis in human monocytes (**manuscript I**).
2. Explore the role of V-ATPase on the biosynthesis of inflammation-related mediators including cytokines and eicosanoids in human M1 macrophages (**manuscript II**).
3. Investigate the anti-tumoral effects of ArchA treated M1 macrophages in a microfluidically-supported tumor biochip model (**manuscript II**).
4. Uncover the role of V-ATPase on lipid mediator (LM) profile and LM biosynthetic enzyme expression in human M1 and M2 macrophages (**manuscript III**).
5. Study the signaling pathways involved in the abrogation of 15-LOX-1 by V-ATPase inhibition in human M2 macrophages (**manuscript III**).

3. MANUSCRIPTS

Manuscript I

Rao Z, Jordan PM, Wang Y, Menche D, Pace S, Gerstmeier J, and Werz O. (2019). "Differential role of V-ATPase for expression and activity of cyclooxygenase-2 in human monocytes." Submitted.

Manuscript II

Thomas L, **Rao Z**, Gerstmeier J, Raasch M, Weinigel C, Rummler S, Menche D, Müller R, Pergola C, Mosig A, Werz O. (2017). "Selective upregulation of TNFalpha expression in classically-activated human monocyte-derived macrophages (M1) through pharmacological interference with V-ATPase." Biochem Pharmacol **130**: 71-82.

Manuscript III

Rao Z, Pace S, Jordan PM, Bilancia R, Troisi F, Börner F, Andreas N, Kamradt T, Menche D, Rossi A, Serhan CN, Gerstmeier J, Werz O. (2019). "Vacuolar (H^+)-ATPase Critically Regulates Specialized Proresolving Mediator Pathways in Human M2-like Monocyte-Derived Macrophages and Has a Crucial Role in Resolution of Inflammation." J Immunol **203**(4): 1031-1043.

3.1 Manuscript I

Differential role of vacuolar (H^+)-ATPase in the expression and activity of cyclooxygenase-2 in human monocytes

Zhigang Rao, Paul M. Jordan, Yan Wang, Simona Pace, Dirk Menche, Jana Gerstmeier and Oliver Werz (2019) Submitted.

In this paper, we presented a differential role of V-ATPase in the expression and in the activity of COX-2 in human monocytes. Pharmacological targeting of V-ATPase elevated the expression of COX-2 protein in LPS-stimulated primary monocytes, which was paralleled by enhanced phosphorylation of p38 MAPK and ERK-1/2, with no significant impact on NF-κB and SAPK/JNK pathways. Targeting of both p38 MAPK and ERK-1/2 pathways with specific inhibitors showed that these kinase pathways are crucial for COX-2 expression in human monocytes. Despite elevated COX-2 protein levels, however, blockade of V-ATPase activity impaired the biosynthesis of COX-derived lipid mediators in monocytes without affecting 12-/15-lipoxygenase (LOX) products with minor suppression of 5-LOX activity, assessed by a metabololipidomics approach using UPLC-MS-MS analysis. Manipulation of the intracellular pH with pH modulators chloroquine confirms the contribution of changes of intracellular pH for COX-2 activity. Our data suggest contrasting roles of V-ATPase on the expression and in the activity of COX-2. On one hand V-ATPase restricts COX-2 protein levels by limiting p38 MAPK and ERK-1/2 activation, while on the other hand it governs the cellular activity of COX-2 through appropriate adjustment of the intracellular pH.

Contribution (75%): Cell culture and performance of blood cell isolation, determination of cell viability and cytokine levels, flow cytometry, SDS-PAGE and Western Blot, UPLC-MS-MS, analysis of data and preparation of graphs, analysis of statistics, co-writing of the manuscript.

Differential role of vacuolar (H^+)-ATPase in the expression and activity of cyclooxygenase-2 in human monocytes

Zhigang Rao[*], Paul M. Jordan[*], Yan Wang[*], Dirk Menche[†], Simona Pace[*], Jana Gerstmeier[*#] and Oliver Werz[*#]

[*]Department of Pharmaceutical/Medicinal Chemistry, Institute of Pharmacy, Friedrich-Schiller-University Jena, Philosophenweg 14, D-07743 Jena, Germany. E-mail addresses: zhigang.rao@uni-jena.de; paul.jordan@uni-jena.de; yan.wang18@stjohns.edu; simona.pace@uni-jena.de; jana.gerstmeier@uni-jena.de; oliver.werz@uni-jena.de.

[†]Kekulé-Institut für Organische Chemie und Biochemie der Rheinischen Friedrich-Wilhelms-Universität Bonn, D-53121, Bonn, Germany; E-mail address: dirk.menche@uni-bonn.de.

[#]**Corresponding authors:** Prof. Dr. Oliver Werz, Chair of Pharmaceutical/ Medicinal Chemistry, Institute of Pharmacy, Friedrich Schiller University Jena, Philosophenweg 14, D-07743 Jena, Germany; Phone: +49-03641-949801; Fax: +49-03641-949802; E-mail: oliver.werz@uni-jena.de; Dr. Jana Gerstmeier, Department of Pharmaceutical/Medicinal Chemistry, Institute of Pharmacy, Friedrich-Schiller-University Jena, Philosophenweg 14, D-07743 Jena, Germany; Phone: +49-03641-949829; Fax: +49-03641-949802; E-mail: jana.gerstmeier@uni-jena.de.

Abstract

Monocytes as professional immune cells produce abundant levels of pro-inflammatory eicosanoids including prostaglandins and leukotrienes during inflammation. Vacuolar (H^+)-ATPase (V-ATPase) is critically involved in a variety of inflammatory processes including cytokine trafficking and lipid mediator biosynthesis. However, its role in eicosanoid biosynthetic pathways in monocytes remain elusive. In this study, we presented a differential role of V-ATPase in the expression and in the activity of COX-2 in human monocytes. Pharmacological targeting of V-ATPase increased the expression of COX-2 protein in lipopolysaccharide-stimulated primary monocytes, which was paralleled by enhanced phosphorylation of p38 MAPK and ERK-1/2, without impacting the NF-κB and SAPK/JNK pathways. Targeting of both p38 MAPK and ERK-1/2 pathways showed that the kinase pathways are crucial for COX-2 expression in human monocytes. Despite increased COX-2 protein levels, however, suppression of V-ATPase activity impaired the biosynthesis of COX-related lipid mediators in monocytes without

affecting 12-/15-lipoxygenase (LOX) products and minor suppression of 5-LOX activity, assessed by a metabololipidomics approach using UPLC-MS-MS analysis. Our results indicate that changes in the intracellular pH may contribute to suppression of COX-2 activity. Our data suggest that V-ATPase on one hand restricts COX-2 protein levels by limiting p38 MAPK and ERK-1/2 activation, while on the other hand it governs the cellular activity of COX-2 through appropriate adjustment of the intracellular pH.

Keywords: Vacuolar (H^+)-ATPase, cyclooxygenase, prostaglandin, p38 MAPK, ERK-1/2, intracellular pH

Abbreviations:

AA, arachidonic acid; ArchA, archazolid A; COX, cyclooxygenase; $cPLA_2$, cytosolic phospholipase A_2; CYP, cytochrome P450; DHA, docosahexaenoic acid; EPA, eicosapentaenoic acid; ERK, extracellular signal-regulated protein kinase; FLAP, 5-lipoxygenase-activating protein; HDHA, hydroxy-DHA; HETE, hydroxyeicosatetraenoic acid; HEPE, hydroxy-EPA; LM, lipid mediator; LPS, lipopolysaccharide; LOX, lipoxygenase; LT, leukotriene; MEK, mitogen-activated protein kinase kinase; p38 MAPK, p38 mitogen-activated protein kinase; PBMC, peripheral blood mononuclear cells; PG, prostaglandin; SAPK/JNK, stress-activated protein kinase/c-Jun N-terminal kinase; TLR, toll-like receptors.

1. Introduction

Monocytes are professional innate immune cells that circulate in the bloodstream and traffic into specific tissues upon recruitment to evoke pivotal roles in the immune defense [1]. Upon challenges like bacterial infection, monocytes produce abundant levels of pro-inflammatory eicosanoids including prostaglandins (PG) and leukotrienes (LT) that maintain the inflammatory microenvironment and promote neutrophil chemotaxis [2]. Excessive and persistent production of pro-inflammatory eicosanoids sustain acute inflammation that turns into a chronic state which is closely related to various diseases including rheumatoid arthritis, diabetes, asthma, Alzheimer or cancer [3]. Therefore, targeting the eicosanoid biosynthetic pathway by suppression of PG and LT the production has emerged as promising strategy to limit the undesired shift from acute to chronic inflammation. The biosynthesis of eicosanoids involves key enzymes including cyclooxygenase (COX) to initiate the production of PG and 5-lipoxygenase (5-LOX), the enzyme responsible for initiation of LT biosynthesis. For COX, two isoforms exist, namely COX-1 and COX-2 [4]. While COX-1 is constitutively expressed in most cells and tissues, COX-2 is an inducible enzyme whose expression is induced by various proinflammatory stimuli (i.e. LPS, TNF-α and IL-1β), and which is responsible for excessive PG formation during inflammation [5]. Thus, various anti-inflammatory drugs including non-

steroidal anti-inflammatory drugs (NSAIDs) have been developed to inhibit COX-2 activity [6-8].

Interestingly, our previous work showed that inhibition of V-ATPase activity caused increased COX-2 expression and formation of COX-derived PG in human M1-like monocyte-derived macrophages (MDM) [9], indicating a detrimental role of V-ATPase for COX-2 biology. V-ATPase is a universal proton pump that is crucial for intracellular pH homeostasis, entry of pathogens, toxins or viruses, and protein degradation in various cell organelles in almost all eukaryotic organisms [10]. V-ATPase pumps protons from the cytosol especially into late endosomes and lysosomes, which serve as major intracellular proton stores with acidic pH [11]. Therefore, V-ATPase contributes to the establishment and maintenance of the reversed pH gradient by elevating the pH in the cytosol while the pH in lysosomes is decreased. Inhibition of V-ATPase elevated TNF-α production, which facilitates the anti-tumoral activities of M1-like MDM [12], while in human M2-like MDM, V-ATPase critically regulates the inflammatory resolution pathway [12]. However, how V-ATPase regulates biosynthesis of lipid mediators (LM) especially the eicosanoid biosynthetic pathway in human monocytes remained elusive. Here, we reveal contrasting roles of V-ATPase in regulating the expression and activity of COX-2 in LPS-stimulated human monocytes: while V-ATPase may limit LPS-induced COX-2 protein levels in a p38 MAPK- and ERK-1/2-dependent manner, it is required for efficient biosynthesis of COX-related PGs.

2. Materials and Methods

2.1. Reagents

Deuterated and non-deuterated LM standards for ultra-performance liquid chromatography-tandem mass spectrometry (UPLC-MS-MS) quantification were purchased from Cayman Chemical/Biomol GmbH (Hamburg, Germany). Archazolid A was isolated from *Archangium gephyra* as previously described. Apicularen A was from the natural compound library of HZI/HIPS (Braunschweig, Germany). Skepinone-L was purchased from Cayman Chemical (Ann Arbor, MI), and U0126 was from Enzo Life Sciences (Farmingdale, NY). Bafilomycin A1, chloroquine, dexamethasone, lipopolysaccharide (LPS) and all other reagents were obtained from Sigma-Aldrich (Taufkirchen, Germany) unless mentioned otherwise.

2.2. Methods

2.2.1. Cell isolation and incubation of human monocytes

Freshly prepared leukocyte concentrates from withdrawn peripheral blood of male and female healthy adult donors (age 18-65 years) were provided by the Institute of Transfusion Medicine at the University Hospital Jena, Germany. The experimental protocol was approved by the ethical committee of the University Hospital Jena. All methods were performed in accordance with the relevant guidelines and regulations. PBMC were separated using dextran sedimentation, followed by centrifugation on lymphocyte

separation medium (Histopaque®-1077, Sigma-Aldrich). PBMC were seeded in RPMI 1640 (Sigma-Aldrich) containing 10% (v/v) heat-inactivated FCS, 100 U/mL penicillin, and 100 µg/mL streptomycin in cell culture flasks (Greiner Bio-one, Frickenhausen, Germany) for 1.5 h at 37 °C and 5% CO_2 for adherence of monocytes. Human monocytes were collected and incubated in RPMI 1640 (Sigma-Aldrich) containing 5% (v/v) heat-inactivated FCS, 100 U/mL penicillin, and 100 µg/mL streptomycin in well plates (Greiner Bio-one, Frickenhausen, Germany).

2.2.2. Analysis of human monocytes for LM metabololipidomics

Human primary monocytes (2×10^6/mL) were incubated in PBS containing 1 mM $CaCl_2$. To evoke LM biosynthesis pathogenic *E. coli* (serotype O6:K2:H1, ratio 1:50) was added for 180 min at 37 °C. The supernatants were then transferred to 2 mL of ice-cold methanol containing 10 µL of deuterium-labeled internal standards (200 nM d8-5S-HETE, d4-LTB_4, d5-LXA_4, d5-RvD2, d4-PGE_2 and 10 µM d8-AA) to facilitate quantification and sample recovery. Sample preparation was conducted by adapting published criteria [13]. In brief, samples were kept at −20 °C for 60 min to allow protein precipitation. After centrifugation (1200 g, 4 °C, 10 min) 8 mL acidified H_2O was added (final pH = 3.5) and samples were subjected to solid phase extraction. Solid phase cartridges (Sep-Pak® Vac 6cc 500 mg/ 6 mL C18; Waters, Milford, MA) were equilibrated with 6 mL methanol and 2 mL H_2O before samples were loaded onto columns. After washing with 6 mL H_2O and additional 6 mL *n*-hexane, LM were eluted with 6 mL methyl formate. Finally, the samples were brought to dryness using an evaporation system (TurboVap LV, Biotage, Uppsala, Sweden) and resuspended in 100 µL methanol-water (50/50, v/v) for UPLC-MS-MS automated injections. LM profiling was analyzed with an Acquity UPLC system (Waters, Milford, MA, USA) and a QTRAP 5500 Mass Spectrometer (ABSciex, Darmstadt, Germany) equipped with a Turbo V™ Source and electrospray ionization. LM were eluted using an Acquity UPLC BEH C18 column (1.7 µm, 2.1 × 100 mm; Waters, Eschborn, Germany) at 50 °C with a flow rate of 0.3 mL/min and a mobile phase consisting of methanol-water-acetic acid of 42:58:0.01 (v/v/v) that was ramped to 86:14:0.01 (v/v/v) over 12.5 min and then to 98:2:0.01 (v/v/v) for 3 min [14]. The QTrap 5500 was operated in negative ionization mode using scheduled multiple reaction monitoring coupled with information-dependent acquisition. The scheduled multiple reaction monitoring window was 60 sec, optimized LM parameters (CE, EP, DP, CXP) were adopted [15], and the curtain gas pressure was set to 35 psi. The retention time and at least six diagnostic ions for each LM were confirmed by means of an external standard (Cayman Chemical/Biomol GmbH, Hamburg, Germany). Quantification was achieved by calibration curves for each LM.

2.2.3. SDS-PAGE and Western blot

Cell lysates of human monocytes, corresponding to 2×10^6 cells, were separated on 8% (for cPLA$_2$-α), 10% (for 5-LOX, COX-

1, COX-2, ERK-1/2, phospho-ERK-1/2, p38 MAPK, phospho-p38 MAPK, NF-κB, phospho-NF-κB, JNK, phospho-JNK, β-actin and GAPDH) and 16% (for FLAP) polyacrylamide gels, and blotted onto nitrocellulose membranes (Amersham Protran Supported 0.45 µm nitrocellulose, GE Healthcare, Freiburg, Germany). The membranes were incubated with the following primary antibodies: rabbit polyclonal anti-cPLA$_2$-α, 1:1000 (2832S, Cell Signaling, MA); rabbit polyclonal anti-5-LOX, 1:1000 (to a peptide with the C-terminal 12 amino acids of 5-LOX: CSPDRIPNSVA; kindly provided by Dr. Marcia E. Newcomer, Louisiana State University, LA); rabbit polyclonal anti-COX-1, 1:1000 (4841S, Cell Signaling); rabbit polyclonal anti-COX-2, 1:1000 (4842S, Cell Signaling); rabbit monoclonal anti-ERK1/2, 1:1000 (4695S, Cell Signaling); mouse monoclonal anti-phospho-ERK1/2 (Thr202/Tyr204), 1:1000 (9106, Cell Signaling); rabbit monoclonal anti-p38 MAPK, 1:1000 (8690S, Cell Signaling); rabbit polyclonal anti-phospho-p38 MAPK (Thr180/Tyr182), 1:1000 (9211S, Cell Signaling); rabbit monoclonal anti-NF-κB p65 (C22B4), 1:1000 (4764S, Cell Signaling); mouse monoclonal anti-phospho-NF-κB (Ser536), 1:1000 (13346S, Cell Signaling); rabbit monoclonal anti-phospho-SAPK/JNK (Thr183/Tyr185), 1:1000 (4668S, Cell Signaling); rabbit polyclonal anti-SAPK/JNK, 1:1000 (9252S, Cell Signaling); rabbit polyclonal anti-FLAP, 1:1000 (ab85227, Abcam); mouse monoclonal anti-β-actin, 1:1000 (3700S, Cell Signaling); rabbit polyclonal anti-β-actin, 1:1000 (4967S, Cell Signaling) and rabbit monoclonal anti-GAPDH, 1:1000 (5174S, Cell Signaling). Immunoreactive bands were stained with IRDye 800CW Goat anti-Mouse IgG (H+L), 1:10,000 (926-32210, LI-COR Biosciences, Lincoln, NE), IRDye 800CW Goat anti-Rabbit IgG (H+L), 1:15,000 (926-32211, LI-COR Biosciences) and/or IRDye 680LT Goat anti-Mouse IgG (H+L), 1:40,000 (926-68020, LI-COR Biosciences), and visualized by an Odyssey infrared imager (LI-COR Biosciences). Data from densitometric analysis were background-corrected.

2.2.4. Determination of cytokine levels

Human monocytes were treated with compounds or vehicle (0.1% DMSO) 30 min before cells were stimulated with LPS (100 ng/mL) for 24 h. For measurement of extracellular cytokine levels, cell supernatants were collected by centrifugation (15,000 rpm, 4 °C, 5 min). The cytokines IL-6, IL-10, IL-1β and TNFα were analyzed using in-house made ELISA kits of (R&D system, Bio-Techne, MN).

2.2.5. Flow cytometry

Fluorescent staining for flow cytometric analysis of monocytes was performed in FACS buffer (PBS with 0.5% BSA, 2 mM EDTA and 0.1% sodium azide). Monocytes were treated with 100 ng/mL LPS and with either 10 nM ArchA or 10 nM bafilomycin for 24 h at 37 °C. Subsequently, monocytes were stained with fluorochrome-labelled antibody mixtures at 4 °C for 20 min. Non-specific antibody binding was blocked by using mouse serum for 10 min at 4°C prior antibody staining. The following antibody was used: FITC anti-human CD14 (2

µg/test, clone M5E2, Biolegend, San Diego, CA). To determine cell viability, monocytes were detached after the respective treatment with PBS plus 0.5% BSA, 5 mM EDTA and 0.4% lidocaine for 20 min. Cells were resuspended in 300 µL FACS buffer containing propidium iodide staining solution (40 ng/test, eBioscience, San Diego, CA). Upon staining, monocytes were assessed using BD LSR Fortessa (BD Bioscience), and data analyzed using FlowJo X Software (BD Bioscience).

2.2.6. Statistical analyses

Results are expressed as mean ± S.E.M. of n observations, where n represents the number of experiments with separate donors performed on different days as indicated. Analyses of data were conducted using GraphPad Prism 8 software (San Diego, CA). Paired *t*-test was used for comparison of two groups. For multiple comparisons, ANOVA with Bonferroni or Dunnett post hoc tests were applied as indicated. The criterion for statistically significant is $p < 0.05$.

3. Results

3.1. Targeting of V-ATPase in human monocytes blocks formation of COX-derived lipid mediators

We used the well-established V-ATPase inhibitor archazolid A (ArchA, [16]) at 3-100 nM as chemical tool to study the role of V-ATPase in the biosynthesis of lipid mediators (LM) in human monocytes. Previous studies of ArchA and the V-ATPase inhibitors bafilomycin and apicularen revealed direct inhibition of 5-LOX and mPGES-1 by ArchA at fairly high concentrations (> 5 µM) but clearly excluded direct inhibition of COX-1 and COX-2 by ArchA in cell-free assays [17]. Human monocytes, freshly isolated from peripheral blood of healthy volunteers, were pretreated with ArchA (3, 10, 30 or 100 nM) for 15 min prior stimulation with LPS. 24 h after LPS addition, high levels of prostanoids (PGD_2, PGE_2, PGF_2-α, TXB_2) were detected in the supernatant of the monocyte cultures in the absence of ArchA, which were clearly reduced when cells were pretreated with ArchA in a concentration-dependent manner (**Fig. 1B**). Dexamethasone, used as positive control, strongly abolished prostanoid formation (**Fig. 1B**) as expected [18]. Next, the monocytes were harvested after 24 h treatment with LPS in the absence or presence of ArchA, and then incubated for 90 min with pathogenic *E. coli* (serotype O6:K2:H1, ratio 1:50) as stimulus to provoke marked LM biosynthesis. LM metabololipidomics using UPLC-MS-MS revealed strong formation of COX-derived prostanoids as well as of 5-LOX- and 12/15-LOX-derived products (**Fig. 1C**). In monocytes that had been pretreated with ArchA prior to LPS, the biosynthesis of COX-derived prostanoids, i.e., PGE_2, PGD_2, PGF_2-α and TXB_2 was strongly reduced (**Fig. 1C**), whereas formation of 5-LOX-derived products (e.g. LTB_4, t-LTB_4 and 5-HETE) was only slightly influenced by ArchA treatment and the release of fatty acids and of other LOX-derived LM like 17-HDHA, 14-HDHA, 12-HETE, 12-HEPE or 4-HDHA was unchanged (**Fig. 1C**). Again, for cells that received dexamethasone prior LPS,

PG biosynthesis was strongly suppressed without marked impairment of LOX-derived LM (**Fig. 1C**).

To explore the role V-ATPase in prostanoid formation in other relevant cellular models, we investigated the effects of ArchA on PGE_2 production in human whole blood using different stimuli. Pretreatment with ArchA for 24 hrs also blocked PGE_2 biosynthesis in LPS-stimulated human whole blood (**Fig. 1D**). To confirm the on-target effects of ArchA and thus the role of V-ATPase, we investigated the two structurally different V-ATPase inhibitors bafilomycin [19] and apicularen [20] for their influence of the LM profile in human primary monocytes. Both compounds caused comparable effects as ArchA and significantly blocked the biosynthesis of COX-derived LM during 24 h treatment with LPS as well as in LPS-treated monocytes that were subsequently challenged with *E. coli* (**Fig. 2A, B**). Again, formation of LOX-derived LM were not or less affected by the V-ATPase inhibitors (**Fig. 2 B**). Together, we show that pharmacological targeting of V-ATPase efficiently blocks the biosynthesis of prostanoids in human monocytes and other COX-2-expressing cells with minor effects on LOX-derived LM formation.

3.2. Targeting of V-ATPase enhances COX-2 expression in human monocytes

Our results prompted us to investigate how suppression of V-ATPase activity would impact the expression of biosynthetic enzymes involved in LM formation in human monocytes. Surprisingly, targeting of V-ATPase by ArchA, bafilomycin or apicularen strongly elevated LPS-induced COX-2 expression in human primary monocytes within 24 h (**Fig. 3A, C**). In contrast, blockade of V-ATPase by ArchA had little impact on the expression of other LM biosynthetic enzymes/proteins such as COX-1, 5-LOX, FLAP and $cPLA_2$-α (**Fig. 3A**). In parallel, we checked how V-ATPase interference would modulate the release of cytokines upon LPS stimulation. Pretreatment of monocytes with ArchA prior LPS also elevated the release of TNF-α and IL-1β levels while IL-10 production was inhibited and IL-6 release was not affected (**Fig. 3B**). To address if targeting V-ATPase modulates the phenotype of human monocytes, we analyzed the expression of the monocytes surface marker CD14 by flow cytometry [21]. In fact, ArchA and bafilomycin reduced the population of total $CD14^+$ cells (**Fig.3D**). In conclusion, targeting of V-ATPase elevates the expression of the COX-2 enzyme along with increased production of TNF-α and IL-1β but at the same time reduces the formation of COX-2-derived LM.

3.3. Temporal modulation of COX-2 expression and LM biosynthesis by V-ATPase inhibition

We recently showed that in M1-like monocyte-derived macrophages the expression of COX-2 was time-dependently induced by LPS treatment, which peaked after 6 h and degraded again after 24 h to 72 h. This finding prompted us to explore the temporal modulation of COX-2 expression along with LM biosynthesis upon V-ATPase inhibition in human monocytes. The

monocytes were pretreated with ArchA for 30 min before LPS stimulation for 6, 24 or 48 h. High and maximal levels of COX-2 protein were induced 6 h after LPS stimulation and declined afterwards (**Fig. 4A**). Of interest, pretreatment with ArchA slightly elevated COX-2 protein levels after 6 h with more pronounced increase after 24 and 48 h, implying the V-ATPase inhibition seemingly prevents the decline of COX-2 expression over time (**Fig. 4A**). Compared to the temporal expression of COX-2, the formation of prostanoids was somewhat delayed, peaking at 24 h with subsequent decline at 48 h LPS treatment (**Fig. 4B**). Again, ArchA consistently blocked the biosynthesis of COX-2-derived prostanoids regardless of the time point (6, 24, or 48 h) to a comparable degree. Also 5-LOX-derived products (5-HETE, 5-HEPE and LTB_4) were inhibited by ArchA but only after 24 h or 48 h (**Fig. 4B**). By contrast, 12/15-LOX-related products (17-HDHA, 14-HDHA and 12-HETE) as well as fatty acids and 4-HDHA that were most prominent after 6 h with subsequent impairment, remained unchanged after ArchA treatment (**Fig. 4B**). Together, we conclude that pharmacologically targeting of V-ATPase prevents the degradation of COX-2 protein expression but despite elevated enzyme levels suppresses COX-2-derived LM formation.

3.4. Elevated COX-2 expression by V-ATPase inhibition is regulated by the p38 MAPK and ERK-1/2 pathway

Toll-like receptor (TLR) activation by TLR ligands including LPS, TNF-α or IL-1β induces COX-2 expression involving different signaling routes and protein kinases like MKK3/6-p38 MAPK, MEK-ERK-1/2, NF-κB and MKK-4/7-SAPK/JNK pathways (**Fig. 5A**, [22-26]). Therefore, we assumed that elevated COX-2 expression due to V-ATPase inhibition in human monocytes may involve (some of) these pathways. In LPS-stimulated monocytes, pretreatment with ArchA for 15 min prior LPS significantly increased the phosphorylation of p38 MAPK and ERK-1/2 after 24 h, whereas phosphorylation of SAPK/JNK and NF-κB was moderately increased but not yet significantly (**Fig. 5B**). Pre-incubation of monocytes with ArchA for 15 min and subsequent short-term treatment with LPS for 15 min or 1 h only did not affect the phosphorylation of these kinases (**Fig. 5C**). Since increased activation of the p38 MAPK and ERK-1/2 pathway by ArchA may account for the elevated COX-2 expression, we used the specific p38 MAPK inhibitor skepinone-L [27] and ERK-1/2 inhibitor U0126 [28] to confirm their involvement, respectively. In particular skepinone-L strongly abrogated COX-2 expression, regardless of ArchA treatment (**Fig. 5D**), and also efficiently blocked the biosynthesis of COX-derived prostanoids upon *E. coli* challenge (**Fig. 5E**). Similar suppressive effects were observed with the ERK-1/2 pathway inhibitor U0126. Moreover, also LPS- and LPS/ArchA-induced 5-LOX product formation was slightly reduced by skepinone-L under these conditions, albeit not significant; note that neither skepinone-L nor U0126 affected 12/15-LOX product formation or release of AA (**Fig. 5E**). Together, we conclude that the elevated COX-2 expression due to targeting of V-ATPase is mediated

through activation of the p38 MAPK and ERK-1/2 pathway.

3.5. COX-2 activity is regulated by V-ATPase through modulation of lysosomal pH

Next, we explored the mechanisms underlying the suppression of COX-derived LM formation due to interference with V-ATPase. Our previous work showed that V-ATPase inhibition in human monocytes causes accumulation of IL-8 in the endoplasmic reticulum (ER), connected to reduced release of this chemokine [29]. Thus, we assumed that the *in situ* biosynthesized COX-derived LM might be trapped inside the cell as well. However, only low amounts of intracellular prostanoids were evident in human monocytes whereas high levels were released into the extracellular medium, regardless of V-ATPase inhibition (**Fig. 6A, B**). V-ATPase is a universal proton pump that is critically involved in the regulation of the intracellular pH [10], and we previously showed that V-ATPase inhibitors elevate the lysosomal pH in human monocytes and macrophages [12, 29]. Therefore, we speculated that decreased cytosolic but increased lysosomal pH due to V-ATPase inhibition might be related to increased COX-2 expression and/or suppressed biosynthesis of prostanoids in human monocytes. As tool compound we used the well-known pH modulator chloroquine [30] that we showed before to increase the lysosomal pH in human monocytes, like ArchA [29]. Propidium iodide staining in human monocytes revealed that neither ArchA nor chloroquine had detrimental effects on cell viability (**Fig. 7A**). In contrast to ArchA treatment, chloroquine strongly blocked the expression of COX-2 protein within 24 h (**Fig. 7B**). In analogy to ArchA, however, chloroquine strongly suppressed the release of COX-derived prostanoids into the medium during 24 h (**Fig. 7C**). Also when monocytes, after 24 h treatment with ArchA, were further stimulated with *E. coli* for another 90 min, formation of COX-derived LM and to a minor degree also of 5-LOX products and AA release were impaired (**Fig. 7D**). Other LOX- or cytochrome P450 (CYP)-derived LM (e.g. 12-HETE, 4-HDHA or 18-HEPE) were not suppressed (**Fig. 7D**). Together, chloroquine mimics the effects of ArchA on the biosynthesis on LM with strong suppression of prostanoids, suggesting that elevation of lysosomal pH is causative for reduced activity of COX-2 and thus impaired prostanoid formation.

4. Discussion

Inflammation is a process in which the immune system defends against exterior stimuli and invaders, and helps the body to return to its healthy state [31]. Acute inflammation is governed by the excessive production of pro-inflammatory LM such as PGs and LTs as well as of cytokines [2]. Our previous research indicates that V-ATPase is involved in the regulation of various inflammatory processes. Thus, we showed that V-ATPase (I) is crucial for cytokine and chemokine trafficking in human monocytes [29], (II) elevates TNF-α production in M1-like MDM to govern anti-tumoral activities [12], and (III) promotes the inflammatory resolution process in M2-like-

MDM by accomplishing 15-LOX-1 expression and SPM formation [9]. Therefore, depending on the cell type, V-ATPase has opposing roles in the regulation of inflammation.

Here, we aimed to investigate how V-ATPase regulates pro-inflammatory LM biosynthetic pathways in human monocytes that are professional innate immune cells with pivotal functions in the immune defense. Our data imply crucial but differential roles of V-ATPase in the regulation of the COX-2 pathway in human monocytes: while V-ATPase has an negative impact on prostanoid biosynthesis by limiting the *de novo*-induced COX-2 protein levels, this proton pump accomplishes efficient COX-2-derived prostanoid formation by favoring cellular COX-2 activity.

We hypothesize that V-ATPase negatively regulates *de novo* biosynthesized COX-2 protein levels in monocytes by rapidly lowering the protein amount of this inducible enzyme over time. This is supported by our previous studies of M1-like MDM, where inhibition of V-ATPase prevents the degradation of COX-2 protein expression that was initially induced by LPS [9]. Also in RAW264 macrophages of murine origin inhibition of V-ATPase was reported to elevate COX-2 levels [32]. Besides higher COX-2 levels, V-ATPase inhibition also increased the amounts of TNF-α and IL-1β that were shown to stimulate COX-2 expression [33, 34] involving p38 MAPK [35] and this kinase seemingly mediates the increased COX-2 levels in the present scenario as well. In fact, several studies reported a crucial role of p38 MAPK in LPS-induced COX-2 expression in human monocytes [22, 23, 36], and it was shown before that both p38 MAPK and ERK-1/2 are essential in the induction of COX-2 protein in LPS-stimulated human neutrophils [26]. In our hands, ArchA increased the phosphorylation of p38 MAPK after 24 h LPS stimulation in human monocytes, and also activation of ERK-1/2 was evident, whereas other relevant signaling pathways like NF-κB and SAPK/JNK were not affected. This suggests that V-ATPase limits p38 MAPK and ERK-1/2 activation in monocytes. Since the p38 MAPK inhibitor skepinone-L as well as the ERK-1/2 inhibitor U0126 abrogated the LPS-induced COX-2 expression, we propose that the enhancement of the p38 MAPK and ERK-1/2 pathway by ArchA is causative for the elevated COX-2 levels in human monocytes.

Although targeting of V-ATPase increased COX-2 protein levels in human monocytes, the concomitant biosynthesis of COX-2-derived prostanoids was surprisingly decreased, suggesting that V-ATPase is overall beneficial for cellular COX-2 activity. Results from previous studies exclude direct interference of the V-ATPase inhibitors ArchA, bafilomycin A and apicularen with the enzymatic activity of COX-2 activity [17], indicating that the suppression of prostanoid formation in monocytes is not the consequence of direct inhibition of the COX-2 enzyme. In contrast to monocytes, in M1-like MDM ArchA (and bafilomycin) elevated COX-2 activity [9], suggesting that the prostanoid-suppressive effects of V-ATPase inhibitors in monocytes is cell type-dependent and due to modulation of processes that govern cellular COX-2 activity.

Since V-ATPase was shown to regulate cytokine and chemokine trafficking in monocytes, where ArchA treatment led to accumulation of IL-8 in the endoplasmic reticulum (ER) [29], it appeared possible that de novo biosynthesized prostanoids might be trapped inside the cell. However, only low amounts of intracellular PGs were evident in *E. coli*-stimulated monocytes whereas high levels were released into the cell supernatant, regardless of V-ATPase inhibition. Together, V-ATPase governs COX-2 activity in monocytes, explaining why V-ATPase interference impairs prostanoid formation.

The main function of V-ATPase is to regulate cellular pH homeostasis by promoting the transport of protons from the cytosol to lysosomes that become acidic [10], and accordingly, targeting of V-ATPase in monocytes led to an elevated lysosomal pH [29]. Therefore, we hypothesized that the reduction of COX-derived prostanoids might be due to intracellular pH changes upon V-ATPase inhibition. Indeed, the pH modulator chloroquine that alkalizes lysosomes and acidifies the cytosol [30] mimicked the effects of V-ATPase inhibitors on the LM profile, as it strongly suppressed COX-dependent LM formation without suppressing 12/15-LOX products and with minor impairment of 5-LOX-derived LM. Cellular activity of 5-LOX is affected by many factors including AA supply, its helper protein FLAP, phosphorylation by MAPKAPK-2 and ERK-1/2 [37]. Note that ArchA did not alter 5-LOX, FLAP or $cPLA_2$-α expression and substrate supply. Thus, the intracellular pH might be crucial for the activity of both the COX-2 and the 5-LOX pathway. In fact, the pH optimum for the enzymatic activities of COX-2 and 5-LOX in cell-free assays is around pH 8.0 [38, 39], implying that cytosolic or nuclear membrane-associated 5-LOX [37] and ER/nuclear envelope-inserted COX-2 [40] may benefit from V-ATPase activity accomplishing alkaline pH in the cytosol. It appeared possible that changes in the intracellular pH might be also the cause for the increased COX-2 expression by ArchA, implying a detrimental role of V-ATPase in this respect. In fact, it was reported before for a human osteoblastic cell line that sensing of pH changes would regulate COX-2 expression and PGE_2 formation [41]. However, the pH modulator chloroquine did not induce COX-2 expression and rather abrogated it, suggesting other mechanisms responsible for elevation of COX-2 levels by ArchA in human monocytes which are mediated by p38 MAPK and ERK-1/2.

In summary, we reveal a crucial role of V-ATPase in the regulation of the biosynthesis of COX-2- and, to a minor extent, in 5-LOX-derived LM in human monocytes. Surprisingly, our V-ATPase-targeting approach implies contrasting requirements of this proton pump: V-ATPase causes an impairment of the protein levels of COX-2 seemingly by suppression of p38 MAPK and ERK-1/2 signaling but accomplishes substantial cellular activity of COX-2 possibly by adjusting a favorable intracellular pH for this enzyme.

Acknowledgments

We thank Petra Wiecha, Bärbel Schmalwasser and Bettina Mönch for expert technical assistance. This work was funded by grants to O.W. (Deutsche Forschungsgemeinschaft, SFB1127 ChemBioSys, SFB1278 Polytarget, and Free State of Thuringia and the European Social Fund (2016 FGR 0045)). Z.R was partly supported by the China Scholarship Council. J.G. received a Carl-Zeiss-Postdoctoral stipend.

Conflict of Interest Statement: None declared.

References

[1] R. van Furth, Z.A. Cohn, The origin and kinetics of mononuclear phagocytes, J Exp Med 128(3) (1968) 415-35.
[2] J.S. Pober, W.C. Sessa, Inflammation and the blood microvascular system, Cold Spring Harb Perspect Biol 7(1) (2014) a016345.
[3] L.M. Coussens, Z. Werb, Inflammation and cancer, Nature 420(6917) (2002) 860-867.
[4] J.R. Vane, Y.S. Bakhle, R.M. Botting, Cyclooxygenases 1 and 2, Annu Rev Pharmacol Toxicol 38 (1998) 97-120.
[5] K. Seibert, J.L. Masferrer, Role of inducible cyclooxygenase (COX-2) in inflammation, Receptor 4(1) (1994) 17-23.
[6] D.J. Bjorkman, The effect of aspirin and nonsteroidal anti-inflammatory drugs on prostaglandins, Am J Med 105(1b) (1998) 8s-12s.
[7] G.A. FitzGerald, C. Patrono, The coxibs, selective inhibitors of cyclooxygenase-2, N Engl J Med 345(6) (2001) 433-42.
[8] R. Flower, R. Gryglewski, K. HerbaczŃSka-Cedro, J.R. Vane, Effects of Anti-inflammatory Drugs on Prostaglandin Biosynthesis, Nature New Biol 238(82) (1972) 104-106.
[9] Z. Rao, S. Pace, P.M. Jordan, R. Bilancia, F. Troisi, F. Borner, N. Andreas, T. Kamradt, D. Menche, A. Rossi, C.N. Serhan, J. Gerstmeier, O. Werz, Vacuolar (H(+))-ATPase Critically Regulates Specialized Proresolving Mediator Pathways in Human M2-like Monocyte-Derived Macrophages and Has a Crucial Role in Resolution of Inflammation, J Immunol (Baltimore, Md. : 1950) 203(4) (2019) 1031-1043.
[10] M. Forgac, Vacuolar ATPases: rotary proton pumps in physiology and pathophysiology, Nat Rev Mol Cell Biol 8(11) (2007) 917-929.
[11] M.E. Maxson, S. Grinstein, The vacuolar-type H^+-ATPase at a glance – more than a proton pump, J Cell Sci 127(23) (2014) 4987-4993.
[12] L. Thomas, Z. Rao, J. Gerstmeier, M. Raasch, C. Weinigel, S. Rummler, D. Menche, R. Muller, C. Pergola, A. Mosig, O. Werz, Selective upregulation of TNFalpha expression in classically-activated human monocyte-derived macrophages (M1) through pharmacological interference with V-ATPase, Biochem Pharmacol 130 (2017) 71-82.
[13] O. Werz, J. Gerstmeier, S. Libreros, X. De la Rosa, M. Werner, P.C. Norris, N. Chiang, C.N. Serhan, Human macrophages differentially produce specific resolvin or leukotriene signals that depend on bacterial pathogenicity, Nat Commun 9(1) (2018) 59.
[14] M. Werner, P.M. Jordan, E. Romp, A. Czapka, Z. Rao, C. Kretzer, A. Koeberle, U. Garscha, S. Pace, H.E. Claesson, C.N. Serhan, O. Werz, J. Gerstmeier, Targeting biosynthetic networks of the proinflammatory and proresolving lipid metabolome, FASEB J 33(5) (2019) 6140-6153.
[15] J.T. English, P.C. Norris, R.R. Hodges, D.A. Dartt, C.N. Serhan, Identification and Profiling of Specialized Pro-Resolving Mediators in Human Tears by Lipid Mediator Metabolomics, Prostag Leukot Ess 117 (2017) 17-27.
[16] F. Sasse, H. Steinmetz, G. Hofle, H. Reichenbach, Archazolids, new cytotoxic macrolactones from Archangium gephyra (Myxobacteria). Production, isolation, physico-chemical and biological properties, J Antibiot 56(6) (2003) 520-5.
[17] D. Reker, A.M. Perna, T. Rodrigues, P. Schneider, M. Reutlinger, B. Mönch, A. Koeberle, C. Lamers, M. Gabler, H. Steinmetz, R. Müller, M. Schubert-Zsilavecz, O. Werz, G. Schneider, Revealing the macromolecular targets of complex natural products, Nat Chem 6 (2014) 1072.
[18] R. Newton, J. Seybold, L.M. Kuitert, M. Bergmann, P.J. Barnes, Repression of cyclooxygenase-2 and prostaglandin E2 release by dexamethasone occurs by transcriptional and post-transcriptional mechanisms involving loss of polyadenylated mRNA, The J Biol Chem 273(48) (1998) 32312-21.
[19] E.J. Bowman, A. Siebers, K. Altendorf, Bafilomycins: a class of inhibitors of membrane ATPases from microorganisms, animal cells, and plant cells, Proc Natl Acad Sci U S A 85(21) (1988) 7972-6.
[20] B. Kunze, R. Jansen, F. Sasse, G. Hofle, H. Reichenbach, Apicularens A and B, new cytostatic macrolides from Chondromyces species (myxobacteria): production, physico-chemical and biological properties, J Antibiot 51(12) (1998) 1075-80.
[21] L. Ziegler-Heitbrock, P. Ancuta, S. Crowe, M. Dalod, V. Grau, D.N. Hart, P.J. Leenen, Y.J. Liu, G. MacPherson, G.J. Randolph, J. Scherberich, J. Schmitz, K. Shortman, S. Sozzani, H. Strobl, M. Zembala, J.M. Austyn, M.B. Lutz, Nomenclature of monocytes and dendritic cells in blood, Blood 116(16) (2010) e74-80.
[22] M. Pouliot, J. Baillargeon, J.C. Lee, L.G. Cleland, M.J. James, Inhibition of prostaglandin

endoperoxide synthase-2 expression in stimulated human monocytes by inhibitors of p38 mitogen-activated protein kinase, J Immunol 158(10) (1997) 4930-4937.
[23] J.L. Dean, M. Brook, A.R. Clark, J. Saklatvala, p38 mitogen-activated protein kinase regulates cyclooxygenase-2 mRNA stability and transcription in lipopolysaccharide-treated human monocytes, The J Biol Chem 274(1) (1999) 264-9.
[24] V.C. Allport, D.M. Slater, R. Newton, P.R. Bennett, NF-κB and AP-1 are required for cyclo-oxygenase 2 gene expression in amnion epithelial cell line (WISH), Mol Hum Reprod 6(6) (2000) 561-565.
[25] R. Nieminen, A. Lahti, U. Jalonen, H. Kankaanranta, E. Moilanen, JNK inhibitor SP600125 reduces COX-2 expression by attenuating mRNA in activated murine J774 macrophages, Int Immunopharmacol 6(6) (2006) 987-96.
[26] S. Nagano, T. Otsuka, H. Niiro, K. Yamaoka, Y. Arinobu, E. Ogami, M. Akahoshi, Y. Inoue, K. Miyake, H. Nakashima, Y. Niho, M. Harada, Molecular mechanisms of lipopolysaccharide-induced cyclooxygenase-2 expression in human neutrophils: involvement of the mitogen-activated protein kinase pathway and regulation by anti-inflammatory cytokines, Int Immunol 14(7) (2002) 733-40.
[27] S.C. Koeberle, J. Romir, S. Fischer, A. Koeberle, V. Schattel, W. Albrecht, C. Grütter, O. Werz, D. Rauh, T. Stehle, S.A. Laufer, Skepinone-L is a selective p38 mitogen-activated protein kinase inhibitor, Nat Chem Biol 8(2) (2012) 141-143.
[28] M.F. Favata, K.Y. Horiuchi, E.J. Manos, A.J. Daulerio, D.A. Stradley, W.S. Feeser, D.E. Van Dyk, W.J. Pitts, R.A. Earl, F. Hobbs, R.A. Copeland, R.L. Magolda, P.A. Scherle, J.M. Trzaskos, Identification of a novel inhibitor of mitogen-activated protein kinase kinase, J Biol Chem 273(29) (1998) 18623-32.
[29] O. Scherer, H. Steinmetz, C. Kaether, C. Weinigel, D. Barz, H. Kleinert, D. Menche, R. Müller, C. Pergola, O. Werz, Targeting V-ATPase in primary human monocytes by archazolid potently represses the classical secretion of cytokines due to accumulation at the endoplasmic reticulum, Biochem Pharmacol 91(4) (2014) 490-500.
[30] B. Poole, S. Ohkuma, Effect of weak bases on the intralysosomal pH in mouse peritoneal macrophages, J Cell Biol 90(3) (1981) 665-9.
[31] R. Medzhitov, Origin and physiological roles of inflammation, Nature 454(7203) (2008) 428-35.
[32] F. Kamachi, M. Yanai, H.S. Ban, K. Ishihara, J. Hong, K. Ohuchi, N. Hirasawa, Involvement of Na+/H+ exchangers in induction of cyclooxygenase-2 by vacuolar-type (H+)-ATPase inhibitors in RAW 264 cells, FEBS Lett 581(24) (2007) 4633-8.
[33] Y. Li, C. Soendergaard, F.H. Bergenheim, D.M. Aronoff, G. Milne, L.B. Riis, J.B. Seidelin, K.B. Jensen, O.H. Nielsen, COX-2-PGE2 Signaling Impairs Intestinal Epithelial Regeneration and Associates with TNF Inhibitor Responsiveness in Ulcerative Colitis, EBioMedicine 36 (2018) 497-507.
[34] E. Porreca, M. Reale, C. Di Febbo, M. Di GioacchinoI, R.C. Barracane, M.L. Castellani, G. Baccante, P. Conti, F. Cuccurullo, Down-regulation of cyclooxygenase-2 (COX-2) by interleukin-1 receptor antagonist in human monocytes, Immunology 89(3) (1996) 424-429.
[35] C.A. Singer, K.J. Baker, A. McCaffrey, D.P. AuCoin, M.A. Dechert, W.T. Gerthoffer, p38 MAPK and NF-kappaB mediate COX-2 expression in human airway myocytes, Am J Physiol Lung Cell Mol Physiol 285(5) (2003) L1087-98.
[36] H. Niiro, T. Otsuka, E. Ogami, K. Yamaoka, S. Nagano, M. Akahoshi, H. Nakashima, Y. Arinobu, K. Izuhara, Y. Niho, MAP kinase pathways as a route for regulatory mechanisms of IL-10 and IL-4 which inhibit COX-2 expression in human monocytes, Biochem Biophys Res Commun 250(2) (1998) 200-5.
[37] O. Radmark, O. Werz, D. Steinhilber, B. Samuelsson, 5-Lipoxygenase, a key enzyme for leukotriene biosynthesis in health and disease, Biochim Biophys Acta 1851(4) (2015) 331-9.
[38] Q. Shi, J. Chen, Y. Wang, Z. Li, X. Li, C. Sun, L. Zheng, Immobilization of Cyclooxygenase-2 on Silica Gel Microspheres: Optimization and Characterization, Molecules 20(11) (2015) 19971-83.
[39] K. Schwarz, M. Walther, M. Anton, C. Gerth, I. Feussner, H. Kuhn, Structural Basis for Lipoxygenase Specificity. Conversion of the human leukocyte 5-lipoxygenase to a 15-lipoxygenating enzyme species by site-directed mutagenesis, J Biol Chem 276(1) (2001) 773-779.
[40] A.G. Spencer, J.W. Woods, T. Arakawa, Singer, II, W.L. Smith, Subcellular localization of prostaglandin endoperoxide H synthases-1 and -2 by immunoelectron microscopy, J Biol Chem 273(16) (1998) 9886-93.
[41] H. Tomura, J.Q. Wang, J.P. Liu, M. Komachi, A. Damirin, C. Mogi, M. Tobo, H. Nochi, K. Tamoto, D.S. Im, K. Sato, F. Okajima, Cyclooxygenase-2 expression and prostaglandin E2 production in response to acidic pH through OGR1 in a human osteoblastic cell line, J Bone Miner Res 23(7) (2008) 1129-39.

Fig. 1

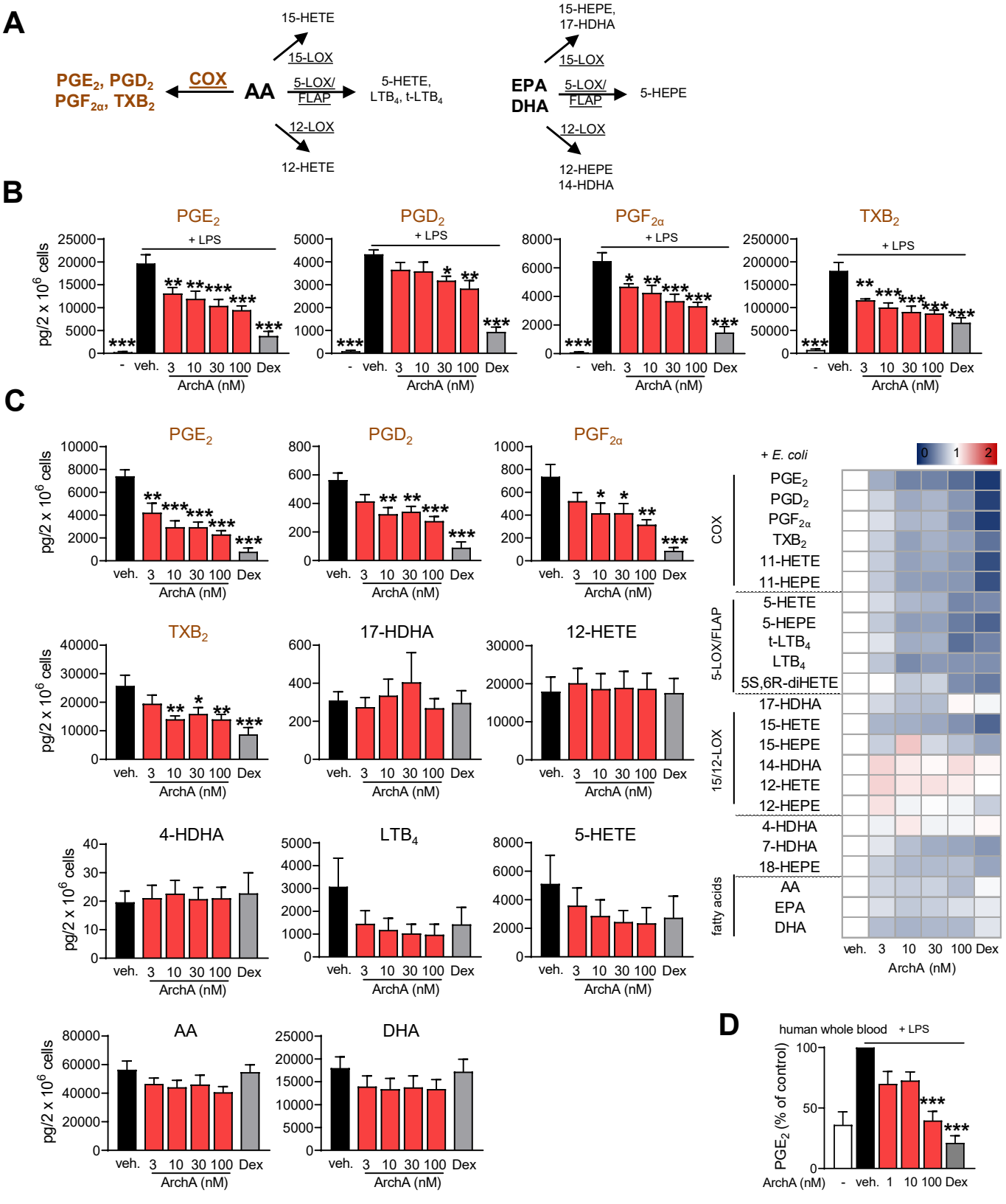

Fig. 1. Targeting of lipid mediator biosynthetic pathways by archazolid A in human monocytes. Human monocytes were pretreated with archazolid A (ArchA, 3-100 nM), dexamethasone (Dex, 1 µM) or vehicle (DMSO 0.1%) for 15 min before stimulation with LPS (100 ng/ml) for 24 h. **A**) Schematic representation of the investigated LM biosynthetic pathways involving COX, 15-LOX, 5-LOX/FLAP, or 12-LOX leading to respective LM. B) LM released from monocytes into the cell culture medium after 24 h were isolated by solid phase extraction and analyzed by UPLC-MS-MS; detection limit: 0.5 pg. Results are given as means ± S.E.M, n = 4. **C**) LM generated from monocytes after exposure to *E. coli* (ratio 1:50, 90 min) were isolated by solid phase extraction and analyzed by UPLC-MS-MS; detection limit: 0.5 pg. Results are given as means ± S.E.M in the bar charts and as ratio to vehicle in the heatmap; n = 7. **D**) Effect of ArchA (1-100 nM) and dexamethasone (Dex, 1 µM) on PGE_2 biosynthesis in human whole blood stimulated with LPS (100 ng/ml, 24 h, n = 6). Results are given as percentage of LPS-vehicle control (= 100%), means ± S.E.M. *p < 0.05, **p < 0.01, ***p < 0.001 vs. LPS-vehicle (veh.), one-way analysis of variance (ANOVA) with Bonferroni test.

Fig. 2

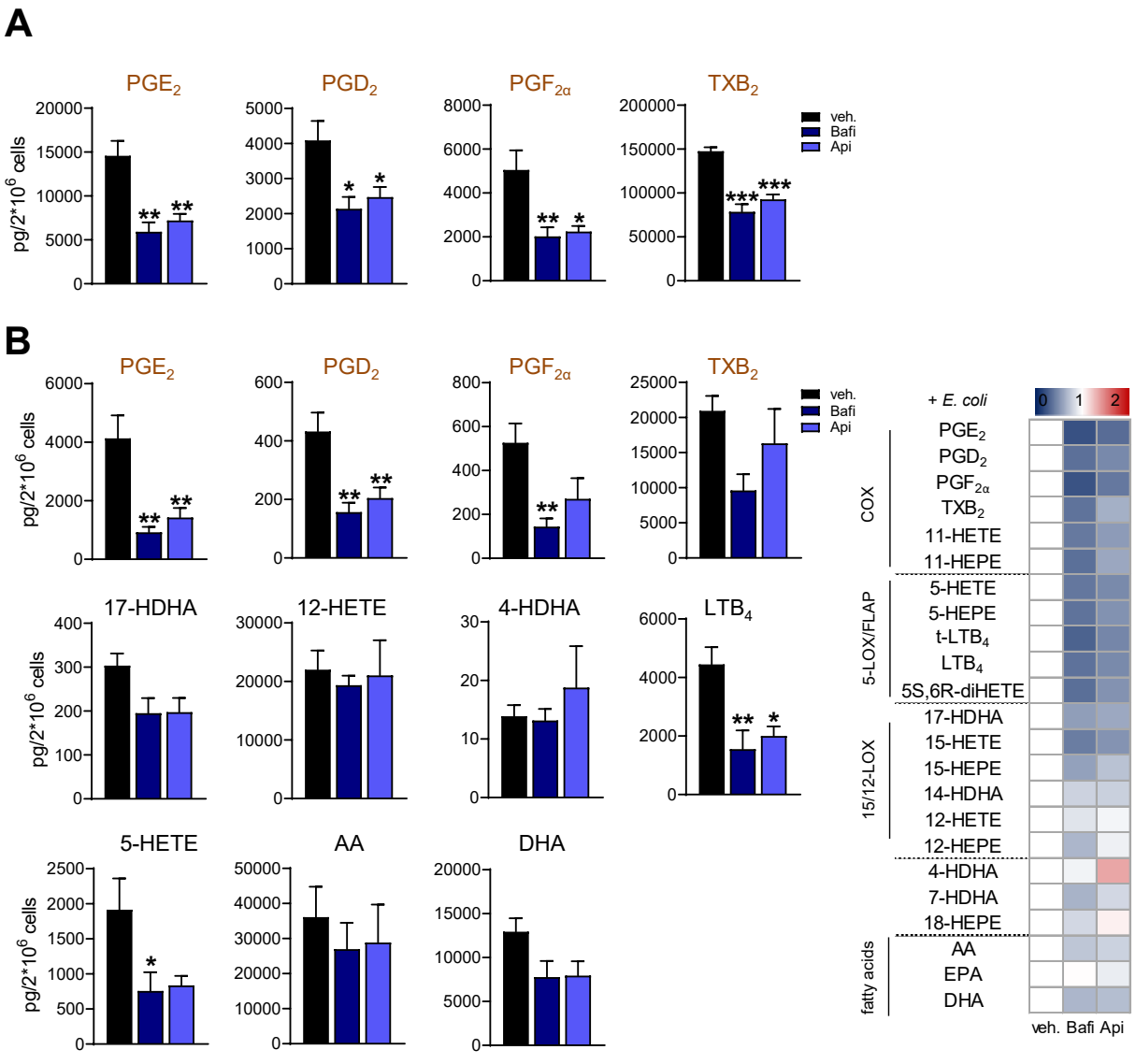

Fig. 2. Class effect of pharmacological targeting V-ATPase. Human monocytes were pretreated with bafilomycin (Bafi, 10 nM) or apicularen (Api, 10 nM) for 15 min before stimulation with LPS (100 ng/ml) for 24 hrs. A) LM produced from cell supernatants were isolated by solid phase extraction and analyzed by UPLC-MS-MS; detection limit: 0.5 pg. Results are given as means ± S.E.M in the bar charts and as ratio to vehicle in the heatmap, n = 4. *p < 0.05, **p < 0.01 vs. vehicle (veh.), one-way analysis of variance (ANOVA) with Bonferroni test. B) LM generated from monocytes after exposure to E. coli (ratio 1:50, 90 min) were isolated by solid phase extraction and analyzed by UPLC-MS-MS; detection limit: 0.5 pg. Results are given as means ± S.E.M in the bar charts and as ratio to vehicle in the heatmap, n = 5. *p < 0.05, **p < 0.01 vs. vehicle (veh.), one-way analysis of variance (ANOVA) with Bonferroni test.

Fig. 3

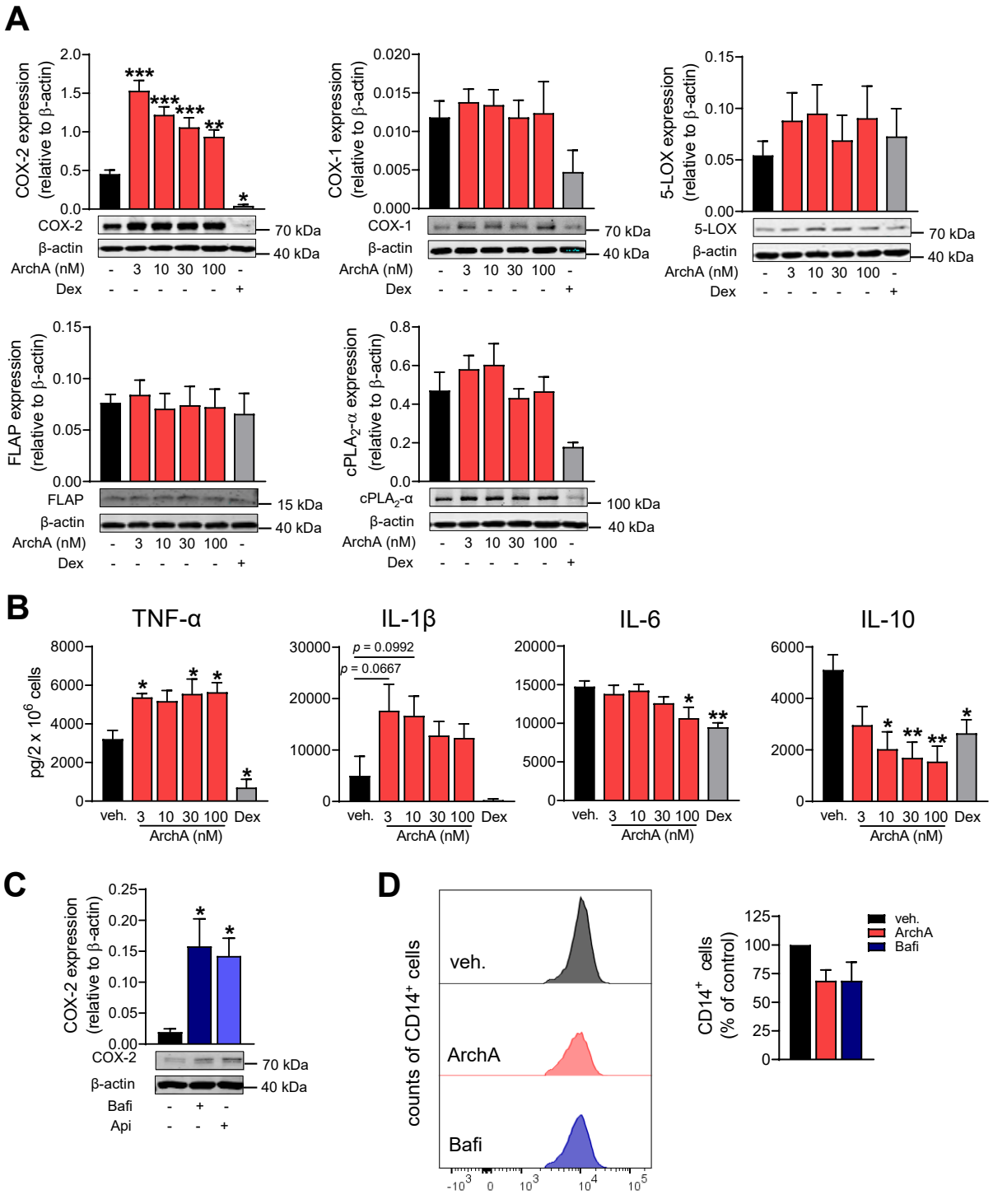

Fig. 3. Pharmacological targeting of V-ATPase induces COX-2 expression in human monocytes. Human monocytes were pretreated with A, B) archazolid A (ArchA, 3-100 nM), dexamethasone (Dex, 1 µM), C) bafilomycin (Bafi, 10 nM) or apicularen (Api, 10 nM) or vehicle (DMSO 0.1%) for 15 min before stimulation with LPS (100 ng/ml) for 24 h. A). Monocyte lysates were immunoblotted for COX-2 (n = 9), COX-1 (n = 6), 5-LOX (n = 6), FLAP (n = 5), cPLA2-α (n = 6) and normalized to β-actin for densitometric analysis. Data are shown as means ± S.E.M, *p < 0.05, **p < 0.01, ***p < 0.001 vs. vehicle (veh.), one-way analysis of variance (ANOVA) with Bonferroni test. B) Cytokines released from monocyte supernatants were analyzed by ELISA; results are given as means ± S.E.M., n = 4. *p < 0.05, **p < 0.01 vs. vehicle (veh.), one-way analysis of variance (ANOVA) with Bonferroni test. C) Cell lysates were immunoblotted for COX-2 and β-actin for densitometric analysis. Data are shown as means ± S.E.M, n = 5. *p < 0.05 vs. vehicle (veh.), one-way analysis of variance (ANOVA) with Bonferroni test. D) Human monocytes were pretreated with ArchA (10 nM), bafilomycin (Bafi, 10 nM) or vehicle (DMSO 0.1%) for 15 min before stimulation with LPS (100 ng/ml) for 24 h. Expression of monocytes surface marker (CD14) analyzed by flow cytometry. Results are shown as percentage of vehicle control (= 100%), means ± S.E.M., n = 3. Representative figure is shown from n = 3 independent experiments.

Fig. 4

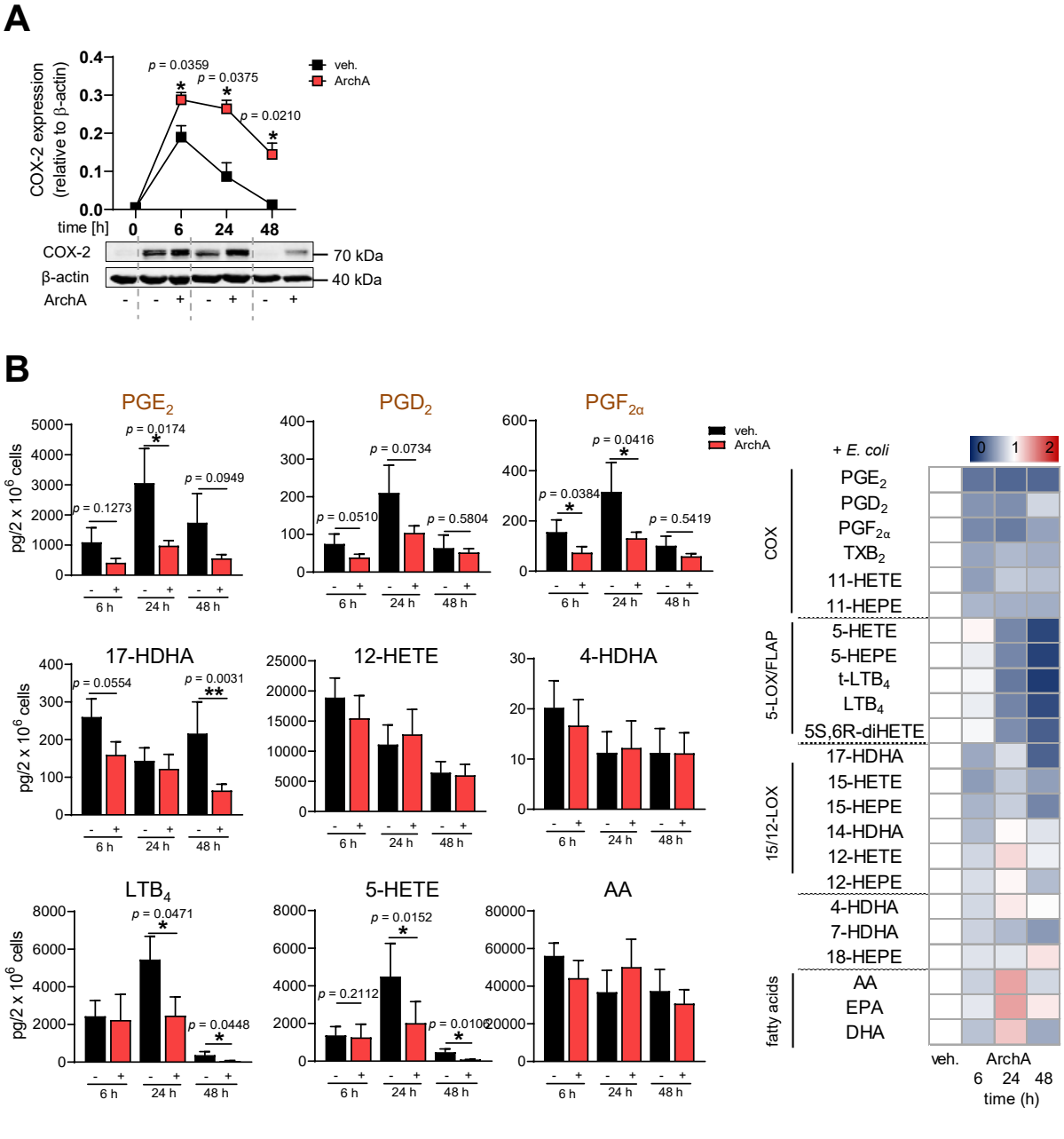

Fig. 4. Temporal modulation of LM biosynthetic pathways by ArchA in human monocytes. Human monocytes were pretreated with archazolid A (ArchA, 10 nM) or vehicle (DMSO 0.1%) for 15 min before stimulation with LPS (100 ng/ml) for 6, 24 or 48 h. A) Monocyte lysates were immunoblotted for COX-2, normalized to β-actin for densitometric analysis. Data are shown as means ± S.E.M, n = 4. *p < 0.05 vs. vehicle, paired t test. B) LM generated from monocytes after exposure to E. coli (ratio 1:50, 90 min) were isolated by solid phase extraction and analyzed by UPLC-MS-MS; detection limit: 0.5 pg. Results are given as means ± S.E.M in the bar charts and as ratio to vehicle in the heatmap, n = 4 for 6 h and n = 7 for 24 h/48 h. *p < 0.05, **p < 0.01 vs. vehicle (veh.), data are log-transformed for statistical analysis, paired t test.

Fig. 5

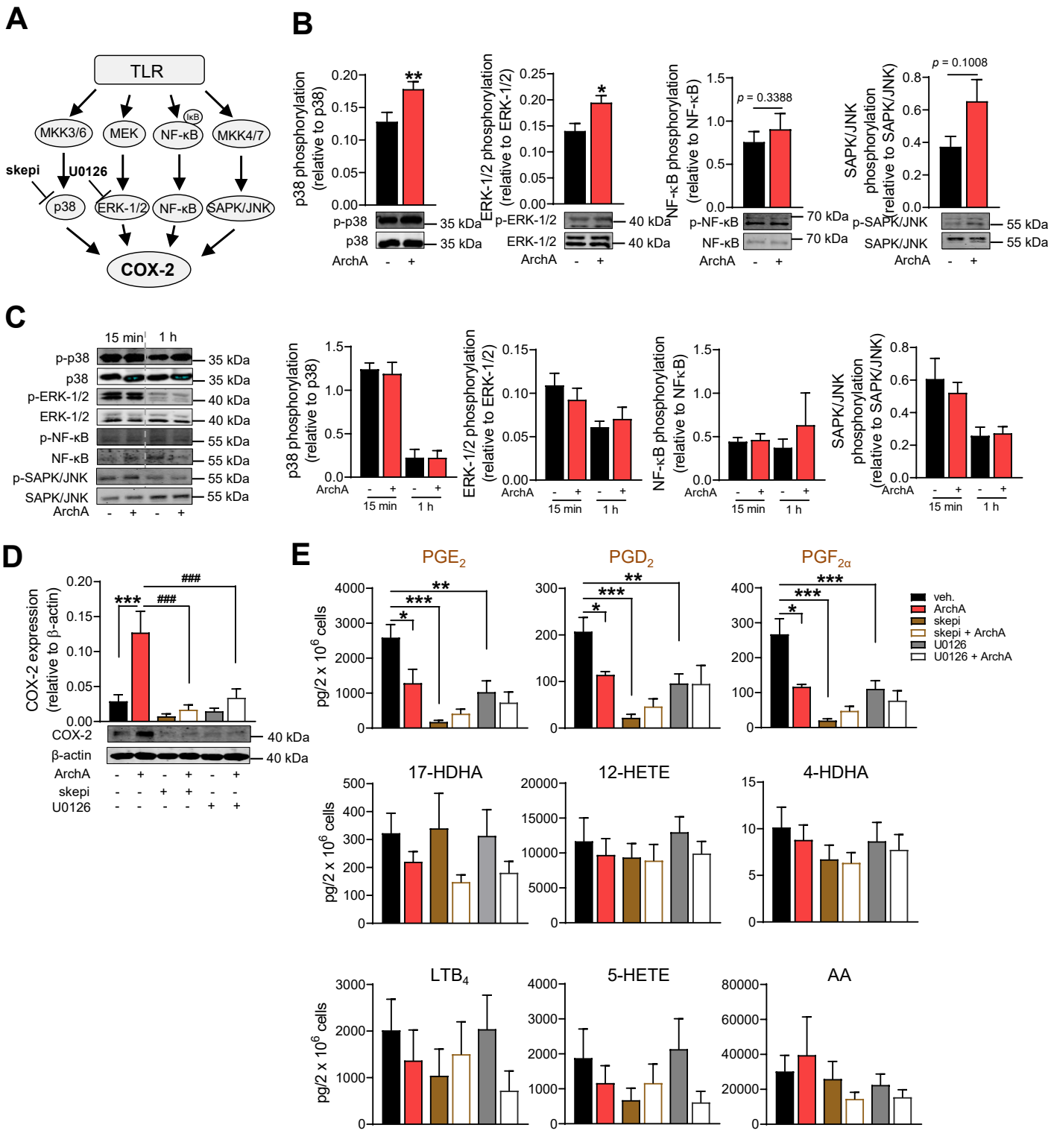

Fig. 5. ArchA-induced COX-2 expression is regulated by p38 MAPK and ERK-1/2. A) Proposed scheme of the COX-2-regulating pathway in monocytes. B, C) Human monocytes were pretreated with archazolid A (ArchA, 10 nM) for 15 min before stimulation with LPS (100 ng/ml) for B) 24 h or C) 15 min and 1 h. Cell lysates were immunoblotted for phospho-p38 MAPK, p38 MAPK, phospho-ERK-1/2, ERK-1/2, phospho-NF-κB, NF-κB, phospho-JNK and JNK for densitometric analysis. Data are shown as means ± S.E.M, n = 6. *p < 0.05, **p < 0.01, vs. LPS-vehicle, paired t test. D, E) Human monocytes were pretreated with ArchA (30 nM), skepinone-L (skepi, 1 μM), U0126 (3 μM) or vehicle (DMSO 0.1%) for 15 min before stimulation with LPS (100 ng/ml) for 24 hrs. D) Monocyte lysates were immunoblotted for COX-2 and β-actin for densitometric analysis. Data are shown as means ± S.E.M from n = 6. E) LM generated from monocytes after exposure to E. coli (ratio 1:50, 90 min) were isolated by solid phase extraction and analyzed by UPLC-MS-MS; detection limit: 0.5 pg. Results are given as means ± S.E.M., n = 5. *p < 0.05, **p < 0.01, ***p < 0.001 vs. vehicle (veh.); ###p < 0.001 vs. ArchA control (ArchA), one-way analysis of variance (ANOVA) with Bonferroni test.

Fig. 6

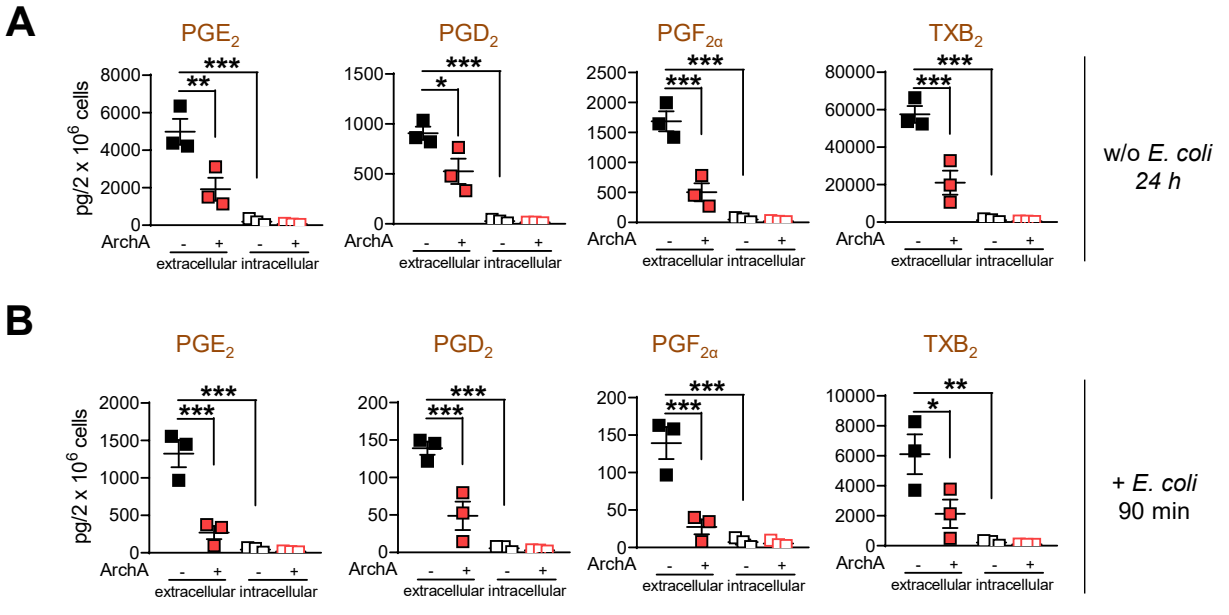

Fig. 6. Effect of ArchA on the production of extracellular and intracellular COX-derived LM in human monocytes. Human monocytes were pretreated with archazolid A (ArchA,10 nM) or vehicle for 15 min before stimulation with LPS (100 ng/ml) for 24 hrs. A) LM from extracellular (cell supernatant) and intracellular (intact cell) origin were isolated by solid phase extraction and analyzed by UPLC-MS-MS; detection limit: 0.5 pg. B) LM from extracellular (cell supernatant) and intracellular (intact cell) origin after exposure to E. coli (ratio 1:50, 90 min) were isolated by solid phase extraction and analyzed by UPLC-MS-MS; detection limit: 0.5 pg. Results are given as means ± S.E.M., n = 3. *p < 0.05, **p < 0.01, ***p < 0.01 vs. vehicle (veh.), one-way analysis of variance (ANOVA) with Bonferroni test.

Fig. 7

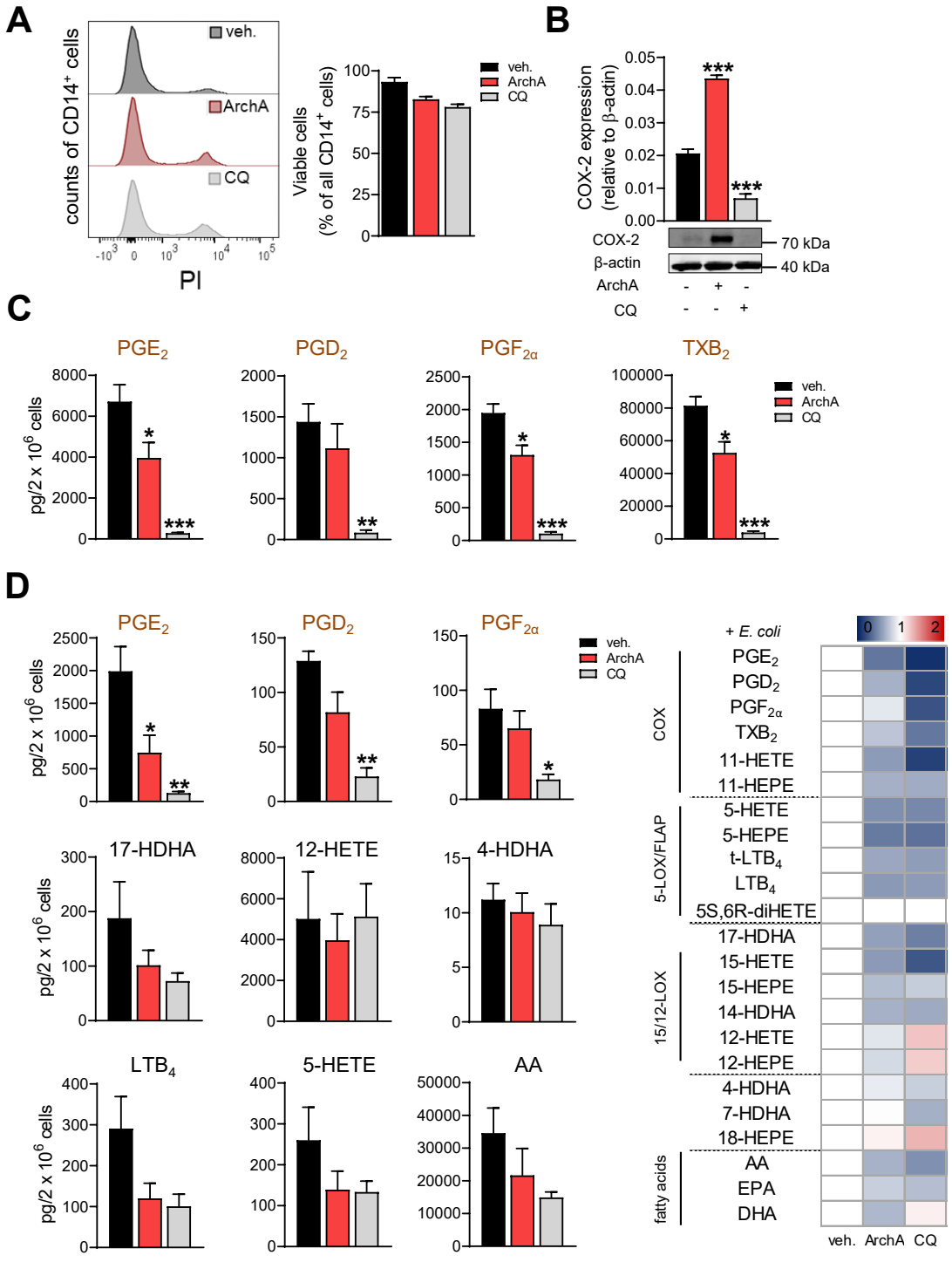

Fig. 7. COX-2 activity is regulated by V-ATPase through modulation of the intracellular pH. Human monocytes were pretreated with archazolid A (ArchA, 10 nM), choloroquine (CQ, 100 µM) or vehicle (DMSO 0.1%) for 15 min before stimulation with LPS (100 ng/ml) for 24 hrs. A) Cell viability determined by propidium iodide staining analyzed by flow cytometry. Data are given as means ± S.E.M. (viable cells as percentage of total cells), n = 3. B) Monocyte lysates were immunoblotted for COX-2 and β-actin for densitometric analysis. Data are shown as means ± S.E.M from n = 3. C) LM present in cell supernatants were isolated by solid phase extraction and analyzed by UPLC-MS-MS; detection limit: 0.5 pg. Results are given as means ± S.E.M in bar charts and as ratio to vehicle in heat-map. n = 3. D) LM generated from monocytes after exposure to E. coli (ratio 1:50, 90 min) were isolated by solid phase extraction and analyzed by UPLC-MS-MS; detection limit: 0.5 pg. Results are given as means ± S.E.M in bar charts and as ratio to vehicle in a heatmap. n = 3. *p < 0.05, **p < 0.01, ***p < 0.001 vs. vehicle (veh.), one-way analysis of variance (ANOVA) with Bonferroni test.

3.2 Manuscript II

Selective upregulation of TNFα expression in classically-activated human monocyte-derived macrophages (M1) through pharmacological interference with V-ATPase

Lea Thomas, **Zhigang Rao**, Jana Gerstmeier, Martin Raasch, Christina Weinigel, Silke Rummler, Dirk Menche, Rolf Müller, Carlo Pergola, Alexander Mosig, Oliver Werz (2017)

Biochemical Pharmacology 130 (2017) 71–82

We show that targeting V-ATPase by the selective inhibitor archazolid (ArchA) upregulates TNF-α mRNA levels and TNF-α secretion in LPS- or LPS/INFγ-activated human M1 macrophages. In contrast, ArchA failed to increase TNF-α levels in uncommitted (M0) or IL-4-treated human M2 macrophages. Secretion of other relevant cytokines like IL-1β, IL-6, IL-10 or chemokines as IL-8 and monocyte chemotactic protein-1 from M1 macrophages was not affected by ArchA. Notably, the phosphorylation and nuclear translocation of the p65 subunit of NF-κB as well as phosphorylation of SAPK/JNK that are responsible for TNF-α expression was enhanced by ArchA. In a microfluidically-supported three-dimensional human tumor biochip model, ArchA-treated human M1 macrophages significantly reduced MCF-7 tumor cell viability via increased secretion of TNFα, whereas in models containing M2 macrophages or in models devoid of macrophages, ArchA failed in this respect. Conclusively, pharmacologically targeting V-ATPase with ArchA activates NF-κB and SAPK/JNK pathways and thus elevates TNF-α levels, which supports the anti-tumoral effects of human M1 macrophages.

Contribution (35%): Cell culture and performance of blood cell isolation, determination of cytokine/chemokine levels, measurement of ROS formation, the microfluidically supported biochip assay, analysis of data and preparation of graphs, analysis of statistics, writing the manuscript.

Biochemical Pharmacology 130 (2017) 71–82

Contents lists available at ScienceDirect

Biochemical Pharmacology

journal homepage: www.elsevier.com/locate/biochempharm

Selective upregulation of TNFα expression in classically-activated human monocyte-derived macrophages (M1) through pharmacological interference with V-ATPase

Lea Thomas [a], Zhigang Rao [a], Jana Gerstmeier [a], Martin Raasch [b], Christina Weinigel [c], Silke Rummler [c], Dirk Menche [d], Rolf Müller [e], Carlo Pergola [a], Alexander Mosig [b], Oliver Werz [a,*]

[a] Institute of Pharmacy, Friedrich Schiller University Jena, Philosophenweg 14, D-7743 Jena, Germany
[b] Institute of Biochemistry II and Center for Sepsis Control and Care, University Hospital Jena, Jena, Germany
[c] Institute of Transfusion Medicine, University Hospital Jena, Jena, Germany
[d] Kekulé-Institut für Organische Chemie und Biochemie der Rheinischen Friedrich-Wilhelms-Universität Bonn, Bonn, Germany
[e] Helmholtz-Institute for Pharmaceutical Research Saarland (HIPS), Helmholtz Centre for Infection Research and Pharmaceutical Biotechnology at Saarland University, Germany

ARTICLE INFO

Article history:
Received 21 December 2016
Accepted 1 February 2017
Available online 9 February 2017

Keywords:
Vacuolar-type H(+)-ATPase
Archazolid
Tumor necrosis factor α
Macrophages
Interleukin
NFκB

ABSTRACT

Pharmacological interference with vacuolar-type H(+)-ATPase (V-ATPase), a proton-translocating enzyme involved in protein transport and pH regulation of cell organelles, is considered a potential strategy for cancer therapy. Macrophages are critically involved in tumor progression and may occur as pro-tumoral M2 phenotype, whereas classically-activated M1 can inhibit tumor development for example by releasing tumor-suppressing molecules, including tumor necrosis factor (TNF)α. Here, we show that targeting V-ATPase by selective inhibitors such as archazolid upregulates the expression and secretion of TNFα in lipopolysaccharide (LPS)- or LPS/interferon (INF)γ-activated M1-like macrophages derived from human blood monocytes. In contrast, archazolid failed to elevate TNFα production from uncommitted (M0) or interleukin (IL)-4-treated M2-like macrophages. Secretion of other relevant cytokines (i.e., IL-1β, IL-6, IL-10) or chemokines (i.e. IL-8 and monocyte chemotactic protein-1) from M1 was not affected by archazolid. Though V-ATPase inhibitors elevated the lysosomal pH in M1 comparable to chloroquine or ammonium chloride, the latter agents suppressed TNFα secretion. Archazolid selectively increased TNFα mRNA levels, which was abolished by dexamethasone. Interestingly, archazolid enhanced the phosphorylation and nuclear translocation of the p65 subunit of NFκB and stimulated phosphorylation of SAPK/JNK. In a microfluidically-supported human tumor biochip model, archazolid-treated M1 significantly reduced tumor cell viability. Together, our data show that V-ATPase inhibition selectively upregulates TNFα production in classically-activated macrophages along with NFκB and SAPK/JNK activation. Such increased TNFα release caused by V-ATPase inhibitors may contribute to tumor suppression in addition to direct targeting cancer cells.

1. Introduction

Combination of direct cytotoxic activity against tumor cells with concomitant capacity to favorably modify the tumor microenvironment might be an appealing option for pharmacological treatment of diverse cancers with clinical relevance [1]. For example, the clinically used chemotherapeutic agent trabectedin, in addition to killing cancer cells, depletes monocytes and tumor-associated macrophages (TAMs) in tumor patients as a key component of its anti-tumor activity [2]. However, the discovery of relevant targets in this respect is still in demand in order to simultaneously repress

Abbreviations: FITC, fluorescein isothiocyanate; IL, interleukin; IFNγ, interferon γ; IκB, inhibitor of nuclear factor kappa B; LPS, lipopolysaccharide; MCP-1, monocyte chemotactic protein-1; M-CSF, macrophage colony-stimulating factor; MTT, 3-(4,5-dimethylthiazol-2-yl)-2,5-diphenyltetrazolium bromide; NFκB, nuclear factor kappa B; p38 MAPK, p38 mitogen-activated protein kinase; PBMC, peripheral blood mononuclear cells; SAPK/JNK, stress-activated protein kinase/Jun amino-terminal kinases; TAM, tumor-associated macrophage; TNFα, tumor necrosis factorα; V-ATPase, vacuolar-type H(+)-ATPase.

* Corresponding author.
E-mail addresses: lea.thomas@uni-jena.de (L. Thomas), zhigang.rao@uni-jena.de (Z. Rao), jana.gerstmeier@uni-jena.de (J. Gerstmeier), Martin.Raasch@med.uni-jena.de (M. Raasch), christina.weinigel@med.uni-jena.de (C. Weinigel), silke.rummler@med.uni-jena.de (S. Rummler), dirk.menche@uni-bonn.de (D. Menche), Rolf.Mueller@helmholtz-hzi.de (R. Müller), pergolacarlo@googlemail.com (C. Pergola), Alexander.MOSIG@med.uni-jena.de (A. Mosig), oliver.werz@uni-jena.de (O. Werz).

http://dx.doi.org/10.1016/j.bcp.2017.02.004
0006-2952/

the viability of cancer cells and to modulate tumor-associated mononuclear cells by a single agent.

The vacuolar-type H(+)-ATPases (V-ATPases) are ATP-dependent proton translocating macromolecular complexes that acidify lysosomes, endosomes, Golgi apparatus, and certain secretory granules in all eukaryotes [3,4]. V-ATPases participate in physiological processes such as cellular pH homeostasis, receptor-mediated endocytosis, virus and toxin entry, intracellular trafficking as well as protein degradation and processing [3]. Aberrant regulation of pH by V-ATPases is implicated in several diseases including osteoporosis, renal tubular acidosis, and malignant neoplasms [5,6]. V-ATPase is highly expressed on the plasma membrane of tumor cells and particularly contributes to the acidification of tumor microenvironments, thus supporting tissue damage, acquisition of metastatic cell phenotypes, and tumor invasiveness [6,7]. Accordingly, specific inhibitors of V-ATPase that decrease the acidity of tumors, reduced the survival of tumor cells and tumor metastasis, and impaired chemoresistance [6,8]. In fact, V-ATPase is considered as promising target in various types of cancer [6].

Cytokines and chemokines significantly impact the tumor microenvironment to which TAMs are exposed, and represent essential factors that impact the heterogeneity of TAM functions [9]. TAMs consist of different phenotypes with partly opposite impact on tumors: the M2-like subtypes play pivotal roles in tumor progression by promoting cancer cell survival, angiogenesis, and immunosuppression, and they represent - as major part of TAMs – a remarkable fraction of tumor-infiltrating immune cells [9,10]. In contrast, classically-activated M1-like subsets are indispensable innate immune cells with microbicidal and tumoricidal activity that produce high levels of anti-tumoral molecules such as tumor necrosis factor (TNF)α, thus opposing cancer cells and preventing the establishment and progression of cancers [1,10].

The role of V-ATPase in cytokine secretion was studied in peritoneal macrophages from mice or rabbits before [11–13]. Here, we aimed to obtain insights into the role of V-ATPase in cytokine and chemokine secretion from human macrophages derived from peripheral blood monocytes, taking into account macrophage plasticity and occurrence as different phenotypes. As a suitable tool to studying the role of V-ATPase we used the myxobacterial compound archazolid [14] that binds to V-ATPase [15–17]. Archazolid has been intensively investigated as anti-tumoral agent that induced apoptosis of cancer cells and reduced migration of invasive tumor cells *in vitro*, and decreased metastatic dissemination of breast tumors *in vivo* [18–20]. In various highly invasive tumor cell lines and leukemic cells, archazolid led to apoptosis due to activation of the hypoxia-inducible factor-1α (HIF1α) [18,21], and to anoikis induction [22]. Thus, archazolid represents a promising candidate for direct targeting of tumor cells via V-ATPase inhibition. We recently reported that archazolid reduces the secretion of cytokines and chemokines in primary human monocytes due to accumulation at the endoplasmic reticulum [23]. However, effects of archazolid on macrophages have not been addressed, and phenotype-specific functions of V-ATPase in cytokine/chemokine secretion from human macrophages have not been reported yet.

2. Materials and methods

2.1. Materials

Archazolid B was isolated from *Archangium gephyra* as previously described [14]. Apicularen A was from the natural compound library of HZI/HIPS (Braunschweig, Germany). RPMI 1640 with L-glutamine, penicillin, streptomycin, and fetal calf serum (FCS) were from PAA Laboratories (Pasching, Germany). For in-house made ELISA, the capture and detection antibodies were from R&D Systems (Abington, UK). U0126, SB203580, nigericin, and SP600125 were from Enzo Life Sciences (Lörrach, Germany), LY294002 from BIOZOL Diagnostica Vertrieb GmbH (Eching, Germany), actinomycin D from Cayman Chemical (Ann Arbor, MI), staurosporine from Calbiochem (Merck, Darmstadt, Germany), interferon (INF)γ and interleukin (IL)-4 from PeproTech (Hamburg, Germany), macrophage colony-stimulating factor (M-CSF) from Cell Guidance Systems Ltd (Cambridge, UK), Calcein-AM and 3-(4,5-dimethylthiazol-2-yl)-2,5-diphenyltetrazolium bromide (MTT) from Thermo Fisher Scientific Inc. (Waltham, MA), LysoTracker dye from Life Technologies (Schwerte, Germany) and ammonium chloride, bafilomycin A1, chloroquine, dexamethasone, diphenyleneiodonium chloride (DPI), LPS, parthenolide, propidium iodide and all other fine chemicals were from Sigma-Aldrich (Steinheim, Germany), unless indicated otherwise.

2.2. Isolation of monocytes, differentiation to macrophages and macrophage activation

The protocols for experiments with human monocytes were approved by the ethical commission of the Friedrich-Schiller-University Jena. All methods were performed in accordance with the relevant guidelines and regulations. Leukocyte concentrates from peripheral blood of healthy human donors which did not take anti-inflammatory medication for the last ten days were obtained from the Institute of Transfusion Medicine, University Hospital Jena, and prepared as described [23]. Peripheral blood mononuclear cells (PBMC) were isolated by dextran sedimentation and density centrifugation on lymphocyte separation medium (LSM 1077, PAA Laboratories, Pasching, Austria). Monocytes from the PBMC fraction were isolated by adherence for 1 h at 37 °C and 5% CO_2 to culture flasks (2×10^7 cells/mL RPMI 1640 medium supplemented with 10% heat-inactivated FCS, 2 mM L-glutamine, 100 U/mL penicillin, and 100 μg/mL streptomycin) [24].

For differentiation towards macrophages, freshly isolated monocytes were incubated for 6 days in RPMI 1640 supplemented with 5% FCS and human recombinant M-CSF (25 ng/mL) [25]. To obtain classically-activated macrophages (M1-like), cells were further treated with 100 ng/mL LPS (designated M_{LPS}) or 100 ng/mL LPS plus 100 ng/mL human recombinant IFNγ (M1) for 24 h. To obtain M2-like cells, macrophages were incubated with human recombinant IL-4 (20 ng/mL) for 24 h [25,26]. To assure correct polarization, cells were assessed by flow cytometry for expression of the M2 surface markers CD163 and CD206, while M1 and M_{LPS} were characterized by expression of CD40 and higher expression of HLA-DR (MHC class II receptor) than M2 [26].

2.3. Determination of cell viability

The viability of human macrophages was assessed by MTT assay as described [27]. Briefly, macrophages after 6 days of differentiation of monocytes were pre-incubated with compounds for 30 min at 37 °C (5% CO_2) and treated for 24 h with (I) 100 ng/mL LPS (M_{LPS}), (II) 100 ng/mL LPS plus 100 ng/mL INFγ (M1), (III) 20 ng/mL IL-4 (M2) or left untreated (M0). MTT was added, cells were further incubated for 4 h, and lysed in a buffer containing 10% (w/v) SDS. Staurosporine, a pan-kinase inhibitor and inducer of apoptosis, was used as positive control.

2.4. Immunofluorescence microscopy and live cell imaging

Macrophages (2.5×10^5/mL) were seeded on glass coverslips and incubated for 1 h at 37 °C and 5% CO_2. After attachment, cells were pre-incubated with test compounds (as indicated) and

stimulated with LPS (100 ng/mL), with LPS (100 ng/mL) plus IFNγ (100 ng/mL) or with IL-4 (20 ng/mL) for the indicated times at 37 °C and 5% CO_2. Then, cells were fixed with 4% (v/v) paraformaldehyde solution, autofluorescence of free formaldehyde was quenched with 50 mM ammonium chloride, and macrophages were permeabilized with 0.2% (v/v) Triton X-100. After blocking with 10% (v/v) non-immune goat serum (Invitrogen, Darmstadt, Germany), samples were incubated with antibodies against the c-subunit of V-ATPase (1:1000 anti-ductin, Biozol, Eching, Germany), LAMP-1 (1:1000, Abcam, Cambridge, UK), IκBα (1:125, mouse monoclonal anti-IκBα, Cell Signaling Technology, Danvers, MA) and NFκB (1:100, rabbit monoclonal anti-NFκB p65, Cell Signaling Technology) over night at 4 °C. The samples were washed and then stained with the fluorophore-labeled secondary antibodies Alexa Fluor 488 goat anti-rabbit IgG (1:500) and Alexa Fluor 555 goat anti-mouse IgG (1:500) (Invitrogen) for 10 min at RT in the dark. DNA was stained using DAPI (0.7 μg/mL) for 3 min at RT. Samples were placed on microscope slides (Roth, Karlsruhe, Germany) using Mowiol containing 0.25% *n*-propyl gallate (Sigma-Aldrich). The fluorescence was visualized with a Zeiss Axio Observer.Z1 inverted microscope (Carl Zeiss, Jena, Germany) and a LCI Plan-Neofluar 63x/1.3 Imm Corr DIC M27 objective. Images were taken with an AxioCam MR3 camera and were acquired, cut, linearly adjusted in the overall brightness and contrast, and exported by the AxioVision 4.8 software.

For imaging of living cells, macrophages (2.5×10^5/mL) were plated into glass bottom dishes (MatTek Corporation, Ashland, MA). After adherence, cells were treated with archazolid (100 nM) or vehicle for 30 min and stimulated for 24 h with either (I) 100 ng/mL LPS, (II) 100 ng/mL LPS plus 100 ng/mL INFγ, or (III) 20 ng/mL IL-4.

For imaging of fluorescein isothiocyanate (FITC) dextran (Thermo Fisher Scientific Inc.) uptake into macrophages, cells were treated as described in pH measurements. Cells were imaged immediately using the Axio Observer Z1 inverted microscope and a Plan-Apochromat 40×/1,3 Oil DIC M27 objective or a LCI Plan-Neofluar 63×/1.3 Imm Corr DIC M27 objective.

2.5. Determination of cytokine/chemokine levels

After 6 days of differentiation of monocytes to macrophages with M-CSF (25 ng/mL) at 37 °C and 5% CO_2, test compounds or vehicle were added to macrophages and 30 min later, cells were incubated for 24 h with either (I) 100 ng/mL LPS, (II) 100 ng/mL LPS plus 100 ng/mL INFγ, or (III) 20 ng/mL IL-4. For measurement of extracellular cytokine levels, supernatants were collected by centrifugation (2000*g*, 4 °C, 10 min). Cytokines and chemokines were either analyzed by using commercially available ELISA kits (IL-8, Assaypro, St. Charles, MO) according to manufacturer's specifications, or by in-house made ELISA (IL-1β, IL-6, IL-10, TNFα, monocyte chemotactic protein (MCP)-1).

2.6. pH measurements in macrophages

pH measurements were performed according to [28], and compositions of sodium and potassium buffers were used as described [29]. For measurements of the vesicular pH, macrophages were incubated with 0.5 mg/mL FITC-dextran (70,000 MW, Sigma-Aldrich) for 1 h. Cells were washed with PBS, pre-incubated with test compounds or vehicle for 30 min and stimulated with 100 ng/mL LPS for 24 h. The pH values were calculated from the ratio of fluorescence intensities excited at 480 nm and 450 nm and emission at 520 nm. *In situ* fluorescence calibration was performed with the ionophore nigericin (10 μM) in potassium buffer at pH values between 4.5 and 7.5.

For analysis by LysoTracker® staining, macrophages (2.5×10^5/mL) were plated into glass bottom dishes (MatTek Corporation). After adherence, cells were treated with test compounds or vehicle for 30 min and stimulated with 100 ng/mL LPS for 24 h. Macrophages were then stained with the fluorescent LysoTracker® dye (50 nM) for 1 h. After washing, the red fluorescence of the accumulated probe in acidic cell organelles was imaged using the Axio Observer Z1 microscope and a LCI Plan-Neofluar 63x/1.3 Imm Corr DIC M27 objective.

2.7. Relative quantification of TNFα and IL-1β mRNA levels in macrophages and determination of TNFα mRNA degradation

After 6 days of differentiation of monocytes to macrophages with M-CSF (25 ng/mL), macrophages were pre-incubated with test compounds or vehicle for 30 min and stimulated with 100 ng/mL LPS for the indicated times at 37 °C and 5% CO_2. For measurement of TNFα mRNA degradation, macrophages were stimulated with 100 ng/mL LPS for 24 h and incubated with archazolid or vehicle for 1 h. Then, transcription was blocked by addition of actinomycin D (5 μg/mL) and cells were incubated for the indicated times. Total RNA was isolated using the E.Z.N.A.® Total RNA Kit I (Omega Biotek, Norcross, GA) and cDNA was generated by reverse transcription with SuperScript® III First-Strand Synthesis SuperMix (Invitrogen). cDNA was amplified by PCR and quantified using Maxima SYBR Green/ROX qPCR Master Mix (Fermentas, Darmstadt, Germany). To calculate the relative TNFα mRNA expression (normalized to B2 M) the $2^{(-\Delta\Delta C(T))}$ method was applied [30]. Primers used: human beta-2-microglobulin (B2 M) forward primer 5′-CTCCGTGGCCTTAGCTGTG-3′, human B2 M reverse primer 5′-TTTGGAGTACGCTGGATAGCCT-3′, human TNFα forward primer 5′-CCCAGGGACCTCTCTCTAATC-3′, human TNFα reverse primer 5′-ATGGGCTACAGGCTTGTCACT-3′, human IL-1β forward primer 5′-ACAGATGAAGTGCTCCTTCCA-3′, human IL-1β reverse primer 5′-GTCGGAGATTCGTAGCTGGAT-3′ (Tib Molbiol, Berlin, Germany).

2.8. Determination of phosphorylation of protein kinases and transcription factors by Western blot analysis

Macrophages, obtained by differentiation of monocytes with M-CSF (25 ng/mL) at 37 °C and 5% CO_2 for 6 days, were first starved for 6 h (AKT, ERK-1/2, p38 MAPK, MEK1/2, SAPK/JNK, MKK3/6) or directly pre-incubated (NFκB p65, STAT-1, STAT-3) with archazolid (100 nM) or vehicle (0.1% DMSO) for 30 min at 37 °C, 5% FCS was added and cells were stimulated with LPS (100 ng/mL) for 15 min. Macrophages were placed on ice, washed once with PBS and lysed with a NP-40 lysis buffer (1% (v/v) NP-40, 1 mM sodium vanadate, 10 mM sodium fluoride, 5 mM sodium pyrophosphate, 25 mM β-glycerophosphate, 5 mM EDTA, and freshly added 10 μg/mL leupeptin hemisulfate salt, 60 μg/mL trypsin inhibitor from soybean, 1 mM phenylmethylsulfonyl fluoride in TBS, pH 7.4). Lysates were centrifuged (10,000*g*, 4 °C, 5 min), and protein concentrations in the supernatants were determined using a Protein Assay (Bio-Rad Laboratories, Hercules, CA). After addition of 4× SDS loading buffer (50 mM Tris-HCl, pH 6.8, 2% (w/v) SDS, 10% (v/v) glycerol, 1% (v/v) β-mercaptoethanol, 12.5 mM EDTA, 0.02% (w/v) bromophenol blue) to the lysates, samples were boiled for 5 min at 95 °C. Proteins were separated by SDS-PAGE and blotted onto nitrocellulose membranes (Amersham Biosciences, Little Chalfont, UK). After blocking with 5% (w/v) bovine serum albumin or low-fat milk powder (Roth, Karlsruhe, Germany), membranes were incubated with primary antibodies overnight at 4 °C. Antibodies, obtained from Cell Signaling Technology (Danvers, MA), were used as follows: NFκB p65, 1:500, rabbit monoclonal anti-NFκB p65; phospho-NFκB p65, 1:500, mouse monoclonal

anti-phospho-NFκB p65; phospho-STAT-1, 1:1000, rabbit polyclonal anti-phospho-STAT-1; phospho-STAT-3, 1:1000, rabbit monoclonal anti-phospho-STAT-3; p38 MAPK, 1:1000, rabbit monoclonal anti-p38 MAPK; phospho-p38 MAPK, 1:1000, rabbit polyclonal anti-phospho-p38 MAPK; ERK-1/2, 1:1000, rabbit polyclonal anti-p44/42 ERK; phospho-ERK-1/2, 1:1000, mouse monoclonal anti-phospho-p44/42 ERK; Akt, 1:1000, mouse monoclonal anti-Akt; phospho-Akt, 1:1000, rabbit polyclonal anti-phospho-Akt; MEK1/2, 1:1000, rabbit polyclonal anti-MEK1/2; phospho-MEK1/2, 1:1000, rabbit polyclonal anti-phospho-MEK1/2; phospho-MKK3, 1:1000, rabbit monoclonal anti-phospho-MKK3/6; phospho-SAPK/JNK, 1:1000, mouse monoclonal anti-phospho-SAPK/JNK. Antibodies against GAPDH: 1:1000, mouse monoclonal anti-GAPDH (Santa Cruz Biotechnology, Heidelberg, Germany) and β-actin, 1:1000, mouse monoclonal anti-β-actin (Santa Cruz Biotechnology). Membranes were washed and incubated with fluorescently-labeled secondary antibodies (LI-COR Biosciences, Bad Homburg, Germany) for 1 h at RT in the dark. Proteins were detected using the Odyssey imaging system (LI-COR Biosciences, Bad Homburg, Germany).

2.9. Measurement of ROS formation

ROS levels were assessed as reported before [31]. Briefly, macrophages were incubated with test compounds or vehicle (0.1% DMSO) for 30 min and stimulated with LPS (100 ng/mL) for 24 h or left untreated. Cells were washed and incubated in HBSS buffer containing 2′-7′-dichlorofluorescein diacetate (DCFH-DA, Sigma-Aldrich) (10 μM) for 30 min at 37 °C/5% CO_2. To detect and quantify intracellular formation of ROS, the fluorescence of the deacetylated dye (2′-7′-dichlorofluorescein) was measured at an excitation wavelength of 485 nm and an emission wavelength of 535 nm using a NOVOstar microplate reader (BMG Labtechnologies GmbH, Offenburg, Germany).

2.10. Microfluidically supported biochip assay

Biochips were prepared by injection moulding from cyclo olefin polymer (COP) Zeonor®, obtained from microfluidic ChipShop GmbH (Jena, Germany), and manufactured as described previously [32]. MCF-7 cells were obtained at LGC Standards (Wesel, Germany). Authentication of MCF-7 was carried out by STR analyses (LGC Standards) and experiments were completed within 4 months of receipt of the cell line. Human umbilical vein endothelial cells (HUVEC) were isolated from human umbilical cords and cultured for up to four passages as described previously [32]. Donors were informed about the aim of the study and gave written consent. HUVEC were seeded at top of the biochip-embedded membrane, MCF-7 cells were seeded at the lower compartment of the biochip. Monocytes (in a six well plate) were differentiated towards macrophages in presence of M-CSF for 6 days, and M1 polarization was induced by addition of LPS plus IFNγ while M2 polarization was induced by addition of IL-4 for 24 h. These M1 and M2 were then added to the HUVEC into the biochip. After 24 h co-culture with HUVECs, medium containing 30 nM archazolid or vehicle (0.1% DMSO) was added, and after 30 min, it was replaced by fresh medium (without archazolid). Then, cells perfused over the vascular layer with a shear stress rate of 3 dyn/cm^2 for 30 min, followed by 24 h incubation with medium. In control experiments, macrophages were omitted and only HUVECs were used in the upper compartment. The viability of the cells was analyzed by immunofluorescence microscopy using Calcein-AM (viable cells, green) and propidium iodide (dead cells, red) staining. Mean fluorescence intensity (MFI) of the Calcein-AM staining was measured by random field analysis of 40 regions of interest per experiment.

2.11. Statistics

Data are presented as mean + standard error of the mean (SEM) of *n* experiments, where *n* represents the number of experiments. Statistical data were calculated using GraphPad InStat program (GraphPad Software, CA), and were analyzed by Student's *t* test for paired groups and by one-way ANOVA for independent or correlated samples followed by a Bonferroni (<5 groups) or Tukey-Kramer (>5 groups) post hoc test for multiple comparisons. A P value of <0.05 (*) was considered significant.

3. Results

3.1. Expression of V-ATPase in macrophages and effects of the V-ATPase inhibitor archazolid on the viability and morphology of macrophages

According to well-established protocols, we induced M-CSF-treated macrophages (designated M0) with LPS/INFγ towards classically-activated M1 or with IL-4 towards M2-like subsets [33]. Moreover, M-CSF-treated macrophages were activated by LPS alone (designated M_{LPS}), which strongly resemble M1 [26] similar to macrophages activated by INFγ alone [33]. Previous studies showed that macrophages from different origins and species express V-ATPase and respond to V-ATPase inhibitors in different ways [13,31,34–39]. We first confirmed V-ATPase expression in human monocyte-derived macrophages [40] by Western blot (not shown) and by using immunofluorescence microscopy where no obvious differences regarding V-ATPase subcellular localization between the macrophage phenotypes were immediately apparent (Fig. 1A). Side-by-side analysis of LAMP-1, a marker protein for lysosomes, revealed colocalisation with V-ATPase (merge, Fig. 1B), suggesting that V-ATPase might be located to vesicles.

The V-ATPase inhibitor archazolid effectively induces apoptosis in cancer cells leading to cell death [18,19]. Since we aimed at using arachzolid as tool compound to study V-ATPase in various human macrophage phenotypes, we first analyzed whether archazolid may affect the viability of macrophages. Incubation of activated macrophages (M_{LPS}, M1 or M2) with archazolid (1, 10, or 100 nM) revealed no loss of cell viability within 24 h, whereas the pan-protein kinase inhibitor and apoptosis inducer staurosporine (3 μM) efficiently reduced cell viability, as expected (Fig. 1C). Microscopic analysis confirmed cellular integrity of M_{LPS}, M1, and M2 upon archazolid treatment but revealed obvious alterations of the cell shape for M_{LPS} and M1 that was not evident for M2, for which the morphology was seemingly not affected by archazolid (Fig. 1D).

3.2. V-ATPase inhibitors induce TNFα secretion in classically-activated macrophages

Having confirmed that archazolid is not detrimental for cellular integrity and viability of macrophages, we next tested whether the compound could modulate cytokine and chemokine release. Differentiated macrophages (M0) were pretreated with archazolid and then either activated by LPS/INFγ (M1) or IL-4 (M2) for 24 h. Analysis of IL-1β, IL-6, IL-8, IL-10 and MCP-1 in the medium revealed no significant modulation of the release of these proteins by archazolid neither in M1 nor in M2 (Fig. 2A). However, the levels of TNFα were upregulated by archazolid (100 nM) about 2.4-fold in M1, whereas the compound failed to alter TNFα levels in M2 (Fig. 2A) and in M0 (not shown). More detailed concentration response experiments showed that for M_{LPS} or M1 the maximal effect (2.9- to 3.4-fold) on TNFα release was obtained at 30 nM archazolid and slightly declined at 100 nM (Fig. 2B). In contrast to archazolid

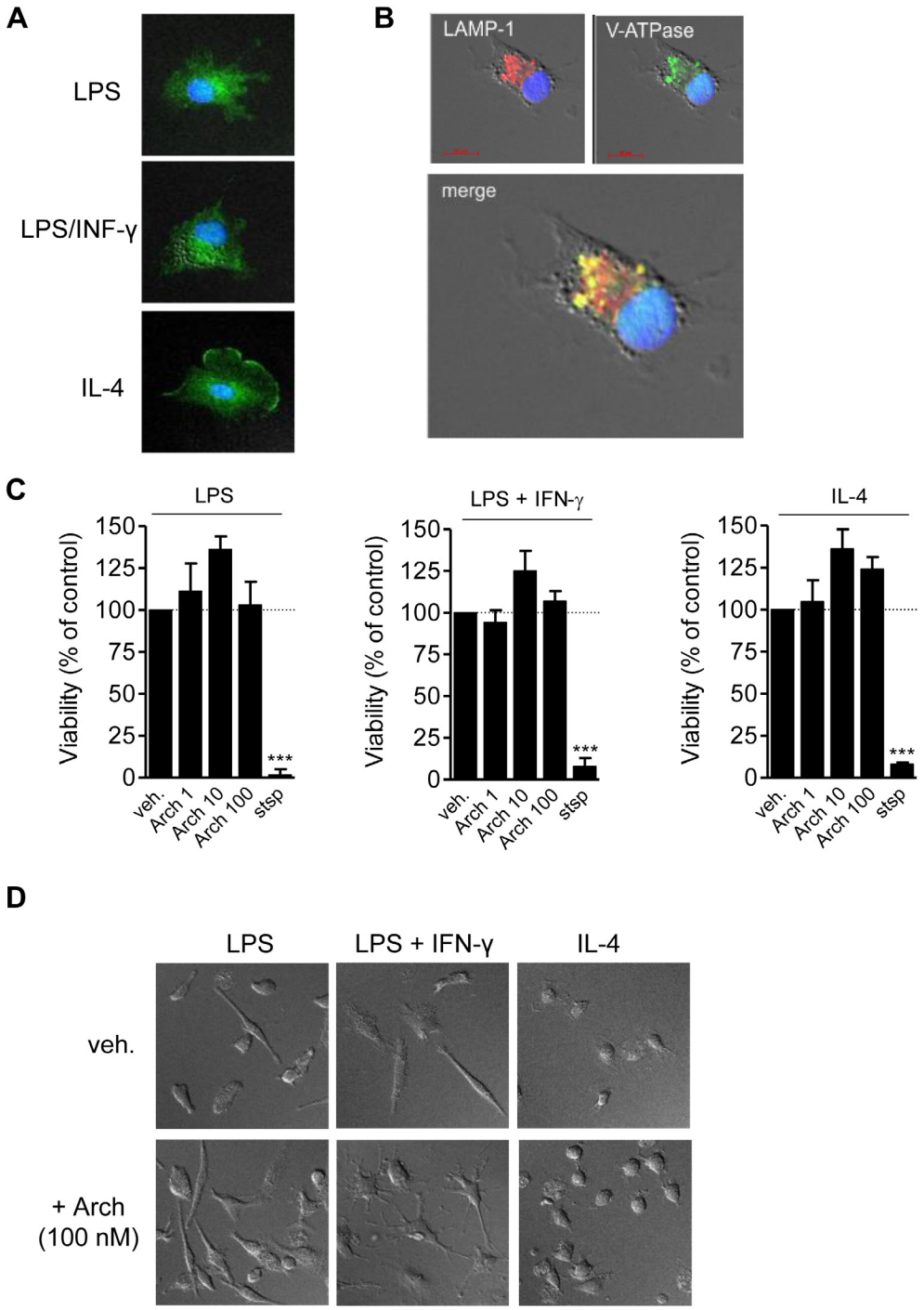

Fig. 1. Expression and subcellular localization of V-ATPase in macrophages and effects of archazolid on macrophage viability and morphology. (A) Macrophages, obtained from human blood monocytes after differentiation with M-CSF (25 ng/mL) for six days, were stimulated with LPS (100 ng/mL), with LPS (100 ng/mL) plus IFNγ (100 ng/mL) or with IL-4 (20 ng/mL) for 24 h. Cells were permeabilized and incubated with an antibody against V-ATPase (green), followed by Alexa Fluor 488 goat anti-rabbit IgG. Nuclei were stained with DAPI (blue). (B) Macrophages were stimulated with LPS (100 ng/mL) plus IFNy (100 ng/mL) for 24 h, permeabilized and incubated with antibodies against v-ATPase (green) or LAMP-1 (red), followed by Alexa Fluor 488 goat anti-rabbit IgG and Alexa Fluor 555 goat anti-rabbit IgG; nuclei were stained with DAPI (blue); differential interference contrast. (C, D) Macrophages were pre-incubated with archazolid (1, 10, 100 nM (C) and 100 nM (D)), staurosporine (3 μM) or vehicle (0.1% DMSO) for 30 min and stimulated with LPS (100 ng/mL), with LPS (100 ng/mL) plus IFNγ (100 ng/mL) or with IL-4 (20 ng/mL) for 24 h. (C) Cell viability was determined by MTT assay. (D) Effects of archazolid (100 nM) on the morphology of macrophages. Microscopic images are shown as differential interference contrast. All results are representative of three independent experiments. Values are given as percentage of vehicle control (=100%), means + SEM; n = 3. $^{***}P < 0.001$ vs. vehicle. ANOVA + Bonferroni post hoc test. (For interpretation of the references to colour in this figure legend, the reader is referred to the web version of this article.)

and as expected, dexamethasone repressed TNFα levels in M_{LPS} and M1 (Fig. 2B). To confirm that the observed effect of archazolid is related to interference with V-ATPase, we tested other V-ATPase inhibitors, that is, apicularen A and bafilomycin A1 (1, 10 and 100 nM, each) in the same experimental settings. For both compounds upregulation of TNFα levels was evident in M_{LPS} and M1 with maximal effects at 10 nM (Fig. 2C), supporting that suppression of V-ATPase accounts for increased TNFα release.

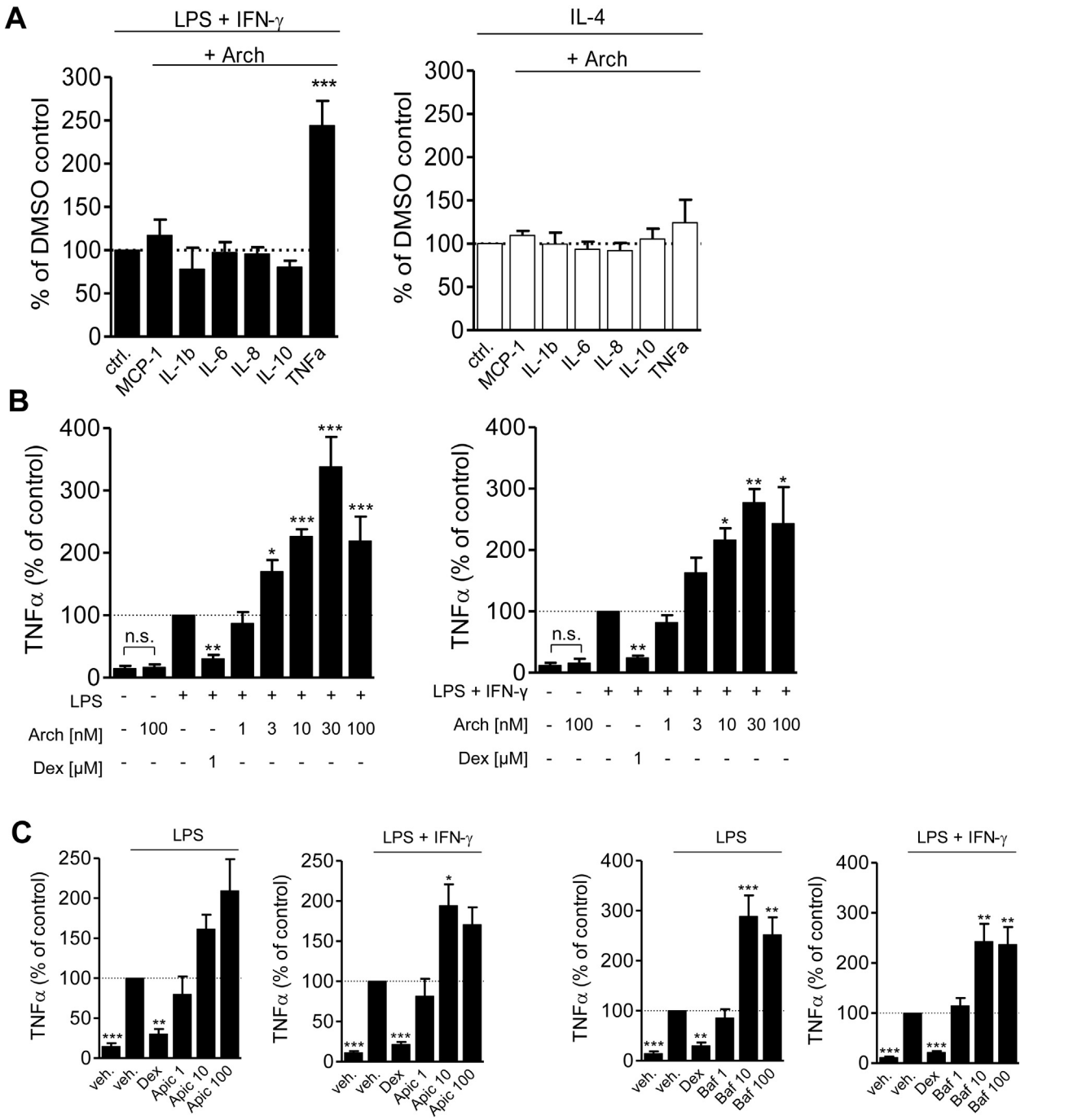

Fig. 2. Effects of V-ATPase inhibitors on cytokine and chemokine release from human macrophages. Human isolated blood monocytes were differentiated to macrophages with M-CSF (25 ng/mL) within six days. For analysis of cytokine release, macrophages were pre-incubated with archazolid, apicularen A, or bafilomycin A1 at the indicated concentrations, with dexamethasone (1 μM) or with vehicle (0.1% DMSO) for 30 min and then stimulated with LPS (100 ng/mL), LPS plus IFN-γ, or IL-4 (20 ng/mL) for another 24 h. Cytokines and chemokines in the supernatants were analyzed by ELISA. Values shown are percentages of vehicle control, means + SEM. $^{*}P < 0.05$, $^{**}P < 0.01$, $^{***}P < 0.001$ vs. vehicle (DMSO). Paired *t*-test (A) or ANOVA + Tukey post hoc test (B, C). (A) Archazolid was used at 100 nM. Absolute values of LPS + IFNγ-stimulated vehicle (100%) control: MCP-1: 98.3 ± 43.4 ng/mL, IL-1β: 1709 ± 1465 pg/mL, IL-6: 30.8 ± 9.3 ng/mL, IL-8: 52.2 ± 4.8 ng/mL, IL-10: 1211 ± 256 pg/mL, TNFα: 1992 ± 653 pg/mL. Absolute values of IL-4-stimulated vehicle (100%) control: MCP-1: 86.1 ± 34.6 ng/mL, IL-1β: 601 ± 403 pg/mL, IL-6: 11.3 ± 1.9 ng/mL, IL-8: 45.1 ± 4.8 ng/mL, IL-10: 819 ± 240 pg/mL, TNFα: 259 ± 87 pg/mL; n = 4. (B, C) Absolute value of LPS-stimulated vehicle (100%) control: 1383 ± 229 pg/mL (n = 6), absolute value of LPS + IFNγ-stimulated vehicle (100%) control: 1906 ± 273 pg/mL (B, n = 3) and 2347 ± 632 pg/mL (C, n = 6).

3.3. Archazolid causes elevation of the lysosomal pH in classically-activated macrophages

Blocking V-ATPase is well-known to cause an elevated lysosomal pH in various cell types [16,41,42], and along these lines, archazolid led to significantly increased lysosomal pH in M_{LPS} as evidenced by the pH-dependent internalization of FITC-labeled dextran (Fig. 3A). Elevation of the lysosomal pH by archazolid was pronounced at 100 nM but only slightly affected at 10 nM. In agreement with the literature [43,44], chloroquine (100 μM) and NH_4Cl (50 mM), used as control tools, elevated the lysosomal pH in M_{LPS} to a comparable degree as 10 nM archazolid (Fig. 3A).

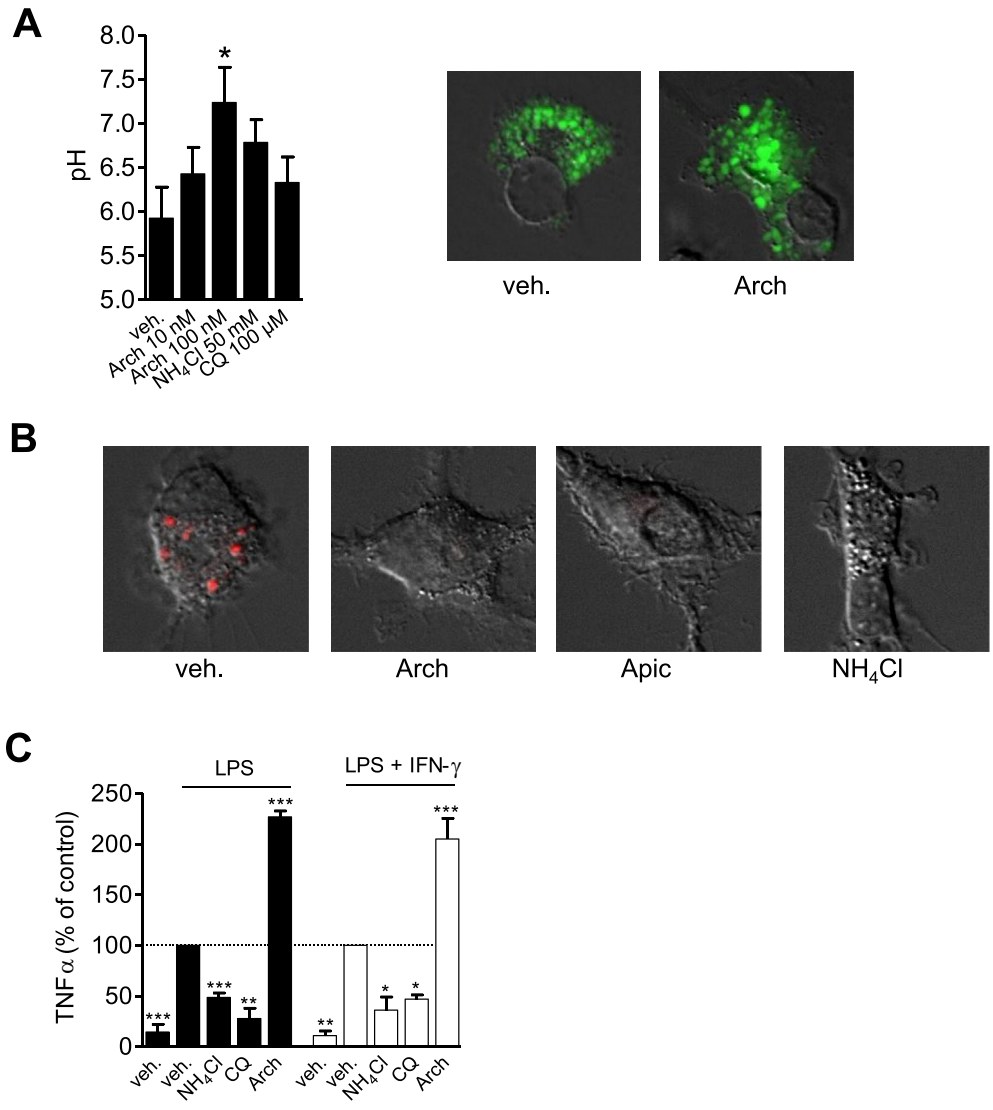

Fig. 3. Effects of V-ATPase inhibition on the lysosomal pH of human macrophages and correlation with cytokine release. Human isolated blood monocytes were differentiated to macrophages with M-CSF (25 ng/mL) within six days. (A) Macrophages were incubated with FITC-dextran (0.5 mg/mL) for 60 min, preincubated with archazolid at the indicated concentrations, ammonium chloride (50 mM), chloroquine (100 μM), or vehicle (0.1% DMSO) for 30 min and stimulated with LPS (100 ng/mL) for 24 h. FITC-Dextran uptake into lysosomes was determined by measurement of emission at 520 nm or by analysis of immunofluorescence pictures (FITC-dextran: green; differential interference contrast). (B) Macrophages were pre-incubated with archazolid (100 nM), apicularen A (100 nM), ammonium chloride (50 mM) or vehicle (DMSO) for 30 min and stimulated with LPS (100 ng/mL) for 24 h. Macrophages were incubated with LysoTracker (50 nM; red) for 60 min and staining of acidic organelles was observed using a fluorescence microscope. (C) Macrophages were pre-incubated with archazolid (10 nM), ammonium chloride (50 mM), chloroquine (100 μM) or vehicle (DMSO) for 30 min and stimulated with LPS (100 ng/mL) or LPS (100 ng/mL) plus IFNγ (100 ng/mL) for 24 h. TNFα levels in supernatants were analyzed by ELISA. Values are given as percentage of vehicle control (=100%), means + SEM; n = 8 (A, left panel), n = 3 (C). $^{*}P < 0.05$, $^{**}P < 0.01$, $^{***}P < 0.001$ vs. the LPS-stimulated vehicle (=100%). ANOVA + Bonferroni post hoc test. Pictures shown are representative of three independent experiments.

A similar result was obtained, when changes of pH in organelles were monitored using the pH sensitive LysoTracker® probe and fluorescence microscopy (Fig. 3B). Note that the structurally distinct V-ATPase inhibitor apicularen A also elevated the pH in organelles of M_{LPS}, just like archazolid.

In order to investigate whether the increased release of TNFα by archazolid and other V-ATPase inhibitors was due to lysosomal pH alterations, we took advantage of chloroquine and NH_4Cl as tool compounds (that also elevated the lysosomal pH) and tested if these agents could increase TNFα release from M_{LPS} and M1 as well. Surprisingly, chloroquine (100 μM) and NH_4Cl (50 mM) failed to enhance TNFα release, but instead markedly repressed it in both M_{LPS} and M1 (Fig. 3C). Therefore, the data suggest that other mechanisms than solely elevation of lysosomal pH is responsible for the TNFα-upregulatory effects by archazolid and other V-ATPase inhibitors.

3.4. Archazolid affects TNFα release on the mRNA level and increases TNFα mRNA expression in classically-activated macrophages

The stimulatory effect of archazolid on TNFα release in classically-activated M1 was abrogated by co-incubation with dexamethasone (Fig. 4A), a glucocorticoid that interferes with TNFα gene expression. This finding led us to assume that archazolid may affect the expression of TNFα at the mRNA level. M(0) were pretreated with or without archazolid in the presence or absence of dexamethasone and 30 min later, LPS was added to obtain M_{LPS}. TNFα mRNA levels after 4 and 8 h were significantly higher in the presence of archazolid versus cells treated with LPS alone, and also after 1 and after 16, 20 and 24 h, archazolid led to elevated levels of TNF mRNA (Fig. 4B). Note that mRNA of IL-1β, studied as control, was not increased by archazolid (Fig. 4B). Coincubation with dexamethasone effectively repressed the up-regulatory effect of

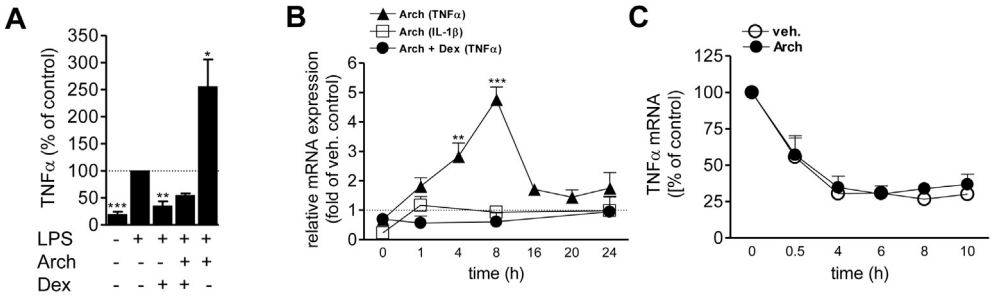

Fig. 4. Effects of archazolid on TNFα mRNA expression and degradation. (A) Macrophages, obtained from human blood monocytes after differentiation with M-CSF (25 ng/mL) for six days, were pre-incubated with archazolid (100 nM), with or without dexamethasone (1 μM) or with vehicle (0.1% DMSO) for 1 h and then stimulated with LPS (100 ng/mL) for 8 h. Levels of TNFα protein in supernatants were analyzed by ELISA. Values are given as percentage of vehicle control (100%, DMSO), means + SEM; n = 3. $^{*}P < 0.05$, $^{**}P < 0.01$, $^{***}P < 0.001$ vs. the LPS-stimulated vehicle control. ANOVA + Bonferroni post hoc test. (B) Macrophages were pre-incubated with archazolid (100 nM), with archazolid (100 nM) plus dexamethasone (1 μM) or with vehicle (0.1% DMSO) for 1 h and then stimulated with LPS (100 ng/mL). At the indicated time points mRNA was extracted and determined by RT-qPCR. mRNA levels of TNFα were normalized against those of B2 M. Values shown are given as fold increase over control, means + SEM; n = 4. $^{**}P < 0.01$, $^{***}P < 0.001$ vs. the unstimulated archazolid-treated sample at time point = 0 h. ANOVA + Tukey post hoc test. (C) Macrophages were stimulated with LPS (100 ng/mL) for 24 h and incubated with archazolid (10 nM) or vehicle (0.1% DMSO) for 60 min. Transcription was stopped by actinomycin D (5 μg/mL) and macrophages were further incubated for the indicated times. TNFα mRNA levels were determined by RT-qPCR. Values are given as percentage of control (100%), means + SEM; n = 4.

archazolid on TNFα mRNA expression (Fig. 4B). Experiments using actinomycin D that blocks mRNA transcription showed that archazolid does not affect TNFα mRNA degradation as possible reason for elevation of mRNA levels (Fig. 4C).

3.5. Effects of archazolid on protein kinases and transcription factors involved in LPS-signaling and on ROS formation

Because archazolid seemingly enhances the LPS-induced expression of TNFα mRNA in M_{LPS}, it appeared possible that the compound modulates LPS-induced signal transduction pathways. We thus analyzed the phosphorylation of typical protein kinases (PK) that are integrated in LPS-induced TNFα expression. M(0) were pre-treated with archazolid or respective reference PK inhibitors, stimulated with LPS for 15 min and analyzed for the phosphorylated form of the kinases by Western blot. LPS caused phosphorylation of Akt, ERK-1/2, p38 MAPK, MEK-1/2, and MEK-3/6 (Fig. 5A) but archazolid (10 or 100 nM) failed to modulate their phosphorylation. The reference inhibitors LY294002 for Akt phosphorylation, U0126 for ERK, and SB203580 for p38 MAPK, used to validate the identity of respective phosphorylated kinases/proteins detected by Western blot, blocked LPS-induced phosphorylation, as expected (Fig. 5A). A tendency for stimulated SAPK/JNK phosphorylation (reference inhibitor SP600125) was observed for 10 and 100 nM archazolid, although statistical significance was not reached (Fig. 5A). However, archazolid (10 and 100 nM) clearly elevated the phosphorylation of the p65 subunit of the transcription factor NFκB in M_{LPS} without marked elevation of NFκB p65 expression (Fig. 5B). An NFκB-stimulatory effect of archazolid was also observed when the translocation of activated NFκB to the nucleus was monitored using immunofluorescence microscopy, in agreement with disappearance of the NFκB chaperon IκB (Fig. 5C). Note that the LPS-induced phosphorylation of other relevant transcription factors, that is, STAT-1 and STAT-3 in M1 was not elevated by archazolid (Fig. 5D).

Because ROS production is closely linked to NFκB and SAPK/JNK signaling [45], we investigated if archazolid could modulate LPS-induced ROS formation in macrophages. Pre-incubation of macrophages with 10 or 30 nM archazolid prior to LPS significantly increased ROS levels within 24 h whereas the NADPH oxidase inhibitor DPI diminished ROS formation induced by LPS, as expected, and also abrogated the elevated ROS levels caused by archazolid (Fig. 6A). Finally, we investigated if the elevated ROS and NFκB activation are involved in archazolid-induced TNFα release. In fact, DPI (5 μM) that reduced archazolid-elicited ROS formation as well as the NFκB activation inhibitor parthenolide (10 μM) efficiently prevented the stimulatory effects of archazolid plus LPS on TNFα release from macrophages (Fig. 6B).

3.6. Archazolid enhances M1-mediated cytotoxicity against MCF-7 cells in a microfluidically biochip assay

To investigate if treatment of macrophages by archazolid influences cancer cell viability in co-cultures, we utilized a microfluidically-supported biochip assay [32], designed as a dynamically perfused three-dimensional human tumor model (Fig. 7A). Macrophages, polarized towards M1 or M2 were added to endothelial cells (ECs) and co-cultured in the upper chamber. The ECs are thought to separate the tumor from the blood cells mimicking the physiological barrier. MCF-7 cells, resembling the tumor component, were cultured underneath the EC-macrophage cell layer. EC-macrophage cell layers treated with archazolid (30 nM) for 30 min and subsequent incubation for 24 h significantly reduced the viability of MCF-7 cells in models containing M1, whereas in models containing M2 or in models devoid of macrophages, archazolid failed in this respect (Fig. 7B, C).

4. Discussion

Here we show that pharmacological targeting of V-ATPase causes selective elevation of TNFα production in classically-activated (i.e., M1 and M_{LPS}) human macrophage phenotypes. Intriguingly, the concomitant release of other cytokines (i.e. IL-1β, IL-6, IL-10) or chemokines (i.e. IL-8, MCP-1) in M1 and M_{LPS} was not elevated, and the corresponding cytokine/chemokine secretion of uncommitted M(0) and of alternatively activated M2 was not affected by archazolid. Because also other V-ATPase inhibitors such as bafilomycin and apicularen led to comparable effects, we suggest that interference with V-ATPase but not with an off-target of archazolid [46] is causative for the elevated TNFα levels. It appears that V-ATPase inhibition enhances the LPS- or LPS/INFγ-induced response of macrophages for TNFα expression, seemingly by augmenting LPS-evoked NFκB activation and ROS formation. Finally, in a biochip tumor model, archazolid caused reduced viability of MCF-7 breast cancer cells in co-culture with M1, but not with M2 or in absence of macrophages. Our data suggest that V-ATPase in classically-activated macrophages may play a regulatory role in TNFα expression implying a therapeutic

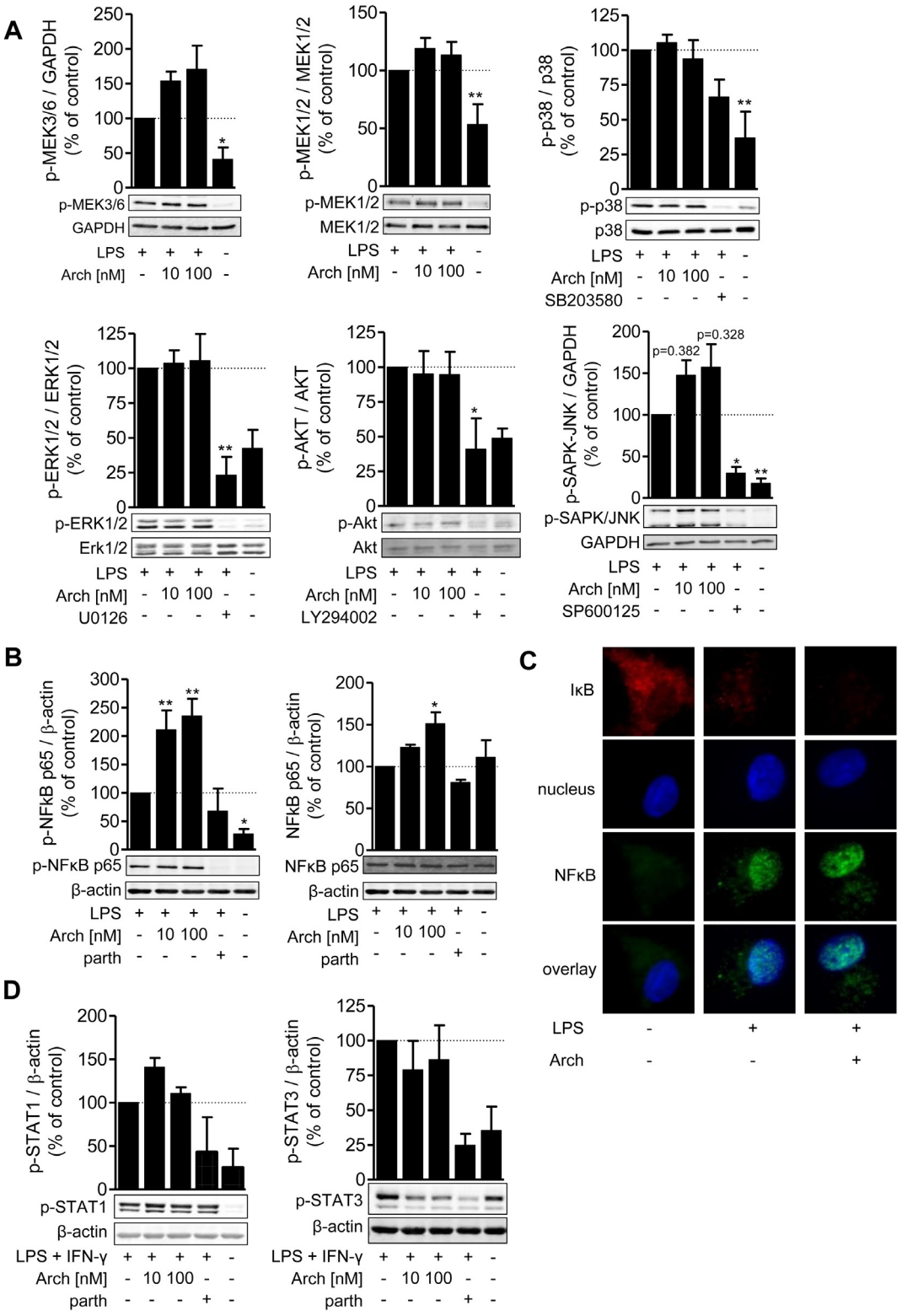

Fig. 5. Effects of archazolid on activation of protein kinases and transcription factors involved in LPS Signaling pathways. (A) Macrophages, obtained from human blood monocytes after differentiation with M-CSF (25 ng/mL) for six days, were first starved for 6 h and then pre-incubated with archazolid at the indicated concentrations, LY294002 (10 μM), U0126 (3 μM), SB203580 (10 μM), SP600125 (10 μM), or vehicle (0.1% DMSO) for 30 min, and stimulated with LPS (100 ng/mL) for 15 min. Protein phosphorylation or expression in cell lysates was analyzed by Western blotting; GAPDH or the respective unphosphorylated proteins were used for normalization. Representative Western blots of 4 independent experiments are shown; data (densitometric analysis) are means + SEM; n = 4. (B, D) Macrophages were pre-incubated with archazolid at the indicated concentrations, parthenolide (10 μM) or vehicle (0.1% DMSO) for 30 min and stimulated with LPS (100 ng/mL) for 15 min. (B) NFκB p65 phosphorylation (left panel) and expression (right panel) or (D) STAT-1 and -3 phosphorylation in cell lysates was analyzed by Western blotting; β-actin was used for normalization. Representative Western blots of 4 independent experiments are shown; data (densitometric analysis) are means + SEM; n = 4 (C) Macrophages were seeded onto coverslips, pre-incubated with archazolid (10 nM), or vehicle (0.1% DMSO) for 30 min and stimulated with LPS (100 ng/mL) for 15 min. Fixed and permeabilized cells were stained with antibodies against IκB (Alexa Fluor 555, red) and NFκB p65 (Alexa Fluor 488, green), nuclei were stained with DAPI (blue). Representative immunofluorescence images of three independent experiments are shown. (For interpretation of the references to colour in this figure legend, the reader is referred to the web version of this article.)

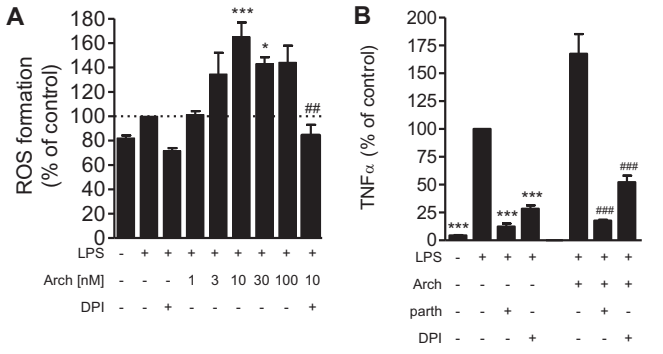

Fig. 6. Archazolid elevates ROS formation in LPS signaling macrophages; effects of ROS and NFκB inhibitors on archazolid-induced TNFα release. (A) Macrophages, obtained from human blood monocytes after differentiation with M-CSF (25 ng/mL) for six days, were pre-incubated with archazolid at the indicated concentrations, DPI (5 μM), or with vehicle (0.1% DMSO) for 30 min and stimulated with LPS (100 ng/mL) for 24 h. Fluorescence of the oxidised 2′,7′-dichlorofluorescin diacetate (5 μg/mL) was measured at an excitation wavelength of 485 nm and an emission wavelength of 535 nm. Values shown are percentages of vehicle control, means + SEM; n = 4. $^{*}P < 0.05$, $^{***}P < 0.001$ vs. the LPS-stimulated vehicle control (100%, DMSO); $^{\#\#}P < 0.01$ vs. cells treated with LPS plus 10 nM archazolid. (B) Macrophages were pre-incubated with DPI (5 μM), parthenolide (10 μM, parth) or vehicle (0.1% DMSO) for 15 min. Then, cells were treated with vehicle or archazolid (30 nM), and after another 15 min, cells were treated with LPS (100 ng/mL) for 24 h. TNFα in the supernatants was analyzed by ELISA. Values shown are percentages of LPS-stimulated controls (=100%), means + SEM. $^{***}P < 0.001$ vs. LPS plus vehicle (DMSO); $^{\#\#\#}P < 0.001$ vs. cells treated with LPS plus archazolid. ANOVA + Tukey post hoc test.

potential for V-ATPase inhibitors to intervene with diseases where increased TNFα levels might be beneficial, such as cancer.

V-ATPase is ubiquitously expressed in mammals and was studied in macrophages before, where it was shown to play roles in lysosomal and cytoplasmic pH homeostasis [34,42,47,48]. Also in our study, using archazolid for the first time as tool for investigating V-ATPase functions in macrophages, modulation of lysosomal pH homeostasis was apparent, since archazolid caused elevation of the pH in lysosomes. Of interest, in contrast to cancer cells that overexpress V-ATPase [5,6] and where V-ATPase inhibition by archazolid induces cell death [18–20,22,49], the viability of human monocyte-derived macrophages was not impaired in response to V-ATPase interference by archazolid. Similarly, archazolid failed to reduce the viability of human primary monocytes [23].

Pharmacological manipulation of V-ATPase in macrophages by respective inhibitors such as bafilomycin A1 was reported before [13,31,35,37,38,48,50]. Many of these studies focused on osteoclasts [51], macrophage cell lines [31] and macrophages from rodents [37,39,48] and from other animals [52], but only few studies addressed V-ATPase functions in human primary macrophages [40,50], and to the best of our knowledge there are no reports that studied the role of V-ATPase on cytokine/chemokine secretion of different macrophage phenotypes, such as M1 and M2. Therefore, one significant novelty of our study is the consideration of distinct human macrophage subtypes, that is, uncommitted M(0), classically-activated M1-like and so-called "resolving" M2-like macrophages that significantly differ in their bioactions [53]. In fact, we show here that blocking V-ATPase upregulates TNFα expression in classically-activated M1-like but not so in M(0) and M2 subtypes.

A previous study demonstrated that bafilomycin A1 reduced the amount of TNFα in LPS-activated alveolar macrophages from rabbits [11], and we recently found that archazolid suppresses TNFα secretion from human monocytes [23]. These opposing results versus our present data emphasize the need of distinguishing between monocyte/macrophage subsets. Recently, a differential role of V-ATPase in M1 and M2 was observed in phagosome pH regulation [40]. In line with our data are previous findings showing that V-ATPase suppresses NFκB and cytokine expression in LPS- or INFγ-activated macrophages [12]. It is noteworthy that among various cytokines and chemokines, solely TNFα was affected by archazolid. The reason for this effect is unknown but selective elevation of TNFα without concomitant increase of Il-1β via NFκB was also observed in LPS-stimulated murine peritoneal macrophages treated with the protein biosynthesis inhibitor cycloheximide [54]. Of interest, V-ATPase might be of importance for polarization towards M2 subsets. Thus, the lysosomal adaptor protein Lamtor1, which forms an amino-acid sensing complex with V-ATPase, was recently shown to be required for M2 polarization [55]. Moreover, V-ATPase was reported to modulate macrophage polarization in tumor-bearing mice [56], and inhibition of the V-ATPase a2 isoform in murine tumor cells delayed tumor growth by decreasing M2-like TAMs in the tumor microenvironment [57].

In our study, targeting of V-ATPase in classically-activated macrophages caused marked elevation of lysosomal pH, a typical effect of V-ATPase inhibitors that block the proton-pumping activity of V-ATPase [16,41,42]. Therefore, it appeared possible that lysosomal pH elevation is causative for increased TNFα expression. However, the control tool compounds chloroquine and NH_4Cl that are known to increase lysosomal pH in macrophages [43,44], also elevated the pH in lysosomes of M_{LPS} comparable as archazolid, but TNFα release was not increased but rather impaired. These data suggest that simply elevation of lysosomal pH is probably not the cause for increased TNFα expression by targeting V-ATPase.

Our detailed analysis of PKs and transcription factors that are potentially involved in induction of TNFα expression [58] excluded the MEK1/2 – ERK, MEK3/6 – p38 MAPK, and Akt pathway as well as STAT-1 and -3 as signaling molecules since archazolid treatment of M_{LPS} did not increase phosphorylation/activation of these proteins. Instead, phosphorylation of the p65 subunit of NFκB and the nuclear translocation of NFκB p65 were markedly promoted by archazolid, along with almost complete disappearance of the NFκB chaperon IκB. Since NFκB regulates TNFα expression in macrophages at the transcriptional level [59,60], we concluded that interference with V-ATPase by archazolid leads to elevation of TNFα mRNA expression. This is supported by the finding that the glucocorticoid dexamethasone which diminishes NFκB levels [59], completely prevented archazolid-induced TNFα mRNA levels. Note that besides NFκB also the SAPK/JNK was slightly activated by archazolid, a signaling molecule controlling TNFα translation in macrophages susceptible to dexamethasone [61]. Based on our experiments with actinomycin D the stability of TNFα mRNA was not affected by archazolid. Although TNFα is well known to augment NFκB signaling [62], it is unlikely that archazolid-induced TNFα is causative for increased NFκB activation, as the later was elevated already 15 min upon exposure to archazolid while TNFα induction was delayed up to hours. Macrophages substantially produce ROS during bacterial killing to clear infections. In agreement with increased ROS formation in murine macrophages exposed to the V-ATPase inhibitors bafilomycin A1 or to concanamycin A [31], archazolid enhanced LPS-induced ROS formation in human macrophages, which was sensitive to the NDAPH oxidase inhibitor DPI. Of interest, DPI also blocked archazolid-induced TNFα release implying a requirement of ROS in this respect. In fact, ROS production was shown to be closely linked to NFκB and SAPK/JNK activity [45].

In summary, we showed that pharmacological targeting of V-ATPase has phenotype-specific consequences for human macrophage functions. Substantial secretion of TNFα is a hallmark of activated macrophages which is increased by V-ATPase inhibition. Although TNFα is a potent pro-inflammatory cytokine that contributes to excessive and unresolved inflammation, controlled temporal and spatial elevation of TNFα may be beneficial in cancer

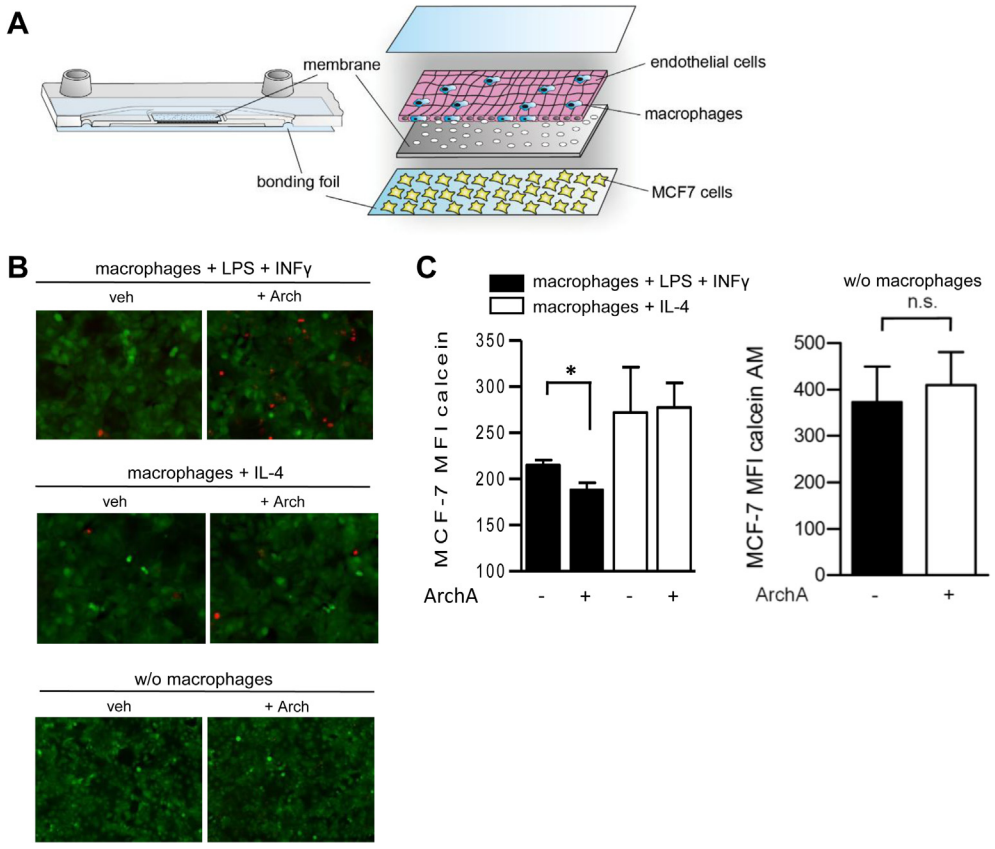

Fig. 7. Archazolid-treatment of M1 reduces the viability of MCF-7 cells in a biochip-based tumor model. (A) Schematic view of the tumor biochip model. HUVEC and polarized macrophages were placed on a membrane in the upper chamber of a microfluidically-supported biochip, while MCF-7 cells are cultured underneath the vascular layer of the biochip. (B, C) Viability of MCF-7 cells by Calcein-AM or propidium iodide staining after 24 h incubation with M1 (macrophages + LPS + INFγ), M2 (macrophages + IL-4) or in absence of macrophages that had been pretreated with 30 nM archazolid or vehicle (0.1% DMSO) for 30 min. (B) Representative images of three independent experiments; green: Calcein-AM staining of viable MCF-7 cells; red: propidium iodide staining of dead MCF-7 cells. (C) Mean fluorescence intensity (MFI) of the Calcein-AM staining of MCF-7 cells was measured by random field analysis of 40 regions of interest per experiment. Left panel, presence of M1 (macrophages + LPS + INFγ) or M2 (macrophages + IL-4), as indicated. Right panel, absence of macrophages. Data are means + SEM, n = 3; $^{*}p < 0.05$. n.s., not significant.

treatment. In fact, attempts have been made to stimulate macrophages for higher TNFα production, for example by TLR-9 activators and CpG oligodeoxynucleotides [63,64] in order to promote immune reactions against the tumor. Our results from the biochip tumor model support anti-tumoral properties of archazolid in combination with M1 but not with M2. Together, V-ATPase inhibitors may have the appeal to act at least in two ways that could synergize in cancer therapy: (i) direct anti-tumoral effects against susceptible cancer cells and (ii) beneficial impact against tumors by phenotype-specific manipulation of macrophages in the tumor microenvironment.

Conflict of interest statement

None declared.

Acknowledgements

This work was supported by the Deutsche Forschungsgemeinschaft FOR1406 (WE2260/11-1) and SFB1127 ChemBioSys. We thank Heidi Traber for expert technical assistance.

References

[1] X. Tang, C. Mo, Y. Wang, D. Wei, H. Xiao, Anti-tumour strategies aiming to target tumour-associated macrophages, Immunology 138 (2013) 93–104.
[2] G. Germano, R. Frapolli, C. Belgiovine, A. Anselmo, S. Pesce, M. Liguori, et al., Role of macrophage targeting in the antitumor activity of trabectedin, Cancer Cell 23 (2013) 249–262.
[3] K. Cotter, L. Stransky, C. McGuire, M. Forgac, Recent insights into the structure, regulation, and function of the V-ATPases, Trends Biochem. Sci. 40 (2015) 611–622.
[4] M. Huss, O. Vitavska, A. Albertmelcher, S. Bockelmann, C. Nardmann, K. Tabke, et al., Vacuolar H(+)-ATPases: intra- and intermolecular interactions, Eur. J. Cell Biol. 90 (2011) 688–695.
[5] V. Marshansky, J.L. Rubinstein, G. Gruber, Eukaryotic V-ATPase: novel structural findings and functional insights, Biochim. Biophys. Acta 1837 (2014) 857–879.
[6] L. Stransky, K. Cotter, M. Forgac, The function of V-ATPases in cancer, Physiol. Rev. 96 (2016) 1071–1091.
[7] D. Neri, C.T. Supuran, Interfering with pH regulation in tumours as a therapeutic strategy, Nat. Rev. Drug Discov. 10 (2011) 767–777.
[8] A. Hernandez, G. Serrano-Bueno, J.R. Perez-Castineira, A. Serrano, Intracellular proton pumps as targets in chemotherapy: V-ATPases and cancer, Curr. Pharm. Des. 18 (2012) 1383–1394.
[9] S.K. Biswas, P. Allavena, A. Mantovani, Tumor-associated macrophages: functional diversity, clinical significance, and open questions, Sem. Immunopathol. 35 (2013) 585–600.
[10] A. Sica, A. Mantovani, Macrophage plasticity and polarization: in vivo veritas, J. Clin. Invest. 122 (2012) 787–795.
[11] A. Bidani, C.Z. Wang, S.J. Saggi, T.A. Heming, Evidence for pH sensitivity of tumor necrosis factor-alpha release by alveolar macrophages, Lung 176 (1998) 111–121.
[12] I.M. Conboy, D. Manoli, V. Mhaiskar, P.P. Jones, Calcineurin and vacuolar-type H+-ATPase modulate macrophage effector functions, Proc. Natl. Acad. Sci. U.S. A. 96 (1999) 6324–6329.
[13] A. Bidani, T.A. Heming, Effects of bafilomycin A1 on functional capabilities of LPS-activated alveolar macrophages, J. Leukoc. Biol. 57 (1995) 275–281.
[14] F. Sasse, H. Steinmetz, G. Hofle, H. Reichenbach, Archazolids, new cytotoxic macrolactones from Archangium gephyra (Myxobacteria). Production, isolation, physico-chemical and biological properties, J. Antibiot. (Tokyo) 56 (2003) 520–525.

[15] S. Bockelmann, D. Menche, S. Rudolph, T. Bender, S. Grond, P. von Zezschwitz, et al., Archazolid A binds to the equatorial region of the c-ring of the vacuolar H+-ATPase, J. Biol. Chem. 285 (2010) 38304–38314.
[16] M. Huss, F. Sasse, B. Kunze, R. Jansen, H. Steinmetz, G. Ingenhorst, et al., Archazolid and apicularen: novel specific V-ATPase inhibitors, BMC Biochem. 6 (2005) 13.
[17] J.P. Golz, S. Bockelmann, K. Mayer, H.J. Steinhoff, H. Wieczorek, M. Huss, et al., EPR studies of V-ATPase with spin-labeled Inhibitors DCC and archazolid: interaction dynamics with proton translocating subunit c, ChemMedChem 11 (2016) 420–428.
[18] K. von Schwarzenberg, R.M. Wiedmann, P. Oak, S. Schulz, H. Zischka, G. Wanner, et al., Mode of cell death induction by pharmacological vacuolar H+-ATPase (V-ATPase) inhibition, J. Biol. Chem. 288 (2013) 1385–1396.
[19] R.M. Wiedmann, K. von Schwarzenberg, A. Palamidessi, L. Schreiner, R. Kubisch, J. Liebl, et al., The V-ATPase-inhibitor archazolid abrogates tumor metastasis via inhibition of endocytic activation of the Rho-GTPase Rac1, Cancer Res. 72 (2012) 5976–5987.
[20] L.S. Schneider, K. von Schwarzenberg, T. Lehr, M. Ulrich, R. Kubisch-Dohmen, J. Liebl, et al., Vacuolar-ATPase inhibition blocks iron metabolism to mediate therapeutic effects in breast cancer, Cancer Res. 75 (2015) 2863–2874.
[21] S. Zhang, L.S. Schneider, B. Vick, M. Grunert, I. Jeremias, D. Menche, et al., Anti-leukemic effects of the V-ATPase inhibitor Archazolid A, Oncotarget 6 (2015) 43508–43528.
[22] C.M. Schempp, K. von Schwarzenberg, L. Schreiner, R. Kubisch, R. Muller, E. Wagner, et al., V-ATPase inhibition regulates anoikis resistance and metastasis of cancer cells, Mol. Cancer Ther. 13 (2014) 926–937.
[23] O. Scherer, H. Steinmetz, C. Kaether, C. Weinigel, D. Barz, H. Kleinert, et al., Targeting V-ATPase in primary human monocytes by archazolid potently represses the classical secretion of cytokines due to accumulation at the endoplasmic reticulum, Biochem. Pharmacol. 91 (2014) 490–500.
[24] C. Pergola, A. Rogge, G. Dodt, H. Northoff, C. Weinigel, D. Barz, et al., Testosterone suppresses phospholipase D, causing sex differences in leukotriene biosynthesis in human monocytes, FASEB J 25 (2011) 3377–3387.
[25] G. Solinas, S. Schiarea, M. Liguori, M. Fabbri, S. Pesce, L. Zammataro, et al., Tumor-conditioned macrophages secrete migration-stimulating factor: a new marker for M2-polarization, influencing tumor cell motility, J. Immunol. 185 (2010) 642–652.
[26] F. Bellora, R. Castriconi, A. Dondero, G. Reggiardo, L. Moretta, A. Mantovani, et al., The interaction of human natural killer cells with either unpolarized or polarized macrophages results in different functional outcomes, Proc. Natl. Acad. Sci. U.S.A. 107 (2010) 21659–21664.
[27] M. Bohnert, O. Scherer, K. Wiechmann, S. Konig, H.M. Dahse, D. Hoffmeister, et al., Melleolides induce rapid cell death in human primary monocytes and cancer cells, Bioorg. Med. Chem. 22 (2014) 3856–3861.
[28] N. Zheng, X. Zhang, G.R. Rosania, Effect of phospholipidosis on the cellular pharmacokinetics of chloroquine, J. Pharmacol. Exp. Ther. 336 (2011) 661–671.
[29] A. Bidani, S.E. Brown, T.A. Heming, R. Gurich, T.D. Dubose Jr., Cytoplasmic pH in pulmonary macrophages: recovery from acid load is Na+ independent and NEM sensitive, Am. J. Physiol. 257 (1989) C65–C76.
[30] K.J. Livak, T.D. Schmittgen, Analysis of relative gene expression data using real-time quantitative PCR and the 2(-Delta Delta C(T)) Method, Methods 25 (2001) 402–408.
[31] A. Yokomakura, J. Hong, K. Ohuchi, S.E. Oh, J.Y. Lee, N. Mano, et al., Increased production of reactive oxygen species by the vacuolar-type (H(+))-ATPase inhibitors bafilomycin A1 and concanamycin A in RAW 264 cells, J. Toxicol. Sci. 37 (2012) 1045–1048.
[32] M. Raasch, K. Rennert, T. Jahn, S. Peters, T. Henkel, O. Huber, et al., Microfluidically supported biochip design for culture of endothelial cell layers with improved perfusion conditions, Biofabrication 7 (2015) 015013.
[33] P.J. Murray, J.E. Allen, S.K. Biswas, E.A. Fisher, D.W. Gilroy, S. Goerdt, et al., Macrophage activation and polarization: nomenclature and experimental guidelines, Immunity 41 (2014) 14–20.
[34] S. Grinstein, A. Nanda, G. Lukacs, O. Rotstein, V-ATPases in phagocytic cells, J. Exp. Biol. 172 (1992) 179–192.
[35] T. Furuchi, K. Aikawa, H. Arai, K. Inoue, Bafilomycin A1, a specific inhibitor of vacuolar-type H(+)-ATPase, blocks lysosomal cholesterol trafficking in macrophages, J. Biol. Chem. 268 (1993) 27345–27348.
[36] T.A. Heming, D.L. Traber, F. Hinder, A. Bidani, Effects of bafilomycin A1 on cytosolic pH of sheep alveolar and peritoneal macrophages: evaluation of the pH-regulatory role of plasma membrane V-ATPases, J. Exp. Biol. 198 (1995) 1711–1715.
[37] J. Xu, H.T. Feng, C. Wang, K.H. Yip, N. Pavlos, J.M. Papadimitriou, et al., Effects of Bafilomycin A1: an inhibitor of vacuolar H (+)-ATPases on endocytosis and apoptosis in RAW cells and RAW cell-derived osteoclasts, J. Cell. Biochem. 88 (2003) 1256–1264.
[38] H. Tapper, R. Sundler, Bafilomycin A1 inhibits lysosomal, phagosomal, and plasma membrane H(+)-ATPase and induces lysosomal enzyme secretion in macrophages, J. Cell. Physiol. 163 (1995) 137–144.
[39] A. Bidani, B.S. Reisner, A.K. Haque, J. Wen, R.E. Helmer, D.M. Tuazon, et al., Bactericidal activity of alveolar macrophages is suppressed by V-ATPase inhibition, Lung 178 (2000) 91–104.
[40] J. Canton, R. Khezri, M. Glogauer, S. Grinstein, Contrasting phagosome pH regulation and maturation in human M1 and M2 macrophages, Mol. Biol. Cell 25 (2014) 3330–3341.
[41] J.A. Mindell, Lysosomal acidification mechanisms, Ann. Rev. Physiol. 74 (2012) 69–86.
[42] R. Sundler, Lysosomal and cytosolic pH as regulators of exocytosis in mouse macrophages, Acta Physiol. Scand. 161 (1997) 553–556.
[43] B. Poole, S. Ohkuma, Effect of weak bases on the intralysosomal pH in mouse peritoneal macrophages, J. Cell Biol. 90 (1981) 665–669.
[44] S. Ohkuma, J. Chudzik, B. Poole, The effects of basic substances and acidic ionophores on the digestion of exogenous and endogenous proteins in mouse peritoneal macrophages, J. Cell Biol. 102 (1986) 959–966.
[45] M.J. Morgan, Z.G. Liu, Reactive oxygen species in TNFalpha-induced signaling and cell death, Mol. Cells 30 (2010) 1–12.
[46] D. Reker, A.M. Perna, T. Rodrigues, P. Schneider, M. Reutlinger, B. Monch, et al., Revealing the macromolecular targets of complex natural products, Nat. Chem. 6 (2014) 1072–1078.
[47] C.J. Swallow, S. Grinstein, R.A. Sudsbury, O.D. Rotstein, Cytoplasmic pH regulation in monocytes and macrophages: mechanisms and functional implications, Clin. Invest. Med. 14 (1991) 367–378.
[48] H. Tapper, R. Sundler, Cytosolic pH regulation in mouse macrophages. Proton extrusion by plasma-membrane-localized H(+)-ATPase, Biochem. J. 281 (Pt 1) (1992) 245–250.
[49] R. Kubisch, T. Frohlich, G.J. Arnold, L. Schreiner, K. von Schwarzenberg, A. Roidl, et al., V-ATPase inhibition by archazolid leads to lysosomal dysfunction resulting in impaired cathepsin B activation in vivo, Int. J. Cancer (2013).
[50] J.Y. Jung, C.M. Robinson, Interleukin-27 inhibits phagosomal acidification by blocking vacuolar ATPases, Cytokine 62 (2013) 202–205.
[51] A. Qin, T.S. Cheng, N.J. Pavlos, Z. Lin, K.R. Dai, M.H. Zheng, V-ATPases in osteoclasts: structure, function and potential inhibitors of bone resorption, Int. J. Biochem. Cell Biol. 44 (2012) 1422–1435.
[52] T.A. Heming, A. Bidani, Plasmalemmal H+ extruders in mammalian alveolar macrophages, Comp. Biochem. Physiol. A: Mol. Integr. Physiol. 133 (2002) 143–150.
[53] F. Ginhoux, J.L. Schultze, P.J. Murray, J. Ochando, S.K. Biswas, New insights into the multidimensional concept of macrophage ontogeny, activation and function, Nat. Immunol. 17 (2016) 34–40.
[54] S.H. Zuckerman, G.F. Evans, L. Guthrie, Transcriptional and post-transcriptional mechanisms involved in the differential expression of LPS-induced IL-1 and TNF mRNA, Immunology 73 (1991) 460–465.
[55] T. Kimura, S. Nada, N. Takegahara, T. Okuno, S. Nojima, S. Kang, et al., Polarization of M2 macrophages requires Lamtor1 that integrates cytokine and amino-acid signals, Nat. Commun. 7 (2016) 13130.
[56] G.K. Katara, M.K. Jaiswal, A. Kulshrestha, B. Kolli, A. Gilman-Sachs, K.D. Beaman, Tumor-associated vacuolar ATPase subunit promotes tumorigenic characteristics in macrophages, Oncogene (2013).
[57] G.K. Katara, A. Kulshrestha, M.K. Jaiswal, S. Pamarthy, A. Gilman-Sachs, K.D. Beaman, Inhibition of vacuolar ATPase subunit in tumor cells delays tumor growth by decreasing the essential macrophage population in the tumor microenvironment, Oncogene 35 (2016) 1058–1065.
[58] B.B. Aggarwal, S.C. Gupta, J.H. Kim, Historical perspectives on tumor necrosis factor and its superfamily: 25 years later, a golden journey, Blood 119 (2012) 651–665.
[59] M.A. Collart, P. Baeuerle, P. Vassalli, Regulation of tumor necrosis factor alpha transcription in macrophages: involvement of four kappa B-like motifs and of constitutive and inducible forms of NF-kappa B, Mol. Cell. Biol. 10 (1990) 1498–1506.
[60] A.N. Shakhov, M.A. Collart, P. Vassalli, S.A. Nedospasov, C.V. Jongeneel, Kappa B-type enhancers are involved in lipopolysaccharide-mediated transcriptional activation of the tumor necrosis factor alpha gene in primary macrophages, J. Exp. Med. 171 (1990) 35–47.
[61] J.L. Swantek, M.H. Cobb, T.D. Geppert, Jun N-terminal kinase/stress-activated protein kinase (JNK/SAPK) is required for lipopolysaccharide stimulation of tumor necrosis factor alpha (TNF-alpha) translation: glucocorticoids inhibit TNF-alpha translation by blocking JNK/SAPK, Mol. Cell. Biol. 17 (1997) 6274–6282.
[62] S. Vallabhapurapu, M. Karin, Regulation and function of NF-kappaB transcription factors in the immune system, Ann. Rev. Immunol. 27 (2009) 693–733.
[63] C. Guiducci, A.P. Vicari, S. Sangaletti, G. Trinchieri, M.P. Colombo, Redirecting in vivo elicited tumor infiltrating macrophages and dendritic cells towards tumor rejection, Cancer Res. 65 (2005) 3437–3446.
[64] A.M. Krieg, Therapeutic potential of Toll-like receptor 9 activation, Nat. Rev. Drug Discov. 5 (2006) 471–484.

3.3 Manuscript III

Vacuolar (H^+)-ATPase Critically Regulates Specialized Proresolving Mediator Pathways in Human M2-like Monocyte-Derived Macrophages and Has a Crucial Role in Resolution of Inflammation

Zhigang Rao, Simona Pace, Paul M. Jordan, Rossella Bilancia, Fabiana Troisi, Friedemann Börner, Nico Andreas, Thomas Kamradt, Dirk Menche, Antonietta Rossi, Charles N. Serhan, Jana Gerstmeier and Oliver Werz (2019)

The Journal of Immunology

In this paper we uncovered the role of V-ATPase in LM biosynthesis in human M1 and M2 macrophages using specific V-ATPase inhibitors archazolid A (ArchA) and bafilomycin. Blockade of V-ATPase during IL-4 triggered M2 polarization abrogated the expression 15-LOX-1 without effects on other LOXs like 15-LOX-2, 12-LOX or 5-LOX. In line with impaired 15-LOX-1 levels, the biosynthesis of SPM precursors as well as related SPM were inhibited by ArchA. In M1 macrophages, inhibition of V-ATPase induced COX-2 expression and the related PG production. Targeting V-ATPase in M2 neither influenced the IL-4 triggered JAK-STAT6 pathway nor the mTORC1 signaling cascade, but strongly suppressed the expression of MEK and ERK-1/2. The MEK inhibitor U0126 and c-Myc inhibitor JQ-1 abrogated the expression of 15-LOX-1 as well as biosynthesis of the related SPM, which confirmed the essential role of MEK/ERK-1/2-c-Myc pathway in 15-LOX-1 expression and SPM formation in M2 macrophages. In a zymosan-induced murine peritonitis model, targeting V-ATPase *in vivo* delayed resolution accompanied by increased neutrophil infiltration and inhibited SPM levels without affecting leukotrienes and prostaglandins.

Contribution (75%): Cell culture and performance of blood cell isolation, determination of cell viability, determination of cytokine levels, SDS-PAGE and Western Blot, Immunofluorescence microscopy, UPLC-MS-MS, analysis of data and preparation of graphs, analysis of statistics, co-writing of the manuscript.

Published July 12, 2019, doi:10.4049/jimmunol.1900236

Vacuolar (H^+)-ATPase Critically Regulates Specialized Proresolving Mediator Pathways in Human M2-like Monocyte-Derived Macrophages and Has a Crucial Role in Resolution of Inflammation

Zhigang Rao,* Simona Pace,* Paul M. Jordan,* Rossella Bilancia,† Fabiana Troisi,* Friedemann Börner,* Nico Andreas,‡ Thomas Kamradt,‡ Dirk Menche,§ Antonietta Rossi,† Charles N. Serhan,¶ Jana Gerstmeier,* and Oliver Werz*

Alternative (M2)-polarized macrophages possess high capacities to produce specialized proresolving mediators (SPM; i.e., resolvins, protectins, and maresins) that play key roles in resolution of inflammation and tissue regeneration. Vacuolar (H^+)-ATPase (V-ATPase) is fundamental in inflammatory cytokine trafficking and secretion and was implicated in macrophage polarization toward the M2 phenotype, but its role in SPM production and lipid mediator biosynthesis in general is elusive. In this study, we show that V-ATPase activity is required for the induction of SPM-biosynthetic pathways in human M2-like monocyte-derived macrophages (MDM) and consequently for resolution of inflammation. Blockade of V-ATPase by archazolid during IL-4–induced human M2 polarization abrogated 15-lipoxygenase-1 expression and prevented the related biosynthesis of SPM in response to pathogenic *Escherichia coli*, assessed by targeted liquid chromatography–tandem mass spectrometry–based metabololipidomics. In classically activated proinflammatory M1-like MDM, however, the biosynthetic machinery for lipid mediator formation was independent of V-ATPase activity. Targeting V-ATPase in M2 influenced neither IL-4–triggered JAK/STAT6 nor the mTOR complex 1 signaling but strongly suppressed the ERK-1/2 pathway. Accordingly, the ERK-1/2 pathway contributes to 15-lipoxygenase-1 expression and SPM formation in M2-like MDM. Targeting V-ATPase in vivo delayed resolution of zymosan-induced murine peritonitis accompanied by decreased SPM levels without affecting proinflammatory leukotrienes or PGs. Together, our data propose that V-ATPase regulates 15-lipoxygenase-1 expression and consequent SPM biosynthesis involving ERK-1/2 during M2 polarization, implying a crucial role for V-ATPase in the resolution of inflammation. ***The Journal of Immunology*****, 2019, 203: 000–000.**

Macrophages are innate immune cells with marked plasticity that, depending on their phenotype, promote acute inflammation and host defense but also can support the resolution of inflammation and the return to homeostasis (1–3). Polarization of macrophages toward proinflammatory M1-like and proresolving M2-like phenotypes is governed by epigenetic and cell survival pathways, tissue microenvironment, and extrinsic factors like microbial products and secreted cytokines (3). $CD4^+$ T cell subtype-derived cytokines determine macrophage polarization, in which the M1 phenotype is obtained by exposure to T_H1-related IFN-γ, particularly in the presence of the TLR agonist LPS, whereas the M2 subtype is achieved upon exposure to T_H2-derived IL-4 or IL-13 (3, 4).

One hallmark characteristic of the opposing functions of M1 and M2 is their differential lipid mediator (LM) profile that they produce, due to their subtype-specific expression of LM-biosynthetic enzymes that distinguish their proinflammatory or proresolving phenotypes (1, 5, 6). Whereas M1 are characterized by marked expression of proinflammatory 5-lipoxygenase (LOX)/5-LOX–activating protein (FLAP), and cyclooxygenase (COX) pathways with substantial leukotriene (LT)B_4 and PGE_2 production, the LM profile of M2 is dominated by the 15-LOX-1 pathway along with strong biosynthesis of specialized proresolving mediators (SPM) (6). These SPM encompass a novel superfamily of highly potent bioactive LM, including lipoxins (LX), resolvins (Rv), maresins (MaR), and protectins (PD), that terminate

*Department of Pharmaceutical/Medicinal Chemistry, Institute of Pharmacy, Friedrich-Schiller-University Jena, 07743 Jena, Germany; †Department of Pharmacy, School of Medicine, University of Naples Federico II, 80131 Naples, Italy; ‡Institute of Immunology, Jena University Hospital, 07743 Jena, Germany; §Kekulé-Institut für Organische Chemie und Biochemie der Rheinischen Friedrich-Wilhelms-Universität Bonn, D-53121 Bonn, Germany; and ¶Center for Experimental Therapeutics and Reperfusion Injury, Department of Anesthesiology, Perioperative, and Pain Medicine, Brigham and Women's Hospital and Harvard Medical School, Boston, MA 02115

ORCIDs: 0000-0002-4591-7037 (N.A.); 0000-0001-8443-5893 (T.K.); 0000-0003-4627-8545 (C.N.S.).

Received for publication February 26, 2019. Accepted for publication June 16, 2019.

This work was supported by the Deutsche Forschungsgemeinschaft (FOR1406, SFB1127, ChemBioSys and SFB1278, Polytarget), and by the Free State of Thuringia and the European Social Fund (2016 FGR 0045). C.N.S. is supported by National Institutes of Health Grants P01-GM095467 and GM038765. Z.R. was partly financed by the China Scholarship Council, and J.G. received a postdoctoral stipend from the Carl Zeiss Foundation.

Address correspondence and reprint requests to Prof. Oliver Werz and Dr. Jana Gerstmeier, Department of Pharmaceutical/Medicinal Chemistry, Institute of Pharmacy, Friedrich-Schiller-University Jena, Philosophenweg 14, 07743 Jena, Germany. E-mail addresses: oliver.werz@uni-jena.de (O.W.) and jana.gerstmeier@uni-jena.de (J.G.)

The online version of this article contains supplemental material.

Abbreviations used in this article: AA, arachidonic acid; ArchA, archazolid A; COX, cyclooxygenase; FLAP, 5-LOX–activating protein; HDHA, hydroxydocosahexaenoic acid; 5-HETE, 5-hydroxyeicosatatraenoic acid; Lamtor1, late endosomal and lysosomal adaptor and MAPK and mTOR activator 1; LM, lipid mediator; LOX, lipoxygenase; LT, leukotriene; LX, lipoxin; LXR, liver X receptor; MDM, monocyte-derived macrophage; mTORC1, mTOR complex 1; PD, protectin; Rv, resolvin; SPM, specialized proresolving mediator; UPLC–MS-MS, ultra-performance liquid chromatography–tandem mass spectrometry; V-ATPase, vacuolar (H^+)-ATPase.

inflammation and promote tissue regeneration (7, 8). Accumulating evidence suggests that the ability of M2 to generate SPM critically determines their inflammation-resolving features (9). However, the signaling pathways involved in SPM biosynthesis during M2 polarization are incompletely understood and remain to be elucidated.

In this article, we show that the vacuolar (H^+)-ATPase (V-ATPase) plays a crucial role in the induction of SPM–biosynthetic pathways during polarization of monocyte-derived macrophages (MDM) to the M2 phenotype. V-ATPases are ATP-dependent proton-translocating macromolecular complexes that acidify lysosomes, endosomes, Golgi apparatus, and certain secretory granules in eukaryotic cells and participate in cellular pH homeostasis, receptor-mediated endocytosis, virus and toxin entry, intracellular trafficking, and protein degradation and processing (10). In macrophages, V-ATPase regulates lysosomal and cytoplasmic pH homeostasis with consequences for reactive oxygen species formation, bactericidal activity, and lysosomal enzyme secretion (11–13). However, little is known about the role of V-ATPase in either LM biosynthesis or the polarization of human macrophages. V-ATPase was shown to participate at M2 polarization in mice, but SPM biosynthesis or expression of 15-LOX-1 was not addressed (14). For human polarized M1 and M2, contrasting phagosome pH regulation and maturation related to V-ATPase was demonstrated (15), and targeting of V-ATPase during polarization of human MDM elevated TNF-α release and ROS formation in M1, but not in M2 (16). Hence, V-ATPase might impact human M1/M2 polarization, but whether V-ATPase is involved in the regulation of LM-biosynthetic pathways related to inflammation and its resolution is unknown. Therefore, we here aimed to reveal the role of V-ATPase in the induction of phenotype-specific profiles of LM with proinflammatory and proresolving properties during human MDM polarization. Our results show that V-ATPase regulates 15-LOX-1 expression and consequent SPM biosynthesis in an ERK-1/2-dependent fashion during acquiring an M2 phenotype and thus imply critical roles of this signaling pathway in the resolution of inflammation.

Materials and Methods

Materials

Deuterated and nondeuterated LM standards for ultra-performance liquid chromatography–tandem mass spectrometry (UPLC–MS-MS) quantification were purchased from Cayman Chemical/Biomol (Hamburg, Germany). Archazolid A (ArchA) was isolated from *Archangium gephyra* as previously described (17). Bafilomycin A1 was obtained from Sigma-Aldrich (Taufkirchen, Germany), CP-690,550 and GSK-2033 were obtained from Tocris Bioscience (Bristol, U.K.), JQ-1 was from AdooQ Bioscience (Irvine, CA), LY294002 was from Cytoskeleton (Denver, CO), skepinone-L and Torin 1 were from Cayman Chemical (Ann Arbor, MI), and U0126 was from Enzo Life Sciences (Farmingdale, NY). AS1517499 and all other reagents were obtained from Sigma-Aldrich unless mentioned otherwise.

Animals

Male CD-1 mice (33–39 g, 6–8 wk; Charles River Laboratories, Calco, Italy) were housed in a controlled environment (21 ± 2°C) and provided with standard rodent chow and water. Animals were allowed to acclimate for 4 d prior to experiments and were subjected to a 12 h light/12 h dark schedule. Mice were randomly assigned for the experiments, which were conducted during the light phase. The experimental procedures were approved by the Italian Ministry according to International and National law and policies (European Union Directive 2010/63/EU and Italian DL 26/2014 for animal experiments.

Cell isolation and polarization of MDM

Leukocyte concentrates from freshly withdrawn peripheral blood of male and female healthy adult human donors (age 18–65 y) were provided by the Institute of Transfusion Medicine at the University Hospital Jena, Jena, Germany. The experimental protocol was approved by the ethical committee of the University Hospital Jena. All methods were performed in accordance with the relevant guidelines and regulations. PBMC were separated using dextran sedimentation, followed by centrifugation on lymphocyte separation medium (Histopaque-1077; Sigma-Aldrich). PBMC were seeded in RPMI 1640 (Sigma-Aldrich) containing 10% (v/v) heat-inactivated FCS, 100 U/ml penicillin, and 100 μg/ml streptomycin in cell culture flasks (Greiner Bio-One, Frickenhausen, Germany) for 1.5 h at 37°C and 5% CO_2 for adherence of monocytes. For differentiation of monocytes to MDM and polarization toward M1 and M2, published criteria were used (4). M1 were generated by incubating monocytes with 20 ng/ml GM-CSF (PeproTech, Hamburg, Germany) for 6 d in RPMI 1640 supplemented with 10% FCS, 2 mmol/L glutamine (Biochrom/Merck, Berlin, Germany), and penicillin–streptomycin (Biochrom/Merck), followed by treatment with 100 ng/ml LPS and 20 ng/ml INF-γ (PeproTech). M2 were generated by incubating monocytes with 20 ng/ml M-CSF (PeproTech) for 6 d, followed by treatment with 20 ng/ml IL-4 (PeproTech). Routinely, cells were polarized for 48 h unless stated otherwise. ArchA (30 nM) and other inhibitors were added 15 min prior to addition of polarization agents (INF-γ, LPS, IL-4) unless mentioned otherwise.

Incubation of MDM for LM formation and LM metabololipidomics

MDM (2×10^6/ml) were incubated in PBS containing 1 mM $CaCl_2$. To evoke LM biosynthesis pathogenic *Escherichia coli* (serotype O6:K2:H1, ratio 1:50) was added for 180 min at 37°C. The supernatants were then transferred to 2 ml of ice-cold methanol containing 10 μl of deuterium-labeled internal standards (200 nM d8-5S-HETE, d4-LTB_4, d5-LXA_4, d5-RvD_2, d4-PGE_2 and 10 μM d8–arachidonic acid [AA]) to facilitate quantification and sample recovery. Sample preparation was conducted by adapting published criteria (6). In brief, samples were kept at −20°C for 60 min to allow protein precipitation. After centrifugation (1200 × *g*, 4°C, 10 min), 8 ml acidified H_2O was added (final pH = 3.5), and samples were subjected to solid phase extraction. Solid phase cartridges (Sep-Pak Vac 6cc 500 mg/6 ml C18; Waters, Milford, MA) were equilibrated with 6 ml methanol and 2 ml H_2O before samples were loaded onto columns. After washing with 6 ml H_2O and additional 6 ml *n*-hexane, LM were eluted with 6 ml methyl formate. Finally, the samples were brought to dryness using an evaporation system (TurboVap LV; Biotage, Uppsala, Sweden) and resuspended in 100 μl methanol–water (50/50, v/v) for UPLC–MS-MS automated injections. LM profiling was analyzed with an Acquity UPLC system (Waters) and a QTRAP 5500 Mass Spectrometer (AB Sciex, Darmstadt, Germany) equipped with a Turbo V Source and electrospray ionization. LM were eluted using an Acquity UPLC BEH C18 column (1.7 μm, 2.1 × 100 mm; Waters, Eschborn, Germany) at 50°C with a flow rate of 0.3 ml/min and a mobile phase consisting of methanol–water–acetic acid of 42:58:0.01 (v/v/v) that was ramped to 86:14:0.01 (v/v/v) over 12.5 min and then to 98:2:0.01 (v/v/v) for 3 min. The QTrap 5500 was operated in negative ionization mode using scheduled multiple reaction monitoring coupled with information-dependent acquisition. The scheduled multiple reaction monitoring window was 60 s, optimized LM parameters (collision energy, entrance potential, declustering potential, collision cell exit potential) were adopted (18), and the curtain gas pressure was set to 35 ψ. The retention time and at least six diagnostic ions for each LM were confirmed by means of an external standard (Cayman Chemical/Biomol). Quantification was achieved by calibration curves for each LM.

SDS-PAGE and Western blot

Cell lysates of MDM, corresponding to 2×10^6 cells, were separated on 8% (for $cPLA_2$-α), 10% (for 5-LOX, 15-LOX-1, 15-LOX-2, COX-1, COX-2, STAT6, phospho-STAT6, Akt, phospho-Akt, p70S6K, phospho-p70S6K, cRaf, phospho-cRaf, MEK, phospho-MEK, ERK-1/2, phospho-ERK-1/2, p38 MAPK, phospho-p38 MAPK, c-Myc, β-actin, and GAPDH), and 16% (for FLAP and late endosomal and lysosomal adaptor and MAPK and mTOR activator 1 [Lamtor1]) polyacrylamide gels and blotted onto nitrocellulose membranes (Amersham Protran supported 0.45 μm nitrocellulose; GE Healthcare, Freiburg, Germany). The membranes were incubated with the following primary Abs: rabbit polyclonal anti-$cPLA_2$-α, 1:1000 (2832S; Cell Signaling Technology); rabbit polyclonal anti-5-LOX, 1:1000 (to a peptide with the C-terminal 12 aa of 5-LOX: CSPDRIPNSVA; kindly provided by Dr. M. E. Newcomer, Louisiana State University, Baton Rouge, LA); mouse monoclonal anti-15-LOX-1, 1:500 (ab119774; Abcam, Cambridge, U.K.); rabbit polyclonal anti-15-LOX-2, 1:500 (ab23691; Abcam); rabbit polyclonal anti-COX-1, 1:1000 (4841S; Cell Signaling Technology); rabbit polyclonal anti-COX-2, 1:1000 (4842S; Cell Signaling Technology); mouse polyclonal anti-STAT6, 1:1000 (ab88540; Abcam);

rabbit polyclonal anti–phospho-STAT6 (Tyr641), 1:1000 (ab28829; Abcam); mouse monoclonal anti-Akt, 1:1000 (2920; Cell Signaling Technology); rabbit polyclonal anti-phospho-Akt, 1:1000 (9271S; Cell Signaling Technology); rabbit monoclonal anti-p70S6K, 1:1000 (2708T; Cell Signaling Technology); mouse monoclonal anti–phospho-p70S6K (Thr389) 1:1000 (9206S; Cell Signaling Technology); rabbit polyclonal anti-MEK1/2, 1:1000 (9122; Cell Signaling Technology); rabbit polyclonal anti–phospho-MEK1/2 (Ser217/Ser221), 1:1000 (9121S; Cell Signaling Technology); rabbit monoclonal anti-ERK1/2, 1:1000 (4695S; Cell Signaling Technology); mouse monoclonal anti–phospho-ERK1/2 (Thr202/Tyr204), 1:1000 (9106; Cell Signaling Technology); rabbit monoclonal anti-p38 MAPK, 1:1000 (8690S; Cell Signaling Technology); rabbit polyclonal anti–phospho-p38 MAPK (Thr180/Tyr182), 1:1000 (9211S; Cell Signaling Technology); rabbit monoclonal anti-cMyc, 1:1000 (5605S; Cell Signaling Technology); rabbit polyclonal anti-FLAP, 1:1000 (ab85227; Abcam); rabbit monoclonal anti-Lamtor1 1:1000 (8975T; Cell Signaling Technology); mouse monoclonal anti-β-actin, 1:1000 (3700S; Cell Signaling); rabbit polyclonal anti–β-actin, 1:1000 (4967S; Cell Signaling Technology) and rabbit monoclonal anti-GAPDH, 1:1000 (5174S; Cell Signaling). Immunoreactive bands were stained with IRDye 800CW Goat anti-Mouse IgG (H+L), 1:10,000 (926-32210; LI-COR Biosciences, Lincoln, NE), IRDye 800CW Goat anti-Rabbit IgG (H+L), 1:15,000 (926 32211; LI-COR Biosciences) and/or IRDye 680LT Goat anti-Mouse IgG (H+L), 1:40,000 (926-68020; LI-COR Biosciences), and visualized by an Odyssey infrared imager (LI-COR Biosciences). Data from densitometric analysis were background corrected.

Determination of cytokine levels

Unpolarized MDM were treated with ArchA (30 nM) or vehicle (0.1% DMSO) 30 min before cells were polarized to M1 or M2 for 48 h. For measurement of extracellular cytokine levels, supernatants were collected by centrifugation (2000 × *g*, 4°C, 10 min). The cytokines IL-6, IL-10, and TNF-α were analyzed by in-house–made ELISA kits (R&D Systems, Bio-Techne).

Flow cytometry

Fluorescent staining for flow cytometric analysis of M1 or M2 was performed in FACS buffer (PBS with 0.5% BSA, 2 mM EDTA, and 0.1% sodium azide). MDM were treated either with vehicle or 30 nM ArchA during 48 h polarization. Nonspecific Ab binding was blocked by using mouse serum for 10 min at 4°C prior Ab staining. Subsequently, MDM were stained with fluorochrome-labeled Ab mixtures at 4°C for 20 min. The following Abs were used: FITC anti-human CD14 (2 μg/test, clone M5E2; BioLegend, San Diego, CA), PE anti-human CD54 (1 μg/test, clone HA58; eBioscience, San Diego, CA), allochycocyanin-H7 anti-human CD80 (0.25 μg/test, clone L307.4; BD Bioscience), PE-Cy7 anti-human CD163 (2 μg/test, clone RM3/1; BioLegend), PerCP-eFluor710 anti-human CD206 (0.06 μg/test, clone 19.2; eBioscience). Upon staining, MDM (M1 or M2) were analyzed using a FACS Canto Plus flow cytometer (BD Bioscience), and data analyzed using FlowJo X Software (BD Bioscience).

Determination of cell viability

The viability of MDM was assessed by MTT assay as described (16). Briefly, MDM after 6 d of differentiation of monocytes were preincubated with test compounds for 15 min at 37°C (5% CO_2), polarization agents were added, and cells were incubated for 48 h. Staurosporine (1 μM), a pan-kinase inhibitor and inducer of apoptosis, was used as positive control. MTT solution was added, and cells were further incubated for 4 h and lysed in a buffer containing 10% (w/v) SDS.

Immunofluorescence microscopy

MDM after 6 d of differentiation of monocytes were pretreated with ArchA (30 nM) for 30 min before polarization for 48 h to M1 and M2, and 10^6 cells were seeded onto glass coverslips. Lysotracker (1:100 dilution; Invitrogen, Thermo Fisher Scientific) was added to the cells for 1 h at 37°C. The fluorescence was visualized with a Zeiss Axio Observer.Z1 inverted microscope (Carl Zeiss, Jena, Germany) and an LCI Plan-Neofluar 63×/1.3 Imm Corr DIC M27 objective. Images were taken with an AxioCam MR3 camera and were acquired, cut, linearly adjusted in the overall brightness and contrast, and exported by the AxioVision 4.8 software (Carl Zeiss).

Zymosan-induced peritonitis in mice

For the zymosan-induced peritonitis, mice (n = 6 per experimental group) received ArchA (1 mg/kg) or vehicle (0.5 ml of 0.9% saline solution containing 2% DMSO) i.p., 60 min prior to peritonitis induction by zymosan, as previously described (19). Zymosan (Sigma-Aldrich) was prepared as a final suspension (2 mg/ml) in 0.9% (w/v) saline and injected i.p. (0.5 ml), followed by a peritoneal lavage with 3 ml of cold PBS. Cells in the inflammatory exudates were immediately counted (dilution 1:10) by using a Bürker chamber and vital trypan blue staining, and then samples were centrifuged (18,000 × *g*, 5 min, 4°C). The blood (~0.7–0.9 ml) was collected by intracardiac puncture using citrate as anticoagulant, and plasma was obtained by centrifugation at 800 × *g* at 4°C for 10 min. LM levels in the supernatants of peritoneal exudates as well as in the plasma were assessed by UPLC–MS-MS analyses as described above (LM metabololipidomics).

Statistical analyses

Results are expressed as mean ± SEM of n observations, where n represents the number of experiments with separate donors performed on different days, or the number of animals per group (n = 6), as indicated. Analyses of data were conducted using GraphPad Prism 7 software (San Diego, CA). LM data were log transformed for statistical analysis and analyzed by paired t test. For multiple comparisons, ANOVA with Bonferroni or Dunnett post hoc tests were applied as indicated. Two-tailed t test was used for comparison of two groups. The criterion for statistically significant is $p < 0.05$.

Results

V-ATPase activity is essential for SPM biosynthesis and 15-LOX-1 expression in human M2-like MDM

To study the requirement of V-ATPase activity during polarization of MDM toward proinflammatory M1- and proresolving M2-like phenotypes with focus on their differential LM profiles they produce, we took advantage of the selective V-ATPase inhibitor ArchA (17). Human monocytes were differentiated for 6 d with GM-CSF toward $M_{GM\text{-}CSF}$ MDM and with M-CSF toward $M_{M\text{-}CSF}$ MDM. Although these MDM are not primary (alveolar or peritoneal) macrophages, for which others have reported LM formation before (20, 21), they are suitable for studying the induction of LM pathways during the acquirement of different human macrophage phenotypes (5, 6). ArchA (30 nM) was added to MDM 30 min prior to 48 h polarization of $M_{GM\text{-}CSF}$ with LPS plus INFγ to M1 or of $M_{M\text{-}CSF}$ with IL-4 to M2, according to our previous report (6). To study the LM profiles by targeted LM metabololipidomics using UPLC–MS-MS, the polarized MDM were incubated with and without pathogenic *E. coli* (serotype O6:K2:H1, ratio 1:50) for 180 min (6). Upon exposure to *E. coli*, M1 and M2 produced opposing LM profiles that clearly distinguish their proinflammatory and proresolving phenotypes: M1 mainly formed COX-derived PGE_2 and 5-LOX/FLAP–derived LTs/5-hydroxyeicosatatraenoic acid (5-HETE), whereas M2 generated SPM (e.g., RvD5, MaR1, PD1, and RvE3), their precursors (i.e., 17-hydroxydocosahexaenoic acid [HDHA], 14-HDHA, 7-HDHA), and 15-LOX-1–derived products (e.g., 15-HETE, 15-HEPE) with low PG and LT/5-HETE levels (Fig. 1A–C, Supplemental Table I). During M1 polarization, ArchA had little impact on LM biosynthesis and caused no significant reduction in LOX products but slightly elevated PGD_2 and TxB_2 levels. By contrast in M2, inhibition of V-ATPase completely prevented the formation of all SPM, their precursors, and 15-LOX-1–derived mediators (Fig. 1B, 1C, Supplemental Table I). Although some monohydroxy 5-LOX products were lowered, formation of LTB_4 was not affected in M2. Moreover, solely in M2, the release of AA, eicosapentaenoic acid, and DHA was significantly impaired because of ArchA treatment (Fig. 1B, Supplemental Table I). In agreement with our previous work (16) ArchA increased the lysosomal pH during M1 and M2 polarization (Fig. 1D), assuring that V-ATPase activity was blocked in both macrophage phenotypes. To confirm on-target effects of ArchA, we used the structurally unrelated V-ATPase inhibitor bafilomycin that caused the

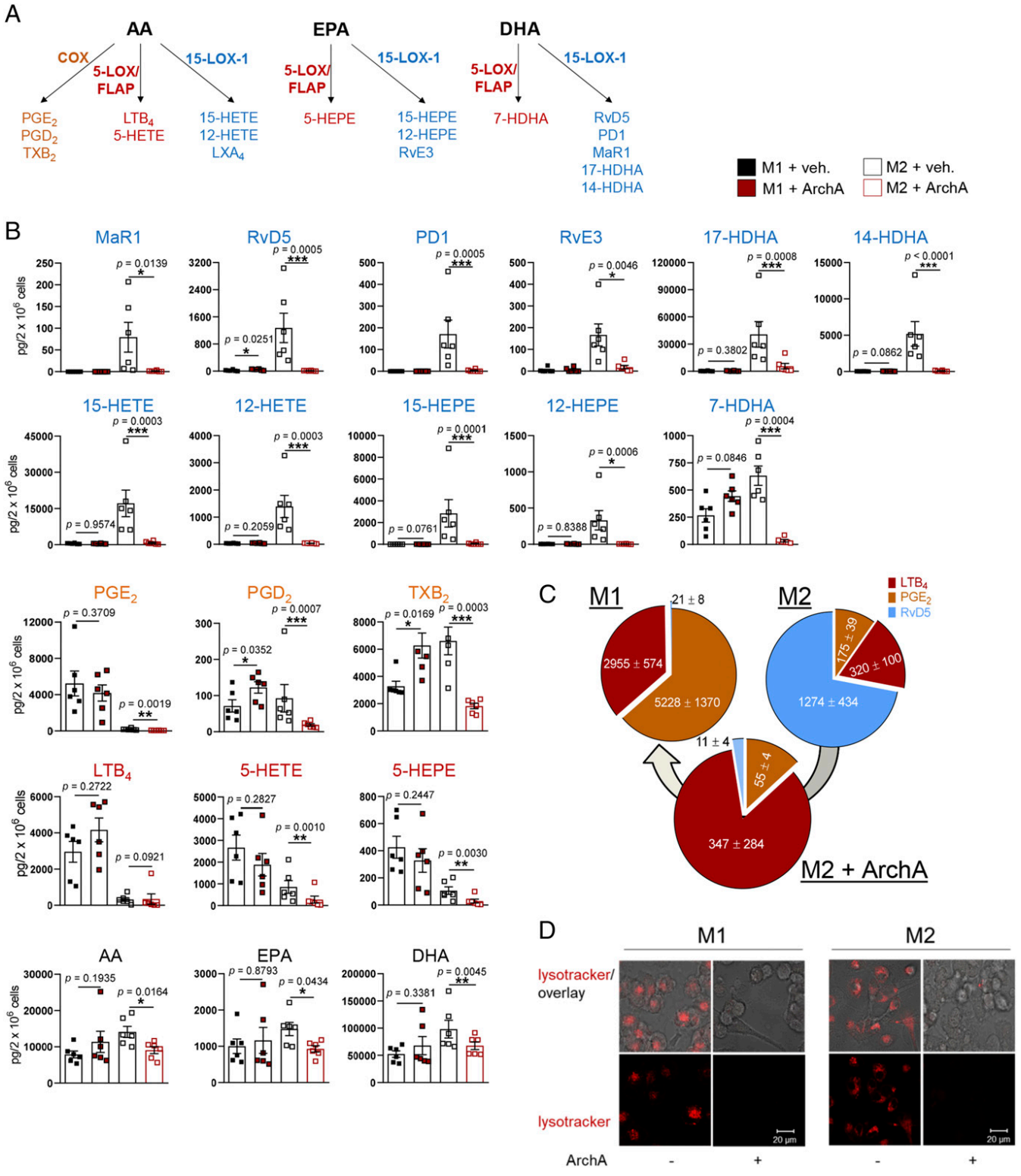

FIGURE 1. Targeting of V-ATPase suppresses SPM formation in human M2. (**A**) Schematic representation of the investigated LM-biosynthetic pathways involving COX, 5-LOX/FLAP, or 15-LOX-1, leading to respective LM. (**B**–**D**) Human monocytes were differentiated by GM-CSF or M-CSF (20 ng/ml, each) for 6 d to get $M_{GM\text{-}CSF}$ or $M_{M\text{-}CSF}$ MDM, respectively. After pretreatment with 30 nM ArchA or vehicle (veh., 0.1% DMSO) for 30 min, the $M_{GM\text{-}CSF}$ were polarized for 48 h with 100 ng/ml LPS plus 20 ng/ml IFN-γ to get M1 whereas the $M_{M\text{-}CSF}$ were polarized with 20 ng/ml IL-4 to get M2. (B) M1 and M2 (2×10^6, each) were incubated for 180 min with pathogenic *E. coli* (serotype O6:K2:H1, ratio 1:50) at 37°C. Biosynthesized LM were isolated from the supernatants by SPE and analyzed by UPLC–MS-MS; detection limit: 0.5 pg. Results are given as means ± SEM ($n = 6$ separate donors). Data were log-transformed for statistical analysis and analyzed by paired t test. $^*p < 0.05$, $^{**}p < 0.01$, $^{***}p < 0.001$, ArchA versus vehicle. (C) Amounts of produced RvD5, LTB_4, and PGE_2 are shown as pie chart in pg/2×10^6 cells (i.e., M1, M2, and M2 plus ArchA, as indicated). (D) Acidic vesicles (red) in M1 and M2 were stained with the LysoTracker probe for 1 h. Fluorescence microscopy pictures are representative of four independent experiments. Scale bar, 20 µm, contrast: differential interference contrast. The fluorescence was visualized with a Zeiss Axio Observer.Z1 microscope and an LCI Plan-Neofluar 63×/1.3 Imm Corr DIC M27 objective or a Plan-Apochromat 100×/1.40 Oil DIC M27 objective. Images were taken with an AxioCam MR3 camera and were acquired, cut, linearly adjusted in the overall brightness and contrast, and exported to TIF by the AxioVision 4.8 software.

same pattern of LM modulation as ArchA, that is, strongly impaired formation of SPM and their precursors with minor effects on 5-LOX and COX products in M2, but rather increased PG in M1 (Supplemental Fig. 1). MTT assays revealed no detrimental effects of ArchA and bafilomycin (up to 100 nM, each) on the viability of MDM during 48 h polarization (not shown).

In line with lower SPM, the protein levels of 15-LOX-1 were strongly impaired in M2 by ArchA (Fig. 2A). In contrast, 15-LOX-2 as well as 5-LOX and FLAP were not markedly affected, neither in M1 nor in M2. COX-1 protein levels were moderately decreased in M2, whereas COX-2 was elevated in M1 by ArchA. Finally, in M2, ArchA downregulated $cPLA_2$ protein expression, but not so in M1. Again, comparable effects were obtained with bafilomycin instead of ArchA, that is, impaired 15-LOX-1 levels in M2 and elevated COX-2 in M1 without change of 5-LOX in either phenotype (Supplemental Fig. 1). Note that in control experiments, addition of ArchA to polarized M1 or M2 and subsequent exposure to *E. coli* for 180 min did not affect biosynthesis of LM formation or the expression of respective biosynthetic enzymes (not shown). Together, V-ATPase activity is critically required during M2 polarization for 15-LOX-1 protein induction, accompanied by increased levels of $cPLA_2$ and COX-1 protein, but with minor importance for expression of LM pathways during M1 polarization.

To investigate if V-ATPase inhibition by ArchA would compromise M2 polarization per se, flow cytometry analysis of the phenotype-characteristic surface markers CD54 and CD80 for M1, and CD163 and CD206 for M2, was performed. In M2, ArchA had no effects on CD206 and CD163 expression, excluding a general influence on M2 polarization. However, ArchA suppressed the release of the M2-related protein IL-10 in M2 but not in M1 (Fig. 2C). In M1, considerable modulation of any macrophage phenotype markers by ArchA was not evident either (Fig. 2B), and M1-like cytokines such as TNF-α and IL-6 were not impaired (Fig. 2C). In conclusion, whereas classical human macrophage phenotype markers are hardly affected by V-ATPase inhibition during polarization, the LM profile in M2 with high SPM levels that distinguishes this proresolving phenotype from the proinflammatory M1 subset is strikingly compromised, suggesting a critical role of V-ATPase in the induction of the SPM-biosynthetic pathway.

Temporal modulation of LM-biosynthetic pathways depending on V-ATPase activity

Previous data show that the expression of the LM-biosynthetic enzymes COX-2 and 15-LOX-1 are temporally modulated during macrophage polarization (6). Thus, we studied manipulation of LM-biosynthetic enzyme expression by ArchA during M1/M2 polarization in more detail. In M2, the protein levels of 15-LOX-1 and COX-1 continuously increased during polarization up to 72 h, whereas 5-LOX slightly decreased, and $cPLA_2$ peaked at 24 h and then declined (Fig. 3A). ArchA did not affect the expression of these enzymes at 6 h but prevented the subsequent polarization-induced increase in the expression of 15-LOX-1, COX-1, and $cPLA_2$ starting at 24 up to 72 h (Fig. 3A). In M1, COX-2 was strongly induced after 6 h with slightly increased $cPLA_2$ levels followed by a continuous decline of both proteins up to 72 h; COX-1 levels were unchanged and 15-LOX-1 protein was not detectable in M1 [Fig. 3B, see also (6)]. In contrast to M2, ArchA failed to decrease COX-1 and $cPLA_2$ levels in M1, and COX-2 levels were rather increased at 24–48 h (Fig. 3B). Like in M2, 5-LOX expression in M1 was unaffected by ArchA. Control experiments assessing V-ATPase protein expression (using Abs against V0 or V1 subunit) revealed continuous presence of the protein during M1 and M2 polarization, without significant influences of ArchA (Fig. 3C, 3D).

Abrogation of 15-LOX-1 expression and SPM formation by targeting V-ATPase is independent of the JAK/STAT6 and the PI3K/Akt–mTOR complex 1–liver X receptor pathways

Induction of M2 polarization and 15-LOX-1 expression is mediated by the JAK/STAT6 pathway that activates transcription of the human ALOX15A gene (Fig. 4A) (22–24). We hypothesized that V-ATPase activity could be required for JAK/STAT6–mediated 15-LOX-1 expression in IL-4–stimulated MDM. However, V-ATPase blockage failed to abolish phosphorylation of STAT6 at Tyr641, and thus its activation, upon 48 h of IL-4 treatment (Fig. 4B) or at other time points (6, 24, or 72 h) during polarization (Fig. 4C). In contrast, the JAK-3 inhibitor CP-690,550 (25), which in analogy to ArchA blocked 15-LOX-1 (but not 5-LOX) expression (Fig. 4D) and thus reduced SPM formation (Fig. 4E), abolished STAT6 phosphorylation in M2 (Fig. 4D), as expected. This confirms that the JAK/STAT6 pathway regulates 15-LOX-1 expression and reveals its involvement in SPM formation but excludes a role for V-ATPase in JAK/STAT6-mediated 15-LOX-1 expression during M2 polarization. Although 5-LOX protein levels were unaffected by CP-690,550 (Fig. 4D), 5-LOX product formation was slightly reduced owing to JAK-3 inhibition (Fig. 4E).

IL-4 was also shown to induce M2 polarization via signaling molecules including PI3K, Akt, mTOR complex 1 (mTORC1), p70S6K, Lamtor1/V-ATPase complex, and liver X receptor (LXR) stimulation (14, 26) (Fig. 5A). Therefore, V-ATPase might be integrated in these downstream signaling pathways of IL-4 to accomplish 15-LOX-1 expression and SPM formation. ArchA impaired phosphorylation of Akt (PI3K substrate) and p70S6K (mTORC1 substrate) in M2 (Fig. 5B, 5C), with minor or no effects in M1, whereas expression of Lamtor1, the activator of mTORC1, was not affected (Fig. 5B). In control experiments, inhibitors of PI3K (i.e., LY294002) and of mTORC1 [i.e., Torin 1 (27)] reduced the phosphorylation of their substrates Akt and p70S6K, respectively (Fig. 5D), without affecting the viability of M2 within 48 h (data not shown). However, in contrast to ArchA, neither the PI3K inhibitor LY294002 nor the mTORC1 inhibitor Torin 1 prevented 15-LOX-1 expression (Fig. 5E) or SPM formation (Fig. 5F) in M2; also, the LXR antagonist GSK-2033 failed in this respect. These data suggest that V-ATPase might be of importance for PI3K/Akt and mTORC1 signaling, but these molecules as well as LXR are dispensable for IL-4–induced 15-LOX-1 protein expression and SPM biosynthesis during M2 polarization.

15-LOX-1 expression and SPM formation in M2 involves MEK/ERK-1/2 signaling

IL-4 activates the MEK/ERK-1/2 pathway (28), and a regulatory role for ERK-1/2 in mediating 15-LOX-1 expression in monocytes was shown (29). Thus, we speculated that the MEK/ERK-1/2 pathway is involved in 15-LOX-1 expression and SPM formation in M2 and that targeting of V-ATPase may suppress the MEK/ERK-1/2 pathway (Fig. 6A). Preincubation with ArchA prior to M2 polarization strongly impaired the phosphorylation of ERK-1/2 and of its upstream kinase MEK at 24, 48, and 72 h (Fig. 6B, 6C), whereas phosphorylation of p38 MAPK was rather increased (Supplemental Fig. 2). Use of NH_4Cl, another tool to elevate the pH in organelles, mimicked the effects of ArchA and suppressed ERK-1/2 phosphorylation in M2 (Supplemental Fig. 3), as expected. Noteworthy, in M1, phosphorylation of ERK-1/2 and MEK was not affected by ArchA.

We next exploited the ERK-1/2 activation inhibitor U0126 (30) to test if ERK-1/2 is required for IL-4–induced 15-LOX-1

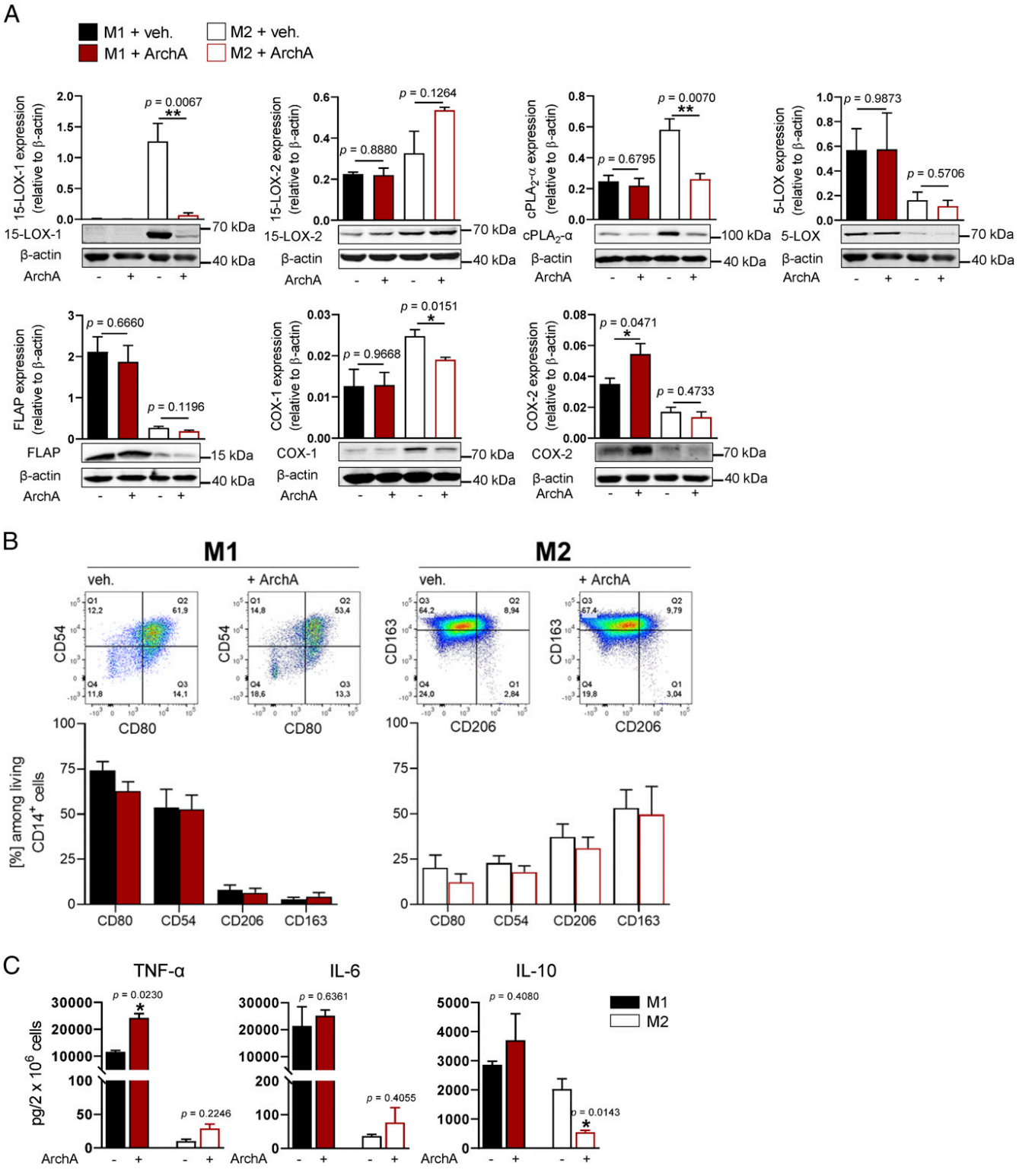

FIGURE 2. Targeting of V-ATPase suppresses 15-LOX-1 expression in human M2. $M_{GM\text{-}CSF}$ and $M_{M\text{-}CSF}$ were pretreated with 30 nM ArchA or vehicle (veh., 0.1% DMSO) for 30 min prior to polarization to M1 and M2 for 48 h. (**A**) Protein expression and densitometric analysis of 15-LOX-1, 15-LOX-2, $cPLA_2$-α, 5-LOX, FLAP, COX-1, and COX-2, normalized to β-actin. Western blots are shown as representatives and data are means ± SEM ($n = 4$ separate donors). $^*p < 0.05$, $^{**}p < 0.01$, ArchA versus vehicle analyzed by two-tailed t test. (**B**) Expression of surface macrophage polarization markers for M1 (CD54, CD80) and M2 (CD206, CD163) analyzed by flow cytometry; representative pseudocolor dot plots from $n = 3$ separate donors; quantification is given as bar charts, data are means ± SEM. Zombie Aqua Fixable viability kit (BioLegend) was used to assess live versus dead status. MDM were first gated using forward scatter and side scatter and then gated on living cells by Zombie Aqua fixable staining. Living cells were gated on CD14 positive and then gated on specific M1 (CD80 and CD206) and M2 (CD163 and CD206) marker. (**C**) Effects of ArchA on cytokine release. Supernatants were analyzed for TNF-α, IL-6 and IL-10 by ELISA and shown in pg/2 × 10^6 cells; means ± SEM ($n = 3$ separate donors). $^*p < 0.05$ compared with vehicle, two-tailed t test.

expression and SPM formation. Pretreatment with U0126 prior to M2 polarization reduced ERK-1/2 phosphorylation as expected and significantly prevented the expression of 15-LOX-1 without affecting 5-LOX protein levels (Fig. 6D). In contrast, the p38 MAPK inhibitor skepinone-L (31) failed to influence 15-LOX-1 levels or LM biosynthesis (Supplemental Fig. 2). The transcription

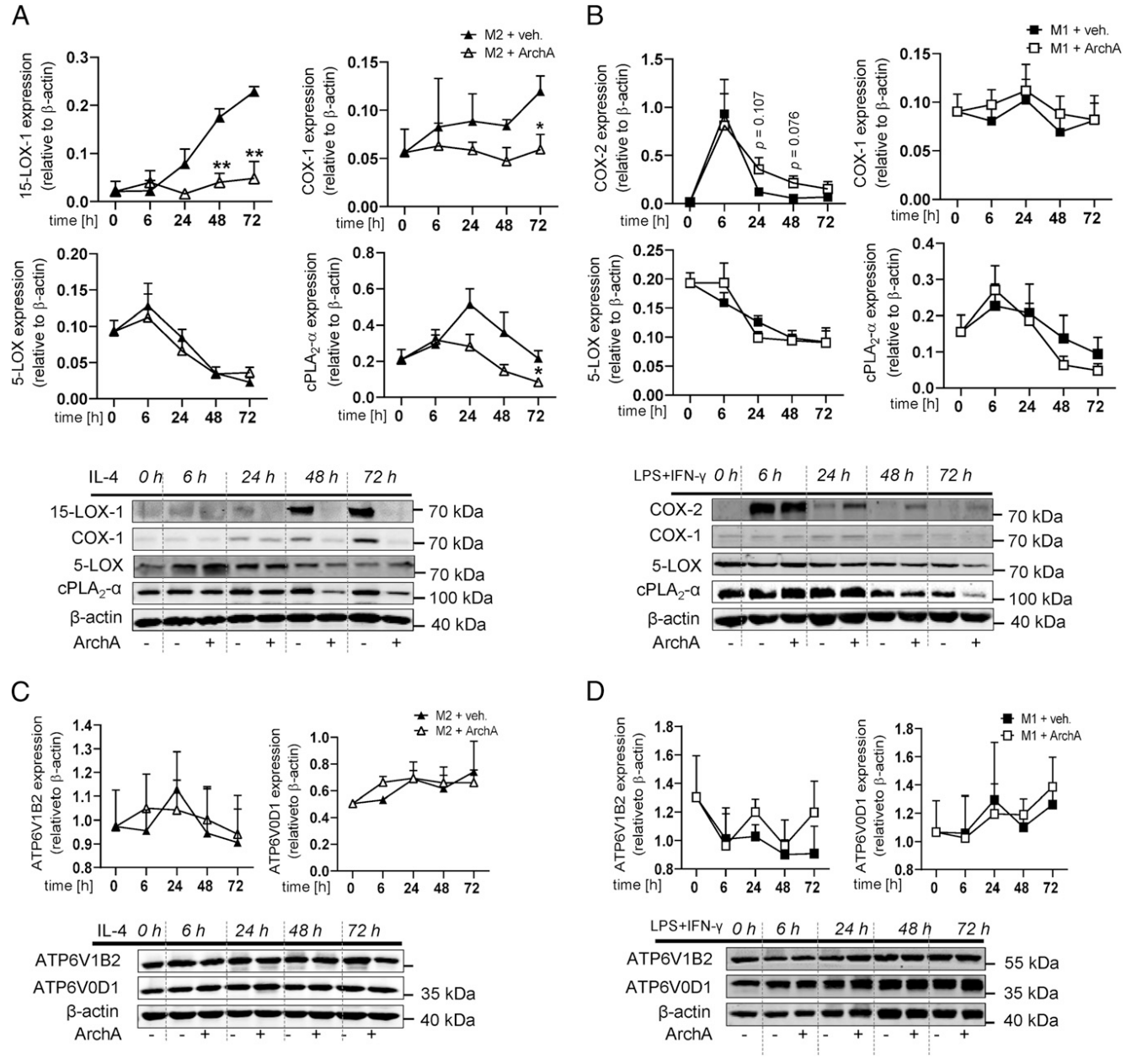

FIGURE 3. Temporal modulation of LM-biosynthetic pathways by targeting V-ATPase. $M_{GM\text{-}CSF}$ and $M_{M\text{-}CSF}$ were pretreated with 30 nM ArchA or vehicle (veh., 0.1% DMSO) for 30 min prior to polarization to M1 and M2 for the indicated periods (0–72 h). (**A** and **B**) Protein expression and densitometric analysis of 15-LOX-1 (only for M2), COX-2 (only for M1), COX-1, 5-LOX, and $cPLA_2$-α, normalized to β-actin in (A) M2 and (B) M1. (**C** and **D**) V-ATPase protein expression during macrophage polarization was assessed by immunoblotting for ATP6V1B2 (V1 subunit), and ATP6V0D1 (V0 subunit) in (C) M2 and (D) M1, and normalized to β-actin for densitometric analysis. Western blots are shown as representatives and results are given as means ± SEM (n = 4 separate donors). $^*p < 0.05$, $^{**}p < 0.01$, ArchA versus vehicle determined by two-tailed t test.

factor c-Myc downstream of the MEK/ERK-1/2 pathway has been shown to regulate 15-LOX-1 expression in macrophages (32), and ArchA downregulated c-Myc in leukemic cells (33) (Fig. 6B). Thus, we tested if the selective c-Myc inhibitor JQ-1 (34) would suppress 15-LOX-1 protein levels (Fig. 6E). As expected, SPM formation and 15-LOX-1-related LM were markedly impaired by U0126 as well as by JQ-1, whereas PG and fatty acid release were unaffected (Fig. 6F). Also, 5-LOX product formation was reduced by U0126 (Fig. 6F) but not so 5-LOX protein expression (Fig. 6D). Finally, the STAT6 inhibitor AS1517499, used to reinforce the link between STAT6 and 15-LOX-1, blocked phosphorylation of STAT6 and expression of 15-LOX-1 (but not 5-LOX) and also ERK-1/2 phosphorylation was moderately inhibited (Supplemental Fig. 3). Together, our data show that V-ATPase is required for functional MEK/ERK-1/2 pathway to accomplish 15-LOX-1 expression and SPM formation during M2 polarization.

Targeting V-ATPase in vivo delays resolution and suppresses SPM formation

To study the consequence of V-ATPase interference for SPM biosynthesis and resolution of inflammation in vivo, we made use of zymosan-induced peritonitis in mice (Fig. 7A), a well-established model of self-limited acute inflammation (19, 35). Application of ArchA (1 mg/kg, i.p., 1 h prior zymosan) caused marked elevation of neutrophil numbers in the peritoneum in the resolving phase 24 h postzymosan versus vehicle-treated mice, reflecting continuation of inflammation, whereas the number of neutrophils during the acute phase (4 h postzymosan) was hardly

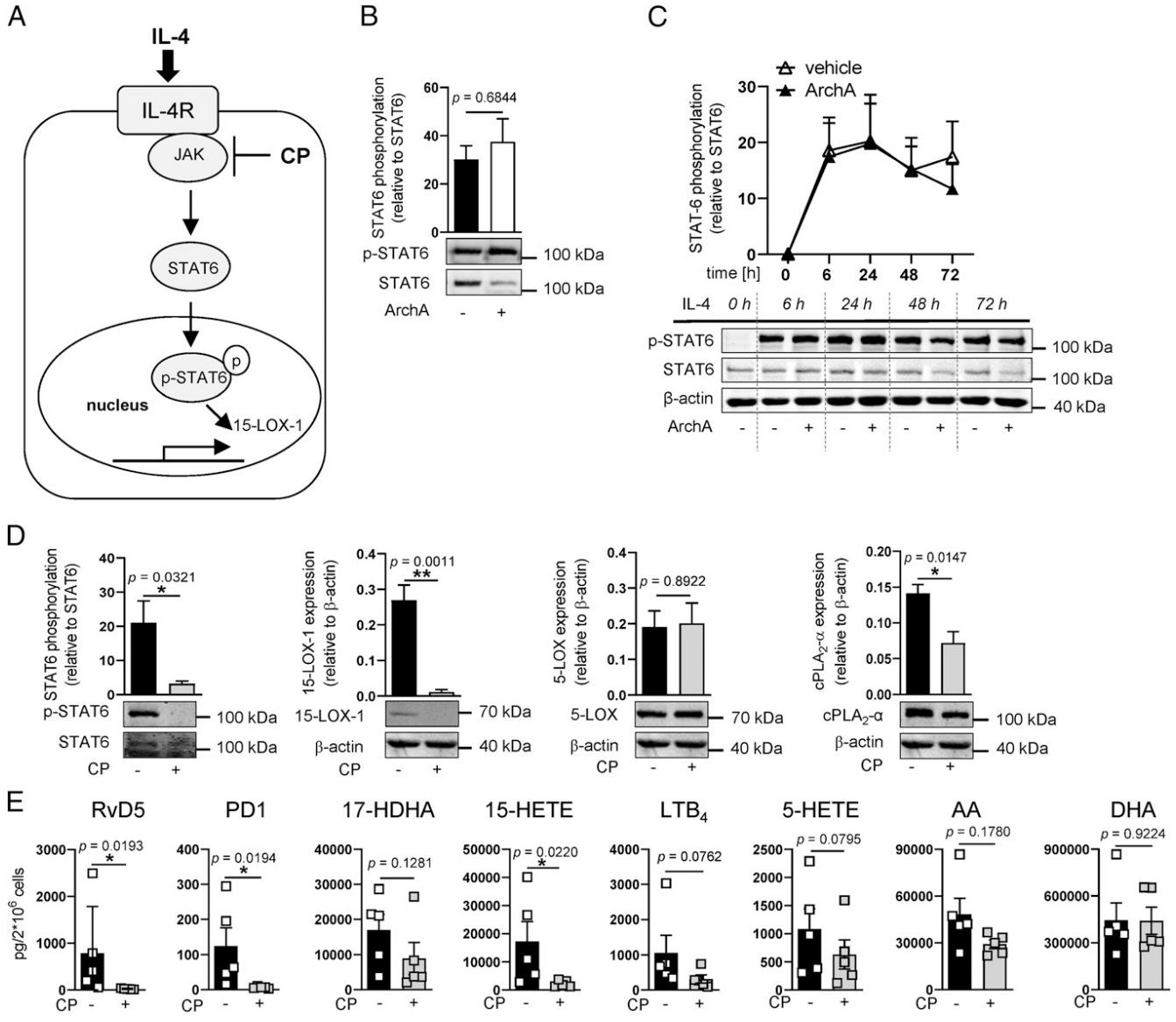

FIGURE 4. Abrogation of 15-LOX-1 expression and SPM formation by targeting V-ATPase is independent of the JAK/STAT6 pathway in M2. (**A**) Schematic draft of the JAK/STAT6 pathway in M2. (**B** and **C**) $M_{GM\text{-}CSF}$ and $M_{M\text{-}CSF}$ were pretreated with 30 nM ArchA or vehicle for 30 min prior to polarization toward M2 for (B) 48 h or for (C) 0–72 h. Cell lysates were immunoblotted for phospho-STAT6, STAT6, and β-actin, and densitometric analysis thereof was performed. Results are given as means ± SEM ($n = 4$ separate donors). (**D** and **E**) $M_{M\text{-}CSF}$ were pretreated with the JAK-3 inhibitor CP-690,550 (CP, 100 nM) for 30 min prior to polarization to M2 for 48 h. (D) Cell lysates were immunoblotted for phospho-STAT6, STAT6, 15-LOX-1, 5-LOX, and $cPLA_2$-α, and normalized to β-actin for densitometric analysis. Results are given as means ± SEM of $n = 4$ separate donors. $^*p < 0.05$, $^{**}p < 0.01$, CP-690,550 versus vehicle; two-tailed t test. (E) Effects of CP-690,550 on LM biosynthesis in M2 that were incubated for 180 min with pathogenic *E. coli* (serotype O6:K2:H1, ratio 1:50) at 37°C. LM were isolated by SPE and analyzed by UPLC–MS-MS, detection limit: 0.5 pg. Results are given as means ± SEM of $n = 5$ separate donors. $^*p < 0.05$, CP versus vehicle. Data were log transformed for statistical analysis, paired t test.

affected by ArchA (Fig. 7B). LM metabololipidomics of the exudates of these mice revealed strongly reduced levels of the SPM RvD2, RvD4, PD1, and LXA_4 in ArchA-treated animals, and also RvD5 and MaR1 levels tended to be lower (Fig. 7C). Moreover, all 15-LOX-1–related SPM precursors (17-HDHA, 14-HDHA, 15-HETE, 15-HEPE, 12-HETE, 12-HEPE, 7-HDHA) were lower in exudates of mice that received ArchA, whereas the levels of 5-LOX-derived LTB_4 and 5-HETE as well as of COX-derived PGs were not different between ArchA- and vehicle-treated groups (Fig. 7C). Similarly, the amounts of various circulating SPM (e.g., RvD1, RvD5) and their precursors in plasma were significantly lower 24 h post zymosan when mice received ArchA, whereas PG and LTB_4 were not reduced but rather elevated (Fig. 7D). Collectively, targeting V-ATPase during inflammation in vivo locally and systemically suppresses SPM biosynthesis and delays resolution of inflammation.

Discussion

One of the hallmarks of host defense during infectious inflammation is the engulfment of invaders by macrophages that transport the invader to the phagosome, an acidic digestive compartment, where the pathogen is degraded to regain homeostasis of the host. Efficient phagosome maturation requires active V-ATPase upon fusion with compartments of the endolysosomal pathway (11, 15). Also, V-ATPase plays a fundamental role in cytokine trafficking and secretion in inflammation (16, 36). However, the function of V-ATPase in the biosynthesis of either proinflammatory or proresolving LM and in resolution of inflammation has not been reported yet.

In this study, our results reveal a novel and critical role for V-ATPase in the biosynthesis of SPM in human M2-like MDM with potential consequences for resolution of inflammation. Alternative

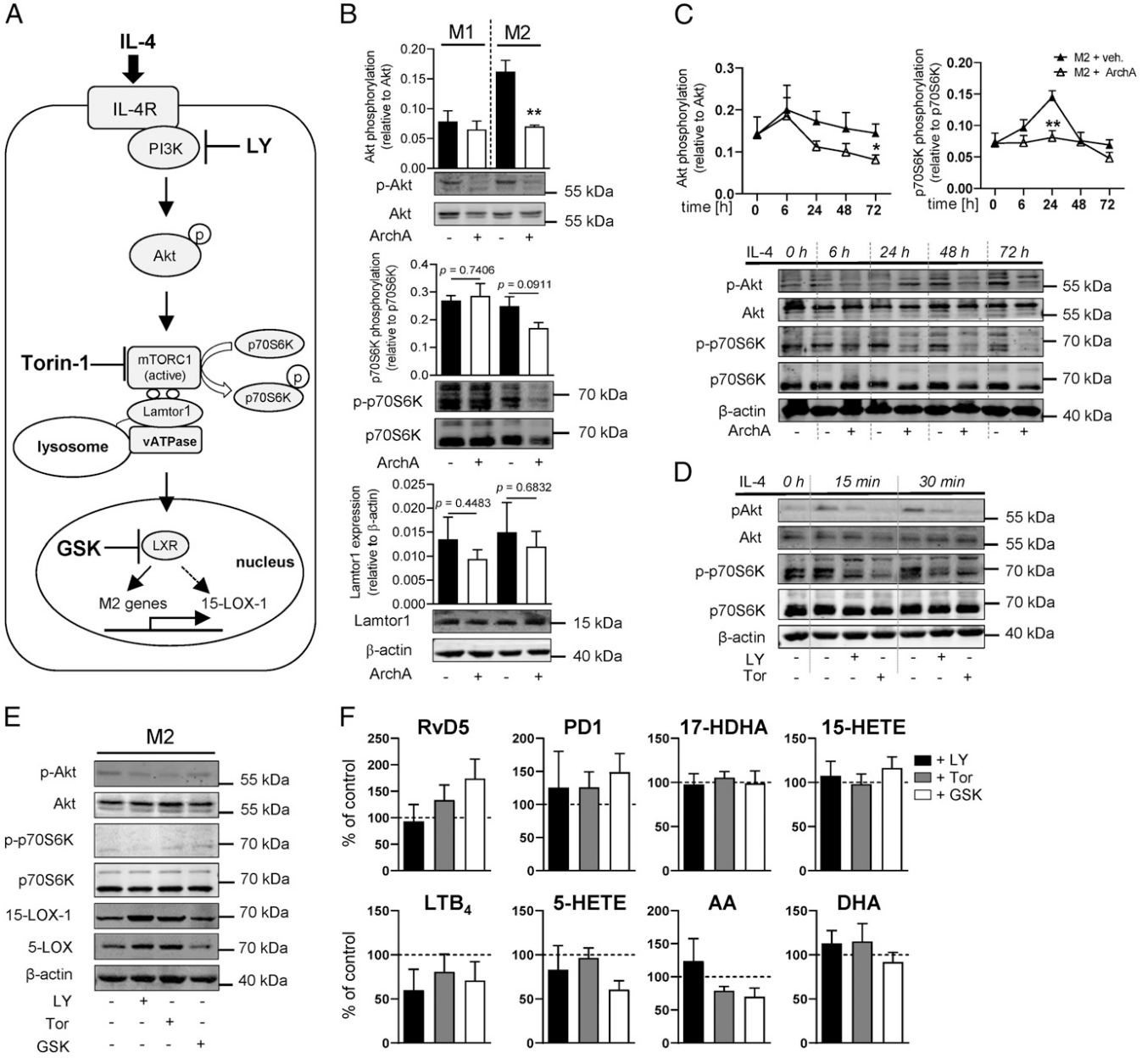

FIGURE 5. Abrogation of 15-LOX-1 expression and SPM formation by targeting V-ATPase is independent of the PI3K/Akt–mTORC1–LXR pathway in M2. (**A**) Schematic draft of the PI3K/Akt–mTORC1–LXR pathway in M2. (**B** and **C**) $M_{GM\text{-}CSF}$ and $M_{M\text{-}CSF}$ were pretreated with 30 nM ArchA or vehicle for 30 min prior to polarization to M1 and M2 (B) for 48 h or (C) for 0–72 h. Cell lysates were immunoblotted for phospho-Akt, Akt, phospho-p70S6K, p70S6K, and Lamtor1 and normalized to β-actin for densitometric analysis. Data are given as means ± SEM. $n = 4$ separate donors, two-tailed t test. $^*p < 0.05$, $^{**}p < 0.01$, ArchA versus vehicle. (**D**) $M_{M\text{-}CSF}$ were pretreated with the PI3K inhibitor LY294002 (LY, 3 μM) or the mTORC1 inhibitor Torin 1 (Tor, 5 nM) for 30 min prior to polarization with IL-4 for 0, 15, and 30 min or (**E**) for 48 h, including also the LXR inhibitor GSK-2033 (GSK, 20 μM). Cell lysates were immunoblotted for phospho-Akt, Akt, phospho-p70S6K, p70S6K, 15-LOX-1, and 5-LOX and normalized to β-actin for densitometric analysis. (**F**) $M_{M\text{-}CSF}$ were pretreated for 30 min with LY (3 μM), Torin 1 (5 nM), and GSK (20 μM) prior to polarization for 48 h to M2, and then incubated with *E. coli* (serotype O6:K2:H1, ratio 1:50) for 180 min at 37°C for LM biosynthesis. Formed LM were isolated by SPE and analyzed by UPLC–MS-MS. Results are given as percentage of vehicle control (= 100%), means ± SEM ($n = 4$ separate donors).

activation of macrophages by IL-4 results in proresolving M2 phenotypes that are featured by high capacities to generate SPM upon challenge with pathogenic bacteria (6) or during efferocytosis of apoptotic neutrophils (1, 5). SPM actively terminate inflammation and promote its resolution by inhibiting neutrophil infiltration, sequestering proinflammatory cytokines, promoting phagocytosis, and finally by clearance of apoptotic cells or cellular debris (7, 8). Moreover, SPM accelerate tissue repair and regeneration (37), typical features promoted by M2 macrophages. Intriguingly, M2-derived SPM, in particular the maresins, switch polarization of M1 toward the M2 phenotype (9). Our results from a pharmacological approach of targeting V-ATPase by two structurally different V-ATPase inhibitors (ArchA and bafilomycin) provide evidences for a critical role of V-ATPase in the induction of the expression of 15-LOX-1, the key enzyme in SPM biosynthesis, which is specifically upregulated during polarization toward M2 (6). Notably, the expression of 15-LOX-2 was not impaired by V-ATPase inhibition, corroborating the specificity of V-ATPase in regulating the 15-LOX-1 isoform. V-ATPase was shown to be required for IL-4–induced murine M2 polarization, but SPM biosynthesis or expression of 15-LOX-1 was not addressed (14). Our results with mice demonstrate a role of

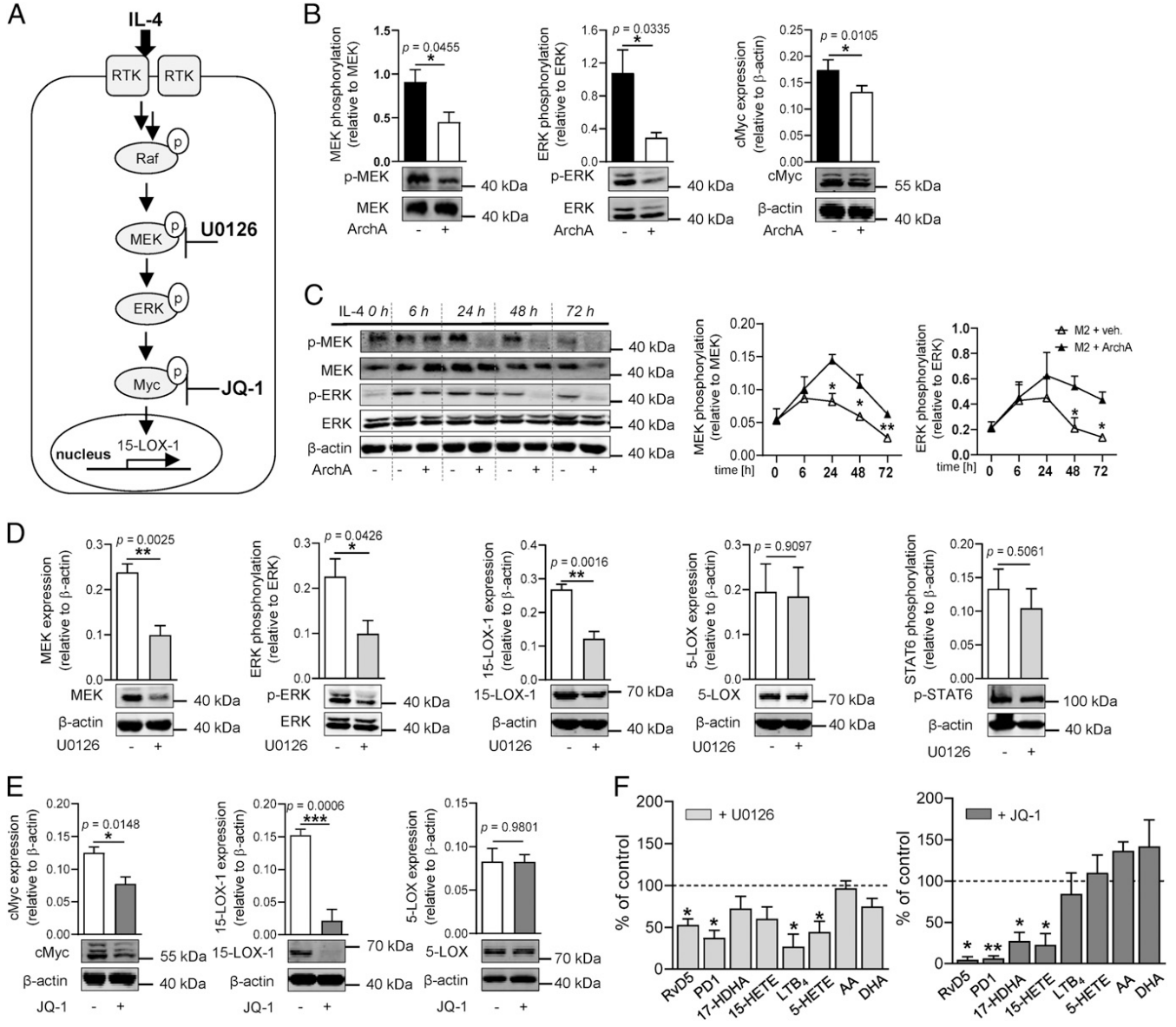

FIGURE 6. 15-LOX-1 expression and SPM formation is accomplished by the MEK/ERK pathway in M2. (**A**) Schematic draft of the Raf–MEK–ERK-1/2 cascade. (**B** and **C**) $M_{GM\text{-}CSF}$ and $M_{M\text{-}CSF}$ were pretreated with 30 nM ArchA or vehicle for 30 min prior to polarization (B) for 48 h to M2 or (C) for a period of 0–72 h to M2. Cell lysates were immunoblotted for phospho-ERK-1/2, ERK-1/2, phospho-MEK, MEK, and c-Myc and normalized to β-actin for densitometric analysis. Data are means ± SEM ($n = 4$ separate donors for 48 h and $n = 3$ separate donors for 0–72 h), two tailed t test. $^{*}p < 0.05$, $^{**}p < 0.01$. (**D**–**F**) $M_{M\text{-}CSF}$ were pretreated with the ERK-1/2 activation inhibitor U0126 (3 μM) and the c-Myc inhibitor JQ-1 (100 nM) or vehicle for 30 min prior to polarization toward M2 for 48 h. (D and E) Cell lysates were immunoblotted for phospho-ERK-1/2, ERK-1/2, MEK, 15-LOX-1, 5-LOX, phospho-STAT6, and cMyc and normalized to β-actin for densitometric analysis. Data are means ± SEM ($n = 4$ separate donors), two tailed t test. $^{*}p < 0.05$, $^{**}p < 0.01$, $^{***}p < 0.001$. (F) Formed LM after incubation of polarized M2 with *E. coli* (serotype O6:K2:H1 ratio 1:50) for 180 min at 37°C. LM were isolated by SPE and analyzed by UPLC–MS-MS. Results are given as percentage of vehicle control (= 100%); means ± SEM ($n = 3$ separate donors); data were log transformed for statistical analysis. $^{*}p < 0.05$, $^{**}p < 0.01$, U0126 and JQ-1 versus vehicle. Data were log transformed for statistical analysis, paired t test.

V-ATPase in SPM biosynthesis also in vivo and implicate its necessity for resolution of inflammation, reflected by unhindered neutrophil infiltration in ArchA-treated mice during peritonitis. Note that besides 15-LOX-1 and SPM, other LM pathways such as PGs and LTs were not affected by V-ATPase inhibition, neither in murine peritonitis nor in human M1. Furthermore, classical M1 and M2 polarization markers or cell viability were not influenced by V-ATPase inhibition and LM formation in the M1 phenotype; where PGs and LTs dominate (5, 6), ArchA had little to no impact. Instead, blocking V-ATPase in M1 increased COX-2 expression accompanied by elevated PG levels, in agreement with (16), a tendency observed also in our present in vivo experiments. Conclusively, V-ATPase is specifically required for induction of 15-LOX-1 and related SPM biosynthesis during M2 polarization and thus may be key for ensuring effective resolution of inflammation. However, 15-LOX-1 is a versatile enzyme, with roles not only in the termination but also in the onset of inflammation (38) and has been implicated in the pathogenesis of chronic inflammatory diseases, particularly related to the airways (39, 40). The induction of 15-LOX-1 expression by IL-4 in various cell types, including primary cultures of human monocytes, strongly depends on STAT6 (22, 23, 29). Therefore, interference with V-ATPase may prevent 15-LOX-1 induction by suppression of STAT6 signaling. However, targeting V-ATPase did neither influence STAT6 expression nor its phosphorylation, suggesting the existence of a STAT6-independent signaling route induced by IL-4 for 15-LOX-1 expression. Another prominent

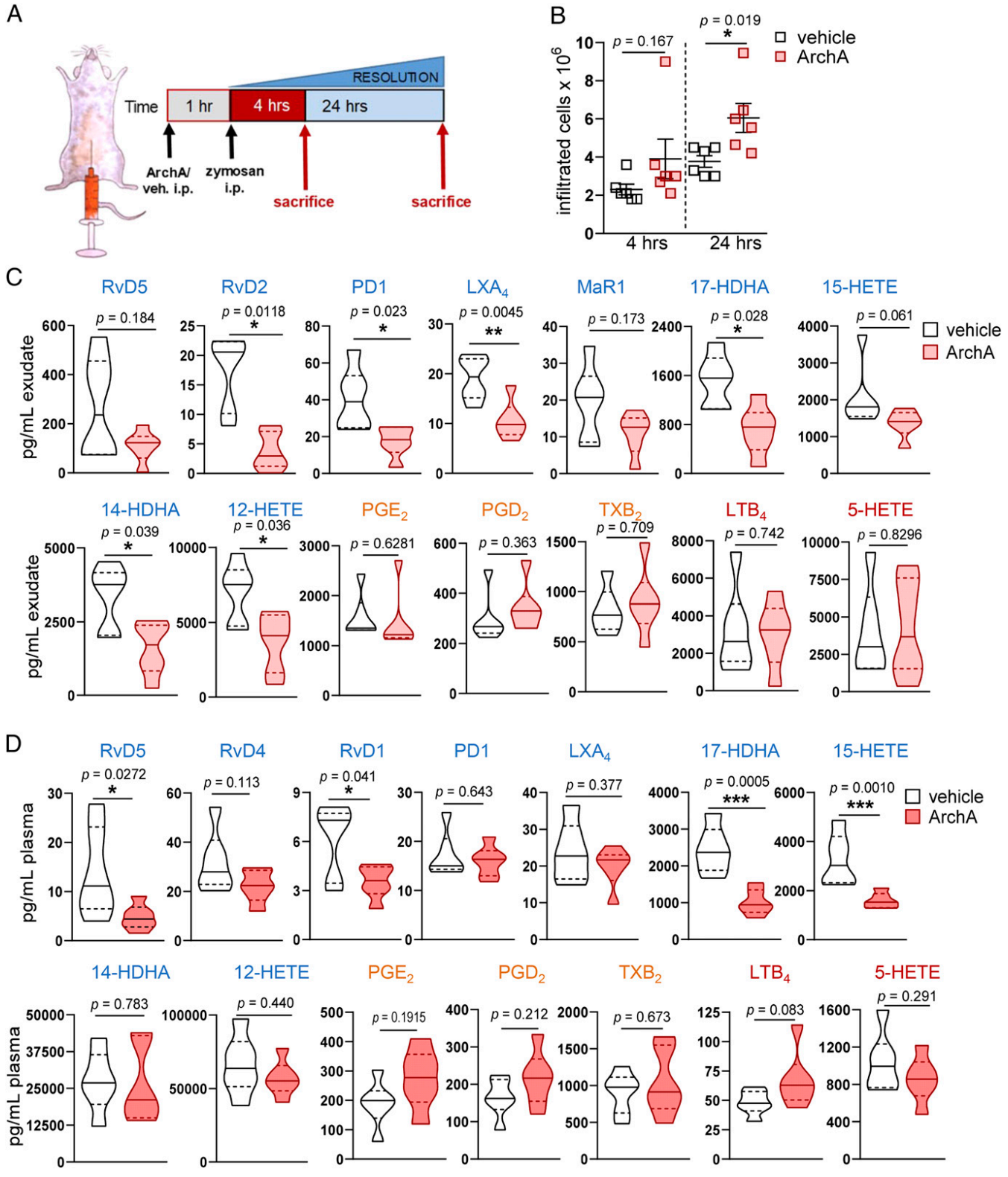

FIGURE 7. Targeting of V-ATPase in vivo delays resolution and suppresses SPM formation in mice. (**A**) Male adult CD1 mice were treated i.p. with ArchA (1 mg/kg) or vehicle 1 h before zymosan-induced peritonitis (1 mg, i.p.). Mice were sacrificed after 4 or 24 h with CO_2, and peritoneal exudates were collected by lavage with 3 ml of PBS, and blood was obtained by cardiac puncture. (**B**) Cell numbers in the peritoneal cavity after 4 and 24 h. (**C**) LM profiles of exudates and (**D**) of plasma after 24 h ArchA treatment. The results are given in picogram per milliliter as means ± SEM ($n = 6$ animals each group). Data were log transformed for statistical analysis, two-tailed t test. *$p < 0.05$, **$p < 0.01$, ***$p < 0.001$, ArchA versus vehicle.

IL-4–induced pathway in mice that governs expression of classical M2 signature genes such as arginase-1, the mannose receptor (CD206), and IL-10, is the PI3K/Akt–mTORC1–LXR cascade in which Lamtor1 forms a complex with active V-ATPase (14). In our study using human MDM, ArchA inhibited phosphorylation of Akt and of the mTORC1 substrate p70S6K in M2, but the expression of Lamtor1, the target of mTORC1, was not affected. Moreover, inhibition of PI3K, of mTORC1, or of LXR did not influence 15-LOX-1 protein levels and SPM formation, suggesting that this pathway is negligible for the SPM-biosynthetic machinery in human M2.

Our results propose that the MEK/ERK-1/2 pathway mediates IL-4–induced 15-LOX-1 expression during M2 polarization and that targeting of V-ATPase prevents 15-LOX-1 induction by blocking MEK/ERK-1/2 signaling. In fact, phosphorylation of ERK-1/2 by MEK was shown to mediate IL-13–induced 15-LOX-1 expression in human monocytes (22, 41). In our hands, the ERK-1/2 activation inhibitor U0126 reduced 15-LOX-1 expression and suppressed SPM biosynthesis, similar to V-ATPase inhibition. As mentioned above, ArchA inhibited Akt phosphorylation, and in fact, the PI3K/Akt cascade is known to activate ERK-1/2. Recently, a direct interaction of phosphorylated PI3K, Akt, and ERK with the subunit E of the V-ATPase V1 domain was reported in cancer cells (42). Thus, the MEK/ERK-1/2 cascade appears to be a focal point for cross-cascade regulation in M2 polarization involving V-ATPase. Along these lines, the transcription factor c-Myc downstream of the MEK/ERK-1/2 pathway was suppressed by ArchA in leukemic cells (33) as well as in our hands in M2, and the c-Myc inhibitor JQ-1 (32) abrogated 15-LOX-1 protein expression and SPM formation. Conclusively, our results suggest that induction of 15-LOX-1 in human M2-like MDM is accomplished by the MEK/ERK-1/2 pathway that requires V-ATPase activity.

In addition to SPM and 15-LOX–derived precursors, 5-LOX products were also reduced by either inhibition of V-ATPase, JAK-3, or ERK-1/2, without impairing 5-LOX protein levels. Cellular 5-LOX activity depends mainly on AA supply, FLAP, Ca^{2+}, and phosphorylations by MAPKAPK-2 and ERK-1/2 (43). ArchA, CP-690,550, or U0126 reduced AA supply and ERK-1/2, and possibly other processes required for substantial 5-LOX product formation, without altering 5-LOX protein levels. Moreover, the ERK-1/2 pathway related to 5-LOX activation and LT biosynthesis is subject of a sex dimorphism due to transient modulation by testosterone in leukocytes (44), implying potential sex differences also for ERK-1/2–mediated 15-LOX-1 regulation. However, the lengthy monocyte/MDM culture conditions in sex hormone-containing FCS (10%) may mask potential sex-dependent modulation and was not explored in this study. Ongoing studies with male and female mice indicate the existence of sex-biased 15-LOX regulation in macrophages in accordance with observations by others (45).

Genetic or pharmacological interference with V-ATPase has been linked to defective wound healing events (46) in which V-ATPase was necessary for the ERK-1/2–dependent transcriptional activation of the repair response around the wound epidermis, and nonhealing chronic wounds display extracellular pH gradients that disrupt epidermal repair (47). This supports our hypothesis on a role of V-ATPase in resolution of inflammation, especially by ensuring effective SPM biosynthesis, because SPMs were shown to effectively increase tissue remodeling and regeneration together with superior wound healing events (48). In fact, we demonstrate in this study that targeting V-ATPase in zymosan-induced peritonitis in vivo, a self-limited model of acute inflammation (19, 35), delays resolution of inflammation reflected by impaired clearance of leukocytes from the inflamed cavity and by reduced SPM levels in both exudates and plasma. Again, other LM such as LTs and PGs were unaltered by V-ATPase inhibition in this model, supporting the selectivity of this pathway for SPM biosynthesis.

Taken together, we show that V-ATPase activity is essential for induction of 15-LOX-1 during polarization of human MDM toward the proresolving M2 phenotype and the consequent capacity to generate SPM. In particular, V-ATPase appears to be crucial for IL-4–induced MEK/ERK-1/2 signaling, which is directly connected to induction of 15-LOX-1 protein expression. We conclude that V-ATPase may be a key component in alternative macrophage activation by regulating 15-LOX-1 expression and related SPM biosynthesis and thus in the resolution of inflammation.

Acknowledgments

We thank Saskia Andreas and Bärbel Schmalwasser for expert technical assistance.

Disclosures

The authors have no financial conflicts of interest.

References

1. Dalli, J., and C. Serhan. 2016. Macrophage proresolving mediators-the when and where. *Microbiol. Spectr.* 4.
2. Motwani, M. P., and D. W. Gilroy. 2015. Macrophage development and polarization in chronic inflammation. *Semin. Immunol.* 27: 257–266.
3. Murray, P. J. 2017. Macrophage polarization. *Annu. Rev. Physiol.* 79: 541–566.
4. Murray, P. J., J. E. Allen, S. K. Biswas, E. A. Fisher, D. W. Gilroy, S. Goerdt, S. Gordon, J. A. Hamilton, L. B. Ivashkiv, T. Lawrence, et al. 2014. Macrophage activation and polarization: nomenclature and experimental guidelines. *Immunity* 41: 14–20.
5. Dalli, J., and C. N. Serhan. 2012. Specific lipid mediator signatures of human phagocytes: microparticles stimulate macrophage efferocytosis and pro-resolving mediators. *Blood* 120: e60–e72.
6. Werz, O., J. Gerstmeier, S. Libreros, X. De la Rosa, M. Werner, P. C. Norris, N. Chiang, and C. N. Serhan. 2018. Human macrophages differentially produce specific resolvin or leukotriene signals that depend on bacterial pathogenicity. *Nat. Commun.* 9: 59.
7. Serhan, C. N. 2014. Pro-resolving lipid mediators are leads for resolution physiology. *Nature* 510: 92–101.
8. Serhan, C. N., and N. Chiang. 2013. Resolution phase lipid mediators of inflammation: agonists of resolution. *Curr. Opin. Pharmacol.* 13: 632–640.
9. Dalli, J., and C. N. Serhan. 2017. Pro-resolving mediators in regulating and conferring macrophage function. *Front. Immunol.* 8: 1400.
10. Cotter, K., L. Stransky, C. McGuire, and M. Forgac. 2015. Recent insights into the structure, regulation, and function of the V-ATPases. *Trends Biochem. Sci.* 40: 611–622.
11. Bidani, A., B. S. Reisner, A. K. Haque, J. Wen, R. E. Helmer, D. M. Tuazon, and T. A. Heming. 2000. Bactericidal activity of alveolar macrophages is suppressed by V-ATPase inhibition. *Hai* 178: 91–104.
12. Grinstein, S., A. Nanda, G. Lukacs, and O. Rotstein. 1992. V-ATPases in phagocytic cells. *J. Exp. Biol.* 172: 179–192.
13. Tapper, H., and R. Sundler. 1995. Bafilomycin A1 inhibits lysosomal, phagosomal, and plasma membrane H(+)-ATPase and induces lysosomal enzyme secretion in macrophages. *J. Cell. Physiol.* 163: 137–144.
14. Kimura, T., S. Nada, N. Takegahara, T. Okuno, S. Nojima, S. Kang, D. Ito, K. Morimoto, T. Hosokawa, Y. Hayama, et al. 2016. Polarization of M2 macrophages requires Lamtor1 that integrates cytokine and amino-acid signals. *Nat. Commun.* 7: 13130.
15. Canton, J., R. Khezri, M. Glogauer, and S. Grinstein. 2014. Contrasting phagosome pH regulation and maturation in human M1 and M2 macrophages. *Mol. Biol. Cell* 25: 3330–3341.
16. Thomas, L., Z. Rao, J. Gerstmeier, M. Raasch, C. Weinigel, S. Rummler, D. Menche, R. Muller, C. Pergola, A. Mosig, and O. Werz. 2017. Selective upregulation of TNFα expression in classically-activated human monocyte-derived macrophages (M1) through pharmacological interference with V-ATPase. *Biochem. Pharmacol.* 130: 71–82.
17. Sasse, F., H. Steinmetz, G. Höfle, and H. Reichenbach. 2003. Archazolids, new cytotoxic macrolactones from Archangium gephyra (Myxobacteria). Production, isolation, physico-chemical and biological properties. *J. Antibiot. (Tokyo)* 56: 520–525.
18. English, J. T., P. C. Norris, R. R. Hodges, D. A. Dartt, and C. N. Serhan. 2017. Identification and profiling of specialized pro-resolving mediators in human tears by lipid mediator metabolomics. *Prostaglandins Leukot. Essent. Fatty Acids* 117: 17–27.
19. Rao, T. S., J. L. Currie, A. F. Shaffer, and P. C. Isakson. 1994. In vivo characterization of zymosan-induced mouse peritoneal inflammation. *J. Pharmacol. Exp. Ther.* 269: 917–925.
20. Gilroy, D. W., M. L. Edin, R. P. De Maeyer, J. Bystrom, J. Newson, F. B. Lih, M. Stables, D. C. Zeldin, and D. Bishop-Bailey. 2016. CYP450-derived oxylipins mediate inflammatory resolution. *Proc. Natl. Acad. Sci. USA* 113: E3240–E3249.
21. Roubin, R., and J. Benveniste. 1985. Formation of prostaglandins, leukotrienes and paf-acether by macrophages. *Comp. Immunol. Microbiol. Infect. Dis.* 8: 109–118.
22. Bhattacharjee, A., M. Shukla, V. P. Yakubenko, A. Mulya, S. Kundu, and M. K. Cathcart. 2013. IL-4 and IL-13 employ discrete signaling pathways for target gene expression in alternatively activated monocytes/macrophages. *Free Radic. Biol. Med.* 54: 1–16.
23. Conrad, D. J., and M. Lu. 2000. Regulation of human 12/15-lipoxygenase by Stat6-dependent transcription. *Am. J. Respir. Cell Mol. Biol.* 22: 226–234.

24. Ishii, M., H. Wen, C. A. Corsa, T. Liu, A. L. Coelho, R. M. Allen, W. F. Carson, IV, K. A. Cavassani, X. Li, N. W. Lukacs, et al. 2009. Epigenetic regulation of the alternatively activated macrophage phenotype. *Blood* 114: 3244–3254.
25. Changelian, P. S., M. E. Flanagan, D. J. Ball, C. R. Kent, K. S. Magnuson, W. H. Martin, B. J. Rizzuti, P. S. Sawyer, B. D. Perry, W. H. Brissette, et al. 2003. Prevention of organ allograft rejection by a specific Janus kinase 3 inhibitor. *Science* 302: 875–878.
26. Covarrubias, A. J., H. I. Aksoylar, J. Yu, N. W. Snyder, A. J. Worth, S. S. Iyer, J. Wang, I. Ben-Sahra, V. Byles, T. Polynne-Stapornkul, et al. 2016. Akt-mTORC1 signaling regulates Acly to integrate metabolic input to control of macrophage activation. *Elife* 5.
27. Thoreen, C. C., S. A. Kang, J. W. Chang, Q. Liu, J. Zhang, Y. Gao, L. J. Reichling, T. Sim, D. M. Sabatini, and N. S. Gray. 2009. An ATP-competitive mammalian target of rapamycin inhibitor reveals rapamycin-resistant functions of mTORC1. *J. Biol. Chem.* 284: 8023–8032.
28. Calvo, K. R., B. Dabir, A. Kovach, C. Devor, R. Bandle, A. Bond, J. H. Shih, and E. S. Jaffe. 2008. IL-4 protein expression and basal activation of Erk in vivo in follicular lymphoma. *Blood* 112: 3818–3826.
29. Bhattacharjee, A., B. Xu, D. A. Frank, G. M. Feldman, and M. K. Cathcart. 2006. Monocyte 15-lipoxygenase expression is regulated by a novel cytosolic signaling complex with protein kinase C delta and tyrosine-phosphorylated Stat3. *J. Immunol.* 177: 3771–3781.
30. Favata, M. F., K. Y. Horiuchi, E. J. Manos, A. J. Daulerio, D. A. Stradley, W. S. Feeser, D. E. Van Dyk, W. J. Pitts, R. A. Earl, F. Hobbs, et al. 1998. Identification of a novel inhibitor of mitogen-activated protein kinase kinase. *J. Biol. Chem.* 273: 18623–18632.
31. Koeberle, S. C., J. Romir, S. Fischer, A. Koeberle, V. Schattel, W. Albrecht, C. Grütter, O. Werz, D. Rauh, T. Stehle, and S. A. Laufer. 2011. Skepinone-L is a selective p38 mitogen-activated protein kinase inhibitor. *Nat. Chem. Biol.* 8: 141–143.
32. Pello, O. M., M. De Pizzol, M. Mirolo, L. Soucek, L. Zammataro, A. Amabile, A. Doni, M. Nebuloni, L. B. Swigart, G. I. Evan, et al. 2012. Role of c-MYC in alternative activation of human macrophages and tumor-associated macrophage biology. *Blood* 119: 411–421.
33. Zhang, S., L. S. Schneider, B. Vick, M. Grunert, I. Jeremias, D. Menche, R. Müller, A. M. Vollmar, and J. Liebl. 2015. Anti-leukemic effects of the V-ATPase inhibitor Archazolid A. *Oncotarget* 6: 43508–43528.
34. Filippakopoulos, P., J. Qi, S. Picaud, Y. Shen, W. B. Smith, O. Fedorov, E. M. Morse, T. Keates, T. T. Hickman, I. Felletar, et al. 2010. Selective inhibition of BET bromodomains. *Nature* 468: 1067–1073.
35. Arnardottir, H. H., J. Dalli, R. A. Colas, M. Shinohara, and C. N. Serhan. 2014. Aging delays resolution of acute inflammation in mice: reprogramming the host response with novel nano-proresolving medicines. *J. Immunol.* 193: 4235–4244.
36. Kwong, C., A. Gilman-Sachs, and K. Beaman. 2011. Tumor-associated a2 vacuolar ATPase acts as a key mediator of cancer-related inflammation by inducing pro-tumorigenic properties in monocytes. *J. Immunol.* 186: 1781–1789.
37. Serhan, C. N., N. Chiang, and T. E. Van Dyke. 2008. Resolving inflammation: dual anti-inflammatory and pro-resolution lipid mediators. *Nat. Rev. Immunol.* 8: 349–361.
38. Ackermann, J. A., K. Hofheinz, M. M. Zaiss, and G. Krönke. 2017. The double-edged role of 12/15-lipoxygenase during inflammation and immunity. Biochim. Biophys. Acta Mol. Cell Biol. Lipids 1862: 371–381.
39. Andersson, C. K., H. E. Claesson, K. Rydell-Törmänen, S. Swedmark, A. Hällgren, and J. S. Erjefält. 2008. Mice lacking 12/15-lipoxygenase have attenuated airway allergic inflammation and remodeling. *Am. J. Respir. Cell Mol. Biol.* 39: 648–656.
40. Kristjansson, R. P., S. Benonisdottir, O. B. Davidsson, A. Oddsson, V. Tragante, J. K. Sigurdsson, L. Stefansdottir, S. Jonsson, B. O. Jensson, J. G. Arthur, et al. 2019. A loss-of-function variant in ALOX15 protects against nasal polyps and chronic rhinosinusitis. *Nat. Genet.* 51: 267–276.
41. Bhattacharjee, A., A. Mulya, S. Pal, B. Roy, G. M. Feldman, and M. K. Cathcart. 2010. Monocyte 15-lipoxygenase gene expression requires ERK1/2 MAPK activity. *J. Immunol.* 185: 5211–5224.
42. Soliman, M., J. Y. Seo, D. S. Kim, J. Y. Kim, J. G. Park, M. M. Alfajaro, Y. B. Baek, E. H. Cho, J. Kwon, J. S. Choi, et al. 2018. Activation of PI3K, Akt, and ERK during early rotavirus infection leads to V-ATPase-dependent endosomal acidification required for uncoating. *PLoS Pathog.* 14: e1006820.
43. Rådmark, O., O. Werz, D. Steinhilber, and B. Samuelsson. 2015. 5-Lipoxygenase, a key enzyme for leukotriene biosynthesis in health and disease. *Biochim. Biophys. Acta* 1851: 331–339.
44. Pergola, C., G. Dodt, A. Rossi, E. Neunhoeffer, B. Lawrenz, H. Northoff, B. Samuelsson, O. Rådmark, L. Sautebin, and O. Werz. 2008. ERK-mediated regulation of leukotriene biosynthesis by androgens: a molecular basis for gender differences in inflammation and asthma. *Proc. Natl. Acad. Sci. USA* 105: 19881–19886.
45. Poeckel, D., K. A. Zemski Berry, R. C. Murphy, and C. D. Funk. 2009. Dual 12/15- and 5-lipoxygenase deficiency in macrophages alters arachidonic acid metabolism and attenuates peritonitis and atherosclerosis in ApoE knock-out mice. *J. Biol. Chem.* 284: 21077–21089.
46. Fraire-Zamora, J. J., and M. Simons. 2018. Vacuolar ATPase is required for ERK-dependent wound healing in the Drosophila embryo. *Wound Repair Regen.* 26: 102–107.
47. Schreml, S., R. J. Meier, M. Kirschbaum, S. C. Kong, S. Gehmert, O. Felthaus, S. Küchler, J. R. Sharpe, K. Wöltje, K. T. Weiß, et al. 2014. Luminescent dual sensors reveal extracellular pH-gradients and hypoxia on chronic wounds that disrupt epidermal repair. *Theranostics* 4: 721–735.
48. Dalli, J., S. Ramon, P. C. Norris, R. A. Colas, and C. N. Serhan. 2015. Novel proresolving and tissue-regenerative resolvin and protectin sulfido-conjugated pathways. *FASEB J.* 29: 2120–2136.

Supplemental Data

Vacuolar (H+)-ATPase critically regulates specialized pro-resolving mediator pathways in human M2-like monocyte-derived macrophages and resolution of inflammation

Rao Z. et al.

		M1				M2			
		-		+ *E. coli*		-		+ *E. coli*	
	Q1 Q3	vehicle	ArchA	vehicle	ArchA	vehicle	ArchA	vehicle	ArchA
SPM									
RvD2	375 175	-	-	-	-	-	-	30.5 ± 15.3	0.5 ± 0.0*
RvD4	375 101							7.9 ± 3.0	0.5 ± 0.0*
RvD5	359 199	-	-	21.4 ± 7.0	45.1 ± 7.1*	-	-	1274 ± 396	10.5 ± 3.4***
RvD6	359 159	-	-	-	-	-	-	18.8 ± 4.3	3.8 ± 0.7*
MaR1	359 250	-	-	-	-	-	-	79.4 ± 13.3	1.5 ± 0.5*
PD1	359 153	-	-	-	-	-	-	171.6 ± 58.9	3.3 ± 1.9***
10S,17SdiHDHA	359 153	-	-	-	-	-	-	45.8 ± 11.2	0.7 ± 0.4***
RvE3	333 201	-	-	4,7 ±3.9	5.8 ± 3.6	-	-	166.7 ± 46.2	18.8 ± 7.2**
LXA_4	351 115	-	-	-		-	-	14.9 ± 3.5	2.8 ± 1.0**
SPM precursors									
17-HDHA	343 245	16.5 ± 4.1	14.4 ± 4.3	306.2 ± 113.7	326.9 ± 116.1	157.8 ± 103.5	40.9 ± 24.9	40702 ± 12935	5680 ± 2804***
15-HETE	319 219	9.1 ± 1.8	15.0 ± 3.2*	462.1 ± 75.0	433.1 ± 47.4	31.5 ± 17.4	16.3 ± 5.1	17,104 ± 5057	766.3 ± 235.1***
15-HEPE	317 219	0.9 ± 0.1	1.2 ± 0.3	7.1 ± 2.6	8.6 ± 2.3	4.4 ± 2.4	1.5 ± 0.3	2849 ± 1145	63.1 ± 24.3***
14-HDHA	343 205	0.9 ± 0.2	0.7 ± 0.1	20.8 ± 3.1	33.6 ± 5.6	19.2 ± 11.7	3.9 ± 1.1	5180 ± 1549	75.5 ± 26.2***
12-HETE	319 179	6.3 ± 1.2	5.8 ± 1.7	33.1 ± 3.2	42.6 ± 4.9	10.0 ± 1.4	8.5 ± 2.2	1391 ± 374	37.4 ± 4.9***
12-HEPE	317 179	-	0.5 ± 0.1	3.9 ± 0.4	4.6 ± 1.3	2.6 ± 1.5	-	331.0 ± 121.5	4.5 ± 1.1***
7-HDHA	343 141	2.3 ± 0.5	2.6 ± 0.2	265.9 ± 56.3	443.6 ± 43.7	9.5 ± 6.1	3.0 ± 0.8	632.0 ± 81.2	33.3 ± 10.0***
4-HDHA	343 101	2.4 ± 0.6	3.1 ± 0.9	49.9 ± 6.1	67.7 ± 12.6	12.1 ± 8.3	3.4 ± 1.4	89.2 ± 13.8	54.9 ± 1.8*
5S,15S-diHETE	335 201	26.8 ± 14.8	54.1 ± 37.5	223.9 ± 52.8	434.6 ± 86.4	72.7 ± 49.9	63.4 ± 24.3	1222 ± 355	168.5 ± 62.4**
5S,15S-diHEPE	333 115	0.8 ± 0.3	1.6 ± 0.4	18.3 ± 3.4	21.2 ± 4.9	1.1 ± 0.5	0.5 ± 0.2	57.5 ± 21.9	2.9 ± 1.3**
COX products									
PGD_2	351 233	7.9 ± 1.3	21.1 ± 3.7**	71.3 ± 15.5	122.4 ± 14.2*	5.3 ± 1.9	4.9 ± 2.5	92.6 ± 34.8	19.0 ± 3.1***
PGE_2	351 271	550.4 ± 83.4	533.9 ± 135.1	5228 ± 1250	4178 ± 811	7.9 ± 1.1	6.7 ± 2.7	147.7 ± 35.5	54.9 ± 3.6**
PGF_2-α	353 193	105.4 ± 40.6	148.1 ± 45.7*	187.4 ± 32.2	414.8 ± 62.1*	8.8 ± 1.7	4.5 ± 1.6	98.4 ± 15.9	73.3 ± 14.8
TXB_2	369 169	1149 ± 195	1497 ± 215*	3284 ± 332	6268 ± 837*	284.9 ± 47.7	71.4 ± 19.6**	6612 ± 925	1827 ± 185***
5-LOX products									
5-HETE	319 115	9.3 ± 5.1	22.9 ± 6.9*	2670 ± 525	1879 ± 474	19.9 ± 8.8	7.7 ± 1.3	856.3 ± 267.4	271.8 ± 147.7**
5-HEPE	317 115	1.0 ± 0.5	3.0 ± 1.2*	425.4 ± 73.8	327.8 ± 79.1	3.5 ± 2.3	0.6 ± 0.3*	105.9 ± 25.1	28.6 ± 13.3**
LTB_4	335 195	2.9 ± 1.2	25.0 ± 9.7**	2955 ± 524	4167 ± 603	2.0 ± 0.5	2.2 ± 0.2	320.0 ± 91.3	347.3 ± 258.8
fatty acids									
AA	303 259	2235 ± 915	3283 ± 1083	7906 ± 868	11385 ± 2658	6867 ± 4189	2392 ± 555	14104 ± 1404	9097 ± 866*
EPA	301 257	315.2 ± 152.8	389.8 ± 166.8	1002 ± 183	1162 ± 328	1401 ± 1031	257.9 ± 87.6	1476 ± 166	929.2 ± 79.8*
DHA	327 283	4163 ± 1089	4323 ± 1262	52,342 ± 5435	67,926 ± 15,179	14,201 ± 9563	3738 ± 805	98,095 ± 14,895	67,701 ± 6402**

Supplementary Table 1. LM profile of ArchA- and vehicle-treated M1 and M2. Human monocytes were differentiated by GM-CSF or M-CSF (20 ng/ml, each) for 6 days to get $M_{GM\text{-}CSF}$ or $M_{M\text{-}CSF}$ macrophages, respectively. After pretreatment with 30 nM ArchA or vehicle for 30 min, the $M_{GM\text{-}CSF}$ were polarized with LPS and INFγ for 48 h towards M1 while the $M_{M\text{-}CSF}$ were polarized with IL-4 for 48 h towards M2. The cells were then incubated for 180 min with pathogenic *E. coli* (serotype O6:K2:H1, ratio 1:50) or vehicle at 37 °C. Formed LM were isolated from the supernatants by solid phase extraction and analyzed by UPLC-MS-MS; detection limit: 0.5 pg. Results are given as means ± S.E.M., n = 6 separate donors. * $P<0.05$, ** $P<0.01$, *** $P<0.001$ ArchA vs. vehicle control, data were log-transformed for statistical analysis; paired t-test.

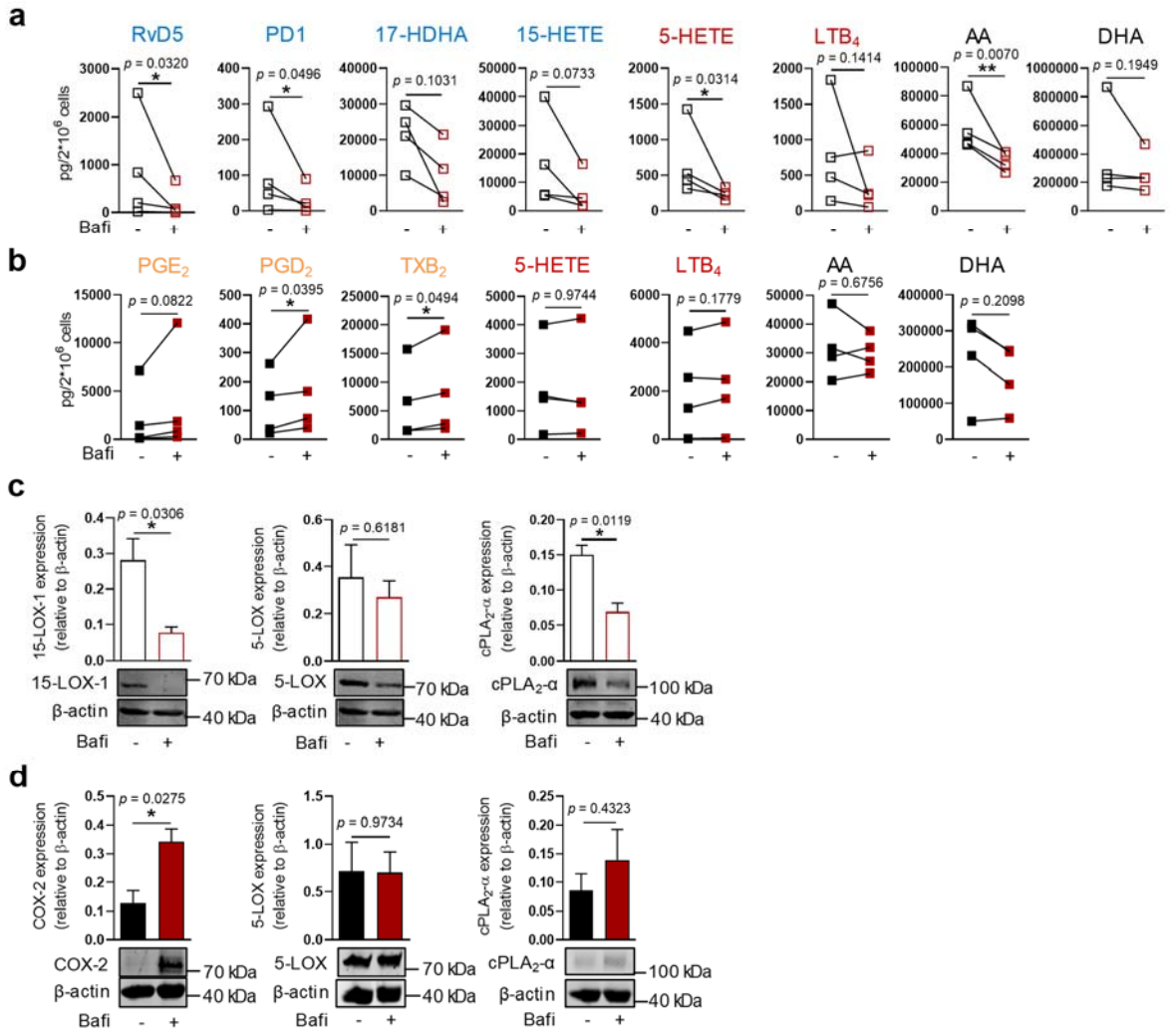

Figure S1. Effects of the vATPase inhibitor bafilomycin on LM formation and LM-biosynthetic enzyme expression in M1 and M2. Human monocytes were differentiated by GM-CSF or M-CSF (20 ng/ml, each) for 6 days to get $M_{GM\text{-}CSF}$ or $M_{M\text{-}CSF}$ macrophages and then pretreated with bafilomycin (Bafi, 30 nM, red) for 30 min prior to polarization for 48 h to M1 and M2. LM produced from (**a**) M2 and (**b**) M1 after exposure to *E. coli* (ratio 1:50) were isolated by solid phase extraction and analyzed by UPLC-MS-MS; detection limit: 0.5 pg. Results are given as means ± S.E.M., n = 4 separate donors; data were log-transformed for statistical analysis; * $P<0.05$ Bafi vs. vehicle, paired t-test. (**c**) Cell lysates of M2 were immunoblotted for 15-LOX-1, 5-LOX, and $cPLA_2$-α and normalized to β-actin for densitometric analysis. (**d**) Cell lysates of M1 were immunoblotted for COX-2, 5-LOX, and $cPLA_2$-α and normalized to β-actin. Results are given as means ± S.E.M., n = 3 separate donors; * $P<0.05$, Bafi vs. vehicle; paired t-test.

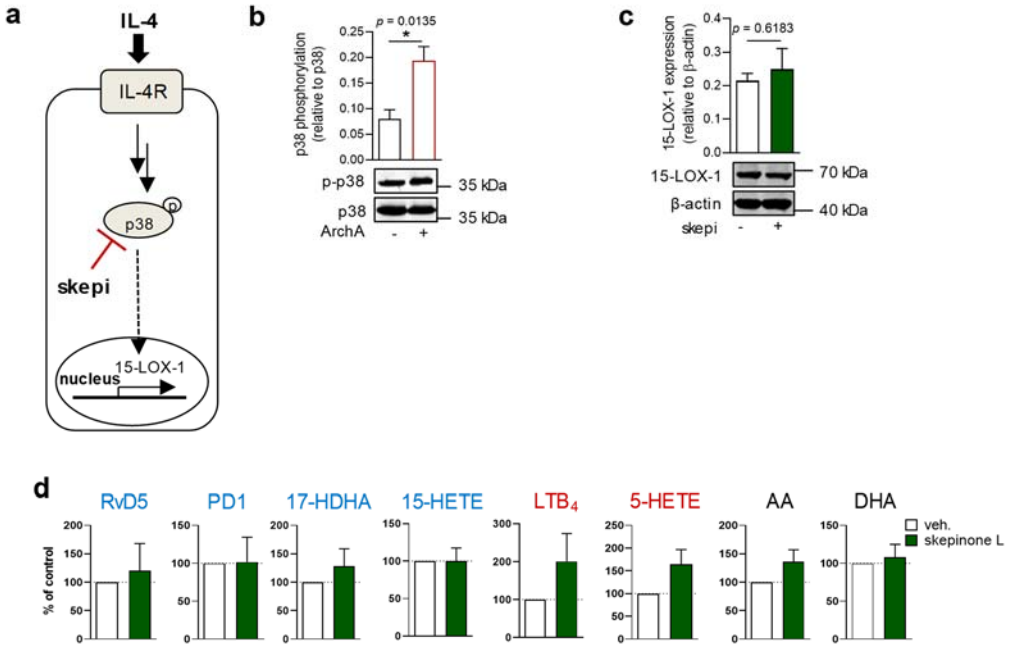

Figure S2. Effect of p38 MAPK inhibitor skepinone-L in M2 on LM formation and LM-biosynthetic enzyme expression. (**a**) Schematic draft of the hypothetic role of p38 MAPK in 15-LOX-1 expression. (**b**) Human monocytes were differentiated by M-CSF (20 ng/ml) for 6 days to get $M_{M\text{-}CSF}$ macrophages, and then pre-treated with ArchA (30 nM) for 30 min prior to polarization for 48 h to M2. Cell lysates were immunoblotted for phospho-p38 MAPK and p38 MAPK and normalized to β-actin for densitometric analysis. Data are means ± S.E.M., n = 4 separate donors, two tailed t-test **P*<0.05. (**c**/**d**) Human macrophages were pretreated with skepinone-L (1 µM) or vehicle (veh.) for 30 min prior to polarization towards M2 for 48 h. (**c**) Cell lysates were immunoblotted for 15-LOX-1, normalized to β-actin. Data are means ± S.E.M., n = 4 separate donors. (**d**) Formed LM after incubation of polarized M2 with *E. coli* (serotype O6:K2:H1 ratio 1:50) for 180 min at 37 °C. LM were analyzed by UPLC-MS-MS. Results are given as percentage of control; means ± S.E.M., n = 4 separate donors.

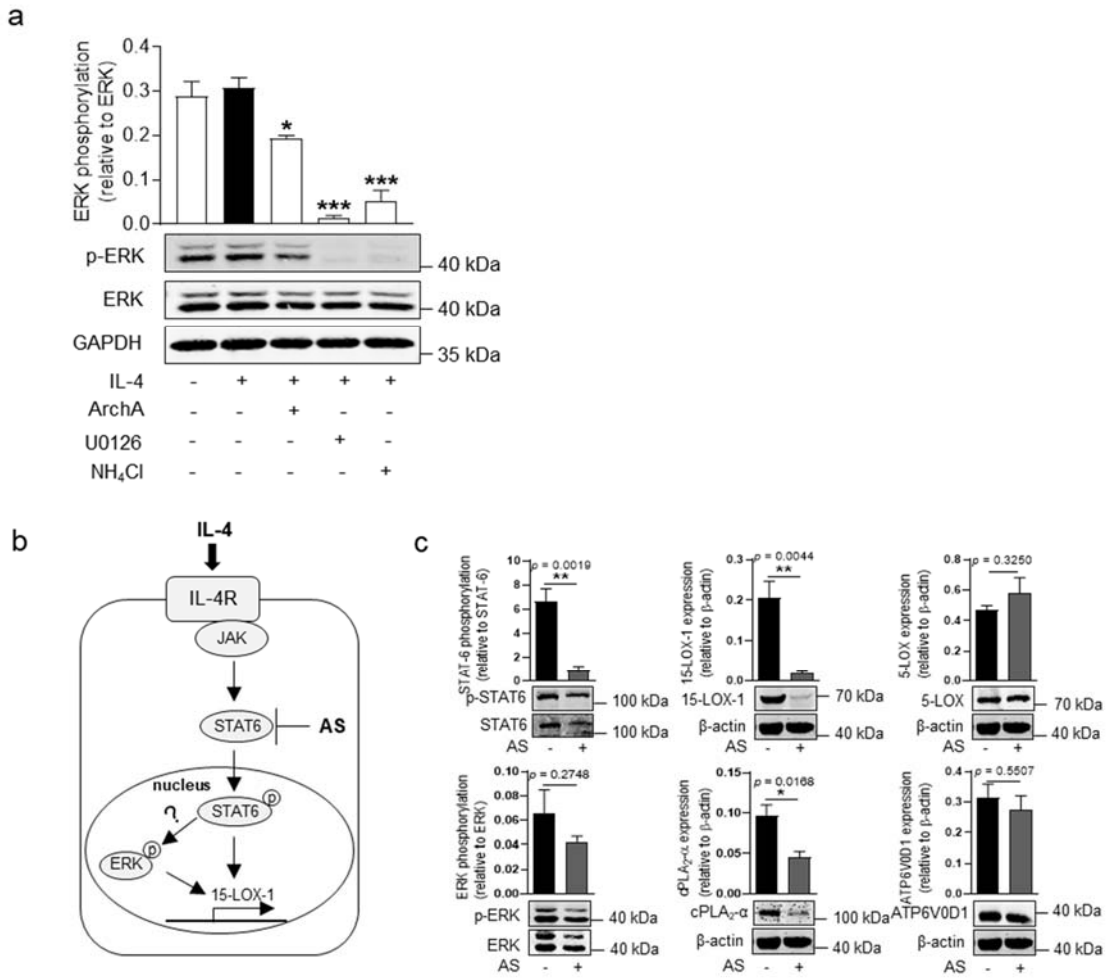

Figure S3. Effects of NH_4Cl and of the STAT6 inhibitor AS1517499 in M2. (a) Human monocytes were differentiated by M-CSF (20 ng/ml, each) for 6 days to get $M_{M\text{-}CSF}$ macrophages and then pretreated with ArchA (30 nM), UO126 (3 μM), NH_4Cl (50 mM) for 30 min prior to activation with IL-4 (20 ng/ml) for 15 min. Cell lysates were immunoblotted for phospho-ERK, ERK and GAPDH, and densitometric analysis was performed. Results are means ± S.E.M., n = 3 separate donors; * P<0.05, *** P<0.001, vs. control (IL-4 vehicle); one-way analysis of variance (ANOVA) with Bonferroni test. (b) Schematic draft of the hypothetic connection between STAT6 and ERK in 15-LOX-1 expression. (c) Human monocytes were differentiated by M-CSF (20 ng/ml, each) for 6 days to get $M_{M\text{-}CSF}$ macrophages and then pretreated with AS1517499 (AS, 1 μM) for 30 min prior to polarization with IL-4 (20 ng/ml) for 48 h. Cell lysates were immunoblotted for phospho-STAT6, STAT6, 15-LOX-1, 5-LOX, phospho-ERK, ERK, $cPLA_2$-α, ATP6V0D1 and β-actin, and densitometric analysis was performed. Results are given as means ± S.E.M., n = 4 separate donors; * P<0.05, *** P<0.001, vs. vehicle control; paired t test.

4. DISCUSSION

Inflammation is a process during which the immune system defends against exterior harmful stimuli and helps the body to return to its healthy state. Acute inflammation is governed by the excessive production of pro-inflammatory mediators such as LTs and PGs as well as of cytokines [1]. Upon challenge, monocytes and macrophages as main human innate immune cells play indispensable roles in both the initiation phase and the resolution of inflammation and release cytokines and chemokines as well as LM including eicosanoids and SPM. The active resolution of inflammation depends largely on the phagocytosis of exterior bacteria during infection, which is facilitated by the function of the V-ATPase-regulated phagolysosome [168]. As a universal pH-regulating proton pump, V-ATPase is involved in multiple cellular processes and thus, V-ATPase is emerging as interesting research target in inflammation and cancer [6, 7, 138, 145, 162, 169, 170]. In this thesis we studied how targeting V-ATPase regulates inflammation-related lipid mediators in human monocytes, M1 macrophages and M2 macrophages.

4.1 Inhibition of V-ATPase in human monocytes

As professional innate immune cells with pivotal functions in the immune defense, human monocytes produce abundant levels of pro-inflammatory mediators including cytokines as well as eicosanoids like LTs and PGs. Our previous research indicates that V-ATPase is crucial for cytokine and chemokine trafficking in human monocytes [6]. Targeting V-ATPase elevates the lysosomal pH and acidifies the intracellular cytosol. Lowered intracellular pH causes endoplasmic reticulum (ER) stress and limits the secretion of cytokines like IL-8. However, how V-ATPase regulates the biosynthesis of LM, especially pro-inflammatory eicosanoids in human monocytes, remained elusive.

Our data imply crucial but differential roles of V-ATPase in the regulation of the COX-2 pathway in human monocytes (manuscript I). While V-ATPase has a negative impact

on prostanoid biosynthesis by limiting the de novo-induced COX-2 protein levels, this proton pump accomplishes efficient COX-2-derived prostanoid formation by favoring cellular COX-2 activity.

We hypothesized that V-ATPase negatively regulates the de novo biosynthesized COX-2 protein levels in monocytes by rapidly lowering the protein amount of this inducible enzyme over time. Actually, it was reported that V-ATPase inhibition by bafilomycin elevates COX-2 levels in RAW264 macrophages of murine origin [6]. Besides higher COX-2 levels, V-ATPase inhibition also increased the amounts of TNF-α and IL-1β that were shown to stimulate COX-2 expression [171, 172] involving p38 MAPK [173], and this kinase seemingly mediates the increased COX-2 levels in the present scenario as well. In fact, several studies reported a crucial role of p38 MAPK in LPS-induced COX-2 expression in human monocytes [174-176], and it was shown before that both p38 MAPK and ERK-1/2 are essential in the induction of COX-2 protein in LPS-stimulated human neutrophils [177]. In our hands, ArchA increased the phosphorylation of p38 MAPK after 24 h LPS stimulation in human monocytes, and activated ERK-1/2, whereas other relevant signaling pathways for COX-2 expression like NF-κB and SAPK/JNK were not affected. This suggests that V-ATPase limits p38 MAPK and ERK-1/2 activation in monocytes. Since the p38 MAPK inhibitor skepinone-L as well as the ERK-1/2 inhibitor U0126 abrogated the LPS-induced COX-2 expression, we propose that the enhancement of the p38 MAPK and ERK-1/2 pathway by ArchA is causative for the elevated COX-2 levels in human monocytes.

Although targeting of V-ATPase increased COX-2 protein levels in human monocytes, the concomitant biosynthesis of COX-2-derived prostanoids was surprisingly decreased, suggesting that V-ATPase is overall beneficial for cellular COX-2 activity. Results from previous studies exclude direct interference of the V-ATPase inhibitors like ArchA, bafilomycin A and apicularen with the enzymatic activity of COX-2 activity [178], indicating that the suppression of prostanoid formation in monocytes is not the consequence of direct inhibition of the COX-2 enzyme. In contrast to monocytes, in M1 macrophages ArchA (and bafilomycin) elevated COX-2 activity, suggesting that the

PG-suppressive effects of V-ATPase inhibitors in monocytes is cell type-dependent and due to modulation of processes that govern cellular COX-2 activity. Since V-ATPase was shown to regulate cytokine and chemokine trafficking in monocytes, where ArchA treatment led to accumulation of IL-8 in the endoplasmic reticulum (ER) [179], it appeared possible that de novo biosynthesized prostanoids might be trapped inside the cell. However, only low amounts of intracellular PGs were evident in *E. coli*-stimulated monocytes whereas high levels were released into the cell supernatant, regardless of V-ATPase inhibition.

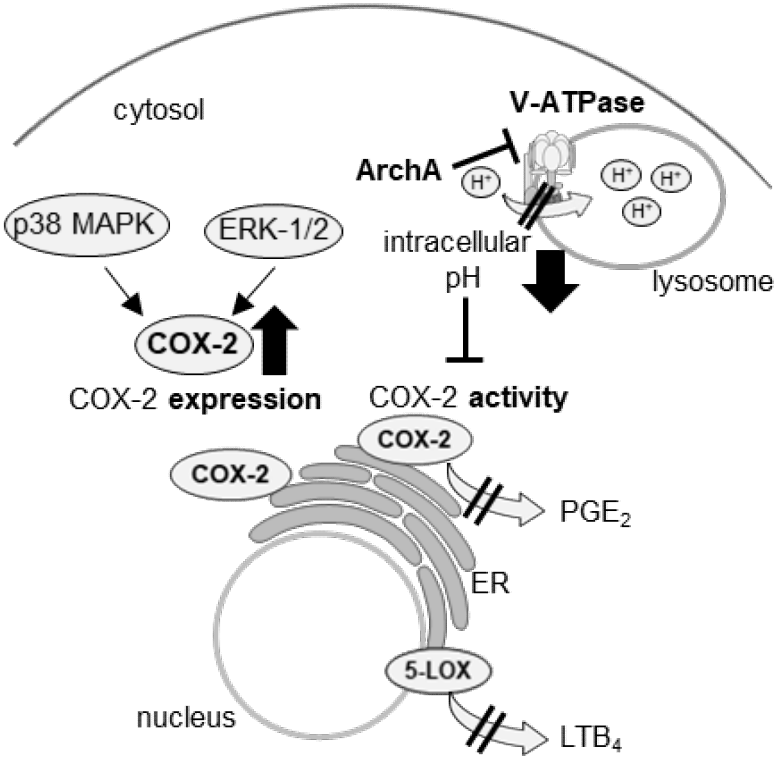

Fig.4.1 Proposed mechanism of V-ATPase inhibition in affecting COX-2 pathways in human monocytes.

The main function of V-ATPase is to regulate cellular pH homeostasis by promoting the transport of protons from the cytosol to lysosomes that become acidic [4], and accordingly, targeting of V-ATPase in monocytes led to an elevated lysosomal pH [179]. Therefore, we hypothesized that the reduction of COX-derived prostanoids might be due to intracellular pH changes upon V-ATPase inhibition. Indeed, the pH modulator

chloroquine that alkalizes lysosomes and acidifies the cytosol [180] mimicked the effects of V-ATPase inhibitors on the LM profile, as it strongly suppressed COX-dependent LM formation without suppressing 12/15-LOX products and with only minor impairment of 5-LOX-derived LM. Cellular activity of 5-LOX is affected by many factors including AA supply, its helper protein FLAP, phosphorylation by MAPKAPK-2 and ERK-1/2 [14]. Note that ArchA did not alter 5-LOX, FLAP or $cPLA_2$-α expression and substrate supply. Thus, the intracellular pH might be crucial for the activity of both the COX-2 and the 5-LOX pathway. In fact, the pH optimum for the enzymatic activities of COX-2 and 5-LOX in cell-free assays is around pH 8.0 [181, 182], implying that cytosolic or nuclear membrane-associated 5-LOX [14] and ER/nuclear envelope-inserted COX-2 [183] may benefit from V-ATPase activity, accomplishing alkaline pH (> pH 7.2) in the cytosol. It appeared possible that changes in the intracellular pH might be also the cause for the increased COX-2 expression by ArchA, implying a detrimental role of V-ATPase in this respect. In fact, it was reported before for a human osteoblastic cell line that sensing of pH changes would regulate COX-2 expression and PGE_2 formation [184]. However, the pH modulator chloroquine did not induce COX-2 expression but rather abrogated it, suggesting other mechanisms are responsible for the elevation of COX-2 protein levels by ArchA in human monocytes which are mediated by the p38 MAPK and ERK-1/2 pathway.

Collectively, we reveal a crucial role of V-ATPase in the regulation of the biosynthesis of COX-2- and, to a minor extent, in 5-LOX-derived LM in human monocytes. Inhibition of V-ATPase results in contrasting requirements of this proton pump: V-ATPase causes an impairment of the protein levels of COX-2 seemingly by suppression of p38 MAPK and ERK-1/2 signaling but accomplishes substantial cellular activity of COX-2 possibly by adjusting a favorable intracellular pH for this enzyme.

4.2 Inhibition of V-ATPase in human M1 macrophages

We showed that targeting V-ATPase activity with ArchA selectively elevates the release

of TNF-α without significant effects on other cytokines like IL-1β, IL-6, IL-10 or chemokines like MCP-1 and IL-8 in both LPS-stimulated macrophages and LPS/IFN-γ-stimulated M1 macrophages (manuscript II). Comparable effects were achieved using two structurally different V-ATPase inhibitors bafilomycin and apicularen, which indicates a class effect on TNF-α release through inhibition of V-ATPase. V-ATPase, as a proton pump, is also well known to regulate lysosomal pH in macrophages. V-ATPase inhibitors including ArchA and bafilomycin were shown to block the function of the proton pump in macrophages and thus elevated the lysosomal pH [6, 162]. To address the involved mechanisms in elevating TNF-α levels, we explored two common pH modulators chloroquine and NH_4Cl on TNF-α release in M1 macrophages [180, 185]. These two tool compounds showed comparable effects on elevating lysosomal pH like ArchA but failed to increase the production of TNF-α. Actually, chloroquine was shown to inhibit the production of LPS-stimulated pro-inflammatory cytokines including TNF-α, IL-1β and IL-6 in a concentration-dependent manner in human whole blood [186]. This report supports our data, which excludes the involvement of pH modulation on elevated TNF-α levels caused by V-ATPase inhibition.

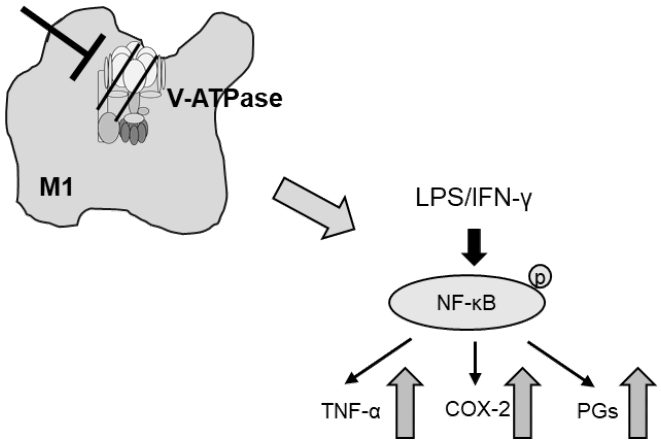

Fig.4.2 Proposed mechanism of V-ATPase inhibition in regulating TNF-α and COX-2 pathways in human M1 macrophages.

Additionally, ArchA significantly upregulated the mRNA levels of TNF-α but not of IL-1β in M1 macrophages. Studies by others revealed various signaling transduction pathways including the SAPK/JNK, NF-κB/IκB, MKK3/6-p38 and MEK/ERK-1/2

cascades that are involved in the production of TNF-α in various cellular systems [187-190]. Analysis of possible involved protein kinases signaling pathways revealed that targeting V-ATPase by ArchA elevated the phosphorylation of NF-κB. Immunofluorescence microscopy results showed that ArchA treatment promoted the translocation of the p65 subunit of NF-κB to nucleus as well as inhibition of IκB. Notably, the phosphorylation of SAPK/JNK was also moderately affected by ArchA treatment. Other kinases were not significantly affected by the treatment with ArchA. Moreover, the elevated TNF-α release and TNF-α mRNA expression was abrogated by parthenolide [191], which inhibits NF-κB phosphorylation and the expression of TNF-α.

Upon bacterial infection, macrophages produce reactive oxygen species (ROS) to clear the trapped bacteria [192]. Consistent with findings by others that V-ATPase inhibitors bafilomycin and concanamycin A increased ROS production in RAW 264 cells [193], we confirmed that V-ATPase inhibition with ArchA also increased the LPS-induced ROS production in M1 macrophages, which was inhibited by the NADPH oxidase inhibitor DPI. Interestingly, DPI also inhibited the ArchA-induced TNF-α release, which indicates an involvement of ROS in TNF-α release. Studies indicated that the regulation of ROS production involves NF-κB and SAPK/JNK signaling [194]. Hence, we concluded that targeting V-ATPase elevated TNF-α expression and ROS production through NF-κB/IκB and SAPK/JNK signaling pathways.

V-ATPase is overexpressed in the plasma membrane in various cancer cells and targeting V-ATPase with specific inhibitors induce apoptosis of tumor cells [144, 145]. Besides tumor cells, the tumor milieu is composed of tumor associated macrophages (TAMs) as well as tumor supporting mediators, which support tumor cells growth and angiogenesis [113]. TAMs are recognized to be M2 macrophages that are anti-inflammatory but pro-tumoral. While classically activated M1 macrophages are well recognized to be more pro-inflammatory but anti-tumoral. Combination of direct cytotoxicity towards tumor cells with modification of tumor environment would be beneficial for anti-cancer therapy [195]. As mentioned previously, we revealed that targeting V-ATPase with ArchA elevated the release of pro-inflammatory TNF-α in M1

macrophages. Next, we utilized a three-dimensional human tumor biochip model to investigate if ArchA affects cancer cell viability in macrophage-tumor cell co-culture system. Human M1 or M2 macrophages were pre-treated with ArchA for 24 h before co-culture with MCF-7 cells for another 24 h. To avoid direct cytotoxicity towards MCF-7 cells, ArchA was removed from the system before the co-culture of macrophages and tumor cells. Of interest, ArchA pre-treatment reduced the viability of MCF-7 cells in the co-culture with M1 but not M2 macrophages. Moreover, elevated TNF-α production was detected in tumor cells co-cultured with M1 macrophages. Thus, our study showed that pharmacological targeting V-ATPase elevated TNF-α release and supported the anti-tumoral effects of M1 macrophages in the tumor milieu. Together, inhibition of V-ATPase with ArchA not only induced direct cytotoxicity towards tumor cells, but also achieved beneficial anti-tumoral effects through manipulation of the tumor microenvironment.

Studies by others showed that TNF-α binds the Toll like receptor (TLR)-2 [196] and thus stimulates COX-2 expression as well as the production of prostaglandins [172, 197]. Our time-course study revealed that COX-2 expression peaked after the 6 h stimulation of LPS stimulation, and was reduced again after 24, 48 or 72 h in human M1 macrophages, which is consistent with our data in human monocytes. Interestingly, pretreatment with ArchA prevented the rapid degradation of COX-2 protein, which kept significantly higher protein levels of COX-2 enzyme up to 72 h. This is consistent with other reports, which indicated that V-ATPase inhibition by bafilomycin induces COX-2 expression in RAW264 macrophages of murine origin [198]. In line with higher COX-2 expression, biosynthesis of COX-related prostanoids were elevated by ArchA pretreatment. By contrast, 15-LOX/12-LOX-related products and 5-LOX/FLAP-related LM remained unchanged.

Compared to M2, LPS-stimulated M1 macrophages are pro-inflammatory but anti-tumoral with higher pro-inflammatory cytokines release, higher COX-2 expression and higher levels of pro-inflammatory PGs [8]. Together, our data revealed that targeting V-ATPase in M1 macrophages promoted the pro-inflammatory phenotype of M1

macrophages in terms of TNF-α release, ROS formation, COX-2 expression and COX-related PG biosynthesis. Moreover, targeting V-ATPase in M1 macrophages enhanced the anti-tumoral effects of M1 macrophages in macrophages-tumor cell coculture through manipulation of the tumor microenvironment.

4.3 Inhibition of V-ATPase in human M2 macrophages

During inflammation, V-ATPase is required for the maturation of the phagolysosome, which is crucial for the phagocytic functions of human macrophages to degrade and clear pathogen invaders [169, 199]. Our previous data showed that V-ATPase regulates cytokine trafficking in human primary monocytes [6]. However, how V-ATPase is involved in the biosynthesis of LM and in the resolution of inflammation remained elusive. Different from the pro-inflammatory M1 macrophages, M2 are generally anti-inflammatory with the capacity to produce abundant levels of SPM during efferocytosis of apoptotic neutrophils or upon challenge with pathogenic bacteria [8, 200]. SPM as biological functional mediators trigger both anti-inflammatory and proresolving actions in both acute inflammation and resolution of inflammation [3]. They are actively involved in various processes like neutrophil transepithelial migration, phagocytosis and tissue regeneration during inflammation [3]. SPM terminate neutrophil transmigration, promote phagocytosis and accelerate tissue regeneration [10]. Here we focused on exploring the roles of V-ATPase in the biosynthesis of LM, especially SPM, in M2.

We show that targeting V-ATPase with two structurally different V-ATPase inhibitors ArchA and bafilomycin significantly suppressed the biosynthesis of SPM, SPM precursors, 15-LOX-1-derived LM as well as fatty acid substrates (manuscript III). In alternative-activated M2 macrophages, IL-4 polarization induces the expression of 15-LOX-1, which is a key enzyme in biosynthesis of SPM precursors and related SPM [8]. In line with lower SPM and 15-LOX-1-related metabolites, inhibition of V-ATPase abrogated the expression of 15-LOX-1 in M2. However, V-ATPase inhibition did not

affect the expression of the other LOXs, namely 15-LOX-2, 12-LOX and 5-LOX. Blockade of V-ATPase also inhibits the expression of $cPLA_2$-α as well as phosphorylation of $cPLA_2$-α and thus might be responsible for lower fatty acids supply. Moreover, biosynthesis of 5-LOX/FLAP-related LM was also inhibited by ArchA in M2 and V-ATPase inhibition suppressed the production of all PGs in M2. Also, ArchA pretreatment moderately suppressed the expression of COX-1 that was shown before to be induced by IL-4 in murine bone-marrow-derived macrophages [29] and also in our hands in human M2. Thus, we propose that lower PG levels correlate to lower fatty acid supply as well as lower COX-1 expression in M2.

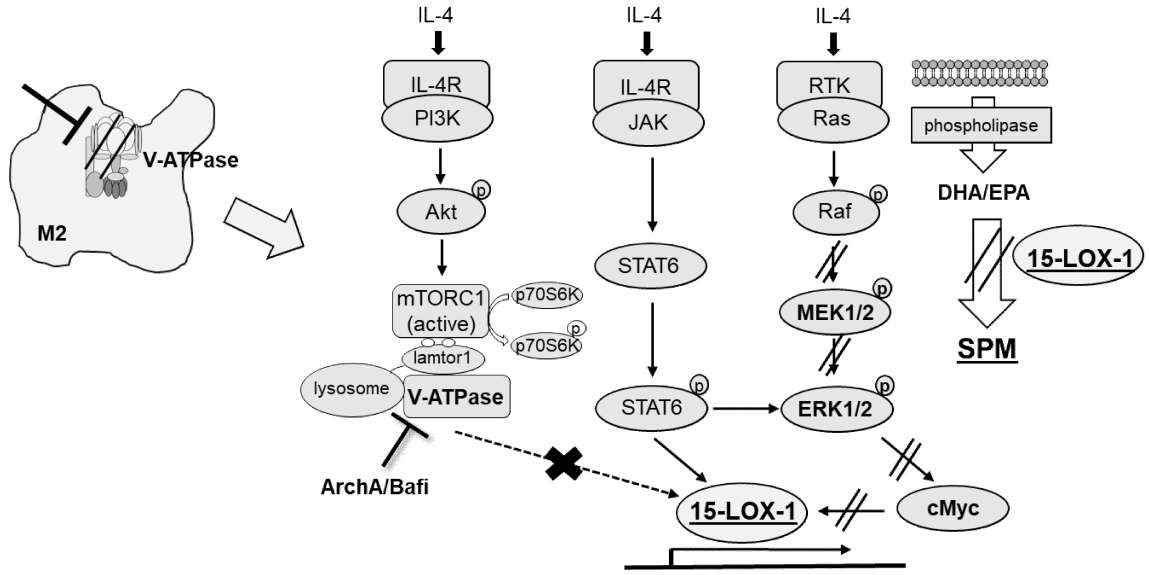

Fig.4.3 Proposed mechanism of V-ATPase inhibition in regulating 15-LOX-1 pathways and biosynthesis of SPM in human M2 macrophages.

Additionally, we investigated the role of V-ATPase in an *in vivo* murine zymosan-induced peritonitis model, where abrogation of 15-LOX-1-related metabolites and SPM in both, exudates of the peritoneal cavity and plasma, by ArchA treatment was addressed. The zymosan-induced peritonitis is a self-resolving model of acute inflammation that peaks within few hours governed by neutrophil infiltration, while later inflammation is resolved after a period of 24 - 72 h [201]. Our *in vivo* data showed that V-ATPase inhibition delayed the resolution phase accompanied by higher numbers of infiltrated cells into the peritoneal cavity. This was in line with lower SPM levels in the

exudates of the peritoneal cavity. The SPMs were shown to impede neutrophils transmigration and accelerate resolution of inflammation [3]. By contrast, pro-inflammatory PGs and LTs were not affected by V-ATPase inhibition with ArchA *in vivo*. Of note, biosynthesis of PGs and LTs were moderately suppressed in M2 macrophages but elevated in M1 macrophages by V-ATPase inhibition. The effects on PGs and LTs by V-ATPase inhibition might be compromised by the consistence of both M1 and M2 phenotypes in the *in vivo* system.

Our previous results suggested that V-ATPase regulates specifically the expression of the 15-LOX-1 isoform (not 15-LOX-2 or 5-LOX) in M2. The regulation of IL-4-stimulated 15-LOX-1 involves multiple possible signaling pathways. The classical IL-4-JAK-STAT6 pathway was shown to regulate 15-LOX-1 expression in various cell systems [110, 202, 203]. By use of the JAK inhibitor CP-690550 and STAT6 inhibitor AS1517499 we confirmed that inhibition of STAT6 phosphorylation abrogated the expression of 15-LOX-1 in IL-4 stimulated M2. However, our data revealed that targeting V-ATPase did not suppress phosphorylation of STAT6. Recently, V-ATPase was shown to be involved in the assembly and activation of mechanistic target of rapamycin complex 1 (mTORC1), which is required in the polarization of IL-4 stimulated murine bone-marrow-derived macrophages [5]. The PI3K-Akt-mTORC-LXR pathway regulated the expression of various M2-specific genes including IL-10, CD206 and Arg-1. Our study in human M2 indicated that V-ATPase inhibition with ArchA inhibited phosphorylation of Akt and p70S6K (substrate of mTORC1 complex), with no effects on the expression of Lamtor1 (subset of mTORC1 complex). However, PI3K inhibitor LY294002, mTORC1 inhibitor Torin 1 or LXR inhibitor GSK-2033 failed to suppress the expression of IL-4-induced 15-LOX-1 expression in M2 macrophages. Thus, neither JAK-STAT6 nor PI3K-Akt-mTORC-LXR pathway was involved in the V-ATPase regulated 15-LOX-1 expression in M2 macrophages.

Our results propose that inhibition of V-ATPase abrogates 15-LOX-1 expression and SPM biosynthesis through regulation of MEK/ERK-1/2 pathway. In fact, an requirement of ERK-1/2 MAPK activity for IL-13 stimulated ALOX15 gene expression in human

monocytes was shown before [112]. We showed that in human M2 macrophages, inhibition of V-ATPase by ArchA inhibited phosphorylation of MEK and ERK-1/2. The activity of p38 MAPK was not affected by ArchA and blockade of p38 MAPK activity with skepinone-L did not impair the expression of 15-LOX-1 enzyme in M2 macrophages. However, blockade of the MEK/ERK-1/2 pathway using the MEK inhibitor U0126 suppressed the expression of 15-LOX-1 as well as biosynthesis of SPM and 15-LOX-1-derived LM in M2 macrophages. Note that a recent study revealed that V-ATPase in Drosophila embryos is required for the ERK-1/2 dependent wound-healing [204] and SPM also possess the capacity in accelerating tissue regeneration [10]. These reports support our hypothesis that V-ATPase regulates MEK/ERK-1/2 signaling and has a role on the resolution of inflammation. The expression of the transcription factor c-Myc, which is downstream of MEK/ERK-1/2, was inhibited by ArchA in leukemic cells [205]. In our hands in human M2, ArchA also inhibited the expression of c-Myc, and the c-Myc inhibitor JQ-1 suppressed 15-LOX-1 expression and SPM biosynthesis. In fact, c-Myc was reported to be a key player in IL-4/IL-13-activated alternative polarization of macrophages and the cleaved product of c-Myc, Myc-nick promoted efferocytosis in M2 macrophages [206, 207]. Together, we show that V-ATPase regulates the MEK/ERK-1/2-c-Myc pathway and thus the expression of 15-LOX-1 as well as SPM formation.

As mentioned before, inhibition of V-ATPase reduced the production of 5-LOX/FLAP-related LM in M2 macrophages, whereas the enzyme expression of 5-LOX nor its helper protein FLAP was affected. Since the activation of 5-LOX involves multiple cellular processes including the presence of FLAP, arachidonic acid (AA) supply, the presence of calcium ion (Ca^{2+}) and ERK-1/2 activity [14, 208, 209], we hypothesized that 5-LOX activation was impaired by V-ATPase inhibition. In M2 macrophages, inhibition of ERK-1/2 activity by U0126 reduced production of 5-LOX-related LM, whereas inhibition of MEK/ERK-1/2 downstream c-Myc did not impair the biosynthesis of 5-LOX-related LM. In addition, both ERK-1/2 activity and AA supply were reduced upon treatment with ArchA (V-ATPase inhibitor), U0126 (MEK inhibitor), or AS1217499 (STAT6 inhibitor). Moreover, due to differences in the levels of sex hormones between

male and female, the ERK-1/2-mediated 5-LOX activity and biosynthesis of 5-LOX metabolites is gender-dependent [210]. Thus, there might also be a potential sex-bias for the MEK/ERK-1/2 regulated 15-LOX-1 expression and SPM formation. However, in our study, since M2 were obtained after long-term polarization (MCSF for 6-7 days) and stimulation (IL-4 for 48 h) from human PBMC in culture with 10% FCS, the sex-differences can mostly be excluded during the long-period incubation. However, the potential sex-differences of 15-LOX-1 regulation are further explored in other cellular and *in vivo* systems and are still ongoing. Collectively, we conclude that V-ATPase critically regulates 15-LOX-1 expression and SPM formation through the MEK/ERK-1/2-c-Myc pathway in M2 macrophages and thus has a crucial role in resolution of inflammation.

Taken together, this thesis revealed pivotal but differential and complex roles of V-ATPase on the biosynthesis of bioactive lipid mediators in human monocytes and macrophage phenotypes. It appears that V-ATPase is crucial for the M2 macrophage-related resolution of inflammation due to accomplishing the expression of 15-LOX-1 and the capacity for SPM formation during M2 polarization. In monocytes, V-ATPase promotes the biosynthesis of pro-inflammatory PG by stimulating COX-2 activity; in contrast, V-ATPase seemingly limits the expression of COX-2 enzyme and production of PG in M1 macrophages. Since V-ATPase is considered as pharmacological target, in particular for cancer therapy where LM play important roles in disease progression, our data will be of importance to judge the outcome of pharmacological intervention with V-ATPase.

5. REFERENCES

1. Pober, J. S., and W. C. Sessa. 2014. Inflammation and the blood microvascular system. *Cold Spring Harb Perspect Biol* 7: a016345.
2. Nathan, C. 2002. Points of control in inflammation. *Nature* 420: 846-852.
3. Serhan, C. N. 2014. Pro-resolving lipid mediators are leads for resolution physiology. *Nature* 510: 92-101.
4. Forgac, M. 2007. Vacuolar ATPases: rotary proton pumps in physiology and pathophysiology. *Nat Rev Mol Cell Biol* 8: 917-929.
5. Kimura, T., S. Nada, N. Takegahara, T. Okuno, S. Nojima, S. Kang, D. Ito, K. Morimoto, T. Hosokawa, Y. Hayama, Y. Mitsui, N. Sakurai, H. Sarashina-Kida, M. Nishide, Y. Maeda, H. Takamatsu, D. Okuzaki, M. Yamada, M. Okada, and A. Kumanogoh. 2016. Polarization of M2 macrophages requires Lamtor1 that integrates cytokine and amino-acid signals. *Nat Commun* 7: 13130.
6. Scherer, O., H. Steinmetz, C. Kaether, C. Weinigel, D. Barz, H. Kleinert, D. Menche, R. Muller, C. Pergola, and O. Werz. 2014. Targeting V-ATPase in primary human monocytes by archazolid potently represses the classical secretion of cytokines due to accumulation at the endoplasmic reticulum. *Biochem Pharmacol* 91: 490-500.
7. Sennoune, S. R., K. Bakunts, G. M. Martinez, J. L. Chua-Tuan, Y. Kebir, M. N. Attaya, and R. Martinez-Zaguilan. 2004. Vacuolar H+-ATPase in human breast cancer cells with distinct metastatic potential: distribution and functional activity. *Am J Physiol Cell Physiol* 286: C1443-1452.
8. Werz, O., J. Gerstmeier, S. Libreros, X. De la Rosa, M. Werner, P. C. Norris, N. Chiang, and C. N. Serhan. 2018. Human macrophages differentially produce specific resolvin or leukotriene signals that depend on bacterial pathogenicity. *Nat Commun* 9: 59.
9. de Oliveira, S., E. E. Rosowski, and A. Huttenlocher. 2016. Neutrophil migration in infection and wound repair: going forward in reverse. *Nat Rev Immunol* 16: 378-391.
10. Serhan, C. N., N. Chiang, and T. E. Van Dyke. 2008. Resolving inflammation: dual anti-inflammatory and pro-resolution lipid mediators. *Nat Rev Immunol* 8: 349-361.
11. Levy, B. D., C. B. Clish, B. Schmidt, K. Gronert, and C. N. Serhan. 2001. Lipid mediator class switching during acute inflammation: signals in resolution. *Nat Immunol* 2: 612-619.
12. Borgeat, P., and B. Samuelsson. 1979. Arachidonic acid metabolism in polymorphonuclear leukocytes: effects of ionophore A23187. *Proc Natl Acad Sci U S A* 76: 2148-2152.
13. Samuelsson, B., P. Borgeat, S. Hammarström, and R. C. Murphy. 1979. Introduction of a nomenclature: Leukotrienes. *Prostaglandins* 17: 785-787.
14. Radmark, O., O. Werz, D. Steinhilber, and B. Samuelsson. 2015. 5-Lipoxygenase, a key enzyme for leukotriene biosynthesis in health and disease. *Biochim Biophys Acta* 1851: 331-339.

15. Samuelsson, B. 1983. Leukotrienes: a new class of mediators of immediate hypersensitivity reactions and inflammation. *Adv Prostaglandin Thromboxane Leukot Res* 11: 1-13.
16. Borgeat, P., and B. Samuelsson. 1979. Metabolism of arachidonic acid in polymorphonuclear leukocytes. Structural analysis of novel hydroxylated compounds. *J Biol Chem* 254: 7865-7869.
17. Borgeat, P., M. Hamberg, and B. Samuelsson. 1976. Transformation of arachidonic acid and homo-gamma-linolenic acid by rabbit polymorphonuclear leukocytes. Monohydroxy acids from novel lipoxygenases. *J Biol Chem* 251: 7816-7820.
18. Weller, P. F., C. W. Lee, D. W. Foster, E. J. Corey, K. F. Austen, and R. A. Lewis. 1983. Generation and metabolism of 5-lipoxygenase pathway leukotrienes by human eosinophils: predominant production of leukotriene C4. *Proc Natl Acad Sci U S A* 80: 7626-7630.
19. Williams, J. D., J. K. Czop, and K. F. Austen. 1984. Release of leukotrienes by human monocytes on stimulation of their phagocytic receptor for particulate activators. *J Immunol* 132: 3034-3040.
20. Palmblad, J., C. L. Malmsten, A. M. Uden, O. Radmark, L. Engstedt, and B. Samuelsson. 1981. Leukotriene B4 is a potent and stereospecific stimulator of neutrophil chemotaxis and adherence. *Blood* 58: 658-661.
21. Brach, M. A., S. de Vos, C. Arnold, H. J. Gruss, R. Mertelsmann, and F. Herrmann. 1992. Leukotriene B4 transcriptionally activates interleukin-6 expression involving NK-chi B and NF-IL6. *Eur J Immunol* 22: 2705-2711.
22. Hanna, C. J., M. K. Bach, P. D. Pare, and R. R. Schellenberg. 1981. Slow-reacting substances (leukotrienes) contract human airway and pulmonary vascular smooth muscle in vitro. *Nature* 290: 343-344.
23. Lewis, R. A., K. F. Austen, J. M. Drazen, D. A. Clark, A. Marfat, and E. J. Corey. 1980. Slow reacting substances of anaphylaxis: Identification of leukotrienes C-1 and D from human and rat sources. *Proc Natl Acad Sci U S A* 77: 3710-3714.
24. Wang, D., and R. N. Dubois. 2010. Eicosanoids and cancer. *Nat Rev Cancer* 10: 181-193.
25. Laitinen, L. A., A. Laitinen, T. Haahtela, V. Vilkka, B. W. Spur, and T. H. Lee. 1993. Leukotriene E4 and granulocytic infiltration into asthmatic airways. *Lancet* 341: 989-990.
26. O'Hickey, S. P., R. J. Hawksworth, C. Y. Fong, J. P. Arm, B. W. Spur, and T. H. Lee. 1991. Leukotrienes C4, D4, and E4 enhance histamine responsiveness in asthmatic airways. *Am Rev Respir Dis* 144: 1053-1057.
27. Drazen, J. M., E. Israel, and P. M. O'Byrne. 1999. Treatment of asthma with drugs modifying the leukotriene pathway. *N Engl J Med* 340: 197-206.
28. Smith, W. L., Y. Urade, and P. J. Jakobsson. 2011. Enzymes of the cyclooxygenase pathways of prostanoid biosynthesis. *Chem Rev* 111: 5821-5865.
29. Shay, A. E., B. T. Diwakar, B. J. Guan, V. Narayan, J. F. Urban, Jr., and K. S. Prabhu. 2017. IL-4 up-regulates cyclooxygenase-1 expression in macrophages. *J Biol Chem* 292: 14544-14555.

30. Funk, C. D. 2001. Prostaglandins and leukotrienes: advances in eicosanoid biology. *Science* 294: 1871-1875.
31. Johnston, M. G., J. B. Hay, and H. Z. Movat. 1976. The modulation of enhanced vascular permeability by prostaglandins through alterations in blood flow (hyperemia). *Agents Actions* 6: 705-711.
32. Vane, J. R. 1971. Inhibition of Prostaglandin Synthesis as a Mechanism of Action for Aspirin-like Drugs. *Nature New Biology* 231: 232.
33. Flower, R., R. Gryglewski, K. HerbaczŃSka-Cedro, and J. R. Vane. 1972. Effects of Anti-inflammatory Drugs on Prostaglandin Biosynthesis. *Nature New Biol* 238: 104.
34. Rhen, T., and J. A. Cidlowski. 2005. Antiinflammatory action of glucocorticoids--new mechanisms for old drugs. *N Engl J Med* 353: 1711-1723.
35. FitzGerald, G. A., and C. Patrono. 2001. The coxibs, selective inhibitors of cyclooxygenase-2. *N Engl J Med* 345: 433-442.
36. Cohen, M. M. 1987. Role of endogenous prostaglandins in gastric secretion and mucosal defense. *Clin Invest Med* 10: 226-231.
37. Hoshino, T., S. Tsutsumi, W. Tomisato, H. J. Hwang, T. Tsuchiya, and T. Mizushima. 2003. Prostaglandin E2 protects gastric mucosal cells from apoptosis via EP2 and EP4 receptor activation. *J Biol Chem* 278: 12752-12758.
38. Ren, K., and R. Torres. 2009. Role of interleukin-1beta during pain and inflammation. *Brain Res Rev* 60: 57-64.
39. Jeanjean, A. P., S. M. Moussaoui, J. M. Maloteaux, and P. M. Laduron. 1995. Interleukin-1 beta induces long-term increase of axonally transported opiate receptors and substance P. *Neuroscience* 68: 151-157.
40. Schweizer, A., U. Feige, A. Fontana, K. Muller, and C. A. Dinarello. 1988. Interleukin-1 enhances pain reflexes. Mediation through increased prostaglandin E2 levels. *Agents actions* 25: 246-251.
41. Braddock, M., and A. Quinn. 2004. Targeting IL-1 in inflammatory disease: new opportunities for therapeutic intervention. *Nat. Rev. Drug Discov* 3: 330-339.
42. Yang, L., R. M. Froio, T. E. Sciuto, A. M. Dvorak, R. Alon, and F. W. Luscinskas. 2005. ICAM-1 regulates neutrophil adhesion and transcellular migration of TNF-alpha-activated vascular endothelium under flow. *Blood* 106: 584-592.
43. Mark, K. S., W. J. Trickler, and D. W. Miller. 2001. Tumor Necrosis Factor-α Induces Cyclooxygenase-2 Expression and Prostaglandin Release in Brain Microvessel Endothelial Cells. *J Pharmaco Exp Ther* 297: 1051-1058.
44. Mosmann, T. R., H. Cherwinski, M. W. Bond, M. A. Giedlin, and R. L. Coffman. 1986. Two types of murine helper T cell clone. I. Definition according to profiles of lymphokine activities and secreted proteins. *J Immunol* 136: 2348-2357.
45. te Velde, A. A., R. J. Huijbens, K. Heije, J. E. de Vries, and C. G. Figdor. 1990. Interleukin-4 (IL-4) inhibits secretion of IL-1 beta, tumor necrosis factor alpha, and IL-6 by human monocytes. *Blood* 76: 1392-1397.
46. Scheller, J., A. Chalaris, D. Schmidt-Arras, and S. Rose-John. 2011. The pro- and anti-inflammatory properties of the cytokine interleukin-6. *Biochima Biophys Acta* 1813: 878-888.
47. Clarke, C. J., A. Hales, A. Hunt, and B. M. Foxwell. 1998. IL-10-mediated

suppression of TNF-alpha production is independent of its ability to inhibit NF kappa B activity. *Eur J Immunol* 28: 1719-1726.

48. de Waal Malefyt, R., C. G. Figdor, R. Huijbens, S. Mohan-Peterson, B. Bennett, J. Culpepper, W. Dang, G. Zurawski, and J. E. de Vries. 1993. Effects of IL-13 on phenotype, cytokine production, and cytotoxic function of human monocytes. Comparison with IL-4 and modulation by IFN-gamma or IL-10. *J Immunol* 151: 6370-6381.
49. Serhan, C. N., and J. Savill. 2005. Resolution of inflammation: the beginning programs the end. *Nat Immunol* 6: 1191.
50. Romano, M., and C. N. Serhan. 1992. Lipoxin generation by permeabilized human platelets. *Biochemistry* 31: 8269-8277.
51. Levy, B. D., M. Romano, H. A. Chapman, J. J. Reilly, J. Drazen, and C. N. Serhan. 1993. Human alveolar macrophages have 15-lipoxygenase and generate 15(S)-hydroxy-5,8,11-cis-13-trans-eicosatetraenoic acid and lipoxins. *J Clin Invest* 92: 1572-1579.
52. Claria, J., and C. N. Serhan. 1995. Aspirin triggers previously undescribed bioactive eicosanoids by human endothelial cell-leukocyte interactions. *Proc Natl Acad Sci U S A* 92: 9475-9479.
53. Chiang, N., C. N. Serhan, S. E. Dahlen, J. M. Drazen, D. W. Hay, G. E. Rovati, T. Shimizu, T. Yokomizo, and C. Brink. 2006. The lipoxin receptor ALX: potent ligand-specific and stereoselective actions in vivo. *Pharmacol Rev* 58: 463-487.
54. Serhan, C. N., J. F. Maddox, N. A. Petasis, I. Akritopoulou-Zanze, A. Papayianni, H. R. Brady, S. P. Colgan, and J. L. Madara. 1995. Design of lipoxin A4 stable analogs that block transmigration and adhesion of human neutrophils. *Biochemistry* 34: 14609-14615.
55. Papayianni, A., C. N. Serhan, and H. R. Brady. 1996. Lipoxin A4 and B4 inhibit leukotriene-stimulated interactions of human neutrophils and endothelial cells. *J Immunol* 156: 2264-2272.
56. Godson, C., S. Mitchell, K. Harvey, N. A. Petasis, N. Hogg, and H. R. Brady. 2000. Cutting Edge: Lipoxins Rapidly Stimulate Nonphlogistic Phagocytosis of Apoptotic Neutrophils by Monocyte-Derived Macrophages. *J Immunol* 164: 1663-1667.
57. Gewirtz, A. T., L. S. Collier-Hyams, A. N. Young, T. Kucharzik, W. J. Guilford, J. F. Parkinson, I. R. Williams, A. S. Neish, and J. L. Madara. 2002. Lipoxin A4 Analogs Attenuate Induction of Intestinal Epithelial Proinflammatory Gene Expression and Reduce the Severity of Dextran Sodium Sulfate-Induced Colitis. *J Immunol* 168: 5260-5267.
58. Korner, A., M. Schlegel, J. Theurer, H. Frohnmeyer, M. Adolph, M. Heijink, M. Giera, P. Rosenberger, and V. Mirakaj. 2018. Resolution of inflammation and sepsis survival are improved by dietary Omega-3 fatty acids. *Cell Death Differ* 25: 421-431.
59. Serhan, C. N., C. B. Clish, J. Brannon, S. P. Colgan, N. Chiang, and K. Gronert. 2000. Novel functional sets of lipid-derived mediators with antiinflammatory actions generated from omega-3 fatty acids via cyclooxygenase 2-nonsteroidal antiinflammatory drugs and transcellular processing. *J Exp Med* 192: 1197-1204.

60. Tjonahen, E., S. F. Oh, J. Siegelman, S. Elangovan, K. B. Percarpio, S. Hong, M. Arita, and C. N. Serhan. 2006. Resolvin E2: identification and anti-inflammatory actions: pivotal role of human 5-lipoxygenase in resolvin E series biosynthesis. *Chem Biol* 13: 1193-1202.
61. Isobe, Y., M. Arita, S. Matsueda, R. Iwamoto, T. Fujihara, H. Nakanishi, R. Taguchi, K. Masuda, K. Sasaki, D. Urabe, M. Inoue, and H. Arai. 2012. Identification and Structure Determination of Novel Anti-inflammatory Mediator Resolvin E3, 17,18-Dihydroxyeicosapentaenoic Acid. *J Bio Chem* 287: 10525-10534.
62. Serhan, C. N., S. Hong, K. Gronert, S. P. Colgan, P. R. Devchand, G. Mirick, and R. L. Moussignac. 2002. Resolvins: a family of bioactive products of omega-3 fatty acid transformation circuits initiated by aspirin treatment that counter proinflammation signals. *J Exp Med* 196: 1025-1037.
63. Hong, S., K. Gronert, P. R. Devchand, R. L. Moussignac, and C. N. Serhan. 2003. Novel docosatrienes and 17S-resolvins generated from docosahexaenoic acid in murine brain, human blood, and glial cells. Autacoids in anti-inflammation. *J Biol Chem* 278: 14677-14687.
64. Krishnamoorthy, S., A. Recchiuti, N. Chiang, S. Yacoubian, C.-H. Lee, R. Yang, N. A. Petasis, and C. N. Serhan. 2010. Resolvin D1 binds human phagocytes with evidence for proresolving receptors. *Proc Natl Acad Sci U S A* 107: 1660-1665.
65. Schmid, M., C. Gemperle, N. Rimann, and M. Hersberger. 2016. Resolvin D1 Polarizes Primary Human Macrophages toward a Proresolution Phenotype through GPR32. *J Immunol* 196: 3429-3437.
66. Colby, J. K., R. E. Abdulnour, H. P. Sham, J. Dalli, R. A. Colas, J. W. Winkler, J. Hellmann, B. Wong, Y. Cui, S. El-Chemaly, N. A. Petasis, M. Spite, C. N. Serhan, and B. D. Levy. 2016. Resolvin D3 and Aspirin-Triggered Resolvin D3 Are Protective for Injured Epithelia. *Am J Pathol* 186: 1801-1813.
67. Dalli, J., J. W. Winkler, R. A. Colas, H. Arnardottir, C.-Y. C. Cheng, N. Chiang, N. A. Petasis, and C. N. Serhan. 2013. Resolvin D3 and aspirin-triggered resolvin D3 are potent immunoresolvents. *Chem Biol* 20: 188-201.
68. Serhan, C. N., K. Gotlinger, S. Hong, Y. Lu, J. Siegelman, T. Baer, R. Yang, S. P. Colgan, and N. A. Petasis. 2006. Anti-Inflammatory Actions of Neuroprotectin D1/Protectin D1 and Its Natural Stereoisomers: Assignments of Dihydroxy-Containing Docosatrienes. *J Immunol* 176: 1848-1859.
69. Deng, B., C.-W. Wang, H. H. Arnardottir, Y. Li, C.-Y. C. Cheng, J. Dalli, and C. N. Serhan. 2014. Maresin Biosynthesis and Identification of Maresin 2, a New Anti-Inflammatory and Pro-Resolving Mediator from Human Macrophages. *PloS one* 9: e102362.
70. Serhan, C. N., R. Yang, K. Martinod, K. Kasuga, P. S. Pillai, T. F. Porter, S. F. Oh, and M. Spite. 2009. Maresins: novel macrophage mediators with potent antiinflammatory and proresolving actions. *J Exp Med* 206: 15-23.
71. van Furth, R., and Z. A. Cohn. 1968. The origin and kinetics of mononuclear phagocytes. *J Exp Med* 128: 415-435.
72. Ebert, R. H., and H. W. Florey. 1939. The Extravascular Development of the

Monocyte Observed In vivo. *Br J Exp Pathol* 20: 342-356.
73. Auffray, C., M. H. Sieweke, and F. Geissmann. 2009. Blood monocytes: development, heterogeneity, and relationship with dendritic cells. *Annu Rev Immunol* 27: 669-692.
74. Sallusto, F., and A. Lanzavecchia. 1994. Efficient presentation of soluble antigen by cultured human dendritic cells is maintained by granulocyte/macrophage colony-stimulating factor plus interleukin 4 and downregulated by tumor necrosis factor alpha. *J Exp Med* 179: 1109-1118.
75. Martinez, F. O., A. Sica, A. Mantovani, and M. Locati. 2008. Macrophage activation and polarization. *Front Biosci* 13: 453-461.
76. Passlick, B., D. Flieger, and H. W. Ziegler-Heitbrock. 1989. Identification and characterization of a novel monocyte subpopulation in human peripheral blood. *Blood* 74: 2527-2534.
77. Ziegler-Heitbrock, L., P. Ancuta, S. Crowe, M. Dalod, V. Grau, D. N. Hart, P. J. Leenen, Y. J. Liu, G. MacPherson, G. J. Randolph, J. Scherberich, J. Schmitz, K. Shortman, S. Sozzani, H. Strobl, M. Zembala, J. M. Austyn, and M. B. Lutz. 2010. Nomenclature of monocytes and dendritic cells in blood. *Blood* 116: e74-80.
78. Ziegler-Heitbrock, H. W., G. Fingerle, M. Strobel, W. Schraut, F. Stelter, C. Schutt, B. Passlick, and A. Pforte. 1993. The novel subset of CD14+/CD16+ blood monocytes exhibits features of tissue macrophages. *Eur J Immunol* 23: 2053-2058.
79. Geissmann, F., S. Jung, and D. R. Littman. 2003. Blood monocytes consist of two principal subsets with distinct migratory properties. *Immunity* 19: 71-82.
80. Amer, A. O., and M. S. Swanson. 2002. A phagosome of one's own: a microbial guide to life in the macrophage. *Curr Opin Micro* 5: 56-61.
81. Epelman, S., K. J. Lavine, and G. J. Randolph. 2014. Origin and functions of tissue macrophages. *Immunity* 41: 21-35.
82. Unanue, E. R. 1984. Antigen-presenting function of the macrophage. *Annu Rev Immunol* 2: 395-428.
83. Aderem, A., and D. M. Underhill. 1999. Mechanisms of phagocytosis in macrophages. *Annu Rev Immunol* 17: 593-623.
84. Gordon, S., and P. R. Taylor. 2005. Monocyte and macrophage heterogeneity. *Nat Rev Immunol* 5: 953-964.
85. Adams, D. O. 1989. Molecular interactions in macrophage activation. *Immunol Today* 10: 33-35.
86. Boehm, U., T. Klamp, M. Groot, and J. C. Howard. 1997. Cellular responses to interferon-gamma. *Annu Rev Immunol* 15: 749-795.
87. Schroder, K., P. J. Hertzog, T. Ravasi, and D. A. Hume. 2004. Interferon-gamma: an overview of signals, mechanisms and functions. *J Leukoc Biol* 75: 163-189.
88. Trinchieri, G. 2003. Interleukin-12 and the regulation of innate resistance and adaptive immunity. *Nat Rev Immunol* 3: 133-146.
89. Hesketh, M., K. B. Sahin, Z. E. West, and R. Z. Murray. 2017. Macrophage Phenotypes Regulate Scar Formation and Chronic Wound Healing. *Inter J Mol Sci* 18: 1545.

90. Mosser, D. M., and J. P. Edwards. 2008. Exploring the full spectrum of macrophage activation. *Nat Rev Immunol* 8: 958-969.
91. MacMicking, J., Q. W. Xie, and C. Nathan. 1997. Nitric oxide and macrophage function. *Annu Rev Immunol* 15: 323-350.
92. Barrios-Rodiles, M., and K. Chadee. 1998. Novel regulation of cyclooxygenase-2 expression and prostaglandin E2 production by IFN-gamma in human macrophages. *J Immunol* 161: 2441-2448.
93. Stein, M., S. Keshav, N. Harris, and S. Gordon. 1992. Interleukin 4 potently enhances murine macrophage mannose receptor activity: a marker of alternative immunologic macrophage activation. *J Exp Med* 176: 287-292.
94. Doyle, A. G., G. Herbein, L. J. Montaner, A. J. Minty, D. Caput, P. Ferrara, and S. Gordon. 1994. Interleukin-13 alters the activation state of murine macrophages in vitro: comparison with interleukin-4 and interferon-gamma. *Eur J Immunol* 24: 1441-1445.
95. Mantovani, A., A. Sica, S. Sozzani, P. Allavena, A. Vecchi, and M. Locati. 2004. The chemokine system in diverse forms of macrophage activation and polarization. *Trends Immunol* 25: 677-686.
96. Hart, P. H., G. F. Vitti, D. R. Burgess, G. A. Whitty, D. S. Piccoli, and J. A. Hamilton. 1989. Potential antiinflammatory effects of interleukin 4: suppression of human monocyte tumor necrosis factor alpha, interleukin 1, and prostaglandin E2. *Proc Natl Acad Sci U S A* 86: 3803-3807.
97. Martinez, F. O., S. Gordon, M. Locati, and A. Mantovani. 2006. Transcriptional profiling of the human monocyte-to-macrophage differentiation and polarization: new molecules and patterns of gene expression. *J Immunol* 177: 7303-7311.
98. Mantovani, A., M. Locati, A. Vecchi, S. Sozzani, and P. Allavena. 2001. Decoy receptors: a strategy to regulate inflammatory cytokines and chemokines. *Trends Immunol* 22: 328-336.
99. Modolell, M., I. M. Corraliza, F. Link, G. Soler, and K. Eichmann. 1995. Reciprocal regulation of the nitric oxide synthase/arginase balance in mouse bone marrow-derived macrophages by TH1 and TH2 cytokines. *Eur J Immunol* 25: 1101-1104.
100. Hesse, M., M. Modolell, A. C. La Flamme, M. Schito, J. M. Fuentes, A. W. Cheever, E. J. Pearce, and T. A. Wynn. 2001. Differential regulation of nitric oxide synthase-2 and arginase-1 by type 1/type 2 cytokines in vivo: granulomatous pathology is shaped by the pattern of L-arginine metabolism. *J Immunol* 167: 6533-6544.
101. Torocsik, D., H. Bardos, L. Nagy, and R. Adany. 2005. Identification of factor XIII-A as a marker of alternative macrophage activation. *Cell Moll Life Sci* 62: 2132-2139.
102. Conrad, D. J., H. Kuhn, M. Mulkins, E. Highland, and E. Sigal. 1992. Specific inflammatory cytokines regulate the expression of human monocyte 15-lipoxygenase. *Proc Natl Acad Sci U S A* 89: 217-221.
103. Chen, B., S. Tsui, W. E. Boeglin, R. S. Douglas, A. R. Brash, and T. J. Smith. 2006. Interleukin-4 Induces 15-Lipoxygenase-1 Expression in Human Orbital Fibroblasts from Patients with Graves Disease. Evidence for anatomic site-

selective actions of Th2 cytokines. *J Bio Chem* 281: 18296-18306.
104. Lee, Y. W., H. Kühn, S. Kaiser, B. Hennig, A. Daugherty, and M. Toborek. 2001. Interleukin 4 induces transcription of the 15-lipoxygenase I gene in human endothelial cells. *J Lipid Res* 42: 783-791.
105. Namgaladze, D., S. Zukunft, F. Schnütgen, N. Kurrle, I. Fleming, D. Fuhrmann, and B. Brüne. 2018. Polarization of Human Macrophages by Interleukin-4 Does Not Require ATP-Citrate Lyase. *Front Immunol* 9.
106. Chaitidis, P., V. O'Donnell, R. J. Kuban, A. Bermudez-Fajardo, U. Ungethuem, and H. Kuhn. 2005. Gene expression alterations of human peripheral blood monocytes induced by medium-term treatment with the TH2-cytokines interleukin-4 and -13. *Cytokine* 30: 366-377.
107. Kuhn, H. 1996. Biosynthesis, metabolization and biological importance of the primary 15-lipoxygenase metabolites 15-hydro(pero)XY-5Z,8Z,11Z,13E-eicosatetraenoic acid and 13-hydro(pero)XY-9Z,11E-octadecadienoic acid. *Prog Lipid Res* 35: 203-226.
108. Wittwer, J., and M. Hersberger. 2007. The two faces of the 15-lipoxygenase in atherosclerosis. *Prostag Leukotr Ess* 77: 67-77.
109. Ihle, J. N., and I. M. Kerr. 1995. Jaks and Stats in signaling by the cytokine receptor superfamily. *Trends Genet* 11: 69-74.
110. Mikita, T., D. Campbell, P. Wu, K. Williamson, and U. Schindler. 1996. Requirements for interleukin-4-induced gene expression and functional characterization of Stat6. *Mol Cell Bio* 16: 5811-5820.
111. Bar-Peled, L., L. D. Schweitzer, R. Zoncu, and D. M. Sabatini. 2012. Ragulator is a GEF for the rag GTPases that signal amino acid levels to mTORC1. *Cell* 150: 1196-1208.
112. Bhattacharjee, A., A. Mulya, S. Pal, B. Roy, G. M. Feldman, and M. K. Cathcart. 2010. Monocyte 15-lipoxygenase gene expression requires ERK1/2 MAPK activity. *J Immunol* 185: 5211-5224.
113. Biswas, S. K., P. Allavena, and A. Mantovani. 2013. Tumor-associated macrophages: functional diversity, clinical significance, and open questions. *Semin Immunopathol* 35: 585-600.
114. Mantovani, A., W. J. Ming, C. Balotta, B. Abdeljalil, and B. Bottazzi. 1986. Origin and regulation of tumor-associated macrophages: the role of tumor-derived chemotactic factor. *Biochim Biophys Acta* 865: 59-67.
115. Movahedi, K., D. Laoui, C. Gysemans, M. Baeten, G. Stange, J. Van den Bossche, M. Mack, D. Pipeleers, P. In't Veld, P. De Baetselier, and J. A. Van Ginderachter. 2010. Different tumor microenvironments contain functionally distinct subsets of macrophages derived from Ly6C(high) monocytes. *Cancer Res* 70: 5728-5739.
116. Balkwill, F., and A. Mantovani. 2001. Inflammation and cancer: back to Virchow? *Lancet* 357: 539-545.
117. Zeisberger, S. M., B. Odermatt, C. Marty, A. H. Zehnder-Fjallman, K. Ballmer-Hofer, and R. A. Schwendener. 2006. Clodronate-liposome-mediated depletion of tumour-associated macrophages: a new and highly effective antiangiogenic therapy approach. *Br J Cancer* 95: 272-281.

118. Mantovani, A., B. Bottazzi, F. Colotta, S. Sozzani, and L. Ruco. 1992. The origin and function of tumor-associated macrophages. *Immunol Today* 13: 265-270.
119. Sica, A., A. Saccani, B. Bottazzi, N. Polentarutti, A. Vecchi, J. van Damme, and A. Mantovani. 2000. Autocrine production of IL-10 mediates defective IL-12 production and NF-kappa B activation in tumor-associated macrophages. *J Immunol* 164: 762-767.
120. Mantovani, A., S. Sozzani, M. Locati, P. Allavena, and A. Sica. 2002. Macrophage polarization: tumor-associated macrophages as a paradigm for polarized M2 mononuclear phagocytes. *Trends immunol* 23: 549-555.
121. Allavena, P., A. Sica, A. Vecchi, M. Locati, S. Sozzani, and A. Mantovani. 2000. The chemokine receptor switch paradigm and dendritic cell migration: its significance in tumor tissues. *Immunol Rev* 177: 141-149.
122. Hagemann, T., T. Lawrence, I. McNeish, K. A. Charles, H. Kulbe, R. G. Thompson, S. C. Robinson, and F. R. Balkwill. 2008. "Re-educating" tumor-associated macrophages by targeting NF-kappaB. *J Exp Med* 205: 1261-1268.
123. Guiducci, C., A. P. Vicari, S. Sangaletti, G. Trinchieri, and M. P. Colombo. 2005. Redirecting in vivo elicited tumor infiltrating macrophages and dendritic cells towards tumor rejection. *Cancer Res* 65: 3437-3446.
124. Watkins, S. K., N. K. Egilmez, J. Suttles, and R. D. Stout. 2007. IL-12 rapidly alters the functional profile of tumor-associated and tumor-infiltrating macrophages in vitro and in vivo. *J Immunol* 178: 1357-1362.
125. Nishi, T., and M. Forgac. 2002. The vacuolar (H+)-ATPases--nature's most versatile proton pumps. *Nat Rev Mol Cell Biol* 3: 94-103.
126. Nelson, N. 2003. A journey from mammals to yeast with vacuolar H+-ATPase (V-ATPase). *J Bioenerg Biomembr* 35: 281-289.
127. Yoshida, M., E. Muneyuki, and T. Hisabori. 2001. ATP synthase--a marvellous rotary engine of the cell. *Nat Rev Mol Cell Biol* 2: 669-677.
128. Sambade, M., and P. M. Kane. 2004. The yeast vacuolar proton-translocating ATPase contains a subunit homologous to the Manduca sexta and bovine e subunits that is essential for function. *J Biol Chem* 279: 17361-17365.
129. Zhao, J., S. Benlekbir, and J. L. Rubinstein. 2015. Electron cryomicroscopy observation of rotational states in a eukaryotic V-ATPase. *Nature* 521: 241.
130. MacLeod, K. J., E. Vasilyeva, J. D. Baleja, and M. Forgac. 1998. Mutational Analysis of the Nucleotide Binding Sites of the Yeast Vacuolar Proton-translocating ATPase. *J Biol Chem* 273: 150-156.
131. Maxfield, F. R., and T. E. McGraw. 2004. Endocytic recycling. *Nat Rev Mol Cell Biol* 5: 121-132.
132. Saftig, P., and J. Klumperman. 2009. Lysosome biogenesis and lysosomal membrane proteins: trafficking meets function. *Nat Rev Mol Cell Biol* 10: 623-635.
133. Kim, K. H., and M. S. Lee. 2014. Autophagy--a key player in cellular and body metabolism. *Nat Rev Endocrinol* 10: 322-337.
134. Gruenberg, J., and F. G. van der Goot. 2006. Mechanisms of pathogen entry through the endosomal compartments. *Nat Rev Mol Cell Biol* 7: 495-504.
135. Toyomura, T., Y. Murata, A. Yamamoto, T. Oka, G. H. Sun-Wada, Y. Wada, and

M. Futai. 2003. From lysosomes to the plasma membrane: localization of vacuolar-type H+ -ATPase with the a3 isoform during osteoclast differentiation. *J Biol Chem* 278: 22023-22030.
136. Wagner, C. A., K. E. Finberg, S. Breton, V. Marshansky, D. Brown, and J. P. Geibel. 2004. Renal vacuolar H+-ATPase. *Physiol Rev* 84: 1263-1314.
137. Pietrement, C., G. H. Sun-Wada, N. D. Silva, M. McKee, V. Marshansky, D. Brown, M. Futai, and S. Breton. 2006. Distinct expression patterns of different subunit isoforms of the V-ATPase in the rat epididymis. *Biol Reprod* 74: 185-194.
138. Williamson, W. R., and P. R. Hiesinger. 2010. On the role of v-ATPase V0a1-dependent degradation in Alzheimer disease. *Commu Integr Biol* 3: 604-607.
139. Pamarthy, S., A. Kulshrestha, G. K. Katara, and K. D. Beaman. 2018. The curious case of vacuolar ATPase: regulation of signaling pathways. *Mol Cancer* 17: 41.
140. Sun-Wada, G.-H., and Y. Wada. 2015. Role of vacuolar-type proton ATPase in signal transduction. *Biochim Biophys Acta* 1847: 1166-1172.
141. Zoncu, R., L. Bar-Peled, A. Efeyan, S. Wang, Y. Sancak, and D. M. Sabatini. 2011. mTORC1 senses lysosomal amino acids through an inside-out mechanism that requires the vacuolar H(+)-ATPase. *Science* 334: 678-683.
142. Kim, D. H., D. D. Sarbassov, S. M. Ali, J. E. King, R. R. Latek, H. Erdjument-Bromage, P. Tempst, and D. M. Sabatini. 2002. mTOR interacts with raptor to form a nutrient-sensitive complex that signals to the cell growth machinery. *Cell* 110: 163-175.
143. Colacurcio, D. J., and R. A. Nixon. 2016. Disorders of lysosomal acidification-The emerging role of v-ATPase in aging and neurodegenerative disease. *Ageing Res Rev* 32: 75-88.
144. Sennoune, S. R., and R. Martinez-Zaguilan. 2007. Plasmalemmal vacuolar H+-ATPases in angiogenesis, diabetes and cancer. *J Bioenerg Biomembr* 39: 427-433.
145. Forgac, M. 2018. A new twist to V-ATPases and cancer. *Oncotarget* 9: 31793-31794.
146. Werner, G., H. Hagenmaier, H. Drautz, A. Baumgartner, and H. Zahner. 1984. Metabolic products of microorganisms. 224. Bafilomycins, a new group of macrolide antibiotics. Production, isolation, chemical structure and biological activity. *J Antibiot* 37: 110-117.
147. Kinashi, H., K. Someno, and K. Sakaguchi. 1984. Isolation and characterization of concanamycins A, B and C. *J Antibiot* 37: 1333-1343.
148. Kinashi, H., K. Sakaguchi, T. Higashijima, and T. Miyazawa. 1982. Structures of concanamycins B and C. *J Antibiot* 35: 1618-1620.
149. Bowman, E. J., A. Siebers, and K. Altendorf. 1988. Bafilomycins: a class of inhibitors of membrane ATPases from microorganisms, animal cells, and plant cells. *Proc Natl Acad Sci U S A* 85: 7972-7976.
150. Droese, S., K. U. Bindseil, E. J. Bowman, A. Siebers, A. Zeeck, and K. Altendorf. 1993. Inhibitory effect of modified bafilomycins and concanamycins on P- and V-type adenosinetriphosphatases. *Biochemistry* 32: 3902-3906.
151. Drose, S., C. Boddien, M. Gassel, G. Ingenhorst, A. Zeeck, and K. Altendorf.

2001. Semisynthetic derivatives of concanamycin A and C, as inhibitors of V- and P-type ATPases: structure-activity investigations and developments of photoaffinity probes. *Biochemistry* 40: 2816-2825.

152. Huss, M., G. Ingenhorst, S. König, M. Gaßel, S. Dröse, A. Zeeck, K. Altendorf, and H. Wieczorek. 2002. Concanamycin A, the Specific Inhibitor of V-ATPases, Binds to the Vo Subunit c. *J Biol Chem* 277: 40544-40548.
153. Bowman, E. J., L. A. Graham, T. H. Stevens, and B. J. Bowman. 2004. The Bafilomycin/Concanamycin Binding Site in Subunit c of the V-ATPases from Neurospora crassa and Saccharomyces cerevisiae. *J Biol Chem* 279: 33131-33138.
154. Bowman, B. J., M. E. McCall, R. Baertsch, and E. J. Bowman. 2006. A Model for the Proteolipid Ring and Bafilomycin/Concanamycin-binding Site in the Vacuolar ATPase of Neurospora crassa. *J Biol Chem* 281: 31885-31893.
155. Bowman, B. J., and E. J. Bowman. 2002. Mutations in subunit C of the vacuolar ATPase confer resistance to bafilomycin and identify a conserved antibiotic binding site. *J Biol Chem* 277: 3965-3972.
156. Erickson, K. L., J. A. Beutler, J. H. Cardellina, and M. R. Boyd. 1997. Salicylihalamides A and B, Novel Cytotoxic Macrolides from the Marine Sponge Haliclona sp. *J Org Chem* 62: 8188-8192.
157. Galinis, D. L., T. C. McKee, L. K. Pannell, J. H. Cardellina, and M. R. Boyd. 1997. Lobatamides A and B, Novel Cytotoxic Macrolides from the Tunicate Aplidium lobatum. *J Org Chem* 62: 8968-8969.
158. Kim, J. W., K. Shin-Ya, K. Furihata, Y. Hayakawa, and H. Seto. 1999. Oximidines I and II: Novel Antitumor Macrolides from Pseudomonas sp. *J Org Chem* 64: 153-155.
159. Kunze, B., R. Jansen, F. Sasse, G. Hofle, and H. Reichenbach. 1998. Apicularens A and B, new cytostatic macrolides from Chondromyces species (myxobacteria): production, physico-chemical and biological properties. *J Antibiot* 51: 1075-1080.
160. Boyd, M. R., C. Farina, P. Belfiore, S. Gagliardi, J. W. Kim, Y. Hayakawa, J. A. Beutler, T. C. McKee, B. J. Bowman, and E. J. Bowman. 2001. Discovery of a novel antitumor benzolactone enamide class that selectively inhibits mammalian vacuolar-type (H+)-atpases. *J Pharmacol Exp Ther* 297: 114-120.
161. Shen, R., C. T. Lin, E. J. Bowman, B. J. Bowman, and J. A. Porco, Jr. 2002. Synthesis and V-ATPase inhibition of simplified lobatamide analogues. *Org Lett* 4: 3103-3106.
162. Huss, M., F. Sasse, B. Kunze, R. Jansen, H. Steinmetz, G. Ingenhorst, A. Zeeck, and H. Wieczorek. 2005. Archazolid and apicularen: Novel specific V-ATPase inhibitors. *BMC Biochem* 6: 13.
163. Osteresch, C., T. Bender, S. Grond, P. von Zezschwitz, B. Kunze, R. Jansen, M. Huss, and H. Wieczorek. 2012. The Binding Site of the V-ATPase Inhibitor Apicularen Is in the Vicinity of Those for Bafilomycin and Archazolid. *J Biol Chem* 287: 31866-31876.
164. Sasse, F., H. Steinmetz, G. Hofle, and H. Reichenbach. 2003. Archazolids, new cytotoxic macrolactones from Archangium gephyra (Myxobacteria). Production,

isolation, physico-chemical and biological properties. *J Antibiot* 56: 520-525.
165. Menche, D., J. Hassfeld, H. Steinmetz, M. Huss, H. Wieczorek, and F. Sasse. 2007. The first hydroxylated archazolid from the myxobacterium Cystobacter violaceus: isolation, structural elucidation and V-ATPase inhibition. *J Antibiot* 60: 328-331.
166. Menche, D., J. Hassfeld, H. Steinmetz, M. Huss, H. Wieczorek, and F. Sasse. 2007. Archazolid-7-O-β-D-glucopyranoside – Isolation, Structural Elucidation and Solution Conformation of a Novel V-ATPase Inhibitor from the Myxobacterium Cystobacter violaceus. *Eur J Org Chem* 2007: 1196-1202.
167. Bockelmann, S., D. Menche, S. Rudolph, T. Bender, S. Grond, P. von Zezschwitz, S. P. Muench, H. Wieczorek, and M. Huss. 2010. Archazolid A binds to the equatorial region of the c-ring of the vacuolar H+-ATPase. *J Biol Chem* 285: 38304-38314.
168. Grinstein, S., A. Nanda, G. Lukacs, and O. Rotstein. 1992. V-ATPases in phagocytic cells. *J Exp Biol* 172: 179-192.
169. Bidani, A., B. S. Reisner, A. K. Haque, J. Wen, R. E. Helmer, D. M. Tuazon, and T. A. Heming. 2000. Bactericidal activity of alveolar macrophages is suppressed by V-ATPase inhibition. *Lung* 178: 91-104.
170. Di Cristofori, A., S. Ferrero, I. Bertolini, G. Gaudioso, M. V. Russo, V. Berno, M. Vanini, M. Locatelli, M. Zavanone, P. Rampini, T. Vaccari, M. Caroli, and V. Vaira. 2015. The vacuolar H+ ATPase is a novel therapeutic target for glioblastoma. *Oncotarget* 6: 17514-17531.
171. PORRECA, E., M. REALE, C. DI FEBBO, M. DI GIOACCHINO, R. C. BARBACANE, M. L. CASTELLANI, G. BACCANTE, P. CONTI, and F. CUCCURULLO. 1996. Down-regulation of cyclooxygenase-2 (COX-2) by interleukin-1 receptor antagonist in human monocytes. *Immunology* 89: 424-429.
172. Li, Y., C. Soendergaard, F. H. Bergenheim, D. M. Aronoff, G. Milne, L. B. Riis, J. B. Seidelin, K. B. Jensen, and O. H. Nielsen. 2018. COX-2-PGE2 Signaling Impairs Intestinal Epithelial Regeneration and Associates with TNF Inhibitor Responsiveness in Ulcerative Colitis. *EBioMedicine* 36: 497-507.
173. Singer, C. A., K. J. Baker, A. McCaffrey, D. P. AuCoin, M. A. Dechert, and W. T. Gerthoffer. 2003. p38 MAPK and NF-kappaB mediate COX-2 expression in human airway myocytes. Am J Physiol Lung Cell Mol Physiol 285: L1087-1098.
174. Pouliot, M., J. Baillargeon, J. C. Lee, L. G. Cleland, and M. J. James. 1997. Inhibition of prostaglandin endoperoxide synthase-2 expression in stimulated human monocytes by inhibitors of p38 mitogen-activated protein kinase. *J Immunol* 158: 4930-4937.
175. Dean, J. L., M. Brook, A. R. Clark, and J. Saklatvala. 1999. p38 mitogen-activated protein kinase regulates cyclooxygenase-2 mRNA stability and transcription in lipopolysaccharide-treated human monocytes. *J Biol Chem* 274: 264-269.
176. Niiro, H., T. Otsuka, E. Ogami, K. Yamaoka, S. Nagano, M. Akahoshi, H. Nakashima, Y. Arinobu, K. Izuhara, and Y. Niho. 1998. MAP kinase pathways as a route for regulatory mechanisms of IL-10 and IL-4 which inhibit COX-2

expression in human monocytes. *Biochem Biophys Res Commun.* 250: 200-205.
177. Nagano, S., T. Otsuka, H. Niiro, K. Yamaoka, Y. Arinobu, E. Ogami, M. Akahoshi, Y. Inoue, K. Miyake, H. Nakashima, Y. Niho, and M. Harada. 2002. Molecular mechanisms of lipopolysaccharide-induced cyclooxygenase-2 expression in human neutrophils: involvement of the mitogen-activated protein kinase pathway and regulation by anti-inflammatory cytokines. *Int Immunol* 14: 733-740.
178. Reker, D., A. M. Perna, T. Rodrigues, P. Schneider, M. Reutlinger, B. Mönch, A. Koeberle, C. Lamers, M. Gabler, H. Steinmetz, R. Müller, M. Schubert-Zsilavecz, O. Werz, and G. Schneider. 2014. Revealing the macromolecular targets of complex natural products. *Nat Chem* 6: 1072.
179. Scherer, O., H. Steinmetz, C. Kaether, C. Weinigel, D. Barz, H. Kleinert, D. Menche, R. Müller, C. Pergola, and O. Werz. 2014. Targeting V-ATPase in primary human monocytes by archazolid potently represses the classical secretion of cytokines due to accumulation at the endoplasmic reticulum. *Biochem Pharmacol* 91: 490-500.
180. Poole, B., and S. Ohkuma. 1981. Effect of weak bases on the intralysosomal pH in mouse peritoneal macrophages. *J Cell Biol* 90: 665-669.
181. Shi, Q., J. Chen, Y. Wang, Z. Li, X. Li, C. Sun, and L. Zheng. 2015. Immobilization of Cyclooxygenase-2 on Silica Gel Microspheres: Optimization and Characterization. *Molecules* 20: 19971-19983.
182. Schwarz, K., M. Walther, M. Anton, C. Gerth, I. Feussner, and H. Kuhn. 2001. Structural Basis for Lipoxygenase Specificity. Conversion of the human leukocyte 5-lipoxygenase to a 15-lipoxygenating enzyme species by site-directed mutagenesis. *J Biol Chem* 276: 773-779.
183. Spencer, A. G., J. W. Woods, T. Arakawa, Singer, II, and W. L. Smith. 1998. Subcellular localization of prostaglandin endoperoxide H synthases-1 and -2 by immunoelectron microscopy. *J Biol Chem* 273: 9886-9893.
184. Tomura, H., J. Q. Wang, J. P. Liu, M. Komachi, A. Damirin, C. Mogi, M. Tobo, H. Nochi, K. Tamoto, D. S. Im, K. Sato, and F. Okajima. 2008. Cyclooxygenase-2 expression and prostaglandin E2 production in response to acidic pH through OGR1 in a human osteoblastic cell line. J Bone Miner Res 23: 1129-1139.
185. Ohkuma, S., J. Chudzik, and B. Poole. 1986. The effects of basic substances and acidic ionophores on the digestion of exogenous and endogenous proteins in mouse peritoneal macrophages. *J Cell Biol* 102: 959-966.
186. Karres, I., J.-P. Kremer, I. Dietl, U. Steckholzer, M. Jochum, and W. Ertel. 1998. Chloroquine inhibits proinflammatory cytokine release into human whole blood. *Am J Physiol* 274: R1058-R1064.
187. Oshio, T., R. Kawashima, Y. I. Kawamura, T. Hagiwara, N. Mizutani, T. Okada, T. Otsubo, K. Inagaki-Ohara, A. Matsukawa, T. Haga, S. Kakuta, Y. Iwakura, S. Hosokawa, and T. Dohi. 2014. Chemokine Receptor CCR8 Is Required for Lipopolysaccharide-Triggered Cytokine Production in Mouse Peritoneal Macrophages. *PloS one* 9: e94445.
188. Zhang, G., and S. Ghosh. 2001. Toll-like receptor–mediated NF-κB activation: a

phylogenetically conserved paradigm in innate immunity. *J Clin Invest* 107: 13-19.
189. Li, D. Q., L. Luo, Z. Chen, H. S. Kim, X. J. Song, and S. C. Pflugfelder. 2006. JNK and ERK MAP kinases mediate induction of IL-1beta, TNF-alpha and IL-8 following hyperosmolar stress in human limbal epithelial cells. *Exp Eye Res* 82: 588-596.
190. Rousseau, S., M. Papoutsopoulou, A. Symons, D. Cook, J. M. Lucocq, A. R. Prescott, A. O'Garra, S. C. Ley, and P. Cohen. 2008. TPL2-mediated activation of ERK1 and ERK2 regulates the processing of pre-TNF alpha in LPS-stimulated macrophages. *J Cell Sci* 121: 149-154.
191. Magni, P., M. Ruscica, E. Dozio, E. Rizzi, G. Beretta, and R. Maffei Facino. 2012. Parthenolide inhibits the LPS-induced secretion of IL-6 and TNF-alpha and NF-kappaB nuclear translocation in BV-2 microglia. *Phytother Res* 26: 1405-1409.
192. Slauch, J. M. 2011. How does the oxidative burst of macrophages kill bacteria? Still an open question. *Mol Microbiol* 80: 580-583.
193. Yokomakura, A., J. Hong, K. Ohuchi, S. E. Oh, J. Y. Lee, N. Mano, T. Takahashi, G. W. Hwang, and A. Naganuma. 2012. Increased production of reactive oxygen species by the vacuolar-type (H(+))-ATPase inhibitors bafilomycin A1 and concanamycin A in RAW 264 cells. *J Toxicol Sci* 37: 1045-1048.
194. Morgan, M. J., and Z. G. Liu. 2010. Reactive oxygen species in TNFalpha-induced signaling and cell death. *Mol Cells* 30: 1-12.
195. Tang, X., C. Mo, Y. Wang, D. Wei, and H. Xiao. 2013. Anti-tumour strategies aiming to target tumour-associated macrophages. *Immunology* 138: 93-104.
196. Syed, M. M., N. K. Phulwani, and T. Kielian. 2007. Tumor necrosis factor-alpha (TNF-alpha) regulates Toll-like receptor 2 (TLR2) expression in microglia. *J Neurochem* 103: 1461-1471.
197. Chen, C. C., Y. T. Sun, J. J. Chen, and K. T. Chiu. 2000. TNF-alpha-induced cyclooxygenase-2 expression in human lung epithelial cells: involvement of the phospholipase C-gamma 2, protein kinase C-alpha, tyrosine kinase, NF-kappa B-inducing kinase, and I-kappa B kinase 1/2 pathway. *J Immunol* 165: 2719-2728.
198. Kamachi, F., M. Yanai, H. S. Ban, K. Ishihara, J. Hong, K. Ohuchi, and N. Hirasawa. 2007. Involvement of Na+/H+ exchangers in induction of cyclooxygenase-2 by vacuolar-type (H+)-ATPase inhibitors in RAW 264 cells. *FEBS letters* 581: 4633-4638.
199. Canton, J., R. Khezri, M. Glogauer, and S. Grinstein. 2014. Contrasting phagosome pH regulation and maturation in human M1 and M2 macrophages. *Mol Biol Cell* 25: 3330-3341.
200. Dalli, J., and C. N. Serhan. 2012. Specific lipid mediator signatures of human phagocytes: microparticles stimulate macrophage efferocytosis and pro-resolving mediators. *Blood* 120: e60-72.
201. Cash, J. L., G. E. White, and D. R. Greaves. 2009. Chapter 17. Zymosan-induced peritonitis as a simple experimental system for the study of inflammation. *Method Enzymol* 461: 379-396.
202. Shankaranarayanan, P., P. Chaitidis, H. Kuhn, and S. Nigam. 2001. Acetylation

by histone acetyltransferase CREB-binding protein/p300 of STAT6 is required for transcriptional activation of the 15-lipoxygenase-1 gene. *J Biol Chem* 276: 42753-42760.
203. Conrad, D. J., and M. Lu. 2000. Regulation of human 12/15-lipoxygenase by Stat6-dependent transcription. *Am J Resp Cell Mol* 22: 226-234.
204. Fraire-Zamora, J. J., and M. Simons. 2018. Vacuolar ATPase is required for ERK-dependent wound healing in the Drosophila embryo. *Wound Repair Regen* 26: 102-107.
205. Zhang, S., L. S. Schneider, B. Vick, M. Grunert, I. Jeremias, D. Menche, R. Muller, A. M. Vollmar, and J. Liebl. 2015. Anti-leukemic effects of the V-ATPase inhibitor Archazolid A. *Oncotarget* 6: 43508-43528.
206. Pello, O. M., M. De Pizzol, M. Mirolo, L. Soucek, L. Zammataro, A. Amabile, A. Doni, M. Nebuloni, L. B. Swigart, G. I. Evan, A. Mantovani, and M. Locati. 2012. Role of c-MYC in alternative activation of human macrophages and tumor-associated macrophage biology. *Blood* 119: 411-421.
207. Zhong, X., H.-N. Lee, S. H. Kim, S.-A. Park, W. Kim, Y.-N. Cha, and Y.-J. Surh. 2018. Myc-nick promotes efferocytosis through M2 macrophage polarization during resolution of inflammation. *FASEB J* 32: 5312-5325.
208. Gerstmeier, J., C. Weinigel, S. Rummler, O. Radmark, O. Werz, and U. Garscha. 2016. Time-resolved in situ assembly of the leukotriene-synthetic 5-lipoxygenase/5-lipoxygenase-activating protein complex in blood leukocytes. *FASEB J* 30: 276-285.
209. Werz, O., E. Burkert, L. Fischer, D. Szellas, D. Dishart, B. Samuelsson, O. Radmark, and D. Steinhilber. 2003. 5-Lipoxygenase activation by MAPKAPK-2 and ERKs. *Adv Exp Med Biol* 525: 129-132.
210. Pergola, C., G. Dodt, A. Rossi, E. Neunhoeffer, B. Lawrenz, H. Northoff, B. Samuelsson, O. Rådmark, L. Sautebin, and O. Werz. 2008. ERK-mediated regulation of leukotriene biosynthesis by androgens: A molecular basis for gender differences in inflammation and asthma. *Proc Natl Acad Sci U S A* 105: 19881-19886.

APPENDIX 1: ACKNOWLEDGEMENTS

As four years went by so quickly, I am coming close to the end of my PhD study in Jena. The period of working time and living life in this lovely town is wonderful, which I will always treasure.

First, I would like to thank my supervisor, prof. Dr. Oliver Werz for taking good care of me both in research fields and in daily life in the Werz group. He is a devoted supervisor, who brings me into the field of inflammation and helps to design the projects step by step. He is an excellent researcher, who is always strict to himself and to us in the scientific field, teaching and guiding me to be an independent researcher.

I would like to thank Prof. Dr. Andrea Huwiler from the University of Bern for the kind agreement to review my dissertation.

Next, I would like to thank Dr. Jana Gerstmeier, who is a great mentor and a nice friend for me. She is patient and helps me to build my research interest by teaching me basic experimental skills, encouraging my enthusiasm and fulfilling my curiosity in science. I am impressed by her big smile and laugh, which encourages me to stay positive whenever there appears a black cloud during the research work or in daily life. It is nice to work together with her, enjoying research and enjoying life.

I would like to thank Dr. Simona Pace, who is an expert in the field of animal experiments and helps with *in vivo* studies for my research projects. She is a nice friend who always encourages me to stay confident and positive during research, and the most important thing, to enjoy life in Jena.

I would like to thank all members in the Werz group and the Scriba group: Andre, Andreas, Anna, Chunyang, Christian, Fabiana, Friedemann, Helmut, Jana F., Kehong, Konstantin L., Konstantin N., Laura, Maria, Markus, Patrick, Paul, Saskia, Stefanie L, Stefanie K., Stefanie S., Sulaiman, Ulrike, Wenfei and Yan. They were always helpful and supportive. Working with these nice people makes great pleasure. We were a big family. Special thanks are given to our secretary Theresa, our lab manager Nadja, Uwe and the technicians Monika, Bärbel, Heidi, Petra, Katrin in our group. Their excellent routine work makes it much easier for us to finish our research work.

I would like to thank all the collaboration partners for their excellent and productive work in all projects. Also, I want to thank the china scholarship council, the Deutsche

Forschungsgemeinschaft and the Free State of Thuringia and the European Social Fund (2016 FGR 0045) for scholarship and project funding.

I would like to thank my friends in Jena. They are always accompanying me and supporting me. Together with you, I enjoyed life in Jena and explored the splendid views all around Europe. I will always treasure the time we spent together in Jena.

Finally, I would like to thank my parents and my younger sister. To start new work and life in a new country is not always easy for me. Their love and support offer me infinite power, helps me to fix all problems when working and living abroad alone. In the near future, I will go back to China and try to spend more time with them.

Danke an alle! Thanks to all of you! 谢谢你们 (xie xie ni men)!

APPENDIX 2*:* CURRICULUM VITAE

PERSONAL INFORMATION

Name:	**Zhigang Rao**
Birthday:	04. May.1992, FuZhou, People´s Republic of China
Nationality:	chinese
Marital status:	single

EDUCATION

Sept. 2002 – June. 2008	High school, Jinxi Nummber.1 Middle School
Sept. 2008 – June. 2012	Bachelor of Science, School of Pharmaceutical Science, Wuhan University
Sept. 2012 – June. 2015	Master of Science, School of Pharmaceutical Science, Wuhan University
Nov. 2015 –	PhD Study in institute of pharmacy, Friedrich-Schiller-Universität Jena (Prof. Dr. Oliver Werz)

CONGRESSES AND SCIRNTIFIC MEETINGS

July 7 - 9, 2016	Annual meeting DFG FOR 1406, Münich, Germany
September 26 - 29, 2017	Annual meeting of the German Pharmaceutical Society (DPhG), Saarbrücken, Germany (**poster presentation)**
March 11 - 14, 2018	Annual program of the Gesellschaft Deutscher Chemiker (GDCh), Jena, Germany
March 29 - 31, 2018	BIOACTIVE LIPIDS conference “From Chemistry to Biology and Medicine”, Athens, Greece **(oral presentation)**
September 2 - 4, 2019	Annual meeting of the German Pharmaceutical Society (DPhG), Heidelberg, Germany (**poster prize)**

Jena, November 21, 2019 Zhigang Rao

APPENDIX 3: LIST OF PUBLICATIONS

1. **Rao Z**, Jordan PM, Wang Y, Menche D, Pace S, Gerstmeier J, and Werz O. (2019). "Differential role of V-ATPase for expression and activity of cyclooxygenase-2 in human monocytes." Submitted.

2. **Rao Z**, Pace S, Jordan PM, Bilancia R, Troisi F, Börner F, Andreas N, Kamradt T, Menche D, Rossi A, Serhan CN, Gerstmeier J, Werz O. (2019). "Vacuolar (H^+)-ATPase Critically Regulates Specialized Proresolving Mediator Pathways in Human M2-like Monocyte-Derived Macrophages and Has a Crucial Role in Resolution of Inflammation." J Immunol **203**(4): 1031-1043.

3. Klapper M, Paschold A, Zhang S, Weigel C, Dahse HM, Götze S, Pace S, König S, **Rao Z**, Reimer L, Werz O, Stallforth P (2019). "Bioactivity and Mode of Action of Bacterial Tetramic Acids." ACS Chem Biol **14**(8): 1693-1697.

4. Freund, R. R. A, Gobrecht P, **Rao Z**, Gerstmeier J, Schlosser R, Görls H, Oliver Werz, Fischer D, Arndt HD. (2019). "Stereoselective total synthesis of parthenolides indicates target selectivity for tubulin carboxypeptidase activity." Chem Sci **10**(31): 7358-7364

5. Werner M, Jordan PM, Romp E, Czapka A, **Rao Z**, Kretzer C, Koeberle A, Garscha U, Pace S, Claesson HE, Serhan CN, Werz O, Gerstmeier J. (2019). "Targeting biosynthetic networks of the proinflammatory and proresolving lipid metabolome." FASEB J **33**(5): 6140-6153.

6. Thomas L, **Rao Z**, Gerstmeier J, Raasch M, Weinigel C, Rummler S, Menche D, Müller R, Pergola C, Mosig A, Werz O. (2017). "Selective upregulation of TNFalpha expression in classically-activated human monocyte-derived macrophages (M1) through pharmacological interference with V-ATPase." Biochem Pharmacol **130**: 71-82.

APPENDIX 4: AUTHOR CONTRIBUTION STATEMENT

Manuscript I

Rao Z, Jordan PM, Wang Y, Menche D, Pace S, Gerstmeier J, and Werz O. (2019). "Differential role of V-ATPase for expression and activity of cyclooxygenase-2 in human monocytes." Submitted.

author	contribution
Rao Z	Cell culture and performance of blood cell isolation, determination of cell viability and cytokine levels, flow cytometry, S2 work with *E. coli*, SDS-PAGE and Western Blot, UPLC-MS-MS, analysis of data and preparation of graphs, analysis of statistics, co-writing of the manuscript. **total contribution: 75%**
Jordan PM	flow cytometry and FACS analysis
Wang Y	SDS-PAGE and Western Blot, determination of cytokine levels
Menche D	biosynthesis of the V-ATPase inhibitor archazolid A
Pace S	experimental design
Gerstmeier J, Werz O	experimental design, conceiving the project, writing the manuscript

Manuscript II

Thomas L, **Rao Z**, Gerstmeier J, Raasch M, Weinigel C, Rummler S, Menche D, Müller R, Pergola C, Mosig A, Werz O. (2017). "Selective upregulation of TNFalpha expression in classically-activated human monocyte-derived macrophages (M1) through pharmacological interference with V-ATPase." Biochem Pharmacol **130**: 71-82.

author	contribution
Rao Z	Cell culture and performance of blood cell isolation, determination of cytokine/chemokine levels, measurement of ROS formation, the microfluidically supported biochip assay, analysis of data and preparation of graphs, analysis of statistics, co-writing the manuscript. **total contribution: 35%**
Thomas L	Cell culture and performance of blood cell isolation, determination of cell viability, determination of cytokine/chemokine/mRNA levels, SDS-PAGE and Western Blot, immunofluorescence microscopy, HPLC analysis, analysis of data and preparation of graphs, analysis of statistics, co-writing the manuscript
Gerstmeier J, Pergola C	experimental design, writing the manuscript
Menche D, Müller R	biosynthesis of the V-ATPase inhibitor archazolid A
Raasch M, Mosig A	the microfluidically supported biochip assay
WeinigelC, Rummler S	buffy coat collection, blood cell isolation
Werz O	experimental design, conceiving the project, writing the manuscript

Manuscript III

Rao Z, Pace S, Jordan PM, Bilancia R, Troisi F, Börner F, Andreas N, Kamradt T, Menche D, Rossi A, Serhan CN, Gerstmeier J, Werz O. (2019). "Vacuolar (H(+))-ATPase Critically Regulates Specialized Proresolving Mediator Pathways in Human M2-like Monocyte-Derived Macrophages and Has a Crucial Role in Resolution of Inflammation." J Immunol **203**(4): 1031-1043.

author	**contribution**
Rao Z	Cell culture and performance of blood cell isolation, determination of cell viability, determination of cytokine levels, SDS-PAGE and Western Blot, Immunofluorescence microscopy, S2 work with *E. coli*, UPLC-MS-MS, analysis of data and preparation of graphs, analysis of statistics, co-writing of the manuscript. **total contribution: 75%**
Pace S, Bilancia R, Troisi F, Rossi A	*in vivo* animal experiments
Jordan PM, Andreas N, Kamradt T	flow cytometry and FACS analysis
Börner F	determination of cytokine levels, analysis of *in vivo* data
Menche D	biosynthesis of the V-ATPase inhibitor archazolid A
Serhan CN	experimental design
Gerstmeier J, Werz O	experimental design, conceiving the project, writing the manuscript

Jena, November 21, 2019 Prof. Dr. Oliver Werz

APPENDIX 5: EIGENSTÄNDIGKEITSERKLÄRUNG

Hiermit erkläre ich, dass mir die Promotionsordnung der Fakultät für Biowissenschaften der Friedrich-Schiller-Universität Jena bekannt ist, ich die Dissertation selbst angefertigt habe und alle von mir benutzten Hilfsmittel, persönlichen Mitteilungen und Quellen in meiner Arbeit angegeben sind.

Ich versichere, dass ich die Hilfe eines Promotionsberaters nicht in Anspruch genommen habe und dass Dritte weder unmittelbar noch mittelbar geldwerte Leistungen von mir für Arbeiten erhalten haben, die im Zusammenhang mit dem Inhalt der vorgelegten Dissertation stehen.

Die vorliegende Dissertation wurde von mir bei keiner bisherigen Prüfungsarbeit für eine staatliche oder andere wissenschaftliche Prüfung eingereicht. Weiterhin versichere ich, dass ich die gleiche, eine in wesentlichen Teilen ähnliche oder eine andere Abhandlung nicht bei einer anderen Universität als Dissertation eingereicht habe.

Jena, November 21, 2019 Zhigang Rao